Methods in Molecular Biology™

VOLUME 208

Peptide Nucleic Acids

Methods and Protocols

Edited by

Peter E. Nielsen

HUMANA PRESS

1

PNA Technology

Peter E. Nielsen

1. Introduction

Peptide nucleic acids (PNA) were originally conceived and designed as sequence-specific DNA binding reagents targeting the DNA major groove in analogy to triplex-forming oligonucleotides. However, instead of the sugar-phosphate backbone of oligonucleotides PNA was designed with a pseudopeptide backbone ***(1).*** Once synthesized, it was apparent that PNA oligomers based on the aminoethylglycin backbone with acetyl linkers to the nucleobases (*see* **Fig. 1**) are extremely good structural mimics of DNA (or RNA), being able to form very stable duplex structures with Watson-Crick complementary DNA, RNA (or PNA) oligomers ***(2–4)***. It also quickly became clear that triplexes formed between one homopurine DNA (or RNA) strand and two sequence complementary PNA strands are extraordinarily stable. Furthermore, this stability is the reason why homopyrimidine PNA oligomers when binding complementary targets in double-stranded DNA do not do so by conventional (PNA-DNA_2) triplex formation, but rather prefer to form a triplex-invasion complex in which the DNA duplex is invaded by an internal PNA_2-DNA triplex (*see* **Fig. 2**) ***(5,6)***. This type of binding is restricted to homopurine/homopyrimidine DNA targets in full analogy to dsDNA targeting by triplex forming oligo-

From: *Methods in Molecular Biology, vol. 208: Peptide Nucleic Acids: Methods and Protocols*
Edited by: P. E. Nielsen © Humana Press Inc., Totowa, NJ

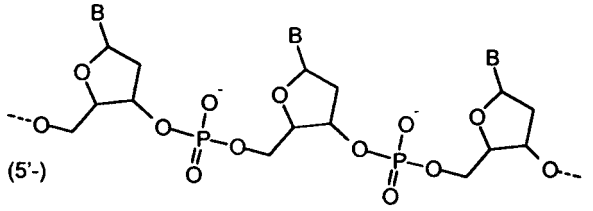

DNA

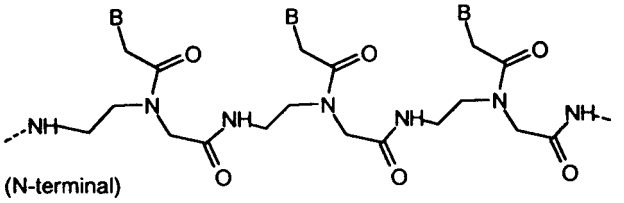

PNA

Fig. 1. Chemical structures of PNA as compared to DNA. In terms of binding properties, the amino-end of the PNA corresponds to the 5'-end of the DNA.

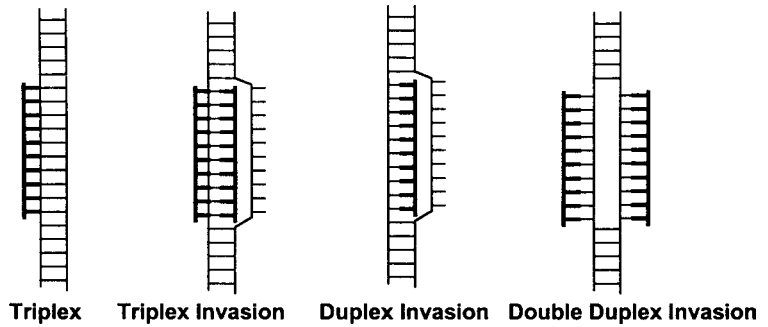

Fig. 2. Structural modes for binding of PNA oligomers to sequence complementary targets in double-stranded DNA.

nucleotides (*see* **Fig. 3**). However, other binding modes for targeting dsDNA is available for PNA *(7)* of which the double duplex invasion *(8)* is believed to become very important, because it allows the formation of very stable complexes at mixed purine-pyrimidine targets

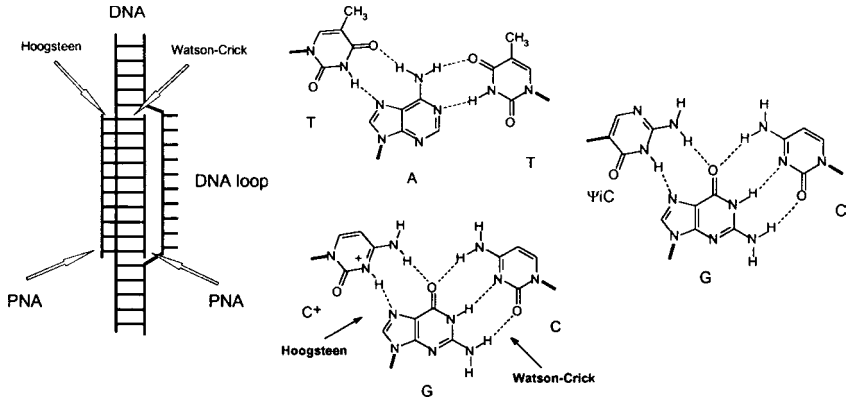

Fig. 3. Triplex invasion by homopyrimidine PNA oligomers. One PNA strand binds via Watson-Crick base pairing (preferably in the antiparallel orientation), whereas the other binds via Hoogsteen base pairing (preferably in the parallel orientation). It is usually advantageous to connect the two PNA strands covalently via a flexible linker into a bis-PNA, and to substitute all cytosines in the Hoogsteen strand with pseudoisocytosines (ΨiC), which do not require low pH for N3 "protonation."

as long as they have a reasonable (~ 50%) A/T content (*see* **Fig. 4**). The DNA/RNA recognition properties of PNA combined with excellent chemical and biological stability and tremendous chemical-synthetic flexibility has made PNA of interest to a range of scientific disciplines ranging from (organic) chemistry to biology to medicine ***(9–16)***.

2. PNA Chemistry

PNA oligomers are easily synthesized by standard solid-phase manual or automated peptide synthesis using either tBoc or Fmoc protected PNA monomers ***(17–19)***, of which the four natural nucleobases are commercially available. Typically the PNA oligomers are deprotected and cleaved off the resin using TFMSA/TFA (tBoc) or and purified by reversed-phase high-performance liquid chromatography (HPLC). While sequencing is not yet a routine option, the oligomers are conveniently characterized by matrix-

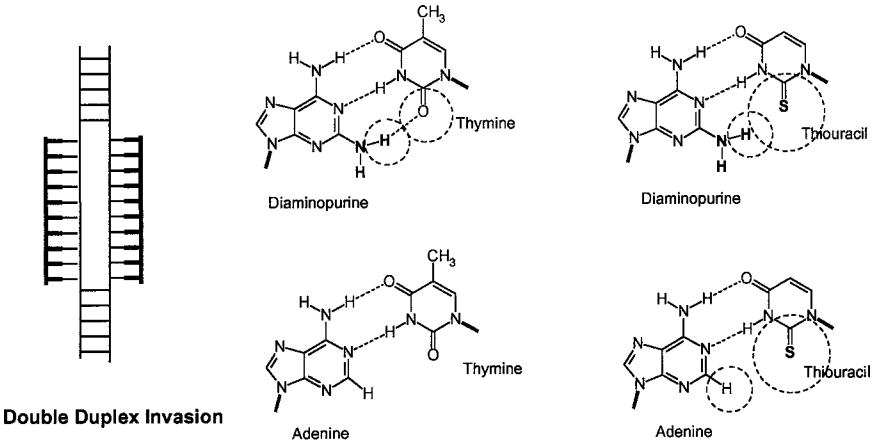

Fig. 4. Double-duplex invasion of pseudo complementary PNAs. In order to obtain efficient binding the target (and thus the PNAs) should contain at least 50% AT (no other sequence constraints), and in the PNA oligomers all A/T base pairs are substituted with 2,6-diaminopurine/2-thiouracil "base pairs." This base pair is very unstable due to steric hindrance. Therefore the two sequence-complementary PNAs will not be able to bind each other, but they bind their DNA complement very well.

assisted laser desorption/ionization time-of-flight (MALDI-TOF) mass spectrometry. PNA oligomers can routinely be labeled with fluorophores (fluorescein, rhodamine) or biotin, while labeling with radioisotopes requires incorporation of tyrosine for ^{125}I-iodination or conjugation to a peptide motif that can be ^{32}P-phosphorylated. Furthermore, PNA-peptide conjugates can be obtained by continuous synthesis or using standard peptide-conjugation techniques, such as maleimide cystein coupling or thioester condensation. Finally, the attractive chemistry of PNA has inspired the synthesis of a large number of PNA analog ***(16)***, including the introduction of a variety of non-natural nucleobases (e.g., ***20–23***) (*see* **Fig. 5**).

3. Cellular Uptake

PNA oligomers used for biological (antisense or antigene) experiments are typically 12–18-mers having a molecular weight of

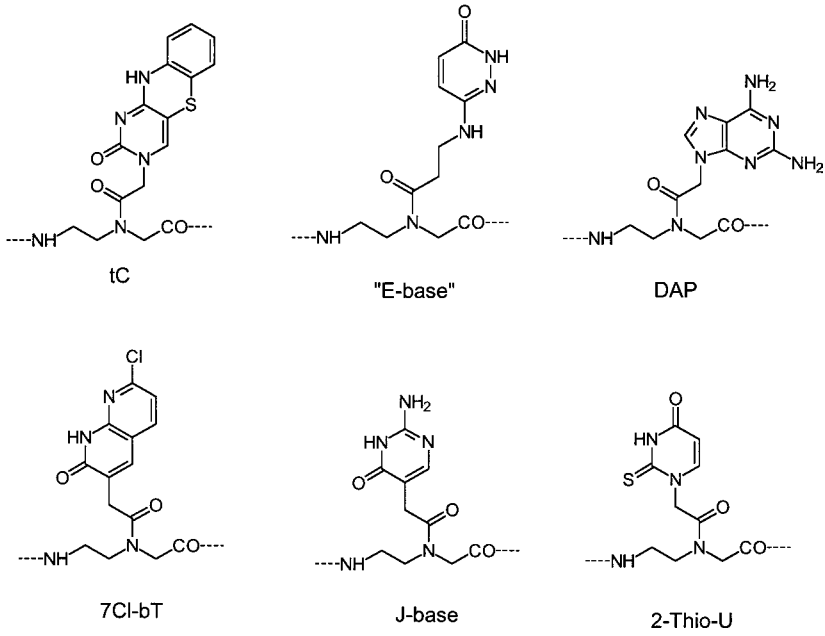

Fig. 5. Chemical structures of non-natural nucleobases used in PNA oligomers.

3–4000. Because PNA oligomers are hydrophilic rather than hydrophobic, these are in analogy to hydrophilic peptides (or oligonucleotides) not readily taken up by pro- or eukaryotic cells in general. Consequently, it has been necessary to devise PNA delivery systems. These include employment of cell-penetrating peptides, such as penetratin ***(24,25)*** transportan ***(25)***, Tat peptide ***(26)***, and nuclear localization signal (NLS) peptide ***(27)*** in PNA-peptide conjugates. Alternatively, cationic liposome carriers, which are routinely and effectively used for cellular delivery of oligonucleotides, can be used to deliver PNAs. However, because PNA oligomers do not inherently carry negative charges, loading of the liposomes with PNA is extremely inefficient. However, efficient loading and hence cell delivery can be attained by using a partly complementary oligonucleotide to "piggy-back" the PNA ***(28)*** or by conjugating a lipophilic tail (a fatty acid) to the PNA ***(29)***. Finally, techniques that

physically disrupt the cell membrane, such as electroporation ***(30)*** or streptolysin treatment ***(31)*** can be used for cell delivery. While all of these delivery systems have successfully been employed to demonstrate PNA-dependent downregulation of gene expression (*see* **Table 1**), it is fair to conclude that a general, easy, and efficient method of delivery is still warranted. In particular, it was recently demonstrated that PNA-peptide (penetratin, Tat, NLS) conjugates, although efficiently internalized in a number of cell lines ***(26)***, were predominently localized in endosomes inside the cell. At present the most general, but rather cumbersome, method is judged to be the oligonucleotide/liposome method ***(28)*** (*see* Chapter 14).

4. Antisense Applications

As mentioned earlier, several examples of PNA-directed (antisense) downregulation of gene expression have been described ***(24,25,27–35)*** (*see* **Table 1**). Cell free in vitro translation experiments indicate that regions around or upstream the translation initiation (AUG) start site of the mRNA are most sensitive to inhibition by PNA unless a triplex-forming PNA is used ***(36–38)*** (as is also the case when using the analogous morpholino oligomers (***[39]***)), although exceptions are reported ***(40)***. In cells in culture, the picture is less clear (*see* **Table 1**), and in one very recent study, it was even reported that among 20 PNA oligomers targeted to the luciferace gene (in HeLa cells) only one at the far 5'end of the mRNA showed good activity ***(34)***.

Because PNA-RNA duplexes are not substrates for RNAseH, antisense inhibition of translation by PNA is mechanistically different from that of phosphorothiates. Consequently, sensitive targets identified for phosphorothioate oligonucleotides are not necessarily expected to be good targets for PNA. Indeed, sensitive RNA targets for PNA oligomers are presumably targets at which the PNA can physically interfere with mRNA function, such as ribosome recognition, scanning, or assembly, whereas ribosomes involved in translation elongation appear much more robust ***(36)***. Interestingly, but not too surprisingly, it was recently demonstrated that intro-exon

Table 1
PNA Cellular Delivery and Ex Vivo Effects

PNA	Target	Method	Modification	Cell type/line	Assay	References
21-mer	Galanin receptor (ORF	Direct delivery	Peptide conjugate (penetratin[a]/ transportation[b]	Human melanoma Bowes	Receptor activity/ protein level (Western blot)	***24***
16-mer	Pre-pro oxytocin	Direct delivery	Peptide conjugate (retro-inverso penetratin[c])	Primary rat neurons	mRNA level (RT-PCR) Immunocytology	***25***
14-mer (homo-pyrimidine)	Nitric oxide synthase	Direct delivery	PNA peptide conjugate (Phe-Leu)[c]	Mouse macrophage RWA264.7	Enzyme activity	***100***
17-mer	c-myc (ORF-sense)	Direct delivery	NLS peptide[d] conjugate	Burkitt's lymphoma	Protein level (Western blot)/ cell viability	***27***
15-mer	PML-Rar-α (AUG)	Cationic liposomes	Adamantyl conjugate	Human lymphocyte (APL) NB4	Protein level (Western blot)/ cell viability	***35***
13-mer	Telomerase (RNA)	Cationic liposomes	PNA/DNA complex	Human prostate cancer DU145	Telomerase activity	***25***
13-mer	Telomerase (RNA)	Cationic liposomes	PNA/DNA complex	Human mammary epithelial (immort.)	Telomerase activity/cell viability/ telomerase length	***32***

(continued)

Table 1 *(continued)*
PNA Cellular Delivery and Ex Vivo Effects

PNA	Target	Method	Modification	Cell type/line	Assay	References
13-mer	Telomerase (RNA)	Electroporation	PNA/DNA complex	AT-SV1, GM05849	Telomerase activity/cell immortality	***33***
11/13-mer	Telomerase (RNA)	Direct delivery	Peptide conjugate (penetratin[c])	JR8/M14, human melanoma	Telomerase activity/cell viability	***102***
11-mer	none	Direct delivery	Mitochondrial uptake peptide[e]	IMR32, HeLa, a.o.	Only uptake	***103***
17-mer	c-myc	Direct delivery	PNA dihydro-testosterone conjugate	Prostatic carcinoma	MYC expression cell viability	***104***
11-18-mer	Luciferase (5-UTR)	Cationic liposomes	PNA/DNA complex	HeLA	Luciferase activity	***34***
15-mer	IL-5Rα (splice site)	Electroporation	None	BCL_1 lymphoma	RNA synthesis (splicing	***30***
11-mer	Mitochondrial DNA	Direct delivery	PNA-phosphonium conjugate	143B osteosarcoma/ fibroblasts (human)	Biotin uptake/ MERRF DNA	***105***
13-mer	Telomerase (RNA)	Direct delivery	PNA-lactose conjugate	HepG2 hepatoblastoma	Fluorescence uptake/telomerase activity	***106***

(continued)

Table 1 *(continued)*
PNA Cellular Delivery and Ex Vivo Effects

PNA	Target	Method	Modification	Cell type/line	Assay	References
15-mer	HIV-1 *gag-pol*	Direct delivery	None	H9	Virus production	***64***
7-mer bis-PNA	ribosomal RNA α-sarcin loop	Direct delivery	None	*E. coli*	Growth inhibition	***54***
10-15-mer	β–lactamase β-glactosidase (AUG)	Direct delivery	None	*E. coli*	Enzyme activity	***101***
10-mer	*acp*P (AUG) α–sarcin loop	Direct delivery	Peptide conjugate (KFF[f])	*E. coli*	Growth inhibition	***56***
17-mer	NTP/EhErd2 (AUG)	Direct delivery	None	*Entamoeba histolytica*	Enzyme activity	***58***
Triplex forming bis-PNA		Electroporation	None	Mouse fibroblasts	Mutation induction	***31***
Triplex forming bis-PNA	Globin gene (dsDNA)	Electroporation	None	Monkey kidney CV1	mRNA level (RT-PCR)	***49***
18-mer	EGFP (nitron)	Electroporation	None/Lys_4	HeLa	GFP synthesis	***41***

[a]penetratin (pAntp): RQIKIWFQNRRMKWKK
[b]transportan: GWTLNSAGYLLGKINLAALAKKIL
[c]reto-inverso penetratin: (D)-KKWKMRRNQFWVKVQR
[d]Nuclear localization signal (NLS): PKKKRKV
[e]MSVLTPLLLRGLTGSARRLPVPRAKIHSL
[f]KFFKFFKFFK

splice junctions are very sensitive targets for PNA antisense inhibition because correct mRNA splicing is prevented ***(34,41)***. Thus in antisense experiments with PNA, as with other DNA analogs and mimics, it is advisable to perform a mRNA scanning (gene-walk) by testing a series of PNAs targeting different regions of the mRNA.

5. Antigene Properties

PNA triplex-invasion complexes have sufficient stability to arrest elongating RNA polymerase, especially when positioned on the template DNA strand ***(38,42)***. Naturally, DNA recognition by proteins, such as transcription factor and RNA polymerase is also totally blocked by PNA binding (both triplex- and double-duplex invasion) ***(8,43,44)*** and the concomitant complete distortion of the DNA helix. Therefore, PNA gene targeting at the DNA level (antigene) should be very efficient. The main obstacle appears to be the access of the PNA to the DNA under physiological conditions that include the presence of cations (K^+, Mg^{2+}, spermine, etc.) that stabilize the DNA double helix and therefore dramatically reduces the rate of helix invasion by the PNA ***(45,46)***. Furthermore, the effect of chromatin structure on PNA binding is not known, but would be expected to decrease the access to the DNA binding sites. Nonetheless, it has been reported that triplex invading PNAs induced mutations in mouse cells, thereby inferring target binding in the cell nucleus ***(31)***. Binding in vivo may be greatly facilitated by negative DNA supercoiling ***(46)***, e.g., induced by active transcription, or by the transcription process *per se* ***(47)***.

Most interestingly, PNA triplex invasion loops are recognized by RNA polymerases as transcription initiation sites, most likely because the loops resembles the loop in a transcription initiation or elongation complex ***(48)***. Thus PNA oligomers may function as artificial transcription factors using the PNA target as a "promotor" (*see* Chapter 17), and the effect has even been reported to take place in cells in culture ***(49)***.

6. Gene Delivery

Gene therapy requires efficient delivery of DNA vectors to the nucleus of cells in desired tissues. The specific and strong binding of PNA to double stranded DNA has been exploited to tag such vectors noncovalently with fluorophores in order to be able to track the vector in the cells ***(50)***, and more recently with targeting ligands conjugated to the PNA. These were either the nuclear localization signal (NLS) peptide improving nuclear entry of the vector ***(51,52)*** or ligands (such as ferritin) for cell-specific receptors ***(53)***, that target the vector to cells expressing this receptor.

7. Antimicrobial PNAs

Microbes have also been targets for PNA antisense. Many antibiotics interfere with protein-synthesis by specifically binding to prokaryotic ribosomes. The binding sites of such antibiotics often map to the ribosomal RNA. In an effort to mimic the action of such antibiotics, PNA oligomers were targeted to functionally essential regions of the 23S *Escherichia coli* ribosomal RNA (*see* **Fig. 6**) ***(54)***. In particular a triplex-forming bis-PNA targeting a 7-mer homopurine stretch in the α-sarcin loop (*see* **Fig. 7**) effectively inhibited translation in a cell free system and were also able to inhibit the growth of *E. coli* , albeit with low potency, which was ascribed to poor uptake of the PNA by the bacteria ***(55)***. Conjugating a simple transporter peptide to the PNA increased the potency significantly, and an even more potent antibacterial PNA was developed by targeting an essential gene involved in fatty acid synthesis, *acp*P. This PNA was shown to inhibit the growth of bacteria *E. coli* in the presence of human (HeLa) cells ***(56)***. Analogous PNA conjugates showed antiinfective efficacy in a mouse model ***(57)***. Unmodified antisense PNA oligomers were also recently shown to downregulate targeted genes in an amoeba (*Entamoeba histolytica*) ***(58)***.

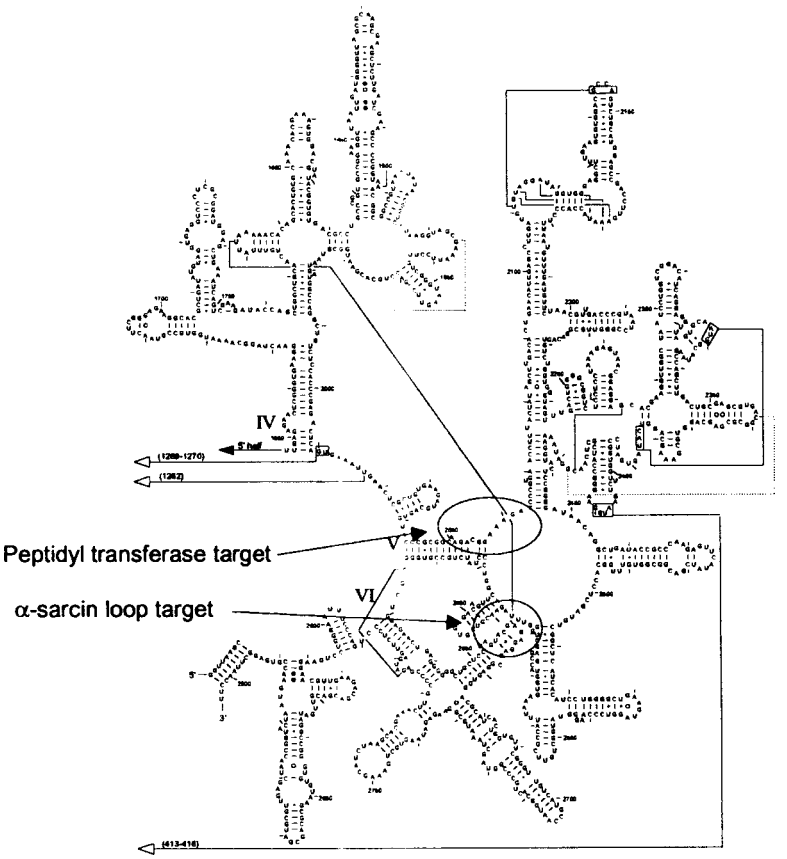

Fig. 6. Sequence of part of the 23S ribosomal RNA from *E. coli*. Two purine rich targets that have been found to be sensitive to tageting by bis-PNAs are indicated. These targets are found in two functional regions: the peptidyl transferase center, and the α-sarcin loop.

8. Antiviral PNAs

Reverse transcriptase, one of the key enzymes in the life cycle of retroviruses (such as HIV), is very sensitive to PNA antisense inhibition. Reverse transcription of the RNA template is effectively arrested by PNA oligomers bound to the template ***(59–63)***. This finding has raised hope that PNA antiviral drugs could be developed, and one report has even shown that HIV replication in cell culture can be inhibited by PNAs targeting the gag-pol gene ***(64)***.

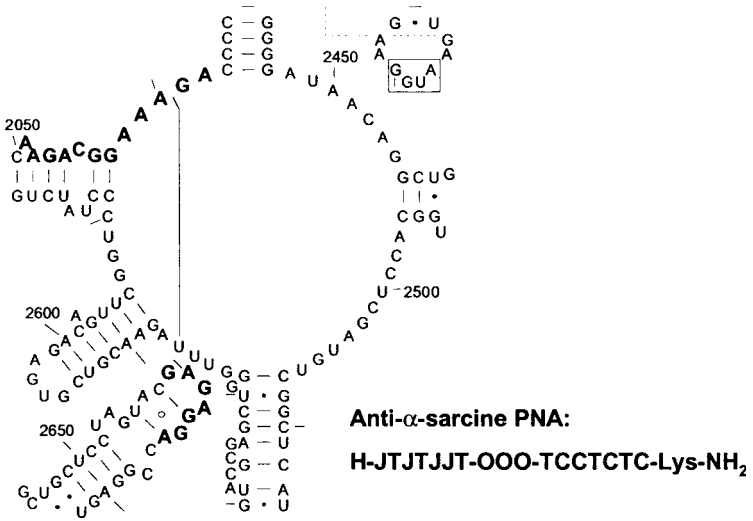

Fig. 7. Close-up view of the peptidyl transferase center and the α-sarcin loop targets (in bold). The bis-PNA targeting the α-sarcin loop is also shown. The linker is composed of three 8-amino-3,6-dioxaoctanoic acid (O) units.

However, very high PNA concentrations were required, emphasizing the need of an efficient cell-delivery system for PNA.

9. Genetic Information Carrier

PNA oligomers are potentially carriers of genetic information through their nucleobase sequence. As PNAs are also peptides, these molecules formally bridge the chemistry and function of proteins (peptides) and nucleic acids (DNA) and in this respect may be of relevance to the discussion of the prebiotic evolution of life ***(65)***. It is well-established that the formation of amino acids and nucleobases could have occurred in a prebiotic soup on the young Earth ***(66)***, whereas it is very difficult to imagine and mimic conditions that would create sugars (ribose) and nucleosides ***(67)***. Thus one may consider the possibility that a PNA-like prebiotic genetic material may have been a predecessor of RNA and the RNA world. Indeed, it has been demonstrated that it is possible to "chemically" transfer" sequence information from one PNA molecule to another

(primitive replication) and likewise from a PNA oligomer to an RNA oligomer ***(68–70)***. Thus, in principle, a PNA world to an RNA world transition scenario is a theoretical possibility. Furthermore, it was recently demonstrated that PNA monomers can be formed under prebiotic soup conditions ***(71)***.

10. PNA in Diagnostics

The excellent hybridization properties of PNA oligomers combined with its unique chemistry has been exploited in a variety of genetic diagnostic techniques. For instance, PNA probes for *in situ* hybridization yield superior signal to noise ratios and often allow milder washing procedures resulting in morphologically better samples. Thus PNA-fluorescence *in situ* hybridization (FISH) techniques (*see* Chapter 12) have been developed for quantitative telomere analyses ***(72–74)***, chromosome painting ***(75)*** and viral and bacterial diagnostics both in medical as well as environmental samples ***(76–83)***.

In another very powerful application, PNA oligomers can be used to silent polymerase chain reaction (PCR) amplifications in single mutation analyses ***(84)*** (*see* Chapters 10 and 11). This technique is so powerful that it is possible to obtain a specific signal from a single mutation oncogene in the presence of a 1,000–10,000-fold excess of the nonmutated wild-type normal gene ***(85–89)***.

Furthermore, various beacon ***(90–91)*** or light-up probe technologies have taken advantage of PNA chemistry ***(92–94)***. PNA oligomers are perfectly suited for MALDI-TOF mass-spectrometry giving very high and distinct signals, and this property has elegantly been exploited in an array hybridization technique in which the hybridized DNA (or RNA) is detected by mass-spectrometry via secondary hybridization of a PNA tag ***(95)***. Such tags are simply made with individual molecular weights, and the presence of a specific PNA tag in the MALDI thus identifies the presence of a specific hybridization and thus the gene variant. Most importantly many PNA tags can be analyzed in the same experiment ***(95)***. Finally, PNA oligomers can be used as capture probes for DNA or RNA purification and sample preparation ***(96–99)***.

The examples given here illustrate the width of PNA applications and, it is hoped, will inspire further use of this versatile DNA mimic both within these already established techniques, but as much in the development of novel applications.

References

1. Nielsen, P. E., Egholm, M., Berg, R. H., and Buchardt, O. (1991) Sequence-selective recognition of DNA by strand displacement with a thymine-substituted polyamide. *Science* **254,** 1497–1500.
2. Egholm, M., Buchardt, O., Christensen, L., Behrens, C., Freier, S. M., Driver, D. A., et al. (1993) PNA hybridizes to complementary oligonucleotides obeying the Watson-Crick hydrogen-bonding rules. *Nature* **365,** 566–568.
3. Jensen, K. K., Ørum, H., Nielsen, P. E., and Nordén, B. (1997) Kinetics for hybridization of peptide nucleic acids (PNA) with DNA and RNA studied with the BIAcore technique. *Biochemistry* **36,** 5072–5077.
4. Wittung, P., Nielsen, P. E., Buchardt, O., Egholm, M., and Nordén, B. (1994) DNA-like double helix formed by peptide nucleic acid. *Nature* **368,** 561–563.
5. Nielsen, P. E., Egholm, M., and Buchardt, O. (1994) Evidence for (PNA)2/DNA triplex structure upon binding of PNA to dsDNA by strand displacement. *J. Mol. Recogn.* **7,** 165–170.
6. Cherny, D. Y., Belotserkovskii, B. P., Frank-Kamenetskii, M. D., Egholm, M., Buchardt, O., Berg, R. H., and Nielsen, P. E. (1993) DNA unwinding upon strand-displacement binding of a thymine-substituted polyamide to double-stranded DNA. *Proc. Natl. Acad. Sci. USA* **90,** 1667–1670.
7. Nielsen, P. E. (2001) Peptide nucleic acid targeting of double-stranded DNA. *Methods Enzymol.* **340,** 329–340.
8. Lohse, J., Dahl, O., and Nielsen, P. E. (1999) Double duplex invasion by peptide nucleic acid: a general principle for sequence-specific targeting of double-stranded DNA. *Proc. Natl. Acad. Sci. USA* **96,** 11,804–11,808.
9. Nielsen, P. E. and Haaima, G. (1997) Peptide nucleic acid (PNA). A DNA mimic with a pseudopeptide backbone. *Chem. Soc. Rev.* **26,** 73–78.
10. Nielsen, P. E. and Egholm, M., ed. (1999) *Peptide Nucleic Acids: Protocols and Applications*. Horizon Press, Wymondham, Norfolk, UK.

11. Nielsen, P. E. (1999) Peptide nucleic acid. A molecule with two identities. *Acc. Chem. Res.* **32,** 624–630.
12. Nielsen, P. E. Antisense peptide nucleic acids. *Curr. Opin. Mol. Ther.* 2000, **2,** 282–287.
13. Nielsen, P. E. (2001) Peptide nucleic acid: a versatile tool in genetic diagnostics and molecular biology. *Curr. Opin. Biotechnol.* **12,** 16–20.
14. Nielsen, P. E. (2001) Peptide nucleic acids as antibacterial agents via the antisense principle. *Expert. Opin. Invest. Drugs* **10,** 331–341.
15. Ray, A. and Nordén, B. (2000) Peptide nucleic acid (PNA): its medical and biotechnical applications and promise for the future. *FASEB J.* **14,** 1041–1060.
16. Ganesh, K. N. and Nielsen, P. E. (2000) Peptide nucleic acids: analogs and derivatives. *Curr. Org. Chem.* **4,** 931–943.
17. Dueholm, K. L., Egholm, M., Behrens, C., Christensen, L., Hansen, H. F., Vulpius, T., et al. (1994) Synthesis of peptide nucleic acid monomers containing the four natural nucleobases: thymine, cytosine, adenine and guanine, and their oligomerization. *J. Org. Chem.* **59,** 5767–5773.
18. Christensen, L., Fitzpatrick, R., Gildea, B., Petersen, K. H., Hansen, H. F., Koch, T., et al. (1995) Solid-phase synthesis of peptide nucleic acids (PNA) *J. Peptide Sci.* **3**, 175–183.
19. Thomson, S. A., Josey, J. A., Cadilla, R., Gaul, M. D., Hassman, C. F., Luzzio, M. J., et al. (1995) Fmoc mediated synthesis of peptide nucleic acids. *Tetrahedr. Lett.* **22,** 6179–6194.
20. Egholm, M., Christensen, L., Dueholm, K. L., Buchardt, O., Coull, J., and Nielsen, P. E. (1995) Efficient pH-independent sequence-specific DNA binding by pseudoisocytosine-containing bis-PNA. *Nucleic Acids Res.* **23,** 217–222.
21. Eldrup, A. B., Dahl, O., and Nielsen, P. E. (1997) A novel peptide nucleic acid monomer for recognition of thymine in triple helix structures. *J. Amer. Chem. Soc.* **119,** 11,116–11,117**.**
22. Haaima, G., Hansen, H. F., Christensen, L., Dahl, O., and Nielsen, P. E. (1997) Increased DNA binding and sequence discrimination of PNA oligomers containing 2,6-diaminopurine. *Nucleic Acids Res.* **25,** 4639–4643.
23. Eldrup, A., Nielsen, B. B., Haaima, G., Rasmussen, H., Kastrup, J. S., Christensen, C., and Nielsen, P. E. (2001) 1,8-Naphthyridin-2(1H)-ones. Novel bi- and tricyclic analogues of thymine in peptide nucleic acids (PNA) *Eur. J. Org. Chem.* 1781–1790.

24. Pooga, M., Soomets, U., Hällbrink, M., Valkna A, Saar, K., Rezaei, K., et al. (1998) Cell penetrating PNA constructs regulate galanin receptor levels and modify pain transmission *in vivo*. *Nat. Biotechnol.* **16,** 857–861.
25. Aldrian-Herrada, G., Desarménien, M.G., Orcel, H., Boissin-Agasse, L., Méry, J., Brugidou, J., and Rabié, A. (1998) A peptide nucleic acid (PNA) is more rapidly internalized in cultured neurons when coupled to a *retro-inverso* delivery peptide. The antisense activity Depresses the target mRNA and protein in magnocellular oxytocin neurons. *Nucleic Acids Res.* **26,** 4910–4916.
26. Koppelhus, U., Awasthi, S., Zachar, V., Holst, H. U., and Nielsen, P. E. Cell Dependent DifferentialCellular Uptake of PNA, Peptides and PNA-peptide conjugates. *Antisense Nucl. Acid Drug Devel.*, in press.
27. Cutrona, G., Carpaneto, E. M., Ulivi, M., Roncella, S., Landt, O., Ferrarini, M., et al. (2000) Effects in live cells of a c-myc anti-gene PNA linked to a nuclear localization signal. *Nature Biotechnol.* **18,** 300–303.
28. Hamilton, S. E., Simmons, C. G., Kathiriya, I. S., and Corey, D. R. (1999) Cellular delivery of peptide nucleic acids and inhibition of human telomerase. *Chem. Biol.* **6,** 343–351.
29. Ljungstrøm, T., Knudsen, H., and Nielsen, P. E. (1999) Cellular uptake of adamantyl conjugated peptide nucleic acids. *Bioconjug. Chem.* **10,** 965–972.
30. Karras, J. G., Maier, M. A., Lu, T., Watt, A., and Manoharan, M. (2001) Peptide nucleic acids are potent modulators of endogenous pre-mRNA splicing of the murine interleukin-5 receptor-alpha chain. *Biochemistry* **40,** 7853–7859.
31. Faruqi, A. F., Egholm, M., and Glazer, P. M. (1998) Peptide nucleic acid-targeted mutagenesis of a chromosomal gene in mouse cells. *Proc. Natl. Acad. Sci. USA* **95,** 1398–1403.
32. Herbert, B. S., Pitts, A. E., Baker, S. I., Hamilton, S. E., Wright, W. E., Shay, J. W. et al. (1999) Inhibition of human telomerase in immortal human cells leads to progressive telomere shortening and cell death. *Proc. Natl. Acad. Sci. USA* **96,** 14,276–14,281.
33. Shammas, M. A., Simmons, C. G., Corey, D. R., and Reis, R. J. S. (1999) Telomerase inhibition by peptide nucleic acids reverses "immortality" of transformed human cells. *Oncogene* **18,** 6191–6200.
34. Doyle, D. F., Braasch, D. A., Simmons, C. G., Janowski, B. A., Corey, D. R. (2001) Inhibition of gene expression inside cells by

peptide nucleic acids: effect of mRNA target sequence, mismatched bases, and PNA length. *Biochemistry* **40,** 53–64.

35. Mologni, L., Marchesi, E., Nielsen, P. E., and Gambacorti-Passerini C. (2001) Inhibition of promyelocytic leukemia (PML)/retinoic acid receptor-alpha and PML expression in acute promyelocytic leukemia cells by anti-PML peptide nucleic acid. *Cancer Res.* **61,** 5468–5473.
36. Knudsen, H. and Nielsen, P. E. (1996) Antisense properties of duplex- and triplex-forming PNAs. *Nucleic Acids Res.* **24,** 494–500.
37. Mologni, L., Lecoutre, P., Nielsen, P. E., and Gambacorti-Passerini, C. (1998) Additive antisense effects of different PNAs on the in vitro translation of the PML/RAR.alpha. gene. *Nucleic Acids Res.* **26,** 1934–1938.
38. Hanvey, J. C., Peffer, N. J., Bisi, J. E., Thomson, S. A., Cadilla, R., Josey, J. A. et al. (1992) Antisense and antigen properties of peptide nucleic acids. *Science (Washington, DC)* **258,** 1481–1485.
39. Summerton, J. (1999) Morpholino antisense oligomers: the case for an RNase H-independent structural type. *Biochim. Biophys. Acta* **1489,** 141–158.
40. Dias, N., Dheur, S., Nielsen, P. E., Gryaznov, S., Van Aerschot, A., Herdewijn, P. et al. (1999) Antisense PNA tridecamers targeted to the coding region of Ha-ras mRNA arrest polypeptide chain elongation. *J. Mol. Biol.* **294,** 403–416.
41. Sazani, P., Kang, S. H., Maier, M. A., Wei, C., Dillman, J., Summerton, J., et al. (2001) Nuclear antisense effects of neutral, anionic and cationic oligonucleotide analogs. *Nucleic Acids Res.* **29,** 3965–3974.
42. Nielsen, P. E., Egholm, M., Buchardt, O. (1994) Sequence-specific transcription arrest by peptide nucleic acid bound to the DNA template strand. *Gene* **149,** 139–145.
43. Nielsen, P. E., Egholm, M., Berg, R. H., and Buchardt, O. (1993) Sequence specific inhibition of DNA restriction enzyme cleavage by PNA. *Nucleic Acids Res.* **21,** 197–200.
44. Vickers, T. A., Griffity, M. C., Ramasamy, K., Risen, L. M., Freier, S. M. (1995) Inhibition of NF-κB specific transcriptional activation by PNA strand invasion. *Nucleic Acids Res.* **23,** 3003–3008.
45. Demidov, V. V., Yavnilovich, M. V., Belotserkovskii, B. P., Frank-Kamenetskii, M. D., and Nielsen, P. E. (1995) Kinetics and mechanism of polyamide ("peptide") nucleic acid binding to duplex DNA. *Proc. Natl. Acad. Sci. USA* **92,** 2637–2641.

46. Bentin, T. and Nielsen, P. E. (1996) Enhanced peptide nucleic acid binding to supercoiled DNA: possible implications for DNA "Breathing" dynamics. *Biochemistry* **35,** 8863–8869.
47. Larsen, H. J. and Nielsen, P. E. (1996) Transcription-mediated binding of peptide nucleic acid (PNA) to double-stranded DNA: sequence-specific suicide transcription. *Nucleic Acids Res.* **24,** 458–463.
48. Møllegaard, N. E., Buchardt, O., Egholm, M., and Nielsen, P. E. (1994) Peptide nucleic acid-DNA strand displacement loops as artificial transcription promoters. *Proc. Natl. Acad. Sci. USA* **91,** 3892–3895.
49. Wang, G., Xu, X., Pace, B., Dean, D. A., Glazer, P. M., Chan, P., et al. (1999) Peptide nucleic acid (PNA) binding-mediated induction of human γ-globin gene expression. *Nucleic Acids Res* **27,** 2806–2813.
50. Zelphati, O., Liang, X., Hobart, P., and Felgner, P. L. (1999) Gene chemistry: functionally and conformationally intact fluorescent plasmid DNA. *Human Gene Ther.* **10,** 15–24.
51. Brandén, L. J., Christensson, B., Smith, C. I. E. (2001) In vivo nuclear delivery of oligonucleotides via hybridizing bifunctional peptides. *Gene Ther.* **8,** 84–87.
52. Brandén, L. J., Mohamed, A. J., and Smith, C. I. E. (1999) A peptide nucleic acid-nuclear localization signal fusion that mediates nuclear transport of DNA. *Nat. Biotechnol.* **17,** 784–787.
53. Liang, K. W., Hoffman, E. P., and Huang, L. (2000) Targeted delivery of plasmid DNA to myogenic cells via transferrin-conjugated peptide nucleic acid. *Mol. Ther.* **1,** 236–243.
54. Good, L. and Nielsen, P. E. (1998) Inhibition of translation and bacterial growth by peptide nucleic acid targeted to ribosomal RNA. *Proc. Natl. Acad. Sci. USA* **95,** 2073–2076.
55. Good, L., Sandberg, R., Larsson, O., Nielsen, P. E., and Wahlestedt, C. (2000) Antisense PNA effects in *Escherichia coli* are limited by the outer-membrane LPS layer. *Microbiology* **146,** 2665–2670.
56. Good, L., Awasthi, S. K., Dryselius, R., Larsson, O., and Nielsen, P. E. (2001) Bactericidal antisense effects of peptide-PNA conjugates. *Nature Biotechnol.* **19,** 360–364.
57. Schou, C., Hansen, H. F., Nielsen, P. E., Beck, F., Ravn, B. T., Kristensen, E., (2000) Antibiotic Effects of PNA (Peptide Nucleic Acid) Antisense Compounds Against Multiresistant *Echerichia coli.* Poster presented at ICAAC, 2000, Toronto).
58. Stock, R. P., Olvera, A., Sanchez, R., Saralegui, A., Scarfi, S., Sanchez-Lopez, R. et al. (2001) Inhibition of gene expression in

Entamoeba histolytica with antisense peptide nucleic acid oligomers. *Nature Biotechnol.* **19,** 231–234.

59. Koppelhus, U., Zachar, V., Nielsen, P. E., Liu, X., Eugen-Olsen, J., and Ebbesen, P. (1997) Efficient in vitro inhibition of HIV-1 gag reverse transcription by peptide nucleic acid (PNA) at minimal ratios of PNA/RNA. *Nucleic Acids Res.* **25,** 2167–2173.
60. Lee, R., Kaushik, N., Modak, M. J., Vinayak, R., and Pandey, V. N. (1998) Polyamide nucleic acid targeted to the primer binding site of the HIV-1 RNA genome blocks *in Vitro* HIV-1 reverse transcription. *Biochemistry* **37,** 900–910.
61. Boulmé, F., Freund, F., Moreau, S., Nielsen, P. E., Gryaznov, S., Toulmé, J. J. et al. (1998) Modified (PNA, 2'-O-methyl and phosphoramidate) anti-TAR antisense oligonucleotides as strong and specific inhibitors of in vitro HIV-1 reverse transcription. *Nucleic Acids Res.* **26,** 5492–5500.
62. Boulme, F., Freund, F., Gryaznov, S., Nielsen, P. E., Tarrago-Litvak, L., and Litvak, S. (2000) Study of HIV-2 primer-template initiation complex using antisense oligonucleotides. *Eur. J. Biochem.* **267,** 2803–2811.
63. Mayhood, T., Kaushik, N., Pandey, P. K., Kashanchi, F., Deng, L., and Pandey, V. N. (2000) Inhibition of Tat-mediated transactivation of HIV-1 LTR transcription by polyamide nucleic acid targeted to TAR hairpin element. *Biochemistry* **39,** 11,532–11,539.
64. Sei, S., Yang, Q. E., O'Neill, D., Yoshimura, K., and Mitsuya, H. (2000) Identification of a key target sequence to block human immunodeficiency virus type 1 replication within the gag-pol transframe domain. *J. Virol.* **74,** 4621–4633.
65. Nielsen, P. E. (1993) Peptide nucleic acid (PNA): A model structure for the primordial genetic material. *Origins Life Evol. Biosph.* **23,** 323–327.
66. Miller, S. L. (1953) A production of amino acids under possible primitive earth conditions, *Science* **117**, 528–529.
67. Oro, J. (1960) Synthesis of adenine from ammonium cyanide, *Biochem. Biophys. Res. Commun.* **2**, 407–412.
68. Böhler, C., Nielsen, P. E., and Orgel, L. E. (1995) Template switching between PNA and RNA oligonucleotides. *Nature* **376,** 578–581.
69. Schmidt, J. G., Nielsen, P. E., Orgel, L. E. (1997) Information transfer from peptide nucleic acids to RNA by template-directed syntheses. *Nucleic Acids Res.* **25,** 4797–4802.

70. Schmidt, J. G., Christensen, L., Nielsen, P. E., and Orgel, L. E. (1997) Information transfer from DNA to peptide nucleic acids by template-directed syntheses. *Nucleic Acids Res.* **25,** 4792–4796.
71. Nelson, K. E., Levy, M., and Miller, S. L. (2000) Peptide nucleic acids rather than RNA may have been the first genetic molecule. *Proc. Natl. Acad. Sci. USA* **97,** 3868–3871.
72. Lansdorp, P. M., Verwoerd, N. P., Van de Rijke, F. M., Dragowska, V., Little, M.-T., Dirks, R. W. et al. (1996) Heterogeneity in telomere length of human chromosomes. *Human Mol. Gen.* **5,** 685–691.
73. Zijlmans, M. J. M., Martens, U. M., Poon, S. S. S., Raap, A. K., Tanke, H. J., Ward, R. K., and Lansdorp, P. M. (1997) Telomeres in the mouse have large inter-chromosomal variations in the number of T_2AG_3 repeats. *Proc. Natl. Acad. Sci. USA* **94,** 7423–7428.
74. Mathioudakis, G., Storb, R., McSweeney, P. A., Torok-Storb, B., Lansdorp, P. M., Brummendorf, T. H., et al. (2000) Polyclonal hematopoiesis with variable telomere shortening in human long-term allogeneic marrow graft recipients. *Blood* **96,** 3991–3994.
75. Chen, C., Wu, B., Wie, T., Egholm, M., and Strauss, W. M. (2000) Unique chromosome identification and sequence-specific structural analysis with short PNA oligomers. *Mamm. Genome* **11,** 384–391.
76. Hongmanee, P., Stender, H., and Rasmussen, O. F. (2001) Evaluation of a fluorescence *in situ* hybridization assay for differentiation between tuberculous and nontuberculous Mycobacterium species in smears of Lowenstein-Jensen and mycobacteria growth indicator tube cultures using peptide nucleic acid probes. *J. Clin. Microbiol.* **39,** 1032–1035.
77. Drobniewski, F. A., More, P. G., and Harris, G. S. (2000) Differentiation of Mycobacterium tuberculosis complex and nontuberculous mycobacterial liquid cultures by using peptide nucleic acid-fluorescence *in situ* hybridization probes. *J. Clin. Microbiol.* **38,** 444–447.
78. Stender, H., Mollerup, T. A., Lund, K., Petersen, K. H., Hongmanee, P., and Godtfredsen, S. E. (1999) Direct detection and identification of Mycobacterium tuberculosis in smear-positive sputum samples by fluorescence *in situ* hybridization (FISH) using peptide nucleic acid (PNA) probes. *Int. J. Tuberc. Lung Dis.* **3,** 830–837.
79. Perry-O'Keefe, H., Stender, H., Broomer, A., Oliveira, K., Coull, J., and Hyldig-Nielsen, J. J. (2001) Filter-based PNA *in situ* hybridization for rapid detection, identification and enumeration of specific micro-organisms. *J. Appl. Microbiol.* **90,** 180–189.

80. Stender, H., Oliveira, K., Rigby, S., Bargoot, F., and Coull, J. (2001) Rapid detection, identification, and enumeration of *Escherichia coli* by fluorescence in situ hybridization using an array scanner. *J. Microbiol. Methods* **45,** 31–39.
81. Stender, H., Sage, A., Oliveira, K., Broomer, A. J., Young, B., and Coull, J. (2001) Combination of ATP-bioluminescence and PNA probes allows rapid total counts and identification of specific microorganisms in mixed populations. *J. Microbiol. Methods* **46,** 69–75.
82. Stender, H., Kurtzman, C., Hyldig-Nielsen, J. J., Sørensen, D., Broomer, A., Oliveira, K. et al. (2001) Identification of Dekkera bruxellensis (Brettanomyces) from wine by fluorescence *in situ* hybridization using peptide nucleic acid probes. *Appl. Environ. Microbiol.* **67,** 938–941.
83. Worden, A. Z., Chisholm, S. W., and Binder, B. J. (2000) *In situ* hybridization of Prochlorococcus and Synechococcus (Marine cyanobacteria) spp. with rRNA-targeted peptide nucleic acid probes. *Appl. Environ. Microbiol.* **66,** 284–289.
84. Ørum, H., Nielsen, P. E., Egholm, M., Berg, R. H., Buchardt, O., and Stanley, C. Single (1993) base pair mutation analysis by PNA directed PCR clamping. *Nucleic Acids Res.* **21,** 5332–5336.
85. Behn, M. and Schuermann, M. (1998) Sensitive detection of *p53* gene mutations by a "mutant enriched" PCR-SSCP technique. *Nucleic Acids Res.* **26,** 1356–1358.
86. Murdock, D. G., Christacos, N. C., and Wallace, D. C. (2000) The age-related accumulation of a mitochondrial DNA control region mutation in muscle, but not brain, detected by a sensitive PNA-directed PCR clamping based method. *Nucleic Acids Res.* **28,** 4350–4355.
87. Myal, Y., Blanchard, A., Watson, P., Corrin, M., Shiu, R., and Iwasiow, B. (2000) Detection of genetic point mutations by peptide nucleic acid-mediated polymerase chain reaction clamping using paraffin-embedded specimens. *Anal. Biochem.* **285,** 169–172.
88. Von Wintzingerode, F., Landt, O., Ehrlich, A., and Gobel, U. B. (2000) Peptide nucleic acid-mediated PCR clamping as a useful supplement in the determination of microbial diversity. *Appl. Environ. Microbiol.* **66,** 549–557.
89. Behn, M., Thiede, C., Neubauer, A., Pankow, W., and Schuermann, M. (2000) Facilitated detection of oncogene mutations from exfoliated tissue material by a PNA-mediated 'enriched PCR' protocol. *J. Pathol.* **190,** 69–75.

90. Ortiz, E., Estrada, G., and Lizardi, P. M. (1998) PNA molecular beacons for rapid detection of PCR amplicons. *Mol. and Cell. Probes* **12(4),** 219–226.
91. Kuhn, H., Demidov, V. V., Gildea, B. D., Fiandaca, M. J., Coull, J. C., and Frank-Kamenetskii, M. D. (2001) PNA beacons for duplex DNA. *Antisense Nucleic Acid Drug Dev.* **11,** 265–270.
92. Isacsson, J., Cao, H., Ohlsson, L., Nordgren, S., Svanvik, N., Westman, G., et al. (2000) Rapid and specific detection of PCR products using light-up probes. *Mol. Cell. Probes* **14,** 321–328.
93. Svanvik, N., Westman, G., Wang, D., and Kubista, M. (2000) Light-up probes: thiazole orange-conjugated peptide nucleic acid for detection of target nucleic acid in homogeneous solution. *Anal. Biochem.* **281,** 26–35.
94. Svanvik, N., Nygren, J., Westman, G., and Kubista, M. (2001) Free-probe fluorescence of light-up probes. *J. Am. Chem. Soc.* **123,** 803–809.
95. Griffin, T., Tang, W., and Smith, L. M. (1997) Genetic analysis by peptide nucleic acid affinity MALDI-TOF mass spectrometry. *Nat. Biotechnol.* **15,** 1368–1370.
96. Ørum, H., Nielsen, P. E., Jørgensen, M., Larsson, C., Stanley, C., and Koch, T. (1995) Sequence-specific purification of nucleic acids by PNA-controlled hybrid selection. *BioTechniques* **19,** 472–480.
97. Seeger, C., Batz, H.-G., Ørum, H. (1997) PNA-mediated purification of PCR amplifiable human genomic DNA from whole blood. *BioTechniques* **23,** 512–516.
98. Chandler, D. P., Stults, J. R., Anderson, K. K., Cebula, S., Schuck, B. L., and Brockman, F. J. (2000) Affinity capture and recovery of DNA at femtomolar concentrations with peptide nucleic scid probes. *Anal. Biochem.* **283,** 241–249.
99. Chandler, D. P., Stults, J. R., Cebula, S., Schuck, B. L., Weaver, D. W., Anderson, K. K., et al. (2000) Affinity purification of DNA and RNA from environmental samples with peptide nucleic acid clamps. *Appl. Environ. Microbiol.* **66,** 3438–3445.
100. Scarfi, S., Giovine, M., Gasparini, A., et al. (1999) Modified peptide nucleic acids are internalized in mouse macrophages RAW 264.7 and inhibit inducible nitric oxide synthase. *FEBS Lett.* **451,** 264–268.
101. Good, L. and Nielsen, P. E. (1998) Antisense inhibition of gene expression in bacteria by PNA targeted to mRNA. *Nat. Biotech.* **16,** 355–358.

102. Villa, R., Folini, M., Lualdi, S., Veronese, S., Daidone, and M. G., Zaffaroni, N. (2000) Inhibition of telomerase activity by a cell-penetrating peptide nucleic acid construct in human melanoma cells. *FEBS Lett.* **473,** 241–248.
103. Chinnery, P. F., Taylor, R. W., Diekert, K., Lill, R., Turnbull, D. M., and Lightowlers, R. N. (1999) Peptide nucleic acid delivery to human mitochondria. *Gene Ther.* **6,** 1919–1928.
104. Boffa, I. C., Scarfi, S., Mariani, M. R., et al. (2000) Dihydro testosterone as a selective cellular/nuclear localization vector for antigene peptide nucleic acid in prostatic carcinoma cells. *Cancer Res.* **60,** 2258–2262.
105. Muratovska, A., Lightowlers, R. N., Taylor, R. W., et al. (2001) Targeting peptide nucleic acid (PNA) oligomers to mitochondria within cells by conjugation to lipophilic cations: implications for mitochondrial DNA replication, expression and disease. *Nucl. Acids Res.* **29,** 1852–1863.
106. Zhang, X., Simmons, C. G., and Corey, D. R. (2001) Liver cell specific targeting of peptide nucleic acid oligomers. *Bioorg. Med. Chem. Lett.* **11,** 1269–1272.

2

Solid Phase Synthesis of PNA Oligomers

Frederik Beck

1. Introduction

Originally the PNA oligomers were assembled on a Merrifield (methylbenzhydrylamine, MBHA) resin in a fritted vial, as shown in **Fig. 1**, using the Boc/Cbz strategy. Fmoc-chemistry was subsequently introduced and most recently the Mmt-monomers have also been used. The first syntheses were made in the above-mentioned glass reaction vial, but later protocols for use on fully automated equipment, both for Boc (ABI synthesizers) and Fmoc chemistry (Expedite, PerSeptive Biosystems), became available. **Subheading 1.1.** will only describe the manual, solid-phase synthesis of PNA oligomers from the commercially available Boc/Cbz monomers.

1.1. Boc/Cbz Synthesis

In **Fig. 2** is depicted the synthesis cycle for the synthesis of PNA oligomers using the Boc/Cbz monomers as published by Christensen et al. ***(1)*** They had initially tested both CPG (controlled pore glass) and polystyrene resins and found, by a comparative study, that MBHA-polystyrene (methylbenzhydrylamine) was the superior solid support. The first monomer coupled to the resin using HBTU activation was typically a Boc-amino acid (Boc-Lysine-N^{ε}-

From: *Methods in Molecular Biology, vol. 208: Peptide Nucleic Acids: Methods and Protocols*
Edited by: P. E. Nielsen © Humana Press Inc., Totowa, NJ

Fig. 1. Reaction vessel.

2-ClZ) to improve solubility of the final oligomer. The Boc group was then removed using trifluoroacetic acid (TFA, m-cresol, 95/5). The m-cresol was added to function as a scavenger for the *tert*-butyl cations in order to avoid alkylation of the nucleobases. The next step, the coupling of the next monomer, was performed with HBTU activation as with the first Boc-amino acid.

As outlined in the figure, *N,N*-dimethylformamide/pyridine (DMF, Pyridine) was used as solvent in the couplings. This was due to the swelling of the MBHA resin in this solvent system, combined with the pyridine working as a catalyst in the amide bond formation during the oligomerization. Initially a protocol employing diisopropylcarbodiimide (DIC) activation was tested. In this protocol a neutralization step using diisopropyl ethylamine (DIEA) was prior to the coupling.

As N-acyl transfer has been known to occur ***(2)*** (*see* **Fig. 3**), when using DIC activation, this type of activation was aborted in favor of the uronium based coupling reagents used in **Fig. 2**, and thus the

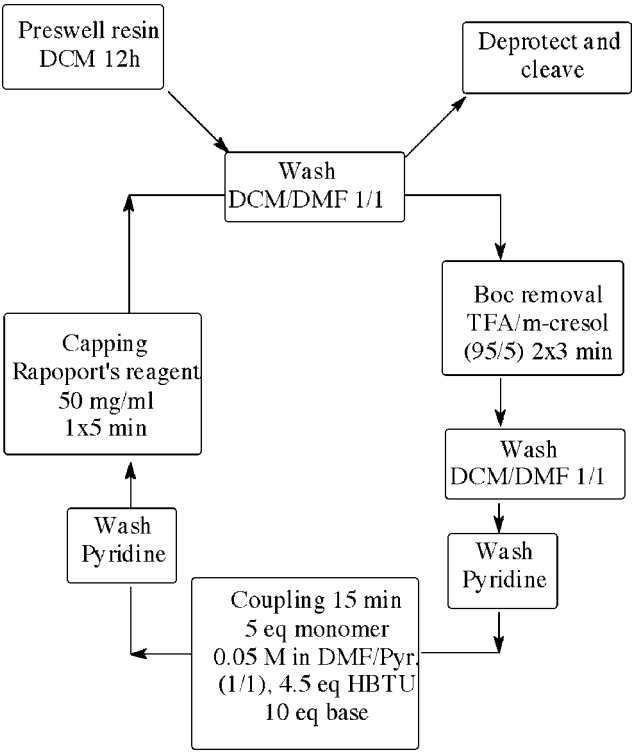

Fig. 2. Boc/Cbz PNA oligomer synthesis.

pre-neutralization step was avoided. As can be seen from **Fig. 2**, the coupling was performed in DMF/Pyridine with *N,N*-diethylcyclohexylamine as base. The coupling efficiency was determined by quantitative high-performance liquid chromatography (HPLC) to be $\geqslant 94\%$. Other uronium based couplings reagents were tested, e.g. TBTU, but HBTU showed the better performance. When using PyBop as coupling reagent in the synthesis of H-CGG ACT AAG TCC ATT GC-Gly-NH_2 a total yield of 40% was obtained as opposed to 61% when using HBTU, underlining that HBTU was the superior coupling reagent.

The choice of base in the coupling reaction was made after testing several tertiary amines. The general choice for this type of coupling chemistry, DIEA, resulted in precipitation of the amine salts

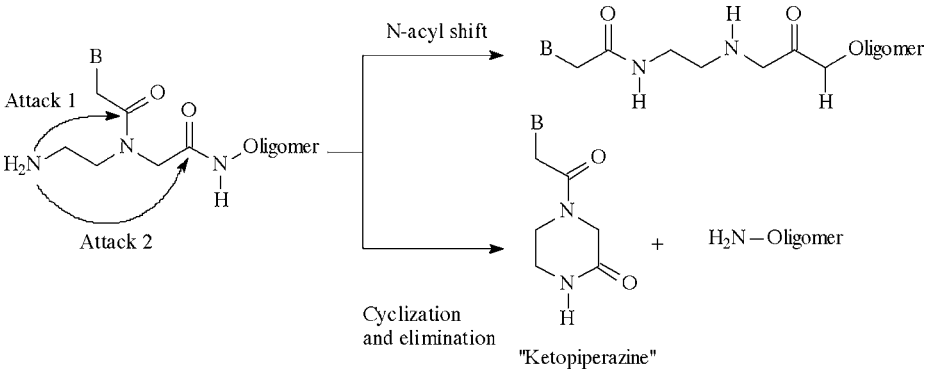

Fig. 3. Side reactions mediated by attack of N-terminal amino group *(2)*.

of the monomers when coupling solutions were made at concentrations greater than 0.05 *M*. When using *N,N*-diethylcyclohexylamine, solutions up to 0.2 *M* could be made without problems. The capping step in the synthesis cycle to cap unreacted amino groups, was initially carried out with acetic anhydride/DIEA in *N,N*-dimethylformamide/methylene chloride (DMF/DCM). This caused the formation of several impurities, which could be observed in reverse phase (RP)-HPLC, corresponding to acylated full-length products probably acylated at the Boc protected *N*-terminal. This was avoided when using "Rapoports reagent" (N^1-benzyloxycarbonyl-N^3-methylimidazolium triflate) in DMF (5%, w/v) that capped unreacted amino groups in 5 min without acylation of other sites on the peptide nucleic acids (PNA). After the final synthesis cycle, the oligomer was cleaved from the resin and deprotected using the low/high trifluoromethanesulfonic acid method developed by Tam et al.*(3)* (*see* **Fig. 4**) followed by precipitation in diethyl ether.

The oligomer was then purified using RP-HPLC and characterized using mass spectrometry. Koch et al. *(4)* also employed the Boc/Cbz monomers for PNA synthesis, but used different washing procedures as well as coupling and capping reagent (*see* **Fig. 5**).

The synthesis cycle outlined in **Fig. 5** gave higher yield and higher product purity than the cycle described by Christensen et al.

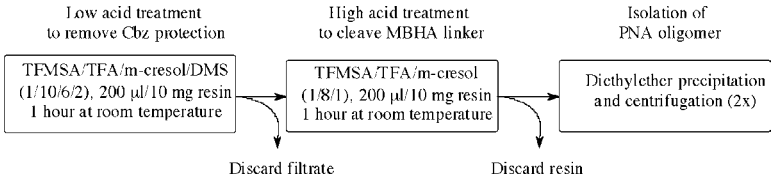

Fig. 4. Low high cleavage of PNA oligomer from resin ***(1)***.

(1). One of the reasons was the change of activation reagent from HBTU to HATU, which increased the average coupling yield from 98.5% to 99.4%. The change of capping reagent to acetic anhydride did not pose a problem, which several experiments clearly showed. The change of solvent from DMF/DCM to DCM gave better washing as the resin swelled better in pure methylene chloride than in the mixed solvent. The piperidine washing step after the capping also helped to increase the product yield and purity as the piperidine functioned as acetyl scavenger for remaining acetic anhydride thus preventing nucleobase acetylation.

2. Materials

1. Methylenechloride (DCM) (Labscan, HPLC grade).
2. Dimethylformamide (DMF) (Labscan, HPLC grade).
3. *N*-Methylpyrrolidone (NMP) (Labscan, HPLC grade).
4. Diisopropylethylamine (DIEA) (Aldrich, + 97%).
5. Methylmorpholine (NMM) (Aldrich, + 97%).
6. 2-(1-H-Benzotriazol-1-yl)-1,1,3,3-tetramethyluronium hexafluorophosphate (HBTU) (Novabiochem, +97%).
7. Trifluoroacetic acid (TFA) (Riedel de Häen, + 99%).
8. Anisole (Sigma, + 97%).
9. Trifluoromethanesulfonic acid (TFMSA) (Fluka, +99%).
10. m-Cresol (Aldrich, + 99%).
11. Acetic anhydride (Ac_2O) (Aldrich, + 97%).
12. Pyridine (Aldrich, + 97%).
13. 4-Methylbenzhydryl amine resin, 100–200 mesh, Hydrochloride salt: (MBHA resin) (Novabiochem).

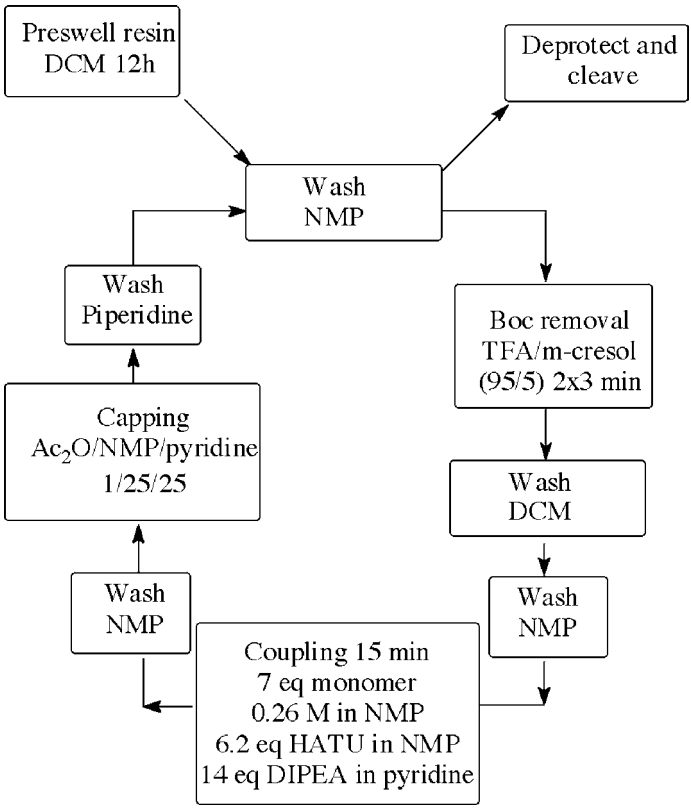

Fig. 5. Automated Boc/Cbz PNA synthesis as described by Koch et al. ***(4)***.

14. *N*-((*N*^{6}-Benzyloxycarbonyl)adenin-9-yl-acetyl)-*N*-(2-Boc-aminoethyl)glycine (Boc-PNA-A(Cbz) monomer) (+ 97%).
15. *N*-((*N*^{4}-Benzyloxycarbonyl)cytosin-1-yl-acetyl)-*N*-(2-Boc-aminoethyl)glycine (Boc-PNA-C(Cbz) monomer) (+ 97%)
16. *N*-((*N2*-Benzyloxycarbonyl)guanine-9-yl-acetyl)-*N*-(2-Boc-aminoethyl)glycine (Boc-PNA-G(Cbz) monomer) (+ 97%).
17. *N*-(2-Boc-aminoethyl)-*N*-(thymin-1-yl-acetyl)glycine (Boc-PNA-T monomer) (+ 97%).
18. Solutions: *see* **Table 1**.
19. Reagent A (Kaiser test): Mix 40 g phenol with10 mL water. Heat gently until all solid is dissolved. Dissolve 65 mg KCN in 100 mL

Table 1
Solutions

Solution	Stability	Special requirements
DIEA in DCM (5/95)	2 mo	None
TFA/DCM/Anisole (50/45/5)	2 wk	Light-sensitive
Pyridine/NMP/Acetic anhydride (50/48/2)	1 wk	Light-sensitive
NMM in NMP (0.5 *M*)	2 wk	None
HBTU in NMP (0.2 *M*)	2 wk	None
Boc-PNA-A(Cbz) monomer (0.26 *M*)	2 wk	None
Boc-PNA-C(Cbz) monomer (0.26 *M*)	2 wk	None
Boc-PNA-G(Cbz) monomer (0.26 *M*)	2 wk	None
Boc-PNA-T monomer (0.26 *M*)	2 wk	None

water. Dilute 2 mL KCN solution with pyridine to a total volume of 100 mL. Mix the phenol and KCN/pyridine solutions.

20. Reagent B (Kaiser test): Dissolve 2.5 g ninhydrine in 50 mL ethanol (99%).

3. Methods

3.1. Downloading

The MBHA resin was downloaded from the initial 0.4–0.8 mmol/g to 0.1 mmol/g to reduce problems with steric hindrance later in the synthesis. This was carried out as follows:

1. MBHA resin (5 g, 0.62 mmol/g) (*see* **Note 1**) was weighed into a 50 mL glass reactor, fitted with a sintered glass filter, (*see* **Fig. 1**), and swelled overnight in DCM.
2. DCM was removed by suction, and the resin was washed with DCM (2×3 min), DIEA/DCM (5/95, 2×3 min) and DMF (2×3 min, twice the volume of the resin) to remove fines (fragments from crushed resin beads, which later can clog the sintered glass filter). Extra DMF is removed from the top immediately after the resin has precipitated. Remaining DMF is removed by filtration.

3. PNA monomer (1 mmol, 2.0 eq) (*see* **Note 2**), was dissolved in NMP (14 mL) and NMM (0.22 mL, 4.0 eq) was added.
4. HBTU (0.38 g, 2.0 eq) was dissolved in NMP (7 mL) and added to the PNA monomer solution
5. Following 2 min preactivation, the mixture was added to the resin and allowed to react for 5 h under gentle shaking.
6. The resin was washed with DMF (2 × 1 min), DCM (4 × 1 min), DIEA/DCM (5/95, 2 × 3 min) and DCM (4 × 1 min).
7. The resin was capped overnight using Ac_2O/NMP/pyridine (2/48/50, 200 mL).
8. The resin was washed using DCM (5 × 1 min) and dried by suction for 2 min.
9. A qualitative Kaiser test must now be negative ***(5)***.

3.2. Qualitative Kaisertest

1. Take 2–5 mg lightly dried resin and add 3 drops reagent A and 2 drops reagent B.
2. Heat to 90°C for 2 min to develop. Blue = positive, Yellow = negative.
3. Finally, the resin loading can be determined as described by Dörner et al. ***(6)***.

3.3. Estimation of Level of First Residue Attachment (6)

1. Swell 50 mg of downloaded PNA resin in DCM overnight.
2. Deprotect resin using TFA/DCM/anisole (50/45/5) (2 × 3 min).
3. Wash with DCM, DMF, DIEA in DCM (5/95), DMF.
4. Couple Fmoc-Glycine to the resin using Fmoc-Gly-OH (29.7 mg dissolved in 200 µL NMP), HBTU (36 mg dissolved in 200 µL NMP) and NMM (22 µL). All three solutions were mixed and allowed to preactivate for one min, after which the mixture was added to the resin and allowed to couple for 30 min under gentle mixing.
5. Wash the resin using DMF, DCM.
6. Test for reaction completion using the Kaiser test as described in **Subheading 3.2.** If the test is positive, repeat coupling (*see* **step 4**). If the test is negative, continue as described in **Subheading 3.3., step 7**.
7. Take 3 × 10 mm matched silica UV cells.

8. Weigh dry Fmoc-Gly resin, prepared as described in **Subheading 3.3., steps 1–6** (approx 1 µmol with respect to Fmoc) into two of the cells. Dispense freshly prepared 20% piperidine in DMF (3 mL) into all three UV cells.
9. Agitate the resin mixture for 2–3 min.
10. Allow the resin beads to settle on the bottom of the UV cell.
11. Place the cells in a UV spectrophotometer using the cell that only contains piperidine as reference cell.
12. Read the absorbance at 290 nm and calculate the degree of first residue attachment from the following equation:

$$\text{Fmoc loading} = \text{PNA monomer loading (mmole/g)} = \frac{(Abs_{Sample} - Abs_{Ref})}{(1.65 \times \text{mg resin})}$$

13. After thorough drying the resin is now ready for use in PNA Synthesis.

3.4. PNA Synthesis

An overview of solid-phase PNA synthesis as described in this section can be seen in **Fig. 6**.

3.4.1. PNA Synthesis 5 (mmol Scale)

The solutions used in this section match the solutions described **Subheading 2., item 18 (Table 1)**.

1. Weigh 50 mg of downloaded PNA resin into a reaction vessel as shown in **Fig. 1**.
2. Swell the resin in DCM overnight while shaking the reaction vessel gently.
3. Remove Boc protection, using TFA/DCM/Anisole (50/45/5) (2 mL, 2 × 3 min).
4. Wash with DCM: Add DCM (2 mL), shake the reaction vessel gently for 30 s, remove DCM by suction. Repeat DCM wash.
5. Wash with DMF: Add DMF (2 mL), shake the reaction vessel gently for 30 s, remove DMF by suction. Repeat DMF wash.

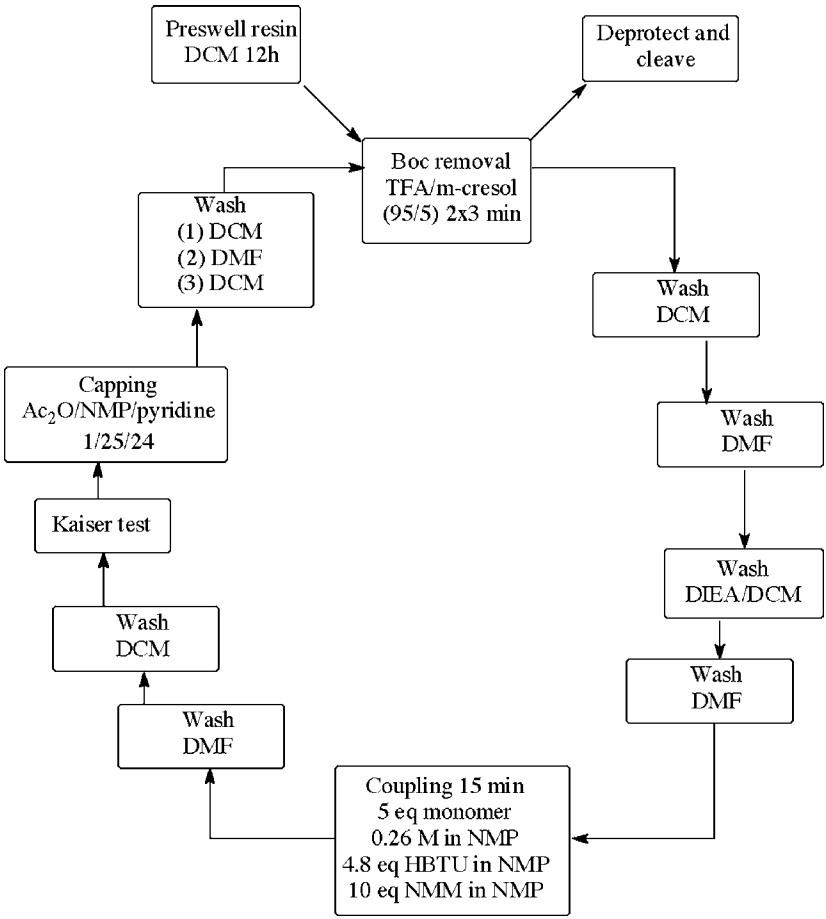

Fig. 6. Solid phase PNA synthesis, 5 μμol scale.

6. Wash with DIEA/DCM (5/95): Add DIEA/DCM (5/95), (2 mL), shake the reaction vessel gently for 30 s, remove DIEA/ DCM (5/95) by suction. Repeat DIEA/DCM (5/95) wash.
7. Wash with DMF: Add DMF (2 mL), shake the reaction vessel gently for 30 s, remove DMF by suction. Repeat DMF wash.
8. Perform Kaiser test. If negative, repeat from **step 3**, if positive continue to **step 9**.
9. Mix: PNA monomer solution (100 μL, 25 μmol, 5 eq), HBTU solution (100 μL, 24 μmol, 4.8 eq) and NMM in NMP (100 μL, 50 μmol, 10 eq) and allow to preactivate for 1 min.

10. Add the activated monomer solution to the resin and allow to couple for 15 min while shaking the reaction vessel gently.
11. Wash with DMF: Add DMF (2 mL), shake the reaction vessel gently for 30 s., remove DMF by suction. Repeat DMF wash.
12. Wash with DCM: Add DCM (2 mL), shake the reaction vessel gently for 30 s, remove DCM by suction. Repeat DCM wash.
13. Perform Kaiser test. If positive repeat from **step 6**; if negative continue to **step 14**.
14. Cap the resin using Ac_2O/NMP/pyridine (2/48/50, 2 mL).
15. Wash with DCM: Add DCM (2 mL), shake the reaction vessel gently for 30 s, remove DCM by suction. Repeat DCM wash.
16. Wash with DMF: Add DMF (2 mL), shake the reaction vessel gently for 30 s, remove DMF by suction. Repeat DMF wash.
17. Wash with DCM: Add DCM (2 mL), shake the reaction vessel gently for 30 s, remove DCM by suction. Repeat DCM wash.
18. Repeat from **step 3**.

After the last coupling, the resin was not capped, but only washed as described in **steps 11** and **12**. Following this, the PNA oligomer was cleaved from the resin as described in **Subheading 3.4.2.**

These reaction conditions are appropriate up to approx 1 g of resin. The amounts of monomer solution, coupling reagent, and base must of course be adjusted to suit the larger amount of resin.

3.4.2. Cleaving of PNA Oligomer from Solid Phase

The directions in this section are suitable for resin amounts of 50–100 mg. When using larger amounts of resin, these amounts must augmented accordingly.

1. Place the resin in a reaction vessel of an appropriate size, e.g., 3–4 mL, and wash with TFA/DCM/anisole (50/45/5, 30 s). Remove TFA solution by suction.
2. Add equal amounts of the two following solutions, both freshly prepared, and shake for 1 h:
   a. TFA/dimethylsulfide/m-cresol (1/3/1, 0.5 mL)
   b. TFA/TFMSA (9/1, 0.5 mL)
3. Remove the liquid by suction and wash, using: TFA/DCM/anisole (50/45/5, 1.0 mL, 30 s).

4. Add the following cleaving mixture and shake for 1.5 h: TFMSA/TFA/m-cresol (2/8/1, 1,0 mL)
5. Transfer the cleaving mixture to a test tube containing cold diethyl ether (8 mL), wash the resin using neat TFA (1 mL). Transfer the TFA to the rest of the cleaving mixture in the test tube.
6. Precipitate the PNA by centrifugation (20 min, 3.000 min^{-1}, –4°C).
7. Discard the diethyl ether, leaving the PNA oligomer in the test tube. Add fresh cold diethyl ether, resuspend the PNA oligomer in the diethyl ether and precipitate by centrifugation as described in **step 6**, then discard the diethyl ether.
8. Leave the PNA oligomer in the test tube overnight for remaining diethyl ether to evaporate. If the oligomer is to be dissolved the following day, for purification, water can be added at this stage (1–2 mL). The diethyl ether will evaporate overnight.

3.4.3. Purification of PNA Oligomer

PNA oligomers were purified using RP-HPLC. The amount of PNA oligomer resulting from a cleaving as described in **Subheading 3.4.2.** could be purified on a Vydac 218TP1022 (2.5 × 25 cm) protein and peptide C_{18} column mounted on a Gilson HPLC system with a Gilson dual-wavelength detector monitoring at 220 nm and 260 nm.

1. A buffer: 0.1% TFA in water.
2. B buffer: 0.1% TFA in acetonitrile.

Gradient: Flow (10 mL/min).

1. 10% B, T = 0 min.
2. 25% B, T = 25 min.
3. 35% B, T = 32 min.
4. 100% B, T = 44 min.
5. 100% B, T = 49 min.
6. 10% B, T = 50 min.
7. 10% B, T = 60 min.

Fractions active at 260 nm were collected and analyzed by analytical RP-HPLC. The pure fractions were characterized using Matrix-Assisted Laser Desorption-Time of Flight mass spectrometry

(MALDI-TOF MS), with sinapinic acid as matrix. The analysis was carried out on a HP G 2025A MALDI-TOF mass spectrometer using positive-mode ionization.

4. Notes

1. This protocol may be scaled down (or up) depending on demand.
2. Downloading is often performed with lysine as PNA oligomers are often synthesized with a C-terminal lysine amide.

References

1. Christensen, L., Epton, R., ed., Fitzpatrick, R., Gildea, B., Warren, B., and Coull, J. (1994) Improved synthesis, purification and characterization of PNA oligomers, in Innovation and Perspectives in Solid Phase Synthesis Peptides, Proteins and Nucleiec Acids Biological and Biomedical Applications. Mayflower Worldwide Limited, Birmingham, Oxford, UK. pp. 149–156.
2. Christensen, L., Fitzpatrick, R. Gildea, B., et al. (1995) Solid-phase synthesis of peptide nucleicAcids. *J. Pept. Sci.* **3,** 175–183.
3. Tam, J. P., Heath, W. F., and Merrifield, R. B. (1986) Mechanism for the removal of benzyl protecting groups in synthetic peptides by trifluoromethane sulfonic acid - trifluoroacetic acid-dimethyl sulfide. *J. Am. Chem. Soc.* **108,** 4242–5251.
4. Koch, T., Hansen, H. F., Andersen, P., et al. (1997) Improvements in automated PNA synthesis using Boc/Z monomers. *J. Pept. Res.* **49,** 80–88.
5. Sarin, V. K., Kent, S. B. H., Tam, J. P., and Merrifield, R. B. (1981) Quantitative monitoring of solid-phase peptide syntehsis by the ninhydrin raction. *Anal. Biochem.* **117,** 147–157.
6. Dörner, B. and White, P. (2000) Resin tests, in *Synthesis Notes* (Dörner, B. and White, P., eds.), Calbiochem-Novabiochem AG, Läufelingen, Sitzerland, pp. P4.

3

Synthesis of PNA-Peptide Conjugates

Satish Kumar Awasthi and Peter E. Nielsen

1. Introduction

Delivery of medium or high molecular-weight compounds (including large proteins) and drugs to cells has recently been achieved through conjugation to certain peptide carriers, such as penetratin, Tat-peptide, and MSP (**Table 1** and **ref**. ***1–15***).

Analogously, peptide nucleic acid (PNA) oligomers may be delivered to eukaryotic cells in culture ***(16–18)*** or to bacteria ***(19)*** as PNA-peptide conjugates. Such conjugates may be prepared by continuous peptide synthesis using either tBoc or Fmoc chemistry or by chemical conjugation in solution of purified PNA and purified peptide. Several types of conjugation chemistry are available and most utilize the specificity obtainable by the soft nucleophile, -SH, which is conveniently introduced in peptides or PNA via a cysteine. Alternatively, the redox chemistry of sulfur can be exploited to form disulfide-(S-S) bridged conjugates ***(16)***. These conjugates may, furthermore, have the advantage of being reduced in the reductive intercellular environment, thereby releasing the PNA cargo inside the cell.

Such conjugation chemistry includes the formation of thioethers via addition to electrophilic substrates like maleimides or by nucleophilic substitution to iodoacetamides. In this chapter, we present

From: *Methods in Molecular Biology, vol. 208: Peptide Nucleic Acids: Methods and Protocols*
Edited by: P. E. Nielsen © Humana Press Inc., Totowa, NJ

Table 1
Cell-Penetrating Peptides

Peptide	Sequence	Length	References
Penetratin	RQIKIWFQNRRMKWKK	16	***(1)***
Tat	GRKKRRQRRRPPQ	13	***(2)***
Transportan	GWTLNSAGYLLGKINLKALAALAKKIL	27	***(3,4)***
TP10	AGYLLGKINLKALAALAKKIL	21	***(4)***
NLS	PKKKRKV	7	***(5–7)***
MPG	GALFLGFLGAAGSTMGAWSQPKSKRKV	27	***(5,8)***
Hel	KLLKLLLKLWLKLLKLLL	18	***(9,10)***
JTS1	GLFEALLELLESLWLLEA	18	***(11)***
LARL	$(LARL)_6$	24	***(9)***
KALA	WEAKLAKALAKALAKHLAKALAKALKACEA	30	***(12)***
Arg	$(Arg)_9$	79	***(13)***
GALA	WEAALAEALAEALAEHLAEALAEALEALAA	30	***(14)***
AMP	KLALKALKALKAALKLA	17	***(15)***

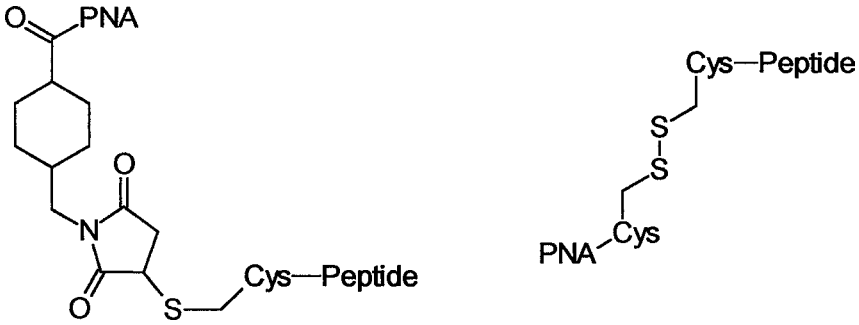

Fig. 1. Chemical structure of the two different coupling linkers, maleimide and disulfide, used to conjugate a PNA to a peptide peptide. In case of the maleimide coupling, the maleimide derivative (at the N-terminal) of the PNA is reacted with a peptide containing one cysteine (usually at the N-terminal), and in case of the disulfide coupling both the peptide and the PNA contains an N-terminal cysteine.

procedures for disulfide-bridge conjugation of a Cys-peptide to a Cys-PNA and a thioether coupling of a Cys-peptide to a maleimide derivatized PNA oligomer **(Fig. 1)**.

2. Materials

1. Succinimidyl-4-[N-maleimidomethyl]-cyclohexan-1-carboxylate (SMCC).
2. Fmoc amino acids.
3. 2-(1-H-benzotriazole-1-yl)-1,1,3,3-tetramethyluronium hexafluorophosphate (HBTU).
4. Boc PNA monomers in which exocyclic amino groups (A, C, G) are protected by the Benzoloxycarbonyl group (Z).
5. Trifluoroacetic acid (TFA).
6. Diisopropylethyl amine (DIEA).
7. Anisol.
8. m-cresol.
9. N-methylpyrrolidone (NMP).
10. Trifluoromethane sulphonic acid (TFMSA).
11. 2,4,6-Collidine.
12. Dimethylformamide (DMF).

13. Dichloromethane (DCM).
14. Acetonitrile, high-performance liquid chromatography (HPLC) grade.
15. Acetic anhydride.
16. PAL-PEG-PS resin.
17. MBHA resin.

3. Methods

3.1. PNA Synthesis

The PNA synthesis is carried out as reported elsewhere (***20***; *see* also Chapter 2). Fluorescein can be incorporated at N-terminal via a fluorescein-lysine derivative in which the fluorescein is attached to side chain amino group (K_{Fluo}) ***(21)***. 8-Amino-2,4-dioxaoctanoic acid linkers (eg1 monomer) can be incorporated at the N-terminal of the PNAs in order to increase the solubility of the resulting PNAs in organic as well as in aqueous solvents. Finally, a cysteine is incorporated at N-terminal of the PNA when the PNA are to be conjugated by disulfide coupling with the peptides.

The HPLC analysis is performed on Delta Pak C_{18} column (5 μ*M*, 3.9 × 150mm) at ambient temperature with the flow rate of 1 mL/min using an acetonitrile/water (containing 0.1% TFA) gradient and using dual UV detection (260 and 230nm). The purification was done on a C_{18} (Delta Pak, Waters, 15 μ*M*, 19 × 300 mm) with 8 mL/min flow rate.

3.2. Peptide Synthesis

The peptides were synthesized by standard procedure. Briefly, the peptides derived from antennapedia (Ac-CRQIKKWFQ NRRMKWKKNH_2) (pAnt, penetratin), and Tat (Ac-CGRKKRR QRRRPPQ-NH_2) (pTat), were synthesized by Fmoc chemistry on a Pal resin. The peptides were acetylated on the resin with 5% acetic anhydride in dimethylformamide for 5 min. The peptide were cleaved from resin with TFA:anisol:ethanedithiol (94:5:1, v/v) at room temperature for 4 h. The peptides were precipitated with dry

cold diethyl ether and washed with diethyl ether several times, and were purified by reverse-phase (RP)-HPLC as described earlier. The homogeneity of the peptides (>95%) were confirmed by analytical HPLC, and their identity was ascertained by mass spectrometry Matrix-Assisted Laser Desorption-Time of Flight (MALDI-TOFMS).

3.3. PNA-SMCC-Peptide Conjugation

1. Dissolve PNA (0.4 μmole, ca. 2 mg) in 2 mL NMP: dimethyl sulfoxide (DMSO) (7:3, v/v) with 15 min vigorous stirring (*see* **Note 1**).
2. Add Succinimidyl-4-[N-maleimidomethyl]-cyclohexan-1-carboxylate, (SMCC) (1 mg, 2.99 μmole) dissolved in 20 μL of NMP to the PNA solution followed by addition of DIEA (16 μL) and kept at room temperature for 2.5 h with gentle shaking (*see* **Note 2**).
3. Add excess dry cold diethyl ether to precipitate the PNA-maleimide conjugate.
4. Wash the precipitate thoroughly with ether containing 10% NMP in order to remove excess SMCC.
5. Dry the PNA-maleimide conjugate under nitrogen and characterize by MALDI-TOF mass spectrometry prior to further reaction.
6. Dissolve the peptide (*see* **Note 3**) (5 mg, 2.09 μmole) in 1.5 mL of 0.1 *M* ammonium bicarbonate solution (NH_4HCO_3).
7. Add DTT (1.54 mg, 9.9 μmole) dissolved in 100 μL water to the peptide solution.
8. Leave the reaction mixture at room temperature under nitrogen for 3 h.
9. Lower the pH to 7.0 by adding acetic acid.
10. Load the reaction mixture on a sephadex G-25 gel-filtration column pre-equilibrated with 10 m*M* Tris-HCl buffer, pH 7.4, and elute with the same buffer.
11. Immediately mix the recovered peptide (2 mL) with the PNA maleimide conjugate predissolved in DMF (200 μL), and allow the reaction to proceed over night (*see* **Note 4**).
12. The product was purified by HPLC and characterized by MALDI TOF (*see* **Notes 5** and **6**).

3.4. PNA-S-S- Peptide Conjugation

1. Dissolve the peptide (*see* **Note 3**) (1.07 μmole, ca, 2 mg) and dithiothreitol (DTT) (1 mg, 6.4 μmol) in 100 μL 0.1 *M* NH_4HCO_3 and keep for 2 h at room temperature.

2. Add dipyridyl disulphide (11 mg, 0.05 mmole) in 100 μL DMF and keep for further 2 h at room temperature.
3. Pass the reaction mixture through a Sephadex-25 gel column pre-equilibrated with 10 m*M* Tris-HCl buffer, pH 7.4, and elute with the same buffer.
4. React the recovered peptide solution (2 mL) immediately with the Cys-PNA (2 mg, 0.4 μmole) for 3 h.
5. Analyze and purify the product by HPLC and characterize by MALDO-TOF mass spectrometry (*see* **Notes 7** and **8**).

All compounds were characterized by mass spectrometry. The masses of PNA, peptide, and PNA-peptide conjugates were analyzed on Kratos MALDI-II TOF mass spectrometer by using the 3,5 dimethoxy 4-hydroxy cinnamic acid as matrix. **Figure 2** shows representative examples of HPLC and mass analysis of some of the peptide-PNA conjugates.

We used PNA extinction coefficient for the concentration determination of the PNA-peptide conjugates. The conjugates were stored at –20°C.

4. Notes

1. PNA solubility in organic solvent can be a problem. The ratio of NMP and DMF for dissolving PNA sequence will vary depending on the specific sequence of the PNA.
2. HPLC analysis showed complete conversion of PNA into PNA-maleimide conjugate.
3. pAnt-S-S-PNA and Tat-S-S-PNA conjugates were prepared in this way.
4. HPLC analysis showed quantitative conversion of the PNA.
5. The coupling yield was about 40% based on HPLC analysis results.
6. Although the protocol represents a general procedure for making PNA-peptide conjugate using bi-functional reagents, PNA solubility in organic solvent can be a problem. The ratio of NMP and DMF for dissolving PNA sequence will vary depending on the specific sequence of the PNA.
7. Furthermore, DTT treatment of the purified conjugate gave the free PNA oligomer and the peptide as major components as analyzed by HPLC and confirmed by mass spectrometry.
8. The yield was more than 70% based on HPLC analysis results.

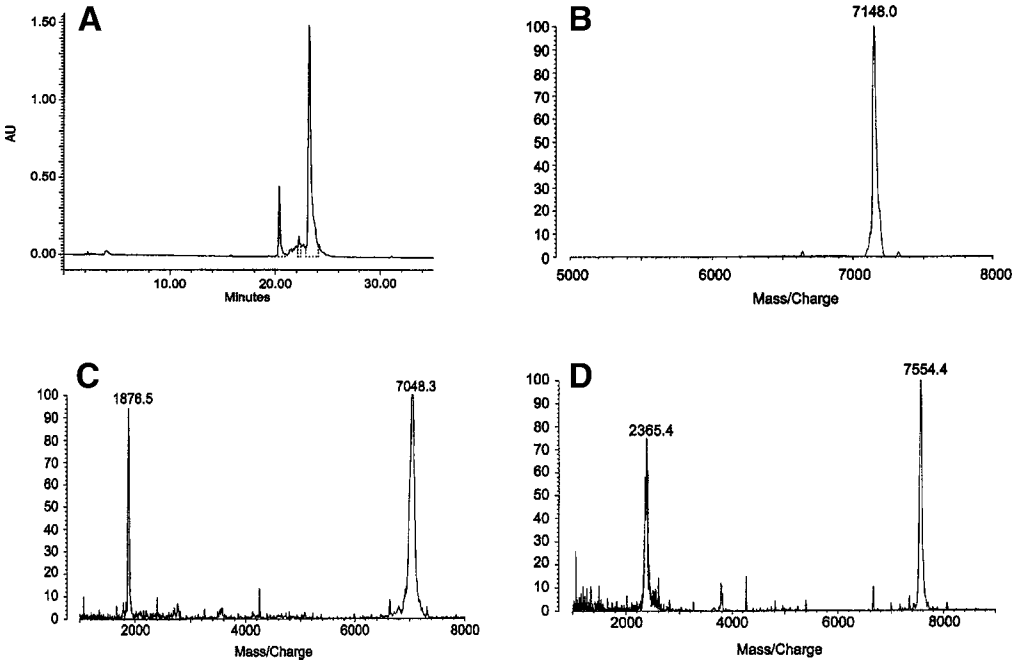

Fig. 2. HPLC chromatogram (**A**) and MALDI-TOF mass spectra (**B–D**) of PNA-peptide conjugates. (A) and (B) H_2N-QPPRRRQRRKKRG-Cys-S-S-Cys-eg1-eg1-eg1-eg1-K_{Fluo}–$GGT_{Lys}GCT_{Lys}CACT_{Lys}GC$ GG-NH_2; (C) H_2N-QPPRRRQRRKKRG-Cys-S-Maleimide-eg1-eg1-eg1-eg1-K_{Fluo}–GGTGCTCACTGC GG-NH_2. (D)) H_2N-KKWKMRRNQFWIKIQR-Cys-S-Maleimide-eg1-eg1-eg1-eg1-K_{Fluo}–GGTGCTCACTGCGG-NH_2.

References

1. Derossi, D., Chassaing, G., Prochiantz, A. (1998) Trojan peptides: the penetratin system for intracellular delivery. *Trends Cell. Biol.* **8,** 84–87.
2. Vives, E., Brodin, P., and Lebleu, B. (1997) A truncated HIV-1 Tat protein basic domain rapidly translocates through the plasma membrane and accumulates in the cell nucleus. *J. Biol. Chem.* **272,**16,010–16,017.
3. Lindgren, M., Gallet, X., Soomets, U., Hallbrink, M., Brakenhielm, E., Pooga, M., et al. (2000) Translocation properties of novel cell penetrating transportan and penetratin analogues. *Bioconjug. Chem.* **11,** 619–626.
4. Soomets, U., Lindgren, M., Gallet, X., Hallbrink, M., Elmquist, A., Balaspiri, L., et al. (2000) Deletion analogues of transportan. *Biochim. Biophys. Acta.* **1467,** 165–176.
5. Morris, M. C., Vidal, P., Chaloin, L., Heitz, F., and Divita, G. (1997) A new peptide vector for efficient delivery of oligonucleotide into nontransformed mammalian cells. *Nucleic Acids Res.* **25,** 2730–2736.
6. Goldfarb, D. S., Gariepy, J., Schoolnik, G., and Kornberg, R. D. (1986) Synthetic peptides as nuclear localization signals. *Nature* **322,** 614–644.
7. Chaloin, L., Vidal, P., Heitz, A., Nguyen Van Mau, N., Mery, J., Divita, G., and Heitz, F. (1997) Conformations of primary amphipathic carrier peptides in membrane mimicking environments. *Biochemistry* **36,** 11,179–11,187.
8. Morris, M. C., Chaloin, L., Mery, J., Heitz, F., and Divita, G. (1999) A novel potent strategy for gene delivery using a single peptide vector as carrier. *Nucleic Acids Res.* **27,** 3510–3517.
9. Niidome, T., Ohmori, N., Ichinose, A., Wada, A., Mihara, H., Harayama, T., and Aoyagi, H. (1997) Binding of cationic α-helical peptides to plasmid DNA and their gene transfer abilities into cells. *J. Biol. Chem.* **272,** 15,307–15,312.
10. Niidome, T., Takaji, K., Urakawa, M., Ohmori, N., Wada, A., Harayama, T., and Aoyagi, H. (1999) Chain length of cationic α-helical peptide sufficient for gene delivery into cells. *Bioconjug. Chem.* **10,** 115–120.

11. Gottschalk, S., Sparrow, J. T., Hauer, J., Mims, M. P., Leland, F. E., Woo, S. L., and Smith, L. C. (1996) A novel DNA–peptide complex for efficient gene transfer and expression in mammalian cells. *Gene Ther.* **3,** 448–457.
12. Wyman, T. B., Nicol, F., Zelphati, O., Scaria, P. V., Plank, C., and Szoka, F. C., Jr., (1997) Design, synthesis and characterization of a cationic peptide that binds to nucleic acids and permeabilizes bilayers. *Biochemistry* **27,** 3008–3017.
13. Wender, P. A., Mitchell, D. J., Pattabiraman, K., Pelkey, E. T., Steinman, L., and Rothbard, J. B. (2000) The design, synthesis, and evaluation of molecules that enable or enhance cellular uptake: peptoid molecular transporters. *Proc. Natl. Acad. Sci. USA* **97,** 13,003–13,008.
14. Parente, R. A., Nadeasdi, L., Subabrao, N. K., and Szoka, F. C., Jr. (1990) Association of a pH-sensitive peptide with membrane vesicles: role of amino-acid sequence. *Biochemistry* **29**, 8713–8719.
15. Oehlke, J., Scheller, A., Wiesner, B., et al. (1998) Cellular uptake of an a-helical amphipathic model peptide with the potential to deliver polar compounds into the cell interior non-endocytically. *Biochim. Biophys. Acta* **1414,** 127–139.
16. Pooga, M., Soomets, U., Hällbrink, M., Valkna, A., Saar, K., Rezaei, K., et al. (1998) Cell penetrating PNA constructs regulate galanin receptor levels and modify pain transmission *in vivo. Nat. Biotechnol.* **16,** 857–861.
17. Aldrian-Herrada, G., Desarménien, M.G., Orcel, H., Boissin-Agasse, L., Méry, J., Brugidou, J., and Rabié, A. (1998) A peptide nucleic acid (PNA) is more rapidly internalized in cultured neurons when coupled to a *retro-inverso* delivery peptide. The antisense activity depresses the target mRNA and protein in magnocellular oxytocin neurons. *Nucleic Acids Res.* **26,** 4910–4916.
18. Cutrona, G., Carpaneto, E. M., Ulivi, M., Roncella, S., Landt, O., Ferrarini, M., et al. (2000) Effects in live cells of a c-myc anti-gene PNA linked to a nuclear localization signal. *Nature Biotechnol.* **18,** 300–303.
19. Good, L., Awasthi, S. K., Dryselius, R., Larsson, O., and Nielsen, P. E. (2001) Bactericidal antisense effects of peptide-PNA conjugates. *Nature Biotechnol.* **19,** 360–364.

20. Christensen, L., Fitzpatrick, R., Gildea, B., Petersen, K. H., Hansen, H. F., Koch, T., et al. (1995) Solid-phase synthesis of peptide nucleic acids. *J. Pept. Sci.* **1,** 185–183.
21. Lohse, J., Nielsen, P. E., Harrit, N., and Dahl, O. (1997) Fluorescein-conjugated lysine monomers for solid phase synthesis of fluorescent peptides. *Bioconjug. Chem.* **8,** 503–509.

4

Parallel Synthesis of PNA-Peptide Conjugate Libraries

Satish Kumar Awasthi and Peter E. Nielsen

1. Introduction

For a large variety of studies, it would be advantageous to be able to synthesize a library of individual peptide nucleic acid (PNA) oligomers in parallel. This is especially useful for screening target positions for antisense reagents along the mRNA (gene walk) as optimal target sites have to be determined emperically to a very large degree. Furthermore, because of the very limited cellular uptake of PNA oligomers in both eukaryotic and bacterial cells and the finding that conjugation of certain relatively simple peptides to the PNA may greatly improve the uptake, it is also of interest to be able to synthesize libraries of PNA-peptide conjugate (*see* Chapter 3). Methods have previously been described for the synthesis of PNA parallel libraries on membranes using Fmoc protection chemistry ***(1,2)***. This chapter describes a protocol for semi-automated parallel synthesis of up to 96-PNA-peptide conjugates (**Table 1**) at 0.5 μmole-scale ***(3)***.

From: *Methods in Molecular Biology, vol. 208: Peptide Nucleic Acids: Methods and Protocols*
Edited by: P. E. Nielsen © Humana Press Inc., Totowa, NJ

Table 1
Examples of Various PNAs and PNA Conjugates Synthesized by the Parallel Manifold Approach

Sequence	Target site
H-GRKKRRQRRRPPQ-eg1-ATCTACTGGCTCC AT-NH_2	tat initiator, HIV-1
H-GRKKRRQRRRPPQ-eg1-CAAGCTTTATTGAGG-NH_2	Poly A signal, HIV-1
H-AAGCCCTCCCCG-NH_2	ras oncogene
H-AAGCCCTCCCC-NH_2	ras oncogene
H-AAGCCCTCCC-NH_2	ras oncogene
Ada-AAGCCCTCCCCG-NH_2	ras oncogene
Ada-AAGCCCTCCCC-NH_2	ras oncogene
Ada-AAGCCCTCCC-NH_2	ras oncogene
H-CCACCAGCACCAT-NH_2	ras oncogene
H-CCCACCAGCACCA-NH_2	ras oncogene
H-CCCCACCAGCACC-NH_2	ras oncogene
Ada-CCACCAGCACCAT-NH_2	ras oncogene
Ada-CCCACCAGCACCA-NH_2	ras oncogene
Ada-CCCCACCAGCACC-NH_2	ras oncogene
H-PKKKRKV-eg1-GGCCGCCAGCTCCAT-NH_2	Her 2 gene
H- PKKKRKV-eg1-GTCTTTATTTCATCTT-NH_2	Her-2 gene
H-KFFKFFKFFK-eg1-CTCATACTCT-NH_2	acpP (*E. coli*)

2. Materials

1. Boc PNA monomers were obtained from Perseptive Biosystem. In Boc monomer, the exocyclic amino groups (A, C, G) were protected by benzoloxycarbonyl group (Z). PNA stock solution in NMP or DMF: 0.24 *M* (G monomer in dimethyl sulfoxide [DMSO]).
2. MBHA resin: 5 mg, loading 0.1 mmol/g (0.5 µmole scale).
3. ABIMED auto-spot robot ASP 222.
4. A 96-well (100 µL per well) filter manifold was provided by ABIMED, Germany.
5. Boc amino acids.
6. HBTU (2-(1-H-benzotriazole-1-yl)-1,1,3,3-tetramethyluronium hexafluorophosphate): 0.23 *M* in DMF.
7. Trifluoroacetic acid (TFA).
8. Diisopropylethyl amine (DIEA): 0.46 *M* in DMF.
9. Anisol

10. m-cresol.
11. N-methylpyrrolidone (NMP).
12. Trifluoromethane sulphonic acid (TFMSA),
13. 2,4,6-Collidine.
14. Dimethylformamide (DMF).
15. Acetonitrile, HPLC grade.
16. Capping reagent: DMF/acetic anhydride/collidine : 8:1:1.
17. Piperidine washing: 5% piperidine DMF.
18. Dichloromethane (DCM).

3. Methods

Steps involved in a single PNA synthesis cycle (*see* **Note 1**):

1. Swell the down-loaded resin (5 mg, 0.5 μmole) in DCM overnight.
2. Deprotect the Boc-groups: 50 μL TFA (3 × 4 min for the first time, subsequently 2 × 4 min).
3. Wash with DMF/dichloromethane (1:1): 3 × 100 μL.
4. Wash with DMF: 100 μL.
5. Wash with pyridine: 2 × 100 μL.
6. Preactivate PNA monomers: Mix: 10 μL PNA monomer +10 μL HBTU+10 μL DIEA from stock solution, leave 1 min at room temperature (RT) (*see* **Note 2**).
7. Coupling. Add: 30 μL (10 μL PNA monomer + 10 μL HBTU + 10 μL DIEA preactivated monomer in each well).
8. Leave 30 min at RT.
9. Wash resin with DMF: 2 × 100 μL.
10. Repeat coupling: **steps 6–9**.
11. Wash with DMF/dichloromethane (1:1): 3 × 100 μL.
12. Add capping reagent (50 μL) (2 min).
13. Wash with DMF/dichloromethane (1:1): 3 × 100 μL.
11. Wash with piperidine:100 μL (4 min).
12. Wash with DMF: 3 × 100 μL.
14. Wash with DMF/dichloromethane: 2 × 100 μL.
15. Repeat from **step 2**.
16. At the and of synthesis, cleave the PNAs from the resin by the low/high TFMSA procedure and precipitate with diethyl ether as described in Chapter 2 (*see* **Note 3**).

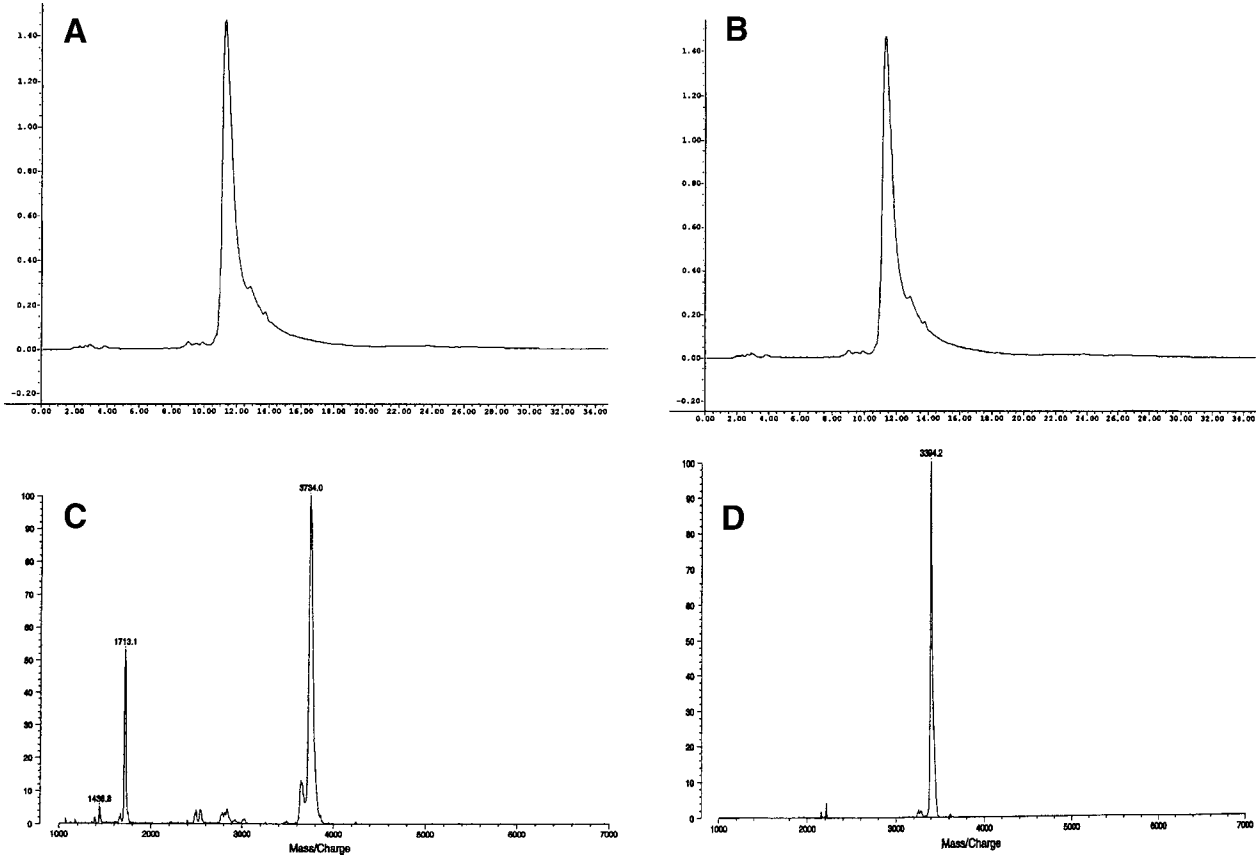

Fig. 1. HPLC analysis of crude **(A)** PNA-peptide (H-PKKKRKV-eg1-TGTACGTCACAACTA-NH_2) and **(B)** PNA (H-CCCACCAGCACCA—NH_2) as well as **(C)** and **(D)** MALDI-TOF mass spectra of these two PNAs synthesized semi-automatically the on multi-well ABIMED robot by Boc chemistry. The found (and calculated) masses for these two PNAs are 3734 (3736) and 3394 (3393), respectively.

4. Notes

1. Only the coupling step (**step 7**) (i.e., the dispensing of all the different activated monomers) is performed on the robot; all deprotection and washing steps are performed manually with the manifold off the robot.
2. Activation of the next monomer was started just before the needle finished delivery of first monomer and the robot started washing the needle. It takes approx 1 min and it can be adjusted.
3. This protocol yields PNA oligomers (10–5-mers) and PNA-peptide conjugates (NLS or Tat peptides) in sufficient amounts (ca. 2 mg) for biological screenings, and of high purity (>90%; *see* **Fig. 1**).

References

1. Weiler, J., Gausepohl, H., Hauser, N., Jensen, O. N., and Hoheisel, J. D. (1997) Hybridisation based DNA screening on peptide nucleic acid (PNA) oligomer arrays. *Nucleic Acids Res.* (1997) **25,** 2792–2799.
2. Matysiak, S., Reuthner, F., Hoheisel, J. D. (2000) Automating parallel peptide synthesis for the production of PNA library arrays. *BioTechniques* **31,** 896–904.
3. Awasthi, S. K., and Nielsen, P. E. (2002) Parallel synthesis of PNA-peptide conjugate libraries. *Comb. Chem. High Through. Screen.* **5,** 251–258.

5

Thermodynamics of PNA Interactions with DNA and RNA

Tommi Ratilainen and Bengt Nordén

1. Introduction

Thermodynamic properties of peptide nucleic acids (PNA) and their complexes with nucleic acids have attracted increasing attention. More detailed thermodynamic information is desired in order to understand and improve the behavior of PNAs in various contexts, e.g., in the design of polymerase chain reaction (PCR) probes and potentially for the use of PNA in therapeutics. The ultimate goal is to predict the thermodynamic properties of PNA-nucleic acid complexes of any sequence. For DNA and RNA thermodynamics, this has been achieved for relatively short (10–30 base pairs) double-stranded complexes (duplexes). These studies have yielded nearest neighbor parameters ($\Delta H°$ and $\Delta S°$) for all possible combinations of base pairs in DNA and RNA ***(1)***, as well as for single mismatches in DNA ***(2)***.

Although numerous PNA studies contain reports of thermal stability of the complexes, only a few of those report thermodynamic parameters, i.e., $\Delta H°$ and $\Delta S°$ ***(3–6)***. The majority of the studies have only given the melting temperature, T_m of the complex ***(7,8)***. For a duplex, the T_m is defined as the temperature at which equal

From: *Methods in Molecular Biology, vol. 208: Peptide Nucleic Acids: Methods and Protocols*
Edited by: P. E. Nielsen © Humana Press Inc., Totowa, NJ

amounts of base-paired duplex and unpaired single strands are in equilibrium. The T_m has been found to correlate well with the thermodynamic equilibrium constant, K, for such a two-state equilibirum and thus is generally a good measure of duplex stability ***(6,9)***.

The main technique used for determination of T_m, as well as for determining enthalpies and entropies of complex association/dissociation for PNA complexes, has been monitoring of changes in UV absorption at about 260 nm as a function of temperature. The resulting profile of absorbance vs temperature is called an equilibrium melting curve because it reflects a transition from an ordered, native structure to a disordered denatured state (or vice versa) analogous to a phase transition. From a van't Hoff analysis of the melting curve, it is possible to calculate T_m, $\Delta H°$ and $\Delta S°$ ***(10,11)***.

The main purpose of this chapter is to give a description of how to use the absorbance melting method mentioned previously for thermodynamic studies of PNA complexes. In addition, two alternative methods based on calorimetric characterization (isothermal titration calorimetry ITC, and differential scanning calorimetry DSC) of the binding will also be described. Finally, a statistical consideration will be made of the drug distribution over a large DNA (genome) and the thermodynamics of strategic targeting of a particular gene.

2. Materials

2.1. General Aspects of Sample Preparation

As for any type of a biophysical experiment, a fundamental factor for good performance is that the solubility of PNA is high enough in order to avoid complications like aggregation. For thermodynamic studies using the absorbance melting curves, the minimum concentrations of oligomers are usually in the μM range. For DNA and RNA, it is normally not a problem to attain such concentrations in aqueous solutions. However, for certain sequences of PNA, especially those with high guanine content, it might be a problem reaching the desired concentration ***(12)***.

PNAs have been modified with various charged amino acids to improve their solubility, with the most common modification being addition of a lysine residue to the carboxy (C) terminal of the peptide backbone. A terminal lysine amide, which is doubly charged at neutral pH, improves the solubility significantly, as do some other polar moieties ***(13)***. The solubility can also be altered undeliberately by labeling of the PNA. For example, PNAs labeled with the dye rhodamine, which is uncharged at neutral pH, are much less soluble than PNAs labeled with fluorescein, which is in mono- and di-anionic form ***(14)***.

The most common method to determine concentrations of PNA is by spectrophotometry. The concentration is calculated from the Beer-Lambert law, $A = \varepsilon cl$, where A is the absorbance, ε is the extinction coefficient [$M^{-1}cm^{-1}$], c is the concentration [M] and, l is the path length [cm]. A complication when working with oligomers of nucleic acids and PNAs is that in most cases the extinction coefficient is not known *a priori* but has to be determined or estimated somehow. Puglisi and Tinoco described an approximate method for calculating the extinction coefficient at 25°C for DNA and RNA oligomers ***(11)***. The method is based on the sum of the extinction coefficients of the constituent nucleosides but with corrections for the hypochromicity due to stacking interactions between neighboring bases. In principle, this method can be applied also to PNAs although it is expected to be less accurate than for nucleic acids due to the different stacking patterns in PNA. Another approximate approach is to denature and measure absorbance of the single strands by heating (80–90°C) and then use the sum of the extinction coefficients (at 25°C) of the corresponding (unstacked) DNA nucleosides ***(15)*** as the PNA extinction coefficient.

Whenever performing studies involving measurements at different temperatures, one must be aware of the effect of temperature on pH of the sample and solvent. Normally, some type of buffer is used as solvent and a critical parameter is the temperature coefficient (dpH/dT) of the buffer which should be as low as possible. A well-behaved buffer in this respect is phosphate buffer with a relatively low dpH/dT = –0.0028/°C ***(15)***.

2.2. Absorbance Melting Curves

The sample is prepared from the appropriate single and/or double strands at high temperature (80–90°C) and then allowed to equilibrate to room temperature. The sample should then be transferred to a suitable quartz cell followed by degassing in order to avoid oxygen-bubble formation at elevated temperatures. Degassing can be easily achieved by purging with an inert gas (N_2 or Ar) for about 10 min or by subjecting the sample to moderate vacuum for about 15 min while stirring it swiftly with a magnet.

After degassing, the cell is sealed and placed into the cell holder of the spectrophotometer. Ideally, the spectrophotometer has a programmable thermostated cell holder allowing precise control of the cell temperature and the heating rate. For melting processes with relatively fast kinetics, such as melting of short duplexes, a heating rate of 0.5°C/min is appropriate. However, in order to avoid errors in cases in which kinetics could be slow, lower heating rates should be tested until no change in the melting curve is observed. Data acquisition should be made typically every 0.5°C.

Often, measurements are performed at only a single wavelength, 260 nm. However, the temperature variation of the refractive index of solvent will effect the base line (via scattering of solution and reflections at cell windows). Therefore, baseline correction must be carried out in order to guarantee a correct absorbance. Furthermore, the absorbance values should not be too low (>0.05) or too high (<2) to obtain satisfactory signal-to-noise ratio.

2.3. Differential Scanning Calorimetry

A DSC experiment is performed as a melting curve experiment, i.e., the solution of interest is heated (or cooled) while monitoring a parameter giving information of the transition from one state to another. In the DSC instrument, it is the excess specific heat C_p of a system that is measured in relation to that of the solvent (buffer). The raw data of a DSC instrument is the (electrical) power required to keep the sample cell at the same temperature as a reference cell, during a constant temperature scan rate of the order of 1°C/min.

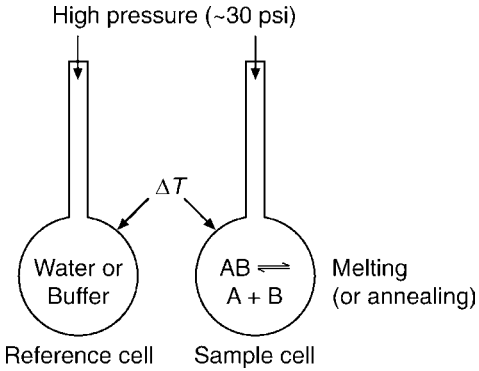

Fig. 1. Schematic picture of the differential scanning calorimeter (DSC). The electrical power (CFB, cell feedback) to keep $\Delta T \approx 0$ is recorded and converted to C_p. The reaction depicted is the (bimolecular) PNA–DNA hybridization.

Modern DSC instruments have sample volumes around 0.5 mL and operate under relatively high pressure (typically 30 psi) enabling melting experiments run up to 130°C. (*see* **Fig. 1**)

Because the DSC measurement resembles the absorbance melting curve method to a large extent, sample preparation can be done accordingly. Degassing of samples is important to avoid bubble-formation (leading to spikes in the response), even though the DSC experiment is performed at high pressure.

2.4. Isothermal Titration Calorimetry

This technique measures at a fixed temperature the released or absorbed heat of reaction, ΔH, as a ligand is titrated into a solution containing the ligand-binding molecule (reactant). The heat of reaction is calculated from the electrical power needed to compensate the temperature change in the sample cell relative to a reference cell containing only buffer. As more ligand is added, the observed heat decreases until saturation of all available binding sites has been reached.

Modern ITC equipment can readily detect relatively small heats of reaction (power 0.1 μcal/s) which allows study of dilute samples

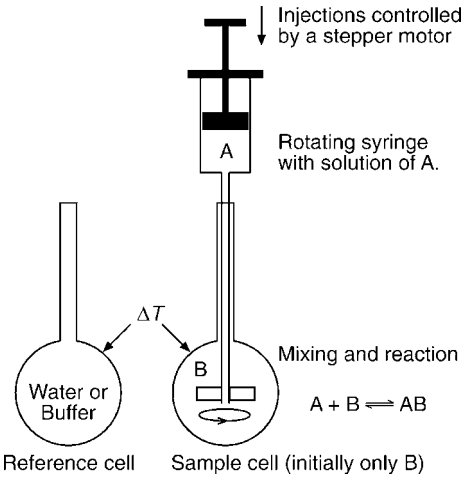

Fig. 2. Schematic picture of the isothermal titration calorimeter (ITC). The electrical power (CFB, cell feed back) to keep $\Delta T \approx 0$ is recorded.

of about 5 μ*M* concentration. For the PNA–DNA hybridization reaction discussed below (*see* **Subheading 3.1.1.**, a typical experiment consists of about 20–30 injections of 4–5 μL, at least 5 min apart from each other, of the ligand solution (about 0.1 m*M*) into the reactant solution (5 μ*M* in 1 mL cell volume). It is integral for a reliable result that the injection syringe can be controlled precisely and that the sample solution is well-stirred. In one of the commercially available instruments, the MicroCal ITC MC-2 system, this is accomplished by a stepper motor controlling a syringe which discharges itself into a paddle-shaped needle rotating at 400 rpm. (*see* **Fig. 2**).

A fundamental difference when preparing for an ITC experiment is that the strands are to be kept separate until titrated during the actual experiment. Degassing is crucial, again to avoid bubble-formation that might lead to spikes in the signal. In contrast to melting curves and DSC, which could be scanned up and down an arbitrarily number of times, ITC is a single-shot experiment consuming the reactants.

3. Methods

3.1. Analysis of Melting Curves

Detailed discussions of how to analyze absorbance melting curves are given in the excellent reviews of Marky and Breslauer ***(10)*** and of Puglisi and Tinoco ***(11)***. Instead of attempting a comprehensive discussion of melting-curve analysis, we will, therefore, address the limitations of the method and what information can be extracted.

To obtain quantitative thermodynamic information from melting curve measurements it is crucial to know the molecularity of the studied transition. Usually this is information available from other experiments, such as electrophoresis or spectroscopic titrations, but when this is not case the molecularity has to be determined separately. It should be noted that the T_m for multi-molecular transitions is dependent upon concentration and, therefore, measurements of T_m can give information about the molecularity ***(11)***.

3.1.1. Bimolecular Association

We will limit our discussion to the reaction between "non-self-complementary" single strands leading to duplex formation because this is the most common reaction studied so far with the absorbance melting-curve technique. This reaction is a bimolecular equilibrium, which can be written as:

$$A + B \overset{K}{\rightleftharpoons} AB \tag{1}$$

where A and B denote the two different single strands and AB denotes the corresponding duplex. K is the equilibrium (binding) constant.

As an example of a melting curve, the melting of a 9-mer PNA–DNA duplex is shown in **Fig. 3**. Included in the figure are also the melting curves of the PNA and DNA single strands making up the duplex. We will return to this example when discussing the analysis of melting curves below.

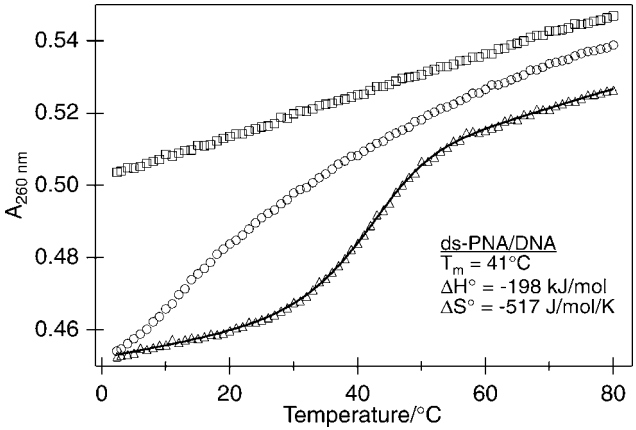

Fig. 3. Melting curves of the PNA 9-mer H-TCACAACTA-Lys-NH_2 (circles), its complementary DNA 9-mer 5'-TAGTTGTGA-3' (squares), and the duplex formed these two single strands (triangles). The total strand concentration = 5 μ*M*. The curves for the single strand melting are displaced 0.005 and 0.01 absorbance units for clarity. The solid line represents the result of a nonlinear least-squares fit of a 6-parameter function to the experimental data (method *iv*, *see* text). The obtained thermodynamic parameters are shown in the inset. Adapted with permission from ref. ***(16)***.

The observed absorbance versus temperature melting curve (*see* **Fig. 3**) can be converted to a curve describing the fraction of single strands (α) in duplex as a function of temperature, assuming that the observed absorbance (A) is sum of contributions form the absorbance of the single strands (A_s) and the absorbance of the duplex (A_d) according to:

$$A = \alpha A_d + (1 - \alpha)\, A_s \qquad (2)$$

In order to make the conversion to a fraction vs temperature curve, it is necessary to take into account the temperature dependence of the absorbance of the double strands and single strands. As seen in **Fig. 3**, the temperature dependencies both for duplex (lower

part of melting curve) and single strands (upper part of melting curve) are both approximately linear. Thus, we can define base lines corresponding to the two end points of the transition according to:

$$A_s = m_s T + b_s \tag{3}$$

$$A_d = m_d T + b_d \tag{4}$$

The deviations of the slopes m_s and m_d from zero can be regarded as a consideration of temperature dependence of nucleobase stacking dynamics.

When the baselines are defined, α can be calculated at each temperature, and the curve can now be analyzed using a suitable model for the equilibrium. For the melting transition of short DNA duplexes (4–20 base pairs), a simple two-state (all-or-none) model ***(17)*** has been found adequate, although some exceptions have been observed ***(18,19)***. The two-state model assumes that each single strand exists in one of two possible states: completely base paired and stacked in a duplex or completely denatured and unstacked. This means that no intermediate states are allowed, such as a partially base-paired duplex or an ordered single strand. Thus, it is not surprising that the two-state model fails for long duplexes because local melting probably starts at many places along such a duplex when the temperature is raised in contrast to the co-operative melting required by a two-state model.

Single-stranded PNA as well as nucleic acid oligomers exhibit in some cases significant order at lower temperatures. For example, for the 9-mer PNA in **Fig. 3** (circles), this gives a tendency to show melting behavior. However, the effect of single-strand order at low temperatures is not a severe complication when analyzing absorbance melting curves. At low temperatures the duplex is strongly favored over the isolated single strands and as the temperature increases and consequently the number of single strands increases, the order of the single strands decreases.

Assuming a two-state model, the fractions α at each temperature can be converted to an equilibrium constant, *K*, at each temperature, where c_t is the total concentration.

$$K = \frac{[\mathrm{A}\cdot\mathrm{B}]}{[\mathrm{A}][\mathrm{B}]} = \frac{2\alpha}{(1-\alpha)^2 c_t} \tag{5}$$

A link between the thermodynamic parameters $\Delta G°$, $\Delta H°$ and $\Delta S°$ with the fraction α is obtained using the standard equations $\Delta G° = -RT \ln K$ and $\Delta G° = \Delta H° - T\Delta S°$

$$K(T) = \left(\frac{-\Delta G°}{RT}\right) = \exp\left(\frac{-\Delta H°}{RT} + \frac{\Delta S°}{R}\right) \tag{6}$$

The set of *K* vs temperature data can then be analyzed using the van't Hoff equation:

$$\frac{d\ln K}{dT^{-1}} + \frac{-\Delta H°}{R} \tag{7}$$

Finally, the T_m can be linked to $\Delta H°$ and $\Delta S°$ by recognizing that for a two-state transition the T_m is defined as the temperature where $\alpha = 0.5$. We then obtain

$$\frac{1}{T_m} = \frac{R}{\Delta H°} \ln c_t + \frac{\Delta S° - R\ln 4}{\Delta H°} \tag{8}$$

which is a very useful relation between two easily measurable quantities, the T_m and the strand concentration c_t. **Equation 8** can be used to extract the thermodynamic properties from a linear fit to a plot of T_m^{-1} vs $\ln c_t$. Expressions analogous to **Eqs. 5** and **8** for other types of equilibria can be found in **ref.** ***(11)***.

3.1.2. Different Approaches

The framework of **Eqs. 2–8** allows a few different approaches for evaluation of melting data ***(10,11)***. These are (1) normal van't Hoff analysis by plotting $\ln K$ vs T^{-1}, (2) analysis of a differentiated melt-

ing curve yielding the van't Hoff enthalpy; (3) analysis of the concentration dependence of T_m (**Eq. 8**), (4) direct nonlinear least-squares fitting of the absorbance *vs* temperature curve using $\Delta H°$ and $\Delta S°$ as parameters together with the baseline parameters m_s, m_d, b_s and b_d giving in total six fitting parameters.

The solid line in **Fig. 3** shows the best fit to the melting curve using method *iv* with the Marquardt-Levenberg algorithm for the nonlinear least-squares minimization ***(20)***. The resulting thermodynamic parameters are shown in the inset.

It is in fact desirable to use more than one of the abovementioned methods because it is a test of the assumption of a two-state transition. If the thermodynamic parameters obtained in different ways disagree, it is an indication of a non-two-state behavior. Furthermore, thermodynamic parameters determined by monitoring other physical properties such as circular dichroism, nuclear magnetic resonance (NMR), and fluorescence or determined by calorimetric methods, should be the same within experimental errors if the transition is truly two-state in character.

3.1.3. Assumptions

Finally, it should be noted that the analysis is made under several assumptions, the justification of which has to be assessed in each case. First, concentrations replace activities in the expression for the equilibrium constant which makes it important to check for solvent and salt effects on activity coefficients. Second, the $\Delta G°$, $\Delta H°$, and $\Delta S°$ values refer to a solution with 1 *M* concentrations of each species but with the properties of an ideal solution. Third, the standard state is defined by the solvent used, which means that the determined parameters might not be applicable in other solvents, at other salt concentrations, and so on. Fourth, the temperature dependence of $\Delta H°$ and $\Delta S°$ is neglected, i.e., ΔC_p is assumed to be 0. This assumption has been found to be reasonable for at least short DNA duplexes ***(21)*** and seems to be justified with PNA ***(4)***, but is generally not true in protein-DNA systems ***(22)***. This last point will be discussed in great detail in a separate section (*see* **Subheading 3.5.**).

3.2. Isothermal Titration Calorimetry

3.2.1. General Concept

Calorimetric methods have the inherent advantage over the van't Hoff based methodology previously described that they can be used to directly measure the heat of reaction, ΔH, or change of heat capacity, ΔC_p, during a reaction. This means that thermodynamic parameters can be determined in a "model-independent" manner. We will here briefly discuss isothermal titration calorimetry and its applications to studies of PNA-nucleic acid complexes.

3.2.2. Example PNA–DNA Titration

In **Fig. 4** (top), the raw ITC data is shown for the titration of the DNA 9-mer shown previously (**Fig. 3**) into a solution of its complementary 9-mer PNA. When the molar ratio of the two single strands approaches 1, the observed reaction heat decreases, i.e., becomes less negative as the reaction saturates. However, the net heat is obviously not zero for the remaining injections. This is due to the heat of dilution that comes from diluting the titrant solution. It is generally assumed that this heat is nearly constant during the series of titrations and, thus, could be subtracted in order to get the true heat of reaction for the hybridization. (*See* **Fig. 4** [bottom]).

3.2.3. Analysis and Information Content

The resulting integrated heat for each titration is shown together with an analysis of the data in **Fig. 4**. The enthalpy of binding is given by the difference between the upper and lower base lines. The remaining thermodynamic parameters can be estimated from the data assuming a suitable model for the binding. In this case it is natural to assume that a single binding site exists in analogy with the two-state model discussed earlier. The best fit of a binding isotherm ***(17)*** is represented by the solid line. The fitting parameters are ΔH, K, and the number of binding sites n.

When interpreting thermodynamic parameters from ITC measurements for PNA-nucleic acid complexes one has to be aware of

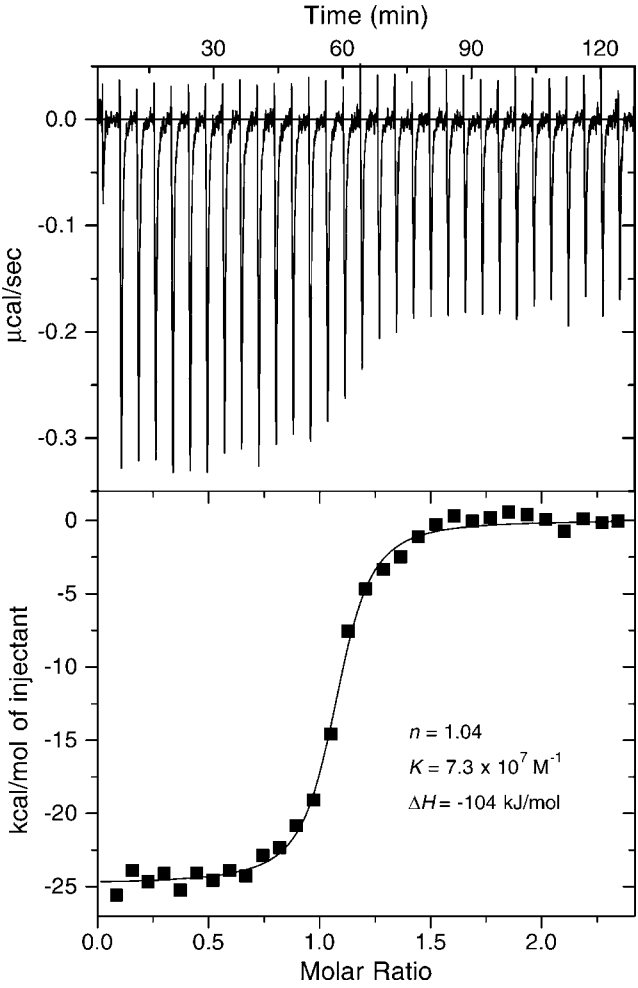

Fig. 4. **Top** panel; The calorimetric response (CFB, cell feed back) for the titration of the DNA 9-mer 5'-TAGTTGTGA-3' into a solution of the complementary PNA 9-mer H-TCACAACTA-Lys-NH_2. **Bottom** panel; Integrated heat of reaction corrected for heat of dilution vs DNA/PNA ratio. The heat of binding is determined as the difference between the upper and lower baselines. The curve represents the result of a non-linear least-squares fit of the data to a binding isotherm. The fitting parameters are the ΔH, the K and the number of binding sites n. The results indicate a single binding site ($n = 1.04 \pm 0.005$), the equilibrium constant is about $7.3(\pm 0.9) \times 10^7\ M^{-1}$ and the reaction enthalpy equals $104(\pm 1)$ kJ·mol^{-1}. Reproduced with permission from **ref.** ***(16)***.

the possible influence from single-strand order at low temperatures ***(23)***. Because the experiments are usually performed at a temperature low enough for the complex to be quite stable, the single strands might have a significant order. In a simplified view, the single-strand order has to broken before the hybridization reaction can occur. Thus, we could potentially have a large contribution from the single strand denaturation/renaturation equilibrium in the measured reaction heat. This has been recognized by Vesnaver and Breslauer, who studied the single-strand order of short DNA oligomers ***(24)***. For our example duplex, the agreement between the van't Hoff enthalpy (–198 kJ·mol^{-1}) and the ITC enthalpy (–104 kJ·mol^{-1}) is very poor, indicating that single-strand order is a severe problem in this particular case. It is possible to correct the ITC enthalpy if data is available for the single strand melting ***(24)***.

3.3. Differential Scanning Calorimetry DSC

3.3.1. General Concept

Differential scanning calorimetry (DSC) measurements might become an increasingly used complement to the abovementioned techniques. The reason for this is that in DSC, the change in heat capacity is directly measured and, thus, the reaction enthalpy and reaction entropy can both be evaluated without applying any model for the binding. The comparison between the thermodynamic parameters determined using the absorbance melting technique in connection with a van't Hoff analysis and those determined in a model free DSC analysis are expected to give important insight about the assumptions of two-state melting behavior and possibly shed light on the nature of any proposed intermediate. The power (CFB, *see* caption for **Fig. 1**) is converted to apparent molar excess heat capacity through

$$C_{p,xs} = \frac{1}{\sigma n}\frac{dCFB}{dt} \tag{9}$$

where time and temperature are linked through the scanrate $\sigma = dT/dt$, and n is the number of moles of the solute.

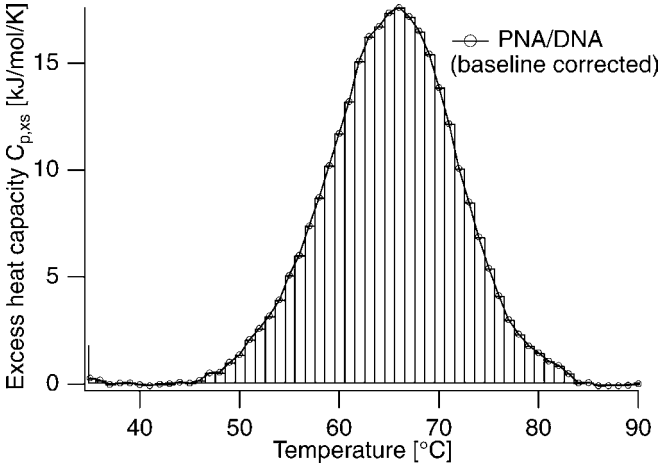

Fig. 5. The calorimetric (baseline-corrected, *see* text) trace of a 1°C/min up-scan of a 34.4 μ*M* solution of PNA–DNA. The area under the peak directly gives the enthalpy of the transition. Adapted from results in **ref.** ***(25)***.

3.3.2. Example PNA–DNA Scan

A baseline-corrected representation of DSC data on PNA–DNA melting is shown (from Chakrabarti and Schwarz ***(25)*** (*see* **Fig. 5**).

3.3.3. Data Analysis

In principle, the integrated area under the peak (*see* **Fig. 5**) gives the enthalpy of the transition

$$\Delta H = \int C_{p,xs} dT \tag{10}$$

If the transition is accompanied with a change of heat capacity (ΔC_p) it would appear as a change of baseline levels from before to after the peak. This is discussed in **Subheading 3.5.1.** Estimation of ΔC_p from thermodynamic parameters or DSC experiments) and will not be other than briefly mentioned here. The most common baselines used are cubic or sigmoidal, and the choice may have a

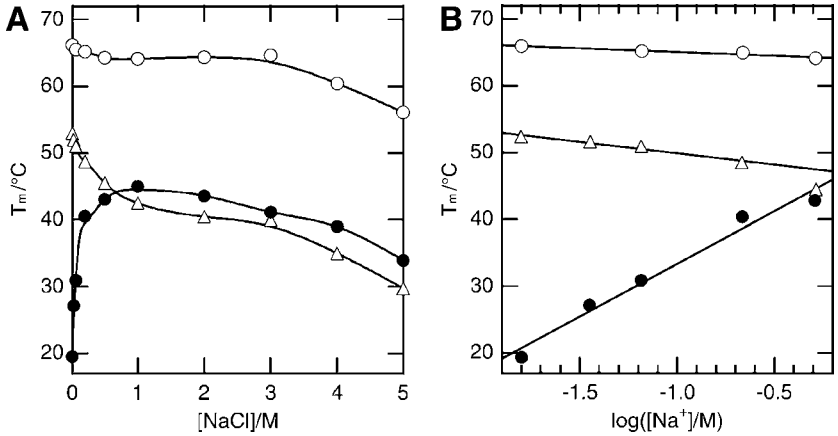

Fig. 6. Effects of ionic strength on the T_m of 10-mer duplexes of PNA–PNA (○), PNA–DNA (▲), and DNA–DNA (●). (**A**) T_m vs [Na^+] in the range 0–5 *M*. (**B**) T_m vs log[Na^+] with [Na^+] in the range 10–500 m*M*. Reproduced with permission from **ref.** ***(4)***.

quite large influence on the results of the fitting. In fact, the procedure of finding appropriate baselines may be the most difficult practical task when analyzing DSC data ***(26)***.

3.4. Thermodynamic Properties of PNA–DNA Duplexes

3.4.1. Ionic Effects

Salts affect the properties of biological macromolecules such as their stability, solubility, and biological activity in widely different manners ***(27)***. At low concentrations, salts generally exert their effects on polyelectrolytes through nonspecific electrostatic interactions depending on the ionic strength of the medium ***(28)***. By contrast, at high salt (>1 *M*), the electrostatic contributions saturate and the salts instead exert specific effects on biopolymers, which depend on the nature of the salt and its concentration and also on its indirect effect on the bulk aqueous solvent ***(29)***.

Figure 6A shows the effect of increasing NaCl concentration on T_m for 10-mer PNA–PNA, PNA–DNA, and DNA–DNA duplexes. At low to moderate salt concentration (≤ 0.5 *M*) the T_m of DNA–DNA increases with NaCl concentration and levels off around 1 *M*, consistent with previous observations ***(30–32)***. In contrast, increas-

ing the NaCl concentration in the 0–1 *M* range resulted in a continuous decrease in the T_m of PNA–DNA such that around 0.7 *M* of NaCl the thermal stabilities of PNA–DNA and DNA–DNA duplexes were equal (**Fig. 6A**).

Unlike the PNA–PNA duplex with its uncharged backbone, both the PNA–DNA and the DNA–DNA duplexes are polyelectrolytes. At low to moderate Na^+ concentrations (10–500 m*M*) the plots of transition temperature T_m vs log[Na^+] follow a linear relationship in the case of both DNA–DNA and PNA–DNA (**Fig. 6B**).

Cations destabilize PNA–DNA, whereas they stabilize DNA–DNA duplexes. The decrease of thermal stability (T_m) of PNA–DNA with increasing ionic strength (10–500 m*M*), is explained by a release of counterions upon hybridization, i.e., quite the opposite to the observation for DNA–DNA formation.

At high concentrations of NaCl (>1 *M*) all the studied duplexes were destabilized (**Fig. 6A**). Here electrostatic effects saturate, and similar trends of decreasing T_m were found for all types of duplexes, irrespective of backbone (charge), suggesting that it is mainly an indirect effect of the surrounding aqueous solvent ***(27,29)***. Changing anions was found to agree with earlier established order in the Hofmeister series, with the degree of destabilization following the series $CH_3COO^- < Cl^- < ClO_4^-$. This suggests that hydrophobic effects are of importance in formation of PNA-containing complexes.

3.4.2. Length Dependence

Our melting curve analysis for different lengths *N* (from 6-mer to 20-mer) of 31 fully complementary mixed-sequence PNA–DNA duplexes ***(6)*** yielded an average contribution of $\partial\Delta G°/\partial N = -(6.5 \pm 0.3)$ kJ·mol^{-1}bp^{-1} corresponding to a binding constant for one base pair (k) of about 14 M^{-1} (at 25 °C), (*see* **Fig. 7A**). For the same set of mixed sequences we determined length-averaged enthalpy and entropy changes as $\partial\Delta H°/\partial N = -(30.0 \pm 2.5)$ kJ·mol^{-1}bp^{-1} and $T\partial\Delta S°/\partial N = -(23.5 \pm 2.3)$ kJ·mol^{-1}bp^{-1}, respectively (**Fig. 7B**). These values, taken at low salt conditions (10–100 m*M*), are quite close to those obtained as an average of DNA–DNA nearest-neigh-

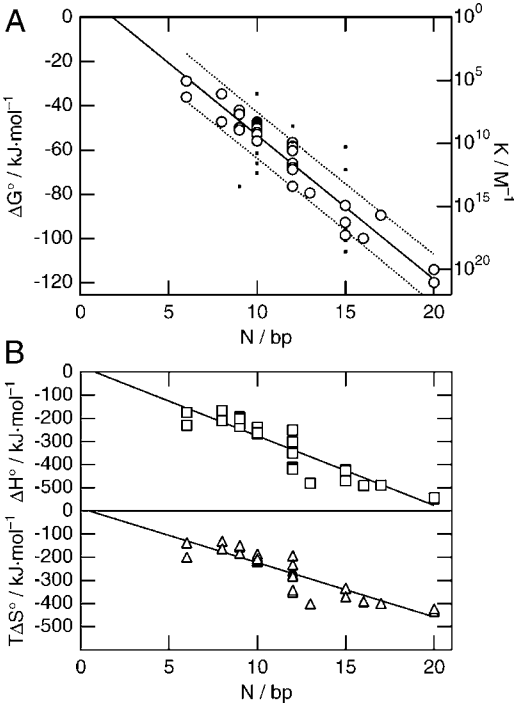

Fig. 7. **(A)** Length dependence of PNA–DNA duplex stability for matched sequences, given as binding free energy ($\Delta G°$, left) and binding constant (K, right). Only data for 'mixed' sequences (circles) were included for the linear fit. Dotted curves show 90% prediction interval (model plus random noise). **(B)** Length dependence of enthalpy $\Delta H°$ (top) and entropy $T\Delta S°$ (bottom) of formation of PNA–DNA duplexes for mixed sequences. Reproduced with permission from **ref.** ***(6)***.

bor parameters at 1 *M* NaCl ***(18)***, again pointing at the superior stability of PNA–DNA at low ionic strength ***(4)***.

3.4.3. Effects of Mismatches on Stability of PNA–DNA Duplexes

The second most important parameter to investigate is the sequence specificity of PNA binding to DNA, i.e., how much lower is the thermal and thermodynamic stability when mismatches are

introduced in the sequence. This has been investigated in a number of studies, three of which are summarized in Table 2 in Ratilainen et al. ***(6)***. Generally a single mismatch costs more in a PNA–DNA duplex than in DNA–DNA, and in most cases, the same relative patterns with respect to the nature of the mismatch are found for both duplexes, e.g., the G•T mismatch was found to be the least destabilizing (ΔT_m = –8°C) in our study as well as in the works by Kilså Jensen et al. ***(9)***, and Igloi ***(33)*** who found a drop of ΔT_m = –13°C. In DNA–DNA systems the G•T mismatch has also been found to be extraordinarily stable and believed to achieve this by forming a so called "wobble" base pair with two hydrogen bonds ***(34)***. In stark contrast, we observe dramatic drops of around 30°C in T_m for both the C•T and T•T mismatches. Mismatches containing C bases have been shown to be the most destabilizing in the DNA–DNA duplexes ***(35)***, and thus our observation for the C•T mismatch suggests the same to be true for the PNA–DNA case.

3.4.4. Sequence and Context Dependence

As for DNA–DNA duplexes with or without mismatches ***(2)***, sequence context is important for PNA–DNA duplexes as well, even though the effects might vary. Here, only the first step considering context dependence is introduced, although more extensive studies are in progress. As found previously for DNA–DNA duplexes ***(19, 34,36)***, we observed that less stable nearest-neighbors (A•T) can increase the negative influence of a mismatched base pair for PNA–DNA systems as well. For example, the A•G mismatch surrounded by two G•C base pairs costs less than the two others with one A•T and one G•C (Table 2 in **ref. *6***). Furthermore, the best agreement between our work and that of Kilså Jensen et al. ***(9)*** and Igloi ***(33)*** is found when we have surroundings of similar stability, e.g., for the C•X mismatches (Table 2 in **ref. *6***).

3.4.5. Enthalpy-Entropy Compensation

Compensation between enthalpy (mainly hydrogen bonding energies and van der Waals interactions) and entropy (mostly

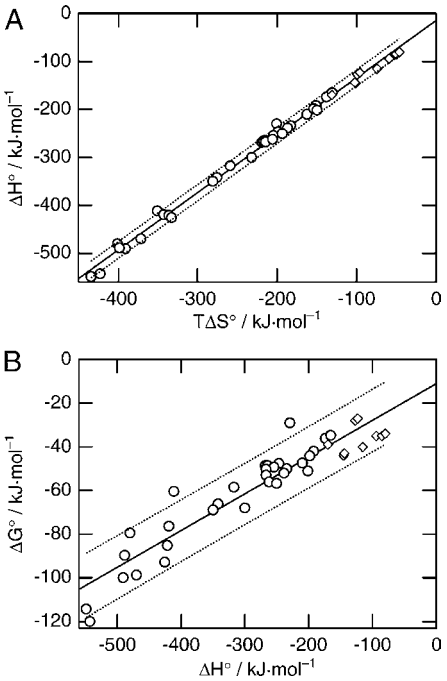

Fig. 8. **(A)** Thermodynamic data ($\Delta H°$ *vs* $T\Delta S°$) showing enthalpy-entropy compensation based on data for the 31 matched PNA–DNA sequences (circles) and for the mismatched systems (rhombs). Dotted curves show the 90% prediction interval for the fit. **(B)** Plot of the corresponding $\Delta G°$ vs $\Delta H°$ pairs. Dotted curves show the 90% prediction interval. Reproduced with permission from **ref**. ***6***.

rearrangements of the two interacting molecules, solvent water, and counterions) is observed for many different biological systems ***(37–39)***.

The general interpretation of this behavior is that tight binding (large $-\Delta H°$) is normally accompanied by a large loss of degrees of freedom (large $-\Delta S°$) in a compensatory manner, resulting in a relatively small change in binding free energy ($\Delta G°$). Considering only the two strands, a strand-association process (dimerization) is *per se* entropically unfavorable, whereas the formation of hydrogen bonds (base pairs) between strands is enthalpically favored, as is the stacking of bases. The classical analysis of data is plotting $\Delta H°$ vs $T\Delta S°$ (**Fig. 8A**) and if the data points correlate linearly this is referred to as

enthalpy-entropy compensation. However a linear plot of corresponding $\Delta H°$ vs $\Delta G°$ values (**Fig. 8B**) is a preferable criterion that the thermodynamic compensation has a chemical nature and is not due to statistical coincidence effects of the data acquisition ***(37,40,41)***.

Our data suggest that the compensation is truly chemically-based, relying on the fundamental nature of binding between the strands as base pairs are formed (**Fig. 8B**). Introducing a single mismatch significantly reduces the binding enthalpy as fewer hydrogen bonds are formed and often also the stacking efficiency decreases. The loosening of the bonds ($-\Delta H°$ smaller) at and in the vicinity of the mismatch is compensated by a less rigid structure ($-\Delta S°$ smaller) upon forming a less perfect sequence-matched duplex (for more details, *see* **Note 1**).

3.5. Temperature Independence of $\Delta H°$ and $\Delta S°$ (Nonzero ΔC_p)?

Using a two-state model and assuming $\Delta C_p = 0$ to determine the enthalpy and entropy changes associated with PNA–DNA hybridization (*see* **Subheading 3.1.3.**), is equivalent to assuming temperature-independent $\Delta H°$ and $\Delta S°$ values, which strictly speaking are extracted from the curve fits at T_m, and thus valid only at T_m in case $\Delta Cp \neq 0$. In general, using $\Delta C_p = 0$ has been an accepted procedure, but there has recently been some concern about the justification of this assumption for DNA–DNA duplexes ***(42–44)***. To find out if the thermodynamic parameters of PNA–DNA hybridization also are considerably temperature-dependent, a couple of different approaches can be used.

3.5.1. Estimation of C_p from Thermodynamic Parameters or DSC Experiments

Following the procedure of Rouzina et al. ***(43)*** to estimate ΔC_p for the set of fully complementary PNA–DNA duplexes (circles in **Fig. 7** and **Fig. 8**), gave $-\Delta C_p = 157 \pm 36$ J·mol^{-1}K^{-1}bp^{-1} (*see* **Note 2**). This appears smaller than even the lowest ones estimated for the DNA–DNA hybridization reaction. Moreover, the important factor

to consider is the ratio $\Delta C_p/\Delta S°$ ***(43)***, which with DNA–DNA data is 2–4, whereas our data are in the low (less severe) end of this range giving $\Delta C_p/\Delta S° \approx 2$.

We have also performed single experiments (unpublished results) with DSC on some of the decameric PNA–DNA duplexes that were investigated in our laboratory ***(5)***, without noticing any indications that there should be any large ΔC_p involved. Schwarz et al. ***(45)*** report on DSC results on some PNA–DNA sequences, getting quite large variations between different experiments and sequences: ΔC_p:s between 0 and 652 $J \cdot mol^{-1}K^{-1}bp^{-1}$ for PNA–DNA and between 0 and 161 $J \cdot mol^{-1}K^{-1}bp^{-1}$ for DNA–DNA. In conclusion, evidence for any significant effect of ΔC_p is still lacking.

3.5.2. Estimation of ΔC_p from Melting Curve Fitting

Formally, it is straightforward to include a non-zero ΔC_p in the expressions needed in the analysis of the melting curves (*see* **Note 3**). Attempts to determine ΔC_p from fitting some of our melting curves to a full analytical expression containing ΔC_p, gave strongly varying results, often with low values of ΔC_p for the best fits, although T_m was practically unaltered.

Significant heat capacity effects are of particular importance if one wants to analyze in detail the respective enthalpic and entropic contributions to the hybridization. Because of the strong enthalpy-entropy compensation that occurs in PNA–DNA hybridization, the individual contributions to $\Delta H°$ and $\Delta S°$ largely mutually cancel in $\Delta G°$. Therefore, for most applications where only T_m (and/or $\Delta G°$) values are used the simplest, model with the historically accepted assumption of $\Delta C_p = 0$, will give sufficiently accurate analysis of PNA–DNA hybridization for comparative purposes.

3.6. Thermodynamic Parameters for Gene-Targeting

Sequence-specific binding to genomic size DNA sequences by artificial agents is of major interest for the development of gene-targeting strategies, gene-diagnostic applications, and biotechnical tools. In order to illustrate the principles of a thermodynamic analysis

of drug distribution over target and mismatched DNA sequences, we have modeled binding of PNA to a randomized human genome with statistical mass action calculations ***(46)***, using our thermodynamic parameters from ref. ***(6)***. **Fig. 9** shows the results schematically.

With the length of the PNA probe, the average per-base binding constant k_0, and the binding affinity loss of a mismatched base-pair as main parameters, the specificity has been characterized as the range of safety of the total drug (PNA) concentration or dose, defined as a "therapeutic ratio" G = maximum safe $[PNA]_{tot}$/minimal efficient $[PNA]_{tot}$. Our simple, but as to principles quite general model suggests that, above a certain threshold length of the PNA, the microscopic binding constant k_0 is the primary determinant for optimal discrimination, and that only a narrow range of rather low k_0 values gives a high therapeutic ratio G ***(46)***.

For diagnostic purposes, the value of k_0 could readily be tuned by changing the temperature, due to the substantial $\Delta H°$ associated with the binding equilibrium. Applied to gene-therapy, our results stress the need for appropriate control of the binding constant and added amount of the gene-targeting agent, to meet the varying conditions (ionic strength, presence of competing DNA-binding molecules) found in the cell.

3.7. Concluding Remarks

We have focussed on the thermodynamics and various ways how to determine the thermodynamical parameters for PNA interacting with nucleic acids and itself. The most common approach, the van't Hoff analysis based on melting curves, for example, recorded in absorbance, is concluded to give generally reliable free energies of binding, and also $\Delta H°$ and $\Delta S°$ values that are useful for most purposes, in the cases when a two-state association model may be applied.

Calorimetric measurements provide an independent check of ΔH; the ITC and DSC methods providing different advantages and disadvantages. The self-structure of the single strands make the analysis of ITC experiments cumbersome, while the DSC instrumentation is not quite as sensitive to measuring at μM concentrations.

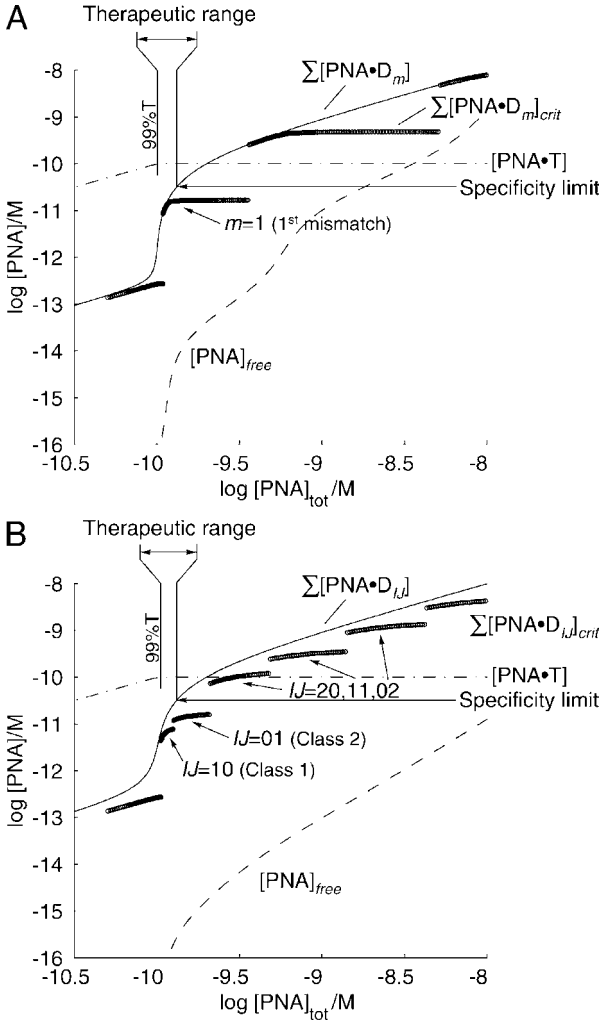

Fig. 9. Graphical representation of the principle and some parameter definitions used in the simulations for the two different binding models. (**A**) Model 1 (one class of mismatches): The graphs show profiles of [PNA•T] (— - —), [PNA]$_{free}$ (— — —), [P•D$_m$] (———), and [P•D$_m$]$_{crit}$ (oooooo). The therapeutic range is defined starting from the concentration at which 99% targeting occurs until the integrated concentration of mismatched complexes reach the specificity level (here chosen to be $10^{-0.5}$ times lower than the concentration of targeted sequence). (**B**) Model 2 (two classes of mismatches): The graphs show profiles of [PNA•T] (— - —), [PNA]$_{free}$ (— — —), [P•D$_{IJ}$] (———), and [P•D$_{IJ}$]$_{crit}$ (oooooo). The bind ing curves appear somewhat more complex, while the therapeutic range

By and large, the thermodynamics of PNA resembles that of natural nucleic acids as to electrostatic and ionic contributions to enthalpy and entropy as well as effects of mismatch and neighboring bases, although detailed studies may reveal differences due to variations in hydrogen bonding in backbone and hydrophobicity.

Finally, although thermodynamics uniquely determines binding affinity and target specificity, the effective use of PNA for therapeutic and diagnostic purposes also depends on reaction kinetics, the rate by which the PNA may find its target. Based on statistical thermodynamical considerations one may estimate the theoretical fidelity by which a PNA will hit its target. However, reality will depend on the rate of diffusion along a genome and the opening dynamics by which the PNA could invade the nucleic acid.

4. Notes

1. Expanding on this simple picture, and as pointed out by Zhong et al., ***(47)*** most probably water structure (hydration) is altered significantly around the mismatched region of a DNA duplex, and also around PNA–DNA duplexes. In addition, it is likely that the water structure around the mismatched regions is different for the various mismatched base pairs. We observe quite different thermodynamic parameters for the mismatches (Table 2 in Ratilainen et al. ***[6]***) but in the end, the unfavorable enthalpic contributions (loosening of intermolecular bonds) when introducing mismatches are still proportionally compensated by a favorable change in the degrees of freedom (the entropic factor).
2. According to Rouzina et al. ***(43)***, ΔC_p was estimated from plots of $\Delta H°$ vs T_m, and $\Delta S°$ vs ln T_m, and averaging the slopes gave us $-\Delta C_p = 157 \pm 36$ J·K^{-1}mol^{-1}bp^{-1}. This value appears smaller than even the lowest ones estimated for DNA–DNA hybridization. The important factor to consider is the ratio $\Delta C_p/\Delta S°$ ***(43)***, which with DNA–DNA data is 2–4 whereas our data are in the low end of this range giving $\Delta C_p/\Delta S° \approx 2$.
3. Denoting all variables valid (only) at a certain reference temperature of our choice (e.g., T_m) with index "*m*", the following applies:

Fig. 9. (*continued from opposite page*) does not change significantly. Reproduced with permission from **ref**. ***(46)***.

$$\Delta H^\circ = \Delta H^{\circ,m} + \Delta C_p\,(T - T_m) \tag{11}$$

$$\Delta S^\circ = \Delta S^{\circ,m} + \Delta C_p\, ln\frac{T}{T_m} \tag{12}$$

which are used in expressing the equilibrium constant at any temperature, *K(T)*

$$K(T) = \exp\left(-\frac{\Delta G^{\circ,m}}{RT_m} + \frac{\Delta H^{\circ,m}}{R}\left(\frac{1}{T} - \frac{1}{T_m}\right) + \frac{\Delta C_p}{R}\left(\ln\frac{T}{T_m} + \frac{T}{T_m} - 1\right)\right) \tag{13}$$

Equation 13 is then used in the analysis instead of **Eq. 6**.

Acknowledgments

The authors would like to thank Anders Holmén for helpful input to the manuscript. Financial support from the Swedish Natural Science Research Council and the Swedish Cancer Foundation is gratefully acknowledged.

References

1. Turner, D. H. (1996) Thermodynamics of base-pairing. *Curr. Opin. Struct. Biol.* **6,** 299–304.
2. Peyret, N., Seneviratne, P. A., Allawi, H. T., and SantaLucia, J. (1999) Nearest-neighbor thermodynamics and NMR of DNA sequences with internal A·A, C·C, G·G, and T·T mismatches. *Biochemistry* **38,** 3468–3477.
3. Egholm, M., Buchardt, O., Christensen, L., Behrens, C., Freier, S. M., Driver, D. A., et al. (1993) PNA hybridizes to complementary oligonucleotides obeying the Watson-Crick hydrogen-bonding rules. *Nature* **365,** 566–568.
4. Tomac, S., Sarkar, M., Ratilainen, T., Wittung, P., Nielsen, P. E., Nordén, B., and Gräslund, A. (1996) Ionic effects on the stability and conformation of peptide nucleic acid (PNA) complexes. *J. Am. Chem. Soc.* **118,** 5544–5552.
5. Ratilainen, T., Holmén, A., Tuite, E., Haaima, G., Christensen, L., Nielsen, P. E., and Nordén, B. (1998) Hybridization of peptide nucleic acid. *Biochemistry* **37,** 12,331–12,342.

6. Ratilainen, T., Holmén, A., Tuite, E., Nielsen, P. E., and Nordén, B. (2000) Thermodynamics of sequence-specific binding of PNA to DNA. *Biochemistry* **39,** 7781–7791.
7. Eriksson, M. and Nielsen, P. E. (1996) PNA nucleic acid complexes. Structure, stability and dynamics. *Q. Rev. Biophys.* **29,** 369–394.
8. Giesen, U., Kleider, W., Berding, C., Geiger, A., Ørum, H., and Nielsen, P. E. (1998) A formula for thermal stability (T_m) prediction of PNA/DNA duplexes. *Nucleic Acids Res.* **26**, 5004–5006.
9. Kilså Jensen, K., Ørum, H., Nielsen, P. E., and Nordén, B. (1997) Kinetics for hybridization of Peptide Nucleic Acids (PNA) with DNA and RNA studied with the BIAcore technique. *Biochemistry* **36,** 5072–5077.
10. Marky, L. A. and Breslauer, K. J. (1987) Calculating thermodynamic data for transitions of any molecularity from equilibrium melting curves. *Biopolymers* **26,** 1601–1620.
11. Puglisi, J. D. and Tinoco, J. I. (1989) Absorbance melting curves of RNA. *Methods Enzymol.* **180,** 304–325.
12. Noble, S. A., Bonham, M. A., Bisi, J. E., Bruckenstein, D. A., Brown, P. H., Brown, S. C., et al. (1995) Impact of biophysical parameters on the biological assessment of peptide nucleic-acids, antisense inhibitors of gene-expression. *Drug Dev. Res.* **34**, 184–195.
13. Gildea, B. D., Casey, S., MacNeill, J., Perry-O'Keefe, H., Sørensen, D., and Coull, J. M. (1998) PNA solubility enhancers. *Tetrahedr. Lett.* **39**, 7255–7258.
14. Sjöback, R., Nygren, J., and Kubista, M. (1995) Absorption and fluorescence properties of fluorescein. *Spectroch. Acta Part A* **51,** L7–L21.
15. Dawson, R. M. C., Elliott, D. C., Elliott, W. H., and Jones, K. M. (1986) *Data for Biochemical Research*, 3rd ed. Oxford University Press, New York.
16. Holmén, A. and Nordén, B. (1999) Thermodynamics of PNA-nucleic acid interactions, in *Peptide Nucleic Acids: Protocols and Applications* (Nielsen, P. E., and Egholm, M., eds.) Horizon Scientific Press, Wymondham, UK, pp 87–97.
17. Cantor, C. R. and Schimmel, P. R. (1980) *Biophysical Chemistry part 3: The Behaviour of Biological Macromolecules*. W. H. Freeman, New York.
18. SantaLucia, J., Allawi, H. T., and Seneviratne, A. (1996) Improved nearest-neighbor parameters for predicting DNA duplex stability. *Biochemistry* **35,** 3555–3562.

19. Allawi, H. T. and SantaLucia, J. (1998) Nearest neighbor thermodynamic parameters for internal GA mismatches in DNA. *Biochemistry* **37,** 2170–2179.
20. Bevington, P. R. (1969) *Data Reduction an Error Analysis for the Physical Sciences*. McGraw-Hill, New York.
21. Breslauer, K. J., Frank, R., Blöcker, H., and Marky, L. A. (1986) Predicting DNA duplex stability from the base sequence. *Proc. Natl. Acad. Sci. USA* **83,** 3746–3750.
22. Lundbäck, T. and Härd, T. (1994) Sequence specific DNA-binding dominated by dehydration. *Proc. Natl. Acad. Sci. USA* **93,** 4754–4759.
23. Sen, S. and Nilsson, L. (2001) MD simulations of homomorphous PNA, DNA, and RNA singles strands: Characterization and comparison of conformations and dynamics. *J. Am. Chem. Soc.* **123,** 7414–7422.
24. Vesnaver, G. and Breslauer, K. J. (1991) The contribution of DNA single-stranded order to the thermodynamics of duplex formation. *Proc. Natl. Acad. Sci. USA* **88,** 3569–3573.
25. Chakrabarti, M. C. and Schwarz, F. P. (1999) Thermal stability of PNA/DNA and DNA/DNA duplexes by differential scanning calorimetry. *Nucleic Acids Res.* **27,** 4801–4806.
26. Haynie, D. T. (1998) in *Biocalorimetry: Applications of Calorimetry in the Biological Sciences* (Ladbury, J. E., and Chowdhry, B. Z., eds.), John Wiley & Sons, Chichester, UK, pp 183–205.
27. Von Hippel, P. H. and Schleich, T. (1969) Structure and stability of biological macromolecules, in *Biological Macromolecules*, (Timasheff, S. N. and Fasman, G., eds.), Marcel Dekker, New York, pp. 417–574.
28. Bloomfield, V., and Carpenter, I. L. (1993) Biological polyelectrolytes, in *Polyelectrolytes; Science and Technology* (Hara, M., ed.), Marcel Dekker New York, pp. 77–125.
29. Collins, K. D. and Washabaugh, M. W. (1985) The Hofmeister effect and the behaviour of water at interfaces. *Q. Rev. Biophys.* **18,** 323–422.
30. Record, M. T., Jr. (1975) Effects of Na^+ and Mg^{2+} ions on the helix-coil transition of DNA. *Biopolymers* **14,** 2137–2158.
31. Krakauer, H. and Sturtevant, J. M. (1968) Heats of the helix-coil transitions of the poly A-poly U complexes. *Biopolymers* **6,** 491–512.

32. Record, M. T., Jr. (1967) Electrostatic effects on polynucleotide transitions. I. Behavior at neutral pH. *Biopolymers* **5,** 975–992.
33. Igloi, G. L. (1998) Variability in the stability of DNA-peptide nucleic acid (PNA) single-base mismatched duplexes: Real-time hybridization during affinity electrophoresis in PNA-containing gels. *Proc. Natl. Acad. Sci. USA* **95,** 8562–8567.
34. Allawi, H. T. and SantaLucia, J. (1997) Thermodynamics and NMR of internal GT mismatches in DNA. *Biochemistry* **36,** 10581–10594.
35. Aboul-ela, F., Koh, D., and Tinoco, I. J. (1985) Base-base mismatches. Thermodynamics of double helix formation for dCA_3XA_3G + dCT_3YT_3G (X, Y = A,C,G,T). *Nucleic Acids Res.* **13,** 4811–4824.
36. Allawi, H. T. and SantaLucia, J. (1998) Nearest-neighbor thermodynamics of internal A center dot C mismatches in DNA: sequence dependence and pH effects. *Biochemistry* **37,** 9435–9444.
37. Gilli, P., Ferretti, V., Gilli, G., and Borea, P. A. (1994) Enthalpy-entropy compensation in drug-receptor binding. *J. Phys. Chem.* **98,** 1515–1518.
38. Gelfand, C. A., Plum, G. E., Grollman, A. P., Johnson, F., and Breslauer, K. J. (1998) The impact of an exocyclic cytosine adduct on DNA duplex properties: significant thermodynamic consequences despite modest lesion-induced structural alterations. *Biochemistry* **37,** 12507–12512.
39. Blasko, A., Dempcy, R. O., Minyat, E. E., and Bruice, T. C. (1996) Association of short-strand DNA oligomers with guanidinium-linked nucleosides. A kinetic and thermodynamic study. *J. Am. Chem. Soc.* **118,** 7892–7899.
40. Krug, R. R., Hunter, W. G., and Grieger, R. A. (1976) Enthalpy-entropy compensation. 2. Separation of the chemical from the statistical effect. *J. Phys. Chem.* **80,** 2341–2351.
41. Krug, R. R., Hunter, W. G., and Grieger, R. A. (1976) Enthalpy-entropy compensation. 1. Some fundamental statistical problems associated with the analysis of van't Hoff and Arrhenius data. *J. Phys. Chem.* **80,** 2335–2341.
42. Chalikian, T. V., Völker, J., Plum, G. E., and Breslauer, K. J. (1999) A more unified picture for the thermodynamics of nucleic acid duplex melting: A characterization by calorimetric and volumetric techniques. *Proc. Natl. Acad. Sci. USA* **96,** 7853–7858.

43. Rouzina, I. and Bloomfield, V. A. (1999) Heat capacity effects on the melting of DNA. 1. General aspects. *Biophys. J.* **77,** 3242–3251.
44. Rouzina, I. and Bloomfield, V. A. (1999) Heat capacity effects on the melting of DNA. 2. Analysis of nearest-neighbor base pair effects. *Biophys. J.* **77,** 3252–3255.
45. Schwarz, F. P., Robinson, S., and Butler, J. M. (1999) Thermodynamic comparisons of PNA/DNA and DNA/DNA hybridization reactions at ambient temperature. *Nucleic Acids Res.* **27,** 4792–4800.
46. Ratilainen, T., Lincoln, P., and Nordén, B. (2001) A simple model for gene-targeting. *Biophys. J.* **81,** 2876–2885.
47. Zhong, M., Marky, L. A., Kallenbach, N. R., and Kupke, D. W. (1997) Thermodynamics of dT-dT base pair mismatching in linear DNA duplexes and three-arm DNA junctions. *Biochemistry* **36,** 2485–2491.

6

Measurement of PNA Binding to Double-Stranded DNA

Thomas Bentin, Georg I. Hansen, and Peter E. Nielsen

1. Introduction

A number of complexes formed between peptide nucleic (PNA) acid and double-stranded (ds) DNA has been described. Each of these complexes involves different structural elements and they consequently exhibit distinct physico-chemical characteristics. Thus, it is important to know in detail with which type of complex one is dealing. To this end, the different techniques described below have proven extremely useful and the rules governing formation of certain types of complexes are, if not fully, then at least partially resolved. In contrast, the mechanism(s) by which peptide nucleic acid (PNA) binds double-stranded DNA has been much more difficult to approach. As for any mechanistic study, the main difficulty is to catch intermediates along the binding pathway, especially those of labile transition-state intermediates. Here we describe (*1*) the currently known PNA-dsDNA complexes, (*2*) the probing methods commonly employed for their analysis, and (*3*) protocols used in our laboratory.

From: *Methods in Molecular Biology, vol. 208: Peptide Nucleic Acids: Methods and Protocols*
Edited by: P. E. Nielsen © Humana Press Inc., Totowa, NJ

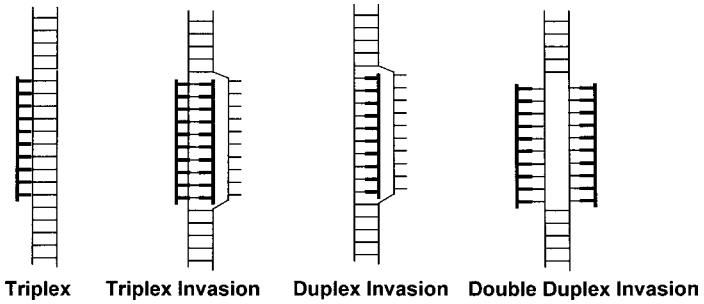

Fig. 1. Complexes formed between PNA and double-stranded DNA. Triplex (PNA·DNA-DNA), triplex invasion (PNA·DNA-PNA/DNA), duplex invasion (PNA-DNA/DNA), double duplex invasion (PNA-DNA/PNA-DNA). PNA moieties are drawn in bold.

1.1. Triplex Invasion

Figure 1 depicts structures of the currently known PNA/dsDNA complexes. The triplex-invasion complex (for PNA nomenclature, *see* **ref.** *[1]*) formed between homopyrimidine PNA molecules and a purine DNA target is by far the best described. Two PNA strands form an internal PNA. DNA–PNA triplex with the purine DNA strand by combined Hoogsteen and Watson-Crick base pairing. As a result, the noncomplementary DNA strand is left extruded in a single-strand loop conformation *(2,3)*. **Figure 2** shows the hydrogen bonding pattern in triplex-invasion complexes. Because two PNAs are required for triplex invasion, bis-PNAs were generated in which two strands of PNA are linked via a flexible ethylene glycol linker. Furthermore, pseudoisocytosine is substituted for cytosine in the PNA strand aimed for binding via Hoogsteen hydrogen bonds because it carries a permanent proton on the N3 position. This overcomes the pH sensitivity of triplex invasion *(4)*. By now bis-PNA technology has chiefly superseded the use of single strand or mono PNAs.

In general, binding of homopyrimidine PNA to dsDNA occurs with high specificity *(5,6)*. The accepted explanation for this is that binding is kinetically controlled – i.e., the activation energy for formation of complexes involving mismatched base pairs is high compared with those encompassing fully matched base pairs. Thus high

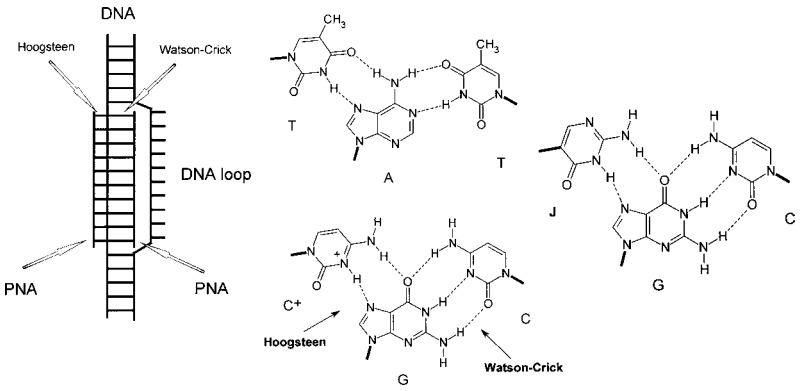

Fig. 2. Interactions in a triplex invasion complex. Left, triplex invasion complex. Right, hydrogen bonds formed in the T·A-T, C+·G-C and J·G-C PNA·DNA-PNA base triplets (J = pseudoisocytosine).

specificity is not obtained under all conditions and careful titration should always be conducted to obtain optimal binding using particular PNA and DNA constructs under a given set of reaction conditions.

In addition to their high specificity of formation, triplex-invasion complexes are extraordinarily stable. For example, a triplex-invasion complex containing decamer homopyrimidine bis-PNA was found to exhibit lifetimes exceeding 100 h ***(7)***. Thus, triplex invasion is generally considered irreversible, at least when using 10-mer bis-PNA molecules and experimental times in the range 1–16 h. Hence, for these PNAs true dissociation constants are not meaningful because $k_{off} \sim 0$. The PNA concentration that gives 50% binding in 1 h at 37°C, referred to as ψKd (pseudo Kd), is used instead.

1.1.1. Ambient Conditions that Influence Triplex Invasion

One of the most pronounced obstacles to efficient triplex invasion under physiologically relevant conditions, and by virtue to the use of PNA in a cellular context, is a strong inhibitory effect of salt on triplex invasion ***(7–10)***. For example a 100-fold reduction in binding rate was seen when going from 10 m*M* to 40 m*M* of sodium chloride ***(11)*** and binding may be further compromised at higher

salt concentrations *(8–10)*. This inhibitory effect is most probably due to DNA duplex stabilization with increasing ionic strength. However, by equipping PNA with lysine residues carrying a positive charge on the ε-amino group at neutral pH, saturation binding was observed at 100 m*M* NaCl although with relatively slow kinetics ***(7)***. While the position of such charges may affect sequence discrimination ***(6)*** it is a general observation that binding is enhanced with at least up to 5 lysine residues per decamer bis-PNA (Nielsen unpublished). Furthermore, charged PNAs bind with increased specificity at elevated ionic strength ***(6)***.

Other factors may also serve to either inhibit or enhance triplex invasion. These include the topology of the DNA and DNA dynamics. Unrestrained DNA supercoiling was found to enhance the rate of triplex invasion by two orders of magnitude at 140 m*M* KCl using a decamer bis-PNA containing 5 positive charges ***(8)***. In another report transcription was shown to catalyze PNA triplex invasion. Transient exposure of a single-stranded target in the "transcription bubble" was suggested as the most probable cause of the observed increase in triplex invasion ***(12)***. Thus, a multitude of factors may coalesce to alleviate the inhibition by salt on triplex invasion under in vivo conditions.

1.1.2. Triplex-Invasion Complex as a Scaffold for Added Features

Recently some new complexes have been developed that are based on the triplex-invasion strategy. The PD-loop ***(13,14)*** exemplifies the use of triplex-invasion complex as a scaffold for the acquisition of new features. In PD-loop, two bis PNA molecules are used to unwind the DNA located in between their targets, which then becomes accessible for binding an oligonucleotide.

1.2. Duplex Invasion

A special case of invasion complex is provided by the duplex-invasion complex formed between homo-purine PNA and a complementary homo-pyrimidine DNA target (**Fig. 1**) ***(15)***. This complex

is much less stable than triplex-invasion complexes and was for example too labile to be analyzed by electrophoretic mobility shift analysis (EMSA). The complex involves an internal Watson-Crick hybridised PNA-DNA duplex and a displaced noncomplementary DNA strand. The low stability of duplex-invasion complexes thus underscores the importance of a Hoogsteen-bound PNA strand in triplex-invasion complexes. More stable duplex-invasion complexes, however, are formed if the DNA target is negatively supercoiled, and in particular if a PNA conjugated to a cationic peptide is employed ***(16)***.

1.3. Double Duplex Invasion

The requirement for a homopurine stretch in the DNA using a triplex-invasion strategy limits the probability for finding suitable targets in a gene of interest. Double duplex invasion solves this by allowing targeting ~ 80% of all sequences, the requirement being the presence of a sufficient number of A-T base pairs (>50%) in the DNA. So-called pseudo complementary PNA molecules are used for strand invasion ***(17)***. These PNAs carry diaminopurine-thiouracil "base pairs" substituted for A-T base pairs to destabilize the competing PNA-PNA duplex by steric interference (**Fig. 3**). The resulting invasion complexes contain two PNA-DNA Watson-Crick base-paired duplexes and thus the entire structure can be written PNA-DNA/PNA-DNA.

1.4. Triplex Formation

Under certain circumstances PNA may bind dsDNA in the DNA major groove without displacement of the noncomplementary DNA strand (**Fig. 1**) ***(18,19)***. This occurs via formation of PNA·DNA-DNA triplexes in which the single PNA strand is bound through Hoogsteen hydrogen bonds. The DNA Watson-Crick hydrogen bonds are preserved. This complex is similar to the conventional triple helix motif formed between homo-pyrimidine oligonucleotides and a cognate purine dsDNA target. Formation of PNA·DNA-DNA triplexes appear to be most stable for homopyrimidine PNA molecules with a high cytosine content ***(19)***.

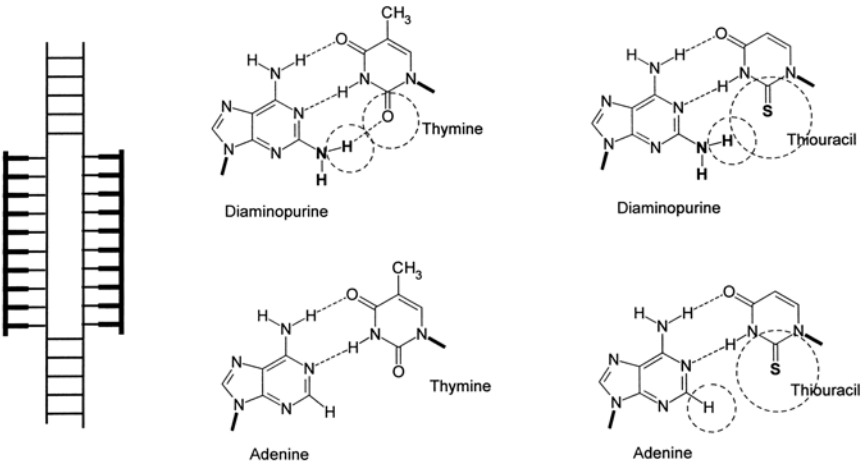

Fig. 3. Interactions in a double duplex invasion complex. Left, double duplex invasion complex. Right: Favorable (diaminopurine-thymine, adenine-thymine, adenine-thiouracil) and unfavorable (diaminopurine-thiouracil) base pairs with the indicated nucleobases and nucleobase analogs.

1.5. Electrophoretic Mobility Shift Assay (EMSA)

EMSA is a simple yet very informative way of obtaining qualitative and quantitative information about PNA/dsDNA interactions. The local denaturation of DNA occurring on DNA duplex invasion provides a hinge or kink, which strongly retards the mobility of DNA in gels (**Fig. 4**) ***(20)***. Such anomaly in migration has been well documented for bent DNA sequences ***(21)***. Often the DNA band shifts to a single new position on the gel, facilitating a straightforward distinction between bound and unbound species. The transformation of free DNA into bound DNA can be followed using a fixed incubation time and variable PNA concentrations. The parameter ψKd can then be obtained and used to evaluate the binding efficiency of different PNAs under a given set of conditions. Alternatively, a fixed PNA concentration may be employed and binding can then be followed over time for determination of the association rate constant.

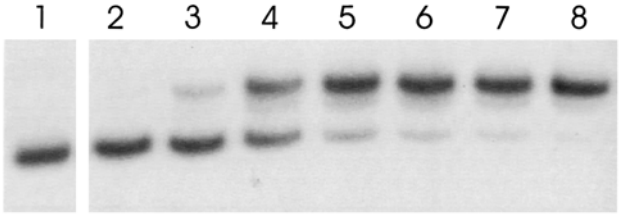

Fig. 4. PNA binding to dsDNA measured by electrophoretic mobility shift analysis. Mono-PNA363 (H-Lys2-TTCTTCTTTT-NH2) was incubated with dsDNA containing the cognate target as described (Methods) and analyzed by PAGE. The following PNA concentrations were used: lane 1 (w/o), lane 2 (0.2 μ*M*), lane 3 (0.4 μ*M*), lane 4 (0.7 μ*M*), lane 5 (1.4 μ*M*), lane 6 (3 μ*M*), lane 7 (6 μ*M*) lane 8 (12 μ*M*).

1.6. Structural Isomers

In some cases multiple bandhifts are observed upon bis-PNA triplex invasion ***(11,22)***. Formation of structural isomers is a cause of such migration differences ***(23)***. One complication to the use of bis-PNA rather than mono-PNA lies in the path of the bis-PNA ethylene glycol linker. It was found that the trajectory of this linker could project around either the targeted (complementary) strand or around the displaced (noncomplementary) DNA strand. Alternatively, it may thread in between the two DNA strands. Moreover, two bis-PNAs may bind to a single DNA target, each using only one of their PNA moieties. However, why only some bis-PNA molecules appear to form structural isomers upon triplex invasion is unknown. Perhaps they all do so but we are unaware of it because of limitations in our probing techniques.

1.7. Chemical Probing

A number of reagents have been used to detect PNA binding to dsDNA. The base-specific probes permanganate ($KMnO_4$) and dimethyl sulphate (DMS) are most useful. Another base-specific probe, diethyl pyrocarbonate, has a lower signal-to-noise ratio but is nevertheless also quite useful because it probes differently than do

$KMnO_4$ and DMS. Finally enzymatic probes such as S1 nuclease ***(24)*** and DNaseI ***(18)*** have been used but these probes require rather low pH (S1) or do not provide single base-pair resolution (DNaseI).

The sequence of events in a typical probing experiment includes (*1*) formation of the relevant PNA/dsDNA complex and verification of the extent of triplex invasion using EMSA, (*2*) probing of the complex, and (*3*) analysis of interaction specificity using high-resolution sequencing gels and phosphorimaging or autoradiography.

1.7.1. Permanganate Probing

Permanganate oxidizes the 5,6-double bond of exposed thymine residues and subsequent alkaline treatment catalyzes specific DNA cleavage at such reacted sites ***(25)***. While dsDNA is relatively resistant to oxidation by $KMnO_4$, PNA triplex invasion greatly perturbs the DNA structure, generally leaving thymine-rich DNA regions in a single strand-like conformation, which is sensitive to $KMnO_4$ oxidation. A local increase of permanganate reactivity is thus an indicator of PNA triplex invasion (**Fig. 5**).

Other elements, including cruciform structures and H-DNA, may produce similar probing results. However, formation of these structures requires specific sequences and DNA superhelical strain as a driving force for their formation. Moreover, $KMnO_4$ probing yields single base-pair resolution so it is easy to correlate the identity of the PNA target with the location of increased permanganate sensitivity based on a sequence ladder.

1.7.2. Dimethyl Sulphate Probing

DMS methylates the N7 position of guanine (and to a much lesser extent N3 of adenine) in double-stranded DNA and subsequent alkali treatment cleaves the DNA at such reacted sites ***(26)***. Protection from DMS methylation indicates that a ligand employs this base position for binding. Using homopyrimidine PNAs, protection from DMS methylation was used to demonstrate PNA "Hoogsteen" binding in the dsDNA major groove via the N7 position of guanine (**Fig. 6**) ***(3)***.

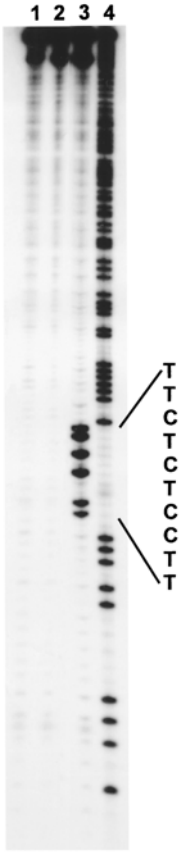

Fig. 5. $KMnO_4$ probing of triplex invasion-complex. Autoradiograph showing the reactivity towards permanganate of a triplex invasion complex. PNA745 [H-Lys2-TTCCTCTCTT-(eg1)3-TTCTCTCCTT-LysNH2] was incubated with a 254-bp *Eco*RI-*Pvu*II restriction fragment containing the cognate target and after triplex invasion probed with potassium permanganate as described in the methods section. Lane 1 (no PNA + $KMnO_4$), lane 2 (control, no PNA and no permanganate probing), lane 3 (triplex invasion complex + $KMnO_4$), lane 4 (A/G sequence marker). Adapted with permission from, ***(23)***.

1.7.3. Diethyl Pyrocarbonate Probing

Diethylpyrocarbonate (DEPC) reacts with the N7 (and also N3) position of purine residues (A>G) resulting in carbethoxylation and

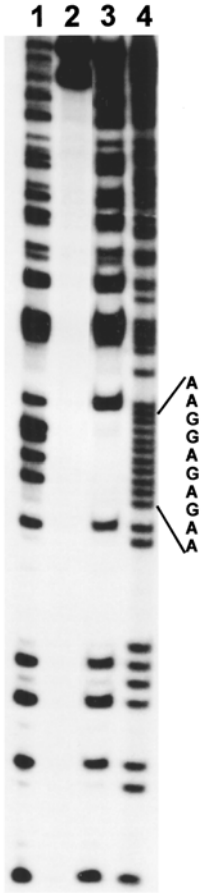

Fig. 6. DMS probing of triplex-invasion complex. Autoradiograph showing the reactivity towards DMS of a triplex invasion complex. PNA745 (*see* **Fig. 5**) was incubated with a 159-bp *Hin*dIII-*Pvu*II fragment containing the complementary target and the triplex-invasion complex formed was probed with DMS as described in the methods section: Lane 1 (control, no PNA + DMS), lane 2 (control, no PNA and no DMS probing), lane 3 (triplex invasion complex + DMS), lane 4 (A/G sequence marker). Adapted with permission from **ref.** ***(23)***.

ring-opening. Alkaline treatment leads to strand scission at DEPC modified sites ***(27,28)***. DEPC does not react very vividly with dsDNA but reacts more strongly with single-stranded DNA. DEPC

probing has been used to demonstrate PNA·DNA/DNA duplex invasion ***(15)***. On incubating homopurine duplex-forming PNA with dsDNA containing a cognate target, the noncomplementary ("A-rich") DNA strand became reactive towards DEPC indicative of strand-invasion.

2. Materials

1. Homopyrimidine PNA at 10-fold the desired final concentration (typically 10–100 μ*M*) in ddH_2O.
2. Appropriately ^{32}P-end-labeled DNA fragment.
3. ddH_2O.
4. 10% (v/v) dimethyl sulphate (20X stock) freshly prepared by dilution in ddH_2O.
5. DNA elution buffer: 0.5 *M* NH_4-acetate, 1 m*M* EDTA).
6. FA-buffer: 80% deionized formamide, 10 m*M* EDTA, 0.25% xylene cyanol FF, 0.25 bromphenol blue.
7. Heating blocks for 37°C and 90°C incubation.
8. 20 m*M* $KMnO_4$ (20X stock).
9. 6X Native loading buffer: 43.5% glycerol, 0.25% xylene cyanol FF, 0.25% bromphenol blue.
10. Polymerase chain reaction (PCR) thermocycler.
11. Phosphorimager or autoradiography.
12. 10% Piperidine in H_2O.
13. 5–10% Native polyacrylamide gels: 30:1 in acrylamide to bisacrylamide.
14. 10% Sequencing gels containing 7 *M* urea: 20:1 in acrylamide to bisacrylamide.
15. Potassium acetate ethanol: (2%/96% w/v).
16. 2X primer extension buffer: 40 m*M* Tris-HC1, pH 8.4, 100 m*M* KCl, 10 m*M* $MgCl_2$, 0.5 m*M* each of dATP, dCTP, dGTP, and dTTP.
17. Pure supercoiled plasmid DNA with a relevant target.
18. Clean scalpel.
19. Sephadex G-25 column.
20. Speed-vac.
21. Stop buffer: 1.5 *M* sodium acetate, 1 *M* 2-mercaptoethanol, pH 7.0.
22. 10 U/μL T4-Kinase: LifeTechnologies.

23. 1X TAE: 40 m*M* Tris-acetate, 1 m*M* EDTA.
24. 5 U/µL Taq DNA polymerase (LifeTechnologies).
25. TBE: 90 m*M* Tris-borate, 2 m*M* EDTA.
26. 100 m*M* Tris-HCl, pH 7.5.
27. 96% Ethanol.
28. 70% Ethanol (optional).

3. Methods

The protocols described below include EMSA, chemical probing in solution and *in situ* in gel slices using DMS and permanganate and finally primer extension analysis of PNA binding.

3.1. PNA

PNA is synthesized and purified as described ***(29)*** and stored as a lyophillized powder at 4°C. Stock solutions are commonly made 10–100 µ*M* in ddH_2O and stored in aliquots at –20°C (*see* **Note 1**).

3.2. Triplex Invasion Analyzed by EMSA

Triplex invasion is usually performed under pseudo first-order binding conditions, i.e., using a PNA concentration that is much higher than the DNA concentration and therefore the free PNA concentration is roughly constant throughout the experiment. Typically very few nano grams of DNA are used in a binding reaction and under such circumstances it is advantageous to employ ^{32}P-radiolabeled DNA to facilitate subsequent analysis. Alternatively, gel-stains including ethidium bromide and ZybrGreen may be used to detect DNA complexes but these detection methods generally have lower sensitivity. DNA fragments with sizes up to ~0.5 kb are convenient for EMSA. Larger DNA fragments can be used but their utility depend on the actual DNA/dsDNA system employed and must be determined empirically in each case (*see* **Note 2**).

1. Dissolve ^{32}P-radiolabeled DNA (100–200 dps) in 16 µL ddH_2O (*see* **Note 3**).
2. Add 2 µL 10X buffer (*see* **Note 4**).

3. Add 2 µL of PNA at 10-fold the desired final concentration.
4. Incubate for the desired length of time and temperature (*see* **Note 5**).
5. Add 4 µL 6X native loading buffer and quencher (optional) (*see* **Note 6**).
6. Analyze an aliquot of each sample on 5–10% native TBE buffered polyacrylamide gels (*see* **Note 7**).
7. Expose the gel to phosphorimaging or autoradiography.

3.3. Permanganate Probing of PNA/dsDNA Complex

1. Form a complex between PNA and dsDNA using the desired PNA and approx 250–500 dps of ^{32}P-endlabeled DNA fragment in a final volume of 20 µL as described in **Subheading 3.2.** (*see* **Note 8**).
2. Add 1 µL 20 m*M* $KMnO_4$ to obtain a final permanganate concentration of 1 m*M* and incubate for 15 s at room temperature (*see* **Note 9**).
3. Add 10 µL stop buffer.
4. Add 60 µL 96% ethanol and collect the DNA by centrifugation at 13,000*g* for 15 min.
5. Remove supernatant completely and rinse pellet using 70% ethanol (optional).
6. Dissolve DNA in 100 µL 10% piperidine and incubate at 90°C for 20 min.
7. Lyophilize sample in a speed-vac.
8. Add 20 µL ddH_2O and re-lyophilize sample to remove traces of piperidine.
9. Resuspend DNA in 8 µL FA-buffer.
10. Denature the DNA at 90°C for 2 min and then chill the tubes on ice.
11. Analyze an aliquot of each sample using 10% polyacrylamide gels containing 7 *M* Urea.
12. Expose gel to phosphorimaging or autoradiography.

3.4. DMS Probing of PNA/dsDNA Complex (see Note 10)

1. Form a complex between PNA and dsDNA using the desired PNA and approx 250–500 dps of ^{32}P-endlabeled DNA fragment in a final volume of 20 µL as described in **Subheading 3.2.** (*see* **Note 8**).
2. Add 1 µL 10% (v/v) DMS to obtain a final concentration of 0.5% and incubate for 10 s at room temperature.
3. Add 10 µL stop buffer.

4. Add 60 µL 96% ethanol and collect precipitated DNA by centrifugation at 13,000*g* for 15 min.
5. Remove supernatant completely and rinse pellet using 70% ethanol (optional).
6. Dissolve DNA in 100 µL 10% piperidine and incubate at 90°C for 20 min.
7. Lyophilize sample in a speed-vac.
8. Add 20 µL ddH_2O and re-lyophilize sample to remove traces of piperidine.
9. Resuspend DNA in 8 µL FA-buffer (*see* **Note 11**).
10. Denature the DNA at 90°C for 2 min and then chill the tubes on ice.
11. Analyze an aliquot of each sample using 10% polyacrylamide gels containing 7 *M* Urea.
12. Expose gel to phosphorimaging or autoradiography.

3.5. In Situ Chemical Probing of Triplex Invasion Complexes in Gel Slices

1. Produce a complex between PNA and dsDNA using the desired PNA and approx 250–500 dps of ^{32}P-endlabeled DNA fragment as described in **Subheading 3.2.**
2. Separate the relevant species employing 5–10% native PAGE (include naked dsDNA as a control).
3. Localize the relevant species by autoradiography and excise the complexes with a scalpel taking care to minimize the amount of gel material.
4. Crush the gel slice by centrifugation through a p2 Gilson pipetman tip (13,000*g*, 2 min).
5. Probing.
   a. Permanganate probing Add 200 µL 1 m*M* $KMnO_4$, incubate for 1 min and terminate reaction with 100 µL stop buffer.
   b. DMS Probing. Add 100 µL 0.5% (v/v) dimethyl sulphate, 100 m*M* sodium phosphate pH 7.0, and incubate for 15 s. Terminate the reaction by addition of 50 µL stop buffer.
6. Add 400 µL DNA elution buffer and elute DNA overnight at room temperature.
7. Spin sample for 20 min at 13,000*g* and withdraw supernatant to another tube. Avoid transferring gel material.

8. Add 1.2 mL 96% ethanol and collect precipitated DNA by centrifugation at 13,000*g* for 15 min.
9. Remove supernatant completely and rinse pellet using 70% ethanol (optional).
10. Dissolve DNA in 100 µL 10% piperidine and incubate at 90°C for 20 min.
12. Lyophilize sample in a speed-vac.
13. Add 20 µL ddH_2O and re-lyophilize sample to remove traces of piperidine.
14. Resuspend DNA in 8 µL FA-buffer (*see* **Note 11**).
15. Denature the DNA at 90°C for 2 min and then chill the tubes on ice.
16. Analyze an aliquot of each sample using 10% polyacrylamide gels containing 7 *M* Urea.
17. Expose the gel to phosphorimaging or autoradiography.

3.6. Primer Extension

1. Form a triplex-invasion complex using the relevant PNA and 50 ng of DNA (typically supercoiled or other topomeric forms) in the desired buffer in a final volume of 20 µL.
2. Add 1 µL 20 m*M* $KMnO_4$ and incubate for 15 s at room temperature (*see* **Note 9**).
3. Add 10 µL stop buffer (1.5 *M* sodium acetate, 1 *M* 2-mercaptoethanol, pH 7.0).
4. Add 60 µL 96% ethanol and collect precipitated DNA by centrifugation at 13,000*g* for 15 min.
5. Remove supernatant completely and rinse pellet using 70% ethanol (optional).
6. Dissolve DNA in 50 µL 2X primer extension buffer (as recommended by the manufacturer or 40 m*M* Tris-HC1, pH 8.4, 100 m*M* KCl, 10 m*M* $MgCl_2$, 0.5 m*M* dATP, dCTP, dGTP and dTTP).
7. Add 0.5–1 pmole (~1500 dps) primer labeled at the 5'-terminus with [γ-32P]ATP using T4 Kinase (*see* **Note 12**).
8. Add water to 100 µL.
9. Add 1 unit Taq DNA polymerase and run a primer extension program using a PCR thermocycler. Include 20–30 cycles of denaturation, annealing and elongation (*see* **Note 13**).
10. Precipitate DNA using 300 µL potassium acetate:ethanol (2/96% w/v).

11. Resuspend DNA in 8 µL FA-buffer (*see* **Note 11**).
12. Denature the DNA at 90°C for 2 min and chill the tubes on ice.
13. Analyze an aliquot of each sample using 10% polyacrylamide gels containing 7 *M* urea.
14. Expose gel to phosphorimaging or autoradiography.

4. Notes

1. To prevent PNA aggregation, avoid multiple freeze-thaw cycles of stock solutions. Polyethylene or polypropylene tubes should always be used, siliconized whenever possible. Avoid using polystyrene because PNA sticks to this material.
2. To facilitate quantitative analyses, the DNA should always be purified using the same procedure, because trace amounts of contaminants (such as polyamines or divalent metal ions) may greatly alter binding efficiency.
3. Sub-microgram DNA quantities are generally required if nonisotopic detection strategies are employed.
4. For triplex invasion we typically use final buffer concentrations of 10 m*M* Tris-HCl or 10 m*M* sodium phosphate, pH 7.0.
5. We use 37°C and 1 h of incubation as a starting point for triplex invasion reactions.
6. If a kinetic experiment is performed using relatively short incubation times it is important to rapidly quench the PNA triplex-invasion reaction. This can be done by adding salt, molar surplus of an oligonucleotide complementary to the PNA or by flash-freezing the samples in dry ice/ethanol.
7. If a triplex-invasion complex contains Hoogsteen-hydrogen bonded cytosines, TAE buffer pH 7.0 may be substituted for TBE because protonization of the cytosine N3 is favoured at lower pH. Note that TAE is a relatively poor buffer, which may require re-circulation using a peristaltic pump or simply occasional exchange.
8. DNA fragments for chemical probing are ideally 100–500 bp long with the PNA target positioned 20–200 from the label.
9. Aqueous solutions of $KMnO_4$ are reduced upon storage. Two signs indicate that the $KMnO_4$ solution should be replaced: a) the clear deep purple color changes to a more reddish- and eventually brown-color and b) the background C-specific reaction increases.
10. DMS is very toxic and should be handled in a suitable fume-hood using appropriate protective clothing. An inactivating agent (e.g.,

10% aqueous ammonia) should be used for disposal of tips and other DMS-contaminated items.

11. Molar surplus of a quencher oligonucleotide complementary to the PNA employed should be included if the PNA is targeted to the DNA strand containing the radiolabel. This will eliminate electrophoretic mobility shifts in sequencing gels.
12. ^{32}P-labeled primers can be purified using sephadex G-25 columns.
13. A primer extension program consisting of 30 cycles of denaturation, annealing, and extension is typical. Template denaturation is performed at 95°C for 4 min in the first step and 30 s in subsequent steps. Annealing and elongation times and temperatures must be determined empirically. Some thermocyclers can run a temperature gradient thus facilitating a simple optimization of the annealing temperature. Elongation is usually performed around 70°C.

References

1. Bentin, T. and Nielsen, P. E. (1999) Nomenclature, in *Peptide Nucleic Acids. Protocols and Applications* (Nielsen, P. E. and Egholm, M., eds.), Horizon Scientific Press, pp. 256.
2. Nielsen, P. E., Egholm, M., Berg, R. H., and Buchardt, O. (1991) Sequence-selective recognition of DNA by strand displacement with a thymine-substituted polyamide. *Science* **254,** 1497–1500.
3. Nielsen, P. E., Egholm, M., and Buchardt, O. (1994) Evidence for $(PNA)_2$/DNA triplex structure upon binding of PNA to dsDNA by strand displacement. *J. Mol. Recog.* **7,** 165–170.
4. Egholm, M., Christensen, L., Dueholm, K. L., Buchardt, O., Coull, J., and Nielsen, P. E. (1995) Efficient pH-independent sequence-specific DNA binding by pseudoisocytosine-containing bis-PNA. *Nucleic Acids Res.* **23,** 217–222.
5. Demidov, V. V., Yavnilovich, M. V., Belotserkovskii, B. P., Frank-Kamenetskii, M. D., and Nielsen, P. E. (1995) Kinetics and mechanism of polyamide ("peptide") nucleic acid binding to duplex DNA. *Proc. Natl. Acad. Sci. USA* **92,** 2637–2641.
6. Kuhn, H., Demidov, V. V., Frank-Kamenetskii, M. D., and Nielsen, P. E. (1998) Kinetic sequence discrimination of cationic bis-PNAs upon targeting of double-stranded DNA. *Nucleic Acids Res.* **26,** 582–587.
7. Griffith, M. C., Riesen, L. M., Greig, M. J., Lesnik, E. A., Sprankle, K. G., Griffey, R. H., et al. (1995) Single and bis peptide nucleic

acids as triplexing agents: binding and stoichiometry. *J. Am. Chem. Soc.* **117,** 831–832.

8. Bentin, T. and Nielsen, P . E. (1996) Enhanced peptide nucleic acid binding to supercoiled DNA: possible implications for DNA "breathing" dynamics. *Biochemistry* **35,** 8863–8869.
9. Cherny, D. Y., Belotserkovskii, B. P., Frank-Kamenetskii, M. D., Egholm, M., Buchardt, O., Berg, R. H., and Nielsen, P. E. (1993) DNA unwinding upon strand-displacement binding of a thymine-substituted polyamide to double-stranded DNA. *Proc. Natl. Acad. Sci. USA* **90,** 1667–1670.
10. Peffer, N. J., Hanvey, J. C., Bisi, J. E., Thomson, S. A., Hassman, C. F., Noble, S. A., and Babiss, L. E. (1993) Strand-invasion of duplex DNA by peptide nucleic acid oligomers. *Proc. Natl. Acad. Sci. USA* **90,** 10,648–10,652.
11. Kurakin, A., Larsen, H. J., and Nielsen, P. E. (1998) Cooperative strand displacement by peptide nucleic acid (PNA). *Chem. Biol.* **5,** 81–89.
12. Larsen, H. J. and Nielsen, P. E. (1996) Transcription-mediated binding of peptide nucleic acid (PNA) to double-stranded DNA: sequence-specific suicide transcription. *Nucleic Acids Res.* **24,** 458–463.
13. Bukanov, N. O., Demidov, V. V., Nielsen, P. E., and Frank-Kamenetskii, M. D. (1998) PD-loop: a complex of duplex DNA with an oligonucleotide. *Proc. Natl. Acad. Sci. USA* **95,** 5516–5520.
14. Broude, N. E., Demidov, V. V., Kuhn, H., Gorenstein, J., Pulyaeva, H., Volkovitsky, P., et al. (1999) PNA openers as a tool for direct quantification of specific targets in duplex DNA. *J. Biomol. Struct. Dyn.* **17,** 237–244.
15. Nielsen, P. E. and Christensen, L. (1996) Strand displacement binding of a duplex forming homopurine PNA to a homopyrimidine duplex DNA target. *J. Am. Chem. Soc.* **118,** 2287–2288.
16. Zhang, X., Ishihara, T., and Corey, D. R. (2000) Strand invasion by mixed base PNAs and a PNA–peptide chimera. *Nucleic Acids Res.* **28,** 3332–3338.
17. Lohse, J., Dahl, O., and Nielsen, P. E. (1999) Double duplex invasion by peptide nucleic acid: A general principle for sequnce specific targeting of double stranded DNA. *Proc. Natl. Acad. Sci. USA* **96,** 11,804–11,808.
18. Praseuth, D., Grigoriev, M., Guieysse, A.-L., Pritchard, L. L., Harel-Bellan, A., Nielsen, P. E., and Hélene, C. (1996) Peptide nucleic acids

directed to the promoter of the α-chain of the interleukin-2 receptor. *Biochim. Biophys. Acta* **1309,** 226–238.

19. Wittung, P., Nielsen, P., and Nordén, B. (1997) Extended DNA-recognition repertoire of peptide nucleic acid (PNA): PNA-dsDNA triplex formed with cytosine-rich homopyrimidine PNA. *Biochemistry* **36,** 7973–7979.
20. Kim, J.-H., Kim, K.-H., Møllegaard, N. E., Nielsen, P. E., and Koo, H. S. (1999) The helical periodicity of $(PNA)_2$-DNA triplexes in strand displacement complexes. *Nucleic Acids Res.* **27,** 2842–2847.
21. Crothers, D. M. and Drak, J. (1992) Global features of DNA structure by comparative gel electrophoresis. *Methods Enzymol.* **212,** 46–71.
22. Kuhn, H., Demidov, V. V., Nielsen, P. E., and Frank-Kamenetskii, M. D. (1999) An experimental study of mechanism and specificity of PNA binding to duplex DNA. *J. Mol. Biol.* **286,** 1337–1345.
23. Hansen, G. I., Bentin, T., Larsen, H. J., and Nielsen, P. E. (2001) Structural isomers of bis-PNA bound to a target in duplex DNA. *J. Mol. Biol.* **307,** 67–74.
24. Demidov, V., Frank-Kamenetskii, M. D., Egholm, M., Buchardt, O., and Nielsen, P. E. (1993) Sequence selective double strand DNA cleavage by PNA targeting using nuclease S1. *Nucleic Acids Res.* **21,** 2103–2107.
25. Rubin, C. M. and Schmid, C. W. (1980) Pyrimidine-specific chemical reactions useful for DNA sequencing. *Nucleic Acids Res.* **8,** 4613–4619.
26. Maxam, A. and Gilbert, W. (1977) A new method for sequencing DNA. *Proc. Natl. Acad. Sci. USA* **74,** 560–564.
27. Furlong, J. C. and Lilley, D. M. J. (1986) Highly selective chemical modification of cruciform loops by diethyl pyrocarbonate. *Nucleic Acids Res.* **14,** 3995–4007.
28. Scholten, P. M. and Nordheim, A. (1986) Diethyl pyrocarbonate: a chemical probe for DNA cruciforms. *Nucleic Acids Res.* **14,** 3981–3993.
29. Christensen, L., Fitzpatrick, R., Gildea, B., Petersen, K. H., Hansen, H. F., Koch, T., et al. (1995). Solid-phase synthesis of peptide nucleic acids. *J. Pept. Sci.* **1,** 175–183.

7

PNA-Mediated Immobilization of Supercoiled DNA

Thomas Bentin and Peter E. Nielsen

1. Introduction

Chromosomal DNA is constrained into topological domains (reviewed in **ref.** *[1]*), and in the cell DNA enzymatic processes function in this framework. To mimic a chromosomal loop, PNA was recently used to site-specifically immobilize double-stranded (ds) DNA to streptavidin-coated paramagnetic beads, and such torsionally constrained DNA was used as a template for transcription by *Escherichia coli* RNA polymerase (RNAP) *(2)*. In more general terms, immobilized supercoiled DNA could be used as templates for assembly and study of enzymatic complexes that require a supercoiled template and various auxiliary factors such as eukaryotic RNAP II.

1.1. Torsionally Constrained DNA

The present approach for generating torsionally constrained DNA is depicted in **Fig. 1**. The high specificity and stability of PNA/dsDNA triplex invasion complexes is exploited. Triplex-invasion complexes contain an internal PNA·DNA-PNA triplex in which two homopyrimidne PNA strands hybridize to the complementary DNA strand by combined Watson-Crick and Hoogsteen base pairing.

From: *Methods in Molecular Biology, vol. 208: Peptide Nucleic Acids: Methods and Protocols*
Edited by: P. E. Nielsen © Humana Press Inc., Totowa, NJ

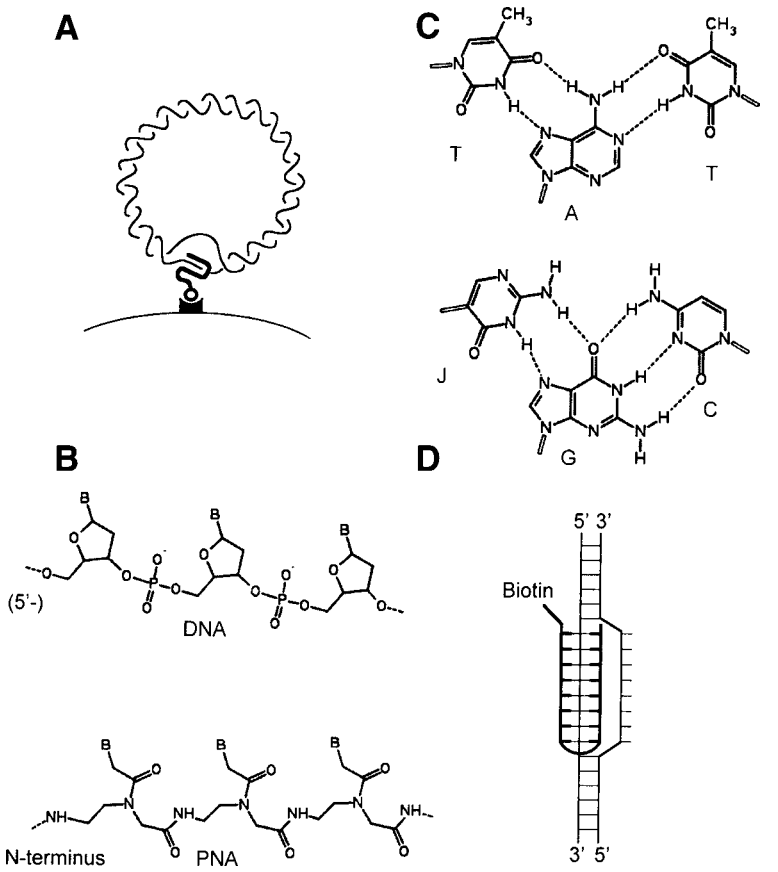

Fig. 1. Structure of PNA and PNA-nucleic acid triplexes. **(A)** Covalently closed circular DNA, for simplicity shown as relaxed circular DNA, bound to streptavidin-beads via a triplex invasion complex. Note that only one DNA strand has to be fixed to prevent rotation of the other. **(B)** Comparison of DNA and PNA chemical structures (B = nucleobase). **(C)** Hydrogen bonds formed in the T·A-T and J·G-C PNA·DNA-PNA base triplets (J = pseudoisocytosine). **(D)** PNA·DNA-PNA/DNA triplex-invasion complex containing bis-PNA equipped with a biotin moiety. In (A) and (D) the PNA is drawn in bold.

Consequently, the noncomplementary DNA strand is displaced as a loop. Supercoiled DNA, or in principle any DNA molecule containing a suitable target, can be attached to streptavidin-coated paramagnetic beads (streptavidin-beads) using biotin-conjugated PNA *(3)*. This preserves the topology of the plasmid (except that

approximately one supercoil is lost due to DNA unwinding at the triplex-invasion complex ***[4]***), and furthermore torsionally constrains the DNA because the streptavidin-bead is too large to rotate within the DNA circle.

We use biotin-conjugated homopyrimidine bis-PNAs for triplex invasion and a plasmid in which the complementary target has been cloned. After triplex invasion, which is carried out using a molar excess of PNA, the nonbound PNA is removed by gel electrophoresis. This somewhat tedious procedure is routinely carried out using up to ~40 μg of supercoiled DNA but larger amounts of DNA are probably best purified using other methods such as gel-filtration fast-performance liquid chromatography (FPLC). Purified triplex-invasion complex is then bound to streptavidin coated beads and non-bound material is removed by extensive washing.

The specificity of the various interactions in the streptavidin-bead/triplex-invasion complex should be examined to ensure well-defined assemblies. To investigate the specificity and efficiency of PNA triplex invasion, and the accessibility of the biotin-PNA conjugate for streptavidin binding, we used electrophoretic mobility shift analysis (EMSA). PNA1021 [biotin-(eg1)3-TTJTTJTTTT-Lys-aha-Lys-aha-Lys-TTTTCTTCTT-Lys-NH2] (*see* **Note 1**) was incubated with a mixture of two plasmids containing (pTEC) or not containing [pT3T7(-)], a cognate PNA target. The DNA was subsequently restriction digested and electrophoresed (**Fig. 2**). The DNA fragment harboring the PNA target displayed reduced mobility after incubation with PNA. The DNA fragments that lack a target were entirely unaffected even at the highest PNA concentration. This suggested that complete and sequence-specific triplex-invasion could be obtained. Further, addition of streptavidin to pre-formed triplex-invasion complex super-shifted the band representing the PNA bound DNA fragment showing that the biotin-PNA conjugate was intact and accessible for streptavidin binding (**Fig. 2A**).

The analysis showed quantitative binding of PNA1021 to its target but this type of analysis examines only a fraction of the DNA. To analyze PNA binding along the entire length of the DNA molecule the triplex-invasion complex can be digested with a frequent

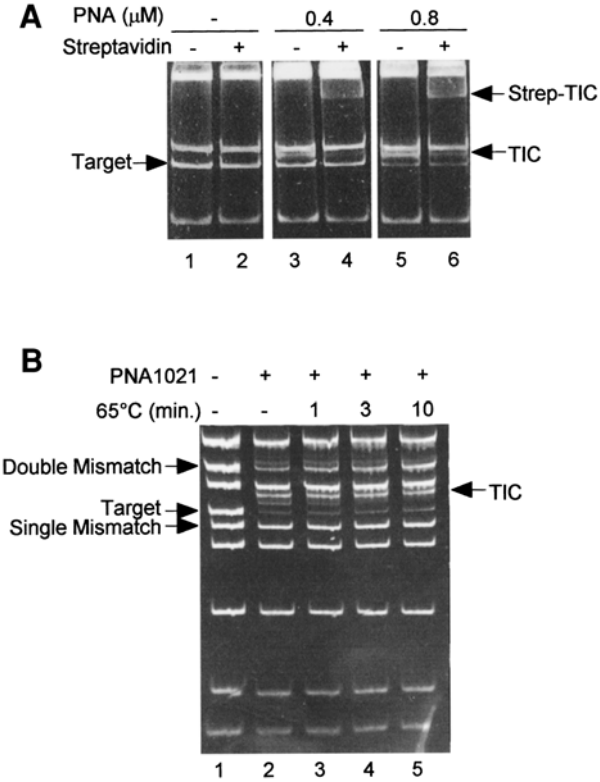

Fig. 2. Specificity of triplex invasion and function of the PNA-biotin conjugate. **(A)** EMSA was used to monitor triplex-invasion and to examine the accessibility of the biotin-PNA conjugate for streptavidin binding. One μg of DNA (0.5 μg pTEC [containing a PNA target] and 0.5 μg pT3T7(-) ([w/o a PNA target]) was incubated with PNA1021 as described (Methods). Following triplex invasion, the DNA was restriction digested with *Eco*RI and *Pvu*II. Each sample was split in two and streptavidin was added as indicated. The samples were analyzed by 6% native PAGE and ethidium bromide staining. The PNA concentrations used is indicated. The different species are indicated with arrows: TIC (Triplex invasion complex), Strep-TIC (streptavidin-triplex invasion complex). **(B)** Specificity of triplex invasion and heat denaturation of mismatched complexes as examined by EMSA. Triplex invasion was conducted using 10 μg of pT3T7 and PNA1021. The triplex invasion complex involving supercoiled DNA was gel-purified and buffer adjusted for restriction digestion. An aliquot (~1 μg) was subject to 65°C for the indicated period of time, restriction digested with *Hae*III, and analyzed. The fragment carrying the fully matched target and those containing single or double-mismatch-binding sites are indicated.

cutter enzyme, e.g., *Hae*III, thereby generating restriction fragments of suitable sizes for EMSA (**Fig. 2B**).

As the example shows, binding occurred to the fragment containing the cloned PNA target. However, two additional DNA fragments changed mobility indicating that nontarget binding also occurred. The mismatched complexes can be gradually dissociated upon heating at 65°C. In contrast, the fully matched triplex-invasion complex should be relatively unaffected by the treatment as expected from the high Tm values for the corresponding PNA·DNA-PNA triplex (in this case T_m >90°C). The entire plasmid except for small fragments encompassing less than 5% of the total template was analyzed in this manner. Furthermore, inspection of the sequence revealed that in the fraction of DNA that could not be examined by this procedure, possible PNA targets contained three or more mismatches. Triplex invasion at such sites should be very inefficient ***(5)***. Thus by using a combination of triplex invasion, gel-purification, and thermal dissociation of nonspecific PNA·DNA-PNA/DNA complexes, it is possible to obtain intact plasmids containing a single site-specifically formed triplex-invasion complex.

2. Materials

1. 2X triplex invasion buffer: 20 m*M* Tris-HC1, 20 m*M* NaCl, pH 7.5.
2. 1X elution buffer/low ionic strength wash: 10 m*M* Tris-HCl, 0.1 m*M* EDTA, pH 7.5.
3. 10–100 µ*M* Biotin-conjugated homopyrimidine bis-PNA in ddH_2O (Perseptive).
4. Pure supercoiled plasmid DNA with a relevant target.
5. 1% Agarose gel.
6. Dialysis tubing boiled in 0.1 m*M* EDTA.
7. 65°C Heating block.
8. 10% Sodium dodecyl sulfate (SDS).
9. 5 *M* NaCl.
10. Streptavidin at 10 µg/µL in ddH_2O. Store flash-frozen in liquid N_2 in aliquots.
11. 6–10% Polyacrylamide gel (30:1 in acrylamide to bisacrylamide).
12. Streptavidin-beads (Dynal or Roche).

13. Mixing wheel.
14. High ionic strength wash solution: 10 m*M* Tris-HCl, 0.1 m*M* EDTA, pH 7.5, + 1/10 vol 5 *M* NaCl.

3. Methods

1. Ten µg supercoiled plasmid DNA containing the relevant PNA target in ddH_2O (*see* **Note 2**).
2. Add 10 µL 10 µ*M* PNA in ddH_2O to establish a triplex invasion complex (*see* **Note 3**).
3. Add 50 µL 20 m*M* Tris-HCl, 20 m*M* NaCl, pH 7.5.
4. Adjust the volume to 100 µL using ddH_2O.
5. Incubate for 1 h at 37°C.
6. Purify the triplex-invasion complex involving supercoiled DNA on a 1% agarose gel (*see* **Note 4**).
7. Dissociate nonspecific PNA/dsDNA complexes by incubation at 25°C below the T_m of the corresponding PNA·DNA-PNA triplex for 10 min (*see* **Note 5**).
8. Wash the streptavidin-beads (20 µL per 0.5–1 µg DNA) once by separating the supernatant from the beads using a magnet followed by addition of 10 m*M* Tris-HCl, pH 7.5, 0.1 *M* EDTA to restore the original volume. Separate beads and wash solution using the magnet and discharge the latter.
9. Add triplex invasion complex and adjust the NaCl concentration to 0.5 *M* in the original volume and incubate for 1 h at room temperature. (Maintain the beads in suspension, e.g., by using a Dynal mixing wheel.)
10. Wash the beads three times in the original streptavidin-bead volume with high and then low (10 m*M* Tris-HCl, pH 7.5, 0.1 m*M* EDTA) ionic strength buffers. Resuspend the streptavidin beads in the desired volume of 10 m*M* Tris, pH 7.5, 0.1 m*M* EDTA (*see* **Note 6**).
11. Examine the extent of DNA-PNA-streptavidin complex formation by heat denaturation of an aliquot in 1% SDS at 80–90°C for 10 min. Analyze the supernatant on a 1% agarose gel. Remember to include a reference of known quantity.

4. Notes

1. The symbols used for PNA molecules are as follows: eg1 (8-amino-2,6-doixaoctanoic acid), Lys (lysine), aha (aminohexanoic acid), J (pseudo-isocytosine ***[6]***).

2. Our standard triplex-invasion reaction contains 1 µg DNA/10 µL total volume. This works well up to at least 40 µg DNA.
3. A titration is necessary to establish the PNA concentration that gives 100% triplex invasion because this depends on the PNA employed as well as the actual DNA preparation.
4. Purification of triplex-invasion complex involving supercoiled DNA is routinely done by electro-transfer of the relevant band onto a dialysis membrane. The nucleic acids are then eluted using 10 m*M* Tris-HCl pH 7.5, 0.1 *M* EDTA. Note that DNA does not stick very well to dialysis tubing so it is important to transfer the membrane from the gel to a tube in a gentle, yet swift manner.
5. After thermal denaturation of nonspecific PNA/dsDNA complexes it is prudent to examine the degree and specificity of triplex invasion. This can conveniently be done by EMSA. Aliquots of the triplex invasion reaction (~1 µg) from before and after thermal denaturation is digested with *Hae*III and analyzed by 6–10% PAGE. Remember to run along unbound DNA as a control.
6. EDTA chelates divalent metal ions such as magnesium and thus inhibits enzymatic reactions that require such metals. Thus if the immobilized DNA is aimed for further enzymatic processing, EDTA can be entirely omitted or the metal ion concentration adjusted accordingly.

Acknowledgments

The Danish Medical Research Council and the Lundbeck Foundation supported this work.

References

1. Sinden, R. R. (1994) DNA Structure and Function. Academic Press, San Diego.
2. Bentin, T. and Nielsen, P. E. (2002) In vitro transcription of a torsionally constrained template. *Nucleic Acids Res.* **30,** 803–809.
3. Demidov, V.V., Cherny, D., Kurakin, A.V., Yavnilovich, M.V., Malkov, V.A., Frank-Kamenetskii, M. D., et al. (1995) Electron microscopy mapping of oligopurine tracts in duplex DNA by peptide nucleic acid (PNA) targeting. *Nucleic Acids Res.* **22,** 5218–5222.
4. Cherny, D. Y., Belotserkovskii, B. P., Frank-Kamenetskii, M. D., Egholm, M., Buchardt, O., et al. (1993). DNA unwinding upon strand-displacement binding of a thymine-substituted polyamide to double-stranded DNA. *Proc. Natl. Acad. Sci. U SA* **90,** 1667–1670.

5. Demidov, V. V., Yavnilovich, M. V., Belotserkovskii, B. P., Frank-Kamenetskii, M. D., and Nielsen, P. E. (1995) Kinetics and mechanism of polyamide ("peptide") nucleic acid binding to duplex DNA. *Proc. Natl. Acad. Sci. USA* **92,** 2637–2641.
6. Egholm, M., Christensen, L., Dueholm, K. L., Buchardt, O., Coull, J., and Nielsen, P. E. (1995) Efficient pH independent sequence-specific DNA binding by pseudoisocytosine-containing bis-PNA. *Nucleic Acids Res.* **23,** 217–222.

8

PNA Openers and Their Applications

Vadim V. Demidov and Maxim D. Frank-Kamenetskii

1. Introduction

Pyrimidine peptide nucleic acids (PNAs) are able to sequence-specifically invade corresponding target sites of double-stranded DNA (dsDNA) yielding P-loops ***(1)***. Within P-loops (also known as invasion triplexes) two PNA oligomers form a triplex with the complementary purine site of one DNA strand, leaving the other DNA strand displaced (**Fig. 1A**). To enhance strand-invasion efficiency, PNA clamps or bis-PNAs are often used. In them, a pair of pyrimidine PNA oligomers with mirror-symmetrical sequences are covalently connected via a flexible linker ***(1–4)***. Linkage of two PNA oligomers offers the possibility to expediently design one PNA strand preferentially for Watson-Crick binding and the other PNA strand preferentially for Hoogsteen binding ***(2)***, as it is required by the structure of PNA_2-DNA triplexes ***(3,4)***. This also reduces the order of the strand-displacement reaction by one, therefore accelerating the PNA invasion ***(1,4)***.

When two individual P-loops are located close to each other, they merge, yielding an extended P-loop (**Fig. 1B**). As a result, a larger open region emerges inside dsDNA in which both strands of duplex DNA are locally exposed ***(5–7)***. In so doing, a pair of bis-PNAs act

From: *Methods in Molecular Biology, vol. 208: Peptide Nucleic Acids: Methods and Protocols*
Edited by: P. E. Nielsen © Humana Press Inc., Totowa, NJ

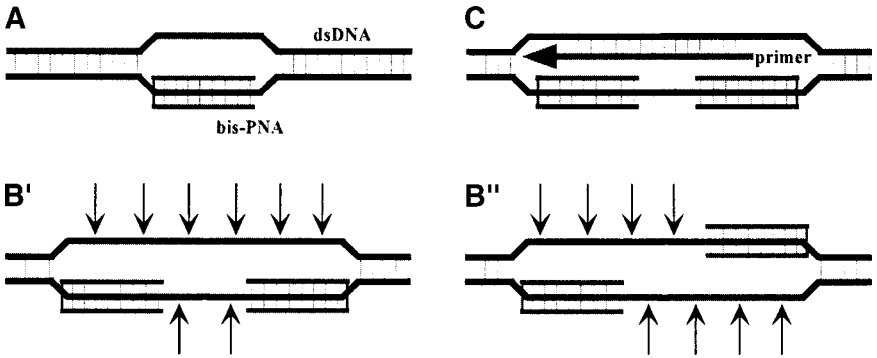

Fig. 1. Looped structures formed within dsDNA by bis-PNA openers: single P-loop (**A**), merged or extended P-loop (**B'** and **B''**) and PD-loop (**C**). PNA openers may bind the same (**B'**) or opposite (**B''**) dsDNA strands; exposed DNA stretches can be attacked by ssDNA-specific nuclease (arrows); oligonucleotide probe can serve as a primer to be extended by DNA polymerase (arrowhead) via strand displacement.

as openers of the DNA double helix allowing the Watson-Crick binding of various probes to designated dsDNA targets *(8–14)* via formation of so-called PD-loops and related complexes (**Fig. 1C**). In addition, this locally exposed region can provide an access of DNA-processing enzymes, like single-stranded DNA (ssDNA)-specific endonucleases or DNA polymerases, to chosen DNA sequences *(5–7,15)*. The use of PNA openers is demonstrated here by two applications, PNA-assisted site-directed rare cleavage of dsDNA with ssDNA-specific endonucleases *(5)* and nondenaturing dsDNA sequencing via design of an artificial primosome *(15)*. Note that the detailed protocols of two other applications of PNA openers, duplex DNA capture and topological labeling, have been recently published elsewhere *(16,17)*.

DNA rare cleavage is used in gene mapping and cloning procedures. The artificial restriction enzyme systems, like methylation-based Rec-A assisted restriction endonuclease (RARE) *(18,19)* and PNA-assisted rare cleavage (PARC) *(20–24)* approaches are complementary to the scarce arsenal of natural rare cutters. PNA openers provide with one more, rather direct approach, which does not require the pre-methylation step intrinsic in the "Achilles' heel"

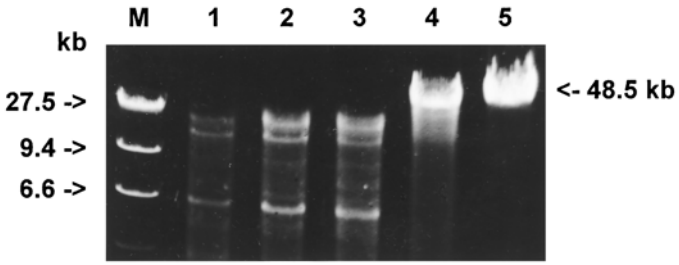

Fig. 2. Use of PNA openers for rare fragmentation of 48.5 kb wild-type λ DNA with mung bean nuclease (the experiment was done in collaboration with Dr. Peter E. Nielsen). Bis-PNA $(T_7)_2$ was used as a single opener to expose the double-target site, $T_7N_6T_7$, located at 6.1 kb within λ DNA. The conditions were as follows: samples of 0.1 μg DNA and 10 μ*M* PNA were incubated for 10 min in TE buffer (buffer A) at 37°C. Then they were digested at room temperature with 20 U nuclease in buffer B (30 m*M* NaAc, 50 m*M* NaCl, 1 m*M* $ZnSO_4$, 0.1% of glycerol, pH 4.5) for 20, 10, and 5 min (lanes 1, 2, and 3, respectively). Lane 4: 10 min incubation with nuclease without PNA pretargeting; lane 5: intact λ DNA; lane M: λ DNA-*Hin*dIII digest used as a size marker (note that the largest, 27.5 kb fragment consists in fact of two end-located λ DNA-*Hin*dIII fragments, 4.4- and 23.1-kb-long, annealed via the *cos*-termini). Electrophoresis was run in 0.5% agarose gel filled with TBE buffer. The expected 6.1-kb-long dsDNA fragment is clearly observed following the quantitative PNA-assisted cleavage; two other major longer fragments, ~17.7- and 24.7-kb-long, could be explained by λ DNA cleaving in one more site, T_5NT_7, located at 23.8 kb. Although this target exhibits a small space between PNA-binding sites, one of which is in addition shorter, it is flanked by AT-rich sequence (87% AT), that becomes easily accessible for nuclease digestion after the PNA nearby binding.

strategy employed by both aforementioned techniques. In this alternative method ***(5)***, ssDNA-specific endonucleases are used, as shown schematically in **Fig. 1B**, to selectively cut the two stretches of ssDNA exposed inside the extended P-loop by PNA invasion. Consequently, the double-stranded break is quantitatively generated at a chosen dsDNA site, thus yielding the corresponding duplex DNA fragment (*see* **Fig. 2** as an example). Besides strand-displacement ability, PNA resistance against nucleases ***(25,26)*** is essential for this method, too.

Use of PNA openers together with the primer and DNA polymerase capable of strand-displacement activity makes it possible to initiate, via the PD-loop formation, the primer-extension reaction directly within linear dsDNA (shown schematically in **Fig. 1C**). Combination of this approach with isothermal dideoxy chain termination protocol *(27)* results in a high-quality sequencing ladder of several hundred nucleotides even for long DNA templates: an example of sequence read obtained by this kind of DNA sequencing for the case of ~50 kb dsDNA is presented in **Fig. 3** *(15)*. Therefore, the method promises to perform sequencing on the excessive background of unrelated DNA to evade target purification procedures. Nondenaturing sequencing of dsDNA also avoids complications caused by folded loops that may form in denatured or ssDNA templates, but not in linear dsDNA templates. We anticipate that sequencing of that type could be used in various DNA diagnostics, e.g., in SNP analysis.

Note that a typical site that is capable of forming the extended P-loops shown in **Fig. 1B**,**C** includes 20 bp or more. Therefore, its sequence is normally unique in the whole genome. Nevertheless, such sites are met every 400–500 base pairs in a random DNA sequence, on average *(8,15–17)*. Thus, normally every genome of interest must contain many of them.

2. Materials

2.1. Materials Common to Methods 1 and 2

1. A pair of appropriate [7 + 7]- and/or [8 + 8]-mer bis-PNAs with achiral and uncharged "classical" *N*-(2-aminoethyl)glycine backbone and pseudoisocytosine instead of cytosine in one half *(2,28,29)* is required. Incorporation of two–three positively charged terminal lysines and use of noncharged linker of three eg1 units (eg1 = 8-amino-3,6-dioxaoctanoic acid *[2]*) is recommended for better stability and specificity of PNA-DNA complex *(28,29)*.
2. Duplex DNA carrying the 20–25 bp target site that is able to form the extended P-loop. This site must contain the 7–8-bp-long oligopurine PNA-binding sites positioned on the same or different

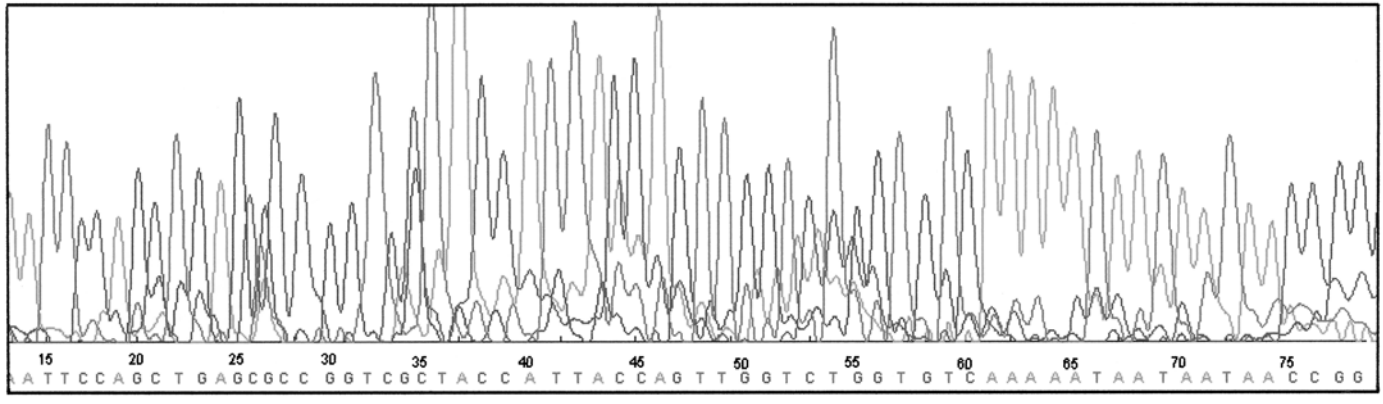

Fig. 3. Application of PNA openers for nondenaturing sequencing of 46.4 kb λ-plasmid recombinant DNA prior digested by *Aat*II. Recombinant DNA was obtained by cloning of the 2.7 kb plasmid carrying the insert, $AGAG_2A_2GCTACTG_2AG_2AGA$, into the *Eco*RI site of the 43.7 kb lgt11 vector. This site is able to form the extended P-loop upon targeting with a pair of PNA openers, $TJTJ_2T_2J$-CT_2C_2TCT and $TCTC_2TC_2$-J_2TJ_2TJT (J denotes pseudoisocytosine), and PD-loop after addition of oligonucleotide primer, fluorescein-$GAG_2A_2GCTACTG_2AG$. To improve the sequence read with Sequenase, fluorescein-labeled dATP was added to all dNTP/ddNTP mixtures (Pharmacia Biotech AutoRead sequencing kit). A part of the sequence data thus obtained is shown, as it was detected using A.L.F. DNA Sequencer (~200 bp of λ-plasmid DNA was sequenced in total).

DNA strands and separated by up to 10 bp of mixed purine-pyrimidine sequence.

3. PNA-binding buffer (buffer A): 25 m*M* MES, pH 6.5 or 10 m*M* Na-phosphate, pH 6.8, or any other appropriate low-salt buffer solution at neutral pH (addition of 1 m*M* EDTA is recommended to bind bivalent cations). Typically, the concentration of the target DNA is much less than the PNA concentration yielding the pseudo-first-order binding kinetics.
4. Sephadex G-50 (Sigma) or microspin G-50 column (Pharmacia Biotech) for removing unbound PNA and replacing the buffer A by one of the two reaction buffers (*see* below) via gel filtration.

2.2. Materials Specific to Method 1

1. Any ssDNA-specific endonucleases like S1 and mung bean nucleases (Promega, New England BioLabs, Gibco-BRL, or Roche MB).
2. Nuclease reaction buffer (buffer B): 30–50 m*M* NaAc, 50–250 m*M* NaCl, 1–2 m*M* $ZnSO_4$, 0.1% of glycerol, pH 4.1–4.6.
3. 500 m*M* EDTA, pH 8.0, or 10% sodium dodecyl sulfate (SDS) to stop nuclease digestion (×10 solutions).
4. Regular or pulsed-field electrophoretic equipment.

2.3. Materials Specific to Method 2

1. Pharmacia Biotech AutoRead sequencing kit ***(30)***, which includes the primer-annealing buffer (buffer C): 100 m*M* Tris-HCl, 10 m*M* $MgCl_2$ pH 7.5; primer-extension buffer (buffer D): 15 m*M* citric acid, 15 m*M* dithiothreitol (DTT), 2 m*M* $MnCl_2$, pH 7.5; and four dNTP/ddNTP mixtures: A-mix (×10 solution) - 5 μ*M* ddATP, 1 m*M* dATP, 1 m*M* dCTP, 1 m*M* dTTP, 1 m*M* 7-deaza-dGTP, 50 m*M* NaCl, 40 m*M* Tris-HCl, pH 7.6; composition of C-mix, G-mix and T-mix is the same as that of A-mix except ddATP, is replaced by ddCTP, ddGTP and ddTTP, respectively.
2. Primer: usually 15–20 nt 5'-fluorescein-labeled oligonucleotide complementary to the displaced DNA strand.
3. *Escherichia coli* SSB protein (Promega): ~1 μg per sample.
4. DNA sequencing equipment, e.g., automated A.L.F. DNA Sequencer (Pharmacia Biotech).

3. Methods

The binding of PNA openers (0.1–10 μ*M* in dependence on the binding affinity of bis-PNAs) to target dsDNA (0.1–10 μg in dependence on the DNA length) with formation of extended P-loops is a common step to both methods. For this, incubate dsDNA with PNAs in the buffer A at 37°C for an appropriate time to complete the formation of PNA-DNA invasion complexes. Remove an excess of unbound PNA at room temperature by gel filtration through a Sephadex G-50 column equilibrated with the buffer required at the next step.

3.1. Method 1: Site-Directed Rare Cleavage of Duplex DNA (see Notes 1–10)

1. Take 5–20 μL of the DNA sample (pre-targeted by PNA openers) in the buffer B.
2. Add ~10 U mung bean or ~100 U of S1 nuclease and incubate ~30 min at room temperature or 37°C.
3. Stop the nuclease digestion of DNA by addition of SDS or EDTA with subsequent cooling of samples on ice.
4. If necessary, check the DNA cleavage by gel electrophoresis.

3.2. Method 2: Nondenaturing Sequencing of Duplex DNA (see Notes 1–4 and 11–14)

1. Take 5–20 μL of the DNA sample (pre-targeted by PNA openers) in buffer C.
2. To form the PD-loop, add 20–40 pmol primer and incubate for 15 min at 37°C.
3. Transfer the sample into buffer D by gel filtration at room temperature.
4. Add DNA polymerase and SSB protein, and perform the Sanger dideoxy sequencing reactions at 37°C using AutoRead sequencing kit and corresponding procedures (omitting the denaturing and neutralization steps).
5. Register sequencing results using corresponding sequencing equipment.

4. Notes

1. If necessary, shorter bis-PNAs could also be used as openers (our unpublished data; *see* also **ref.** ***[31]***). However, their binding may not be stable enough and use of [7 + 7]-mer bis-PNAs or longer is recommended, when possible.
2. PE Biosystems (Framingham, MA) offers custom synthesis of bis-PNA oligomers using automated protocols. Manual PNA synthesis (up to 20 μ*M*) is less expensive and could be advantageous for small-budget laboratories with synthetic experience ***(32–34)***.
3. Use of siliconized micro/mini test tubes is recommended to avoid a loss of PNA via its binding to the tube's surface.
4. The PNA binding could be quantitatively checked by the gel-shift assay ***(1,35,36)***, if required.
5. In case of cutting the large DNAs significant background cleavage can be observed due two reasons: a) the formation of mismatched PNA-DNA complexes exposing incorrect, unwanted sites; and b) the nonspecific background cleavage of dsDNA regardless of the PNA targeting.
6. The formation of mismatched PNA-DNA complexes can be minimized by the choice of optimal targeting conditions ***(31)***. Key factors are: PNA quantity and/or time of PNA targeting as well as salt concentration and pH of buffer A. If, by some reason, the selectivity of dsDNA targeting by PNA openers under optimized experimental conditions is still not satisfactory, preferential dissociation of mismatched DNA-PNA complexes at elevated temperature or alkaline pH can be used to enhance the selectivity ***(37–39)***.
7. If nonspecific background cleavage is large, reduce the amount of nuclease. Also, use of mung bean nuclease instead of S1 can decrease the nonspecific background ***(5)***, especially in case of longer DNA molecules. Although both nucleases have similar catalytic activities, it is known that S1 nuclease effectively cleaves the DNA strand opposite a nick in the duplex, whereas the mung bean nuclease can only attack a gap consisting of a few nucleotides. Prior treatment of target dsDNA by DNA ligase to heal ligatable nicks may eliminate part of background cleavage, too.
8. Note that higher salt concentration of buffer B and lower temperature may also reduce the background cleavage though at the expense of a less efficient digest.

9. Usually, the mung bean nuclease allows to accomplish the method on sub-megabase DNAs (*see* **Fig. 2** as an example). Still, inherent in this method nonspecific dsDNA cleavage, that is higher than in case of the methylation-based approaches ***(18–24)***, most probably will limit its use for selective cutting of megabase DNAs. Note that high molecular-weight DNAs have to be embedded in agarose plugs for preserving their integrity. In that case, all manipulations should be adapted to handle with gel pieces as in ***(18–24)***.
10. Though we have no experience with other ssDNA-specific endonucleases, they (e.g., nuclease P1; Roche MB) could also be of potential use.
11. Modified T7 DNA polymerase (Sequenase), Klenow enzyme or any other DNA polymerase with strand-displacement activity can be used.
12. Digestion of longer dsDNA templates with appropriate restriction enzyme into ~1 kb fragments may enhance quality of the sequencing data.
13. Addition of 1 m*M* fluorescein-labeled dATP to dNTP/ddNTP mixtures (×10 solution) and some variation of dNTP: ddNTP ratio may significantly improve sequence read.
14. Other primer-extension applications, e.g., incorporation of multiple labels into primer to amplify the hybridization signal ***(9,15)*** and mapping of DNA-binding ligands ***(40)***, can be done in a similar way.

Acknowledgment

We dedicate this chapter to Professor Yurii S. Lazurkin, a pioneer of DNA biophysics and the elder in the PNA field, in connection with his 85th birthday.

References

1. Demidov, V. V., Yavnilovich, M. V., Belotserkovskii, B. P., Frank-Kamenetskii, M. D., and Nielsen, P. E. (1995) Kinetics and mechanism of polyamide ("peptide") nucleic acid binding to duplex DNA. *Proc. Natl. Acad. Sci. USA* **92,** 2637–2641.
2. Egholm, M., Christensen, L., Dueholm, K. L., Buchardt, O., Coull, J., and Nielsen, P. E. (1995) Efficient pH-independent sequence-specific DNA binding by pseudoisocytosine-containing bis-PNA. *Nucleic Acids Res.* **23,** 217–222.

3. Betts, L., Josey, J. A., Veal, J. M., and Jordan, S. R. (1995) A nucleic acid triple helix formed by a peptide nucleic acid-DNA complex. *Science* **270,** 1838–1841.
4. Griffith, M. C., Risen, L. M., Greig, M. J., Lesnik, E. A., Sprankle, K. G., Griffey, R. H., et al. (1995) Single and bis peptide nucleic acids as triplexing agents: binding and stoichiometry. *J. Am. Chem. Soc*. **117,** 831–832.
5. Demidov, V., Frank-Kamenetskii, M. D., Egholm, M., Buchardt, O., and Nielsen, P. E. (1993) Sequence selective double strand DNA cleavage by PNA targeting using nuclease S1. *Nucleic Acids Res*. **21,** 2103–2107.
6. Nielsen, P. E., Egholm, M., Berg, R. H., and Buchardt, O. (1993) Peptide nucleic acids (PNAs): potential anti-sense and anti-gene agents. *Anti-Cancer Drug Design* **8,** 53–63.
7. Nielsen, P. E., Egholm, M., and Buchardt, O. (1994) Evidence for $(PNA)_2$/DNA triplex structure upon binding of PNA to dsDNA by strand displacement. *J. Mol. Recog*. **7,** 165–170.
8. Bukanov, N. O., Demidov, V. V., Nielsen, P. E., and Frank-Kamenetskii, M. D. (1998) PD-loop: a complex of duplex DNA with an oligonucleotide. *Proc. Natl. Acad. Sci. USA* **95,** 5516–5520.
9. Broude, N. E., Demidov, V. V., Kuhn, H., Gorenstein, J., Pulyaeva, H., Volkovitsky, P., et al. (1999) PNA openers as a tool for direct quantification of specific targets in duplex DNA. *J. Biomol. Struct. Dynam*. **17,** 237–244.
10. Kuhn, H., Demidov, V. V., and Frank-Kamenetskii, M. D. (1999) Topological links between duplex DNA and a circular DNA single strand. *Angew. Chem. Int. Ed.* **38,** 1446–1449.
11. Kuhn, H., Demidov, V. V., and Frank-Kamenetskii, M. D. (2000) An earring for the double helix: assembly of topological links comprising duplex DNA and a circular oligodeoxynucleotide. *J. Biomol. Struct. Dyn*. **11,** 221–225.
12. Kuhn, H., Demidov, V. V., Gildea, B. D., Fiandaca, M. J., Coull, J. M., and Frank-Kamenetskii, M. D. (2001) PNA beacons for duplex DNA. *Antisense Nucleic Acid Drug Dev.* **11,** 265–270.
13. Kuhn, H., Demidov, V. V., Coull, J. M., Gildea, B. D., Fiandaca, M. J., and Frank-Kamenetskii, M. D. (2002) Hybridization of DNA and PNA molecular beacons to single-stranded and double-stranded DNA targets. *J. Am. Chem. Soc.* **124,** 1097–1103.
14. Kuhn, A., Demidov, V. V., and Frank-Kamenetskii, M. D. (2002) Rolling-circle amplification under topological constraints. *Nucleic Acids Res.* **30,** 574–580.

15. Demidov, V. V., Broude, N. E., Lavrentyeva-Smolina, I. V., Kuhn, H., and Frank-Kamenetskii, M. D. (2001) An artificial primosome: design, function, and applications. *ChemBioChem.* **2,** 133–139.
16. Demidov, V. V., Bukanov, N. O., and Frank-Kamenetskii, M. D. (2000) Duplex DNA capture. *Curr. Issues Mol. Biol.* **2,** 31–35.
17. Demidov, V. V., Kuhn, H., Lavrentyeva-Smolina, I. V., and Frank-Kamenetskii, M. D. (2001) Peptide nucleic acid-assisted sequence-specific topological labeling of duplex DNA. *Methods* **23,** 123–131.
18. Ferrin, L. J. and Camerini-Otero, R. D. (1991) Selective cleavage of human DNA: RecA-assisted restriction endonuclease (RARE) cleavage. *Science* **254,** 1494–1497.
19. Ferrin, L. J. and Camerini-Otero, R. D. (1994) Long-range mapping of gaps and telomeres with RecA-assisted restriction endonuclease (RARE) cleavage. *Nature Genet.* **6,** 379–383.
20. Veselkov, A. G., Demidov, V. V., Frank-Kamenetskii, M. D., and Nielsen, P. E. (1996) PNA as a rare genome-cutter. *Nature* **379,** 214.
21. Veselkov, A. G., Demidov, V. V., Nielsen, P. E., and Frank-Kamenetskii, M. D. (1996) A new class of genome rare cutters. *Nucleic Acids Res.* **24,** 2483–2488.
22. Izvolsky, K. I., Demidov, V. V., Bukanov, N. O., and Frank-Kamenetskii, M. D. (1998) Yeast artificial chromosome segregation from host chromosomes with similar lengths. *Nucleic Acids Res.* **26,** 5011–5012.
23. Demidov, V. V. and Frank-Kamenetskii, M. D. (1999) PNA directed genome rare cutting, in *Peptide Nucleic Acids: Protocols & Applications* (Nielsen, P. E. and Egholm, M., eds.), Horizon Scientific Press, Wymondham, UK, pp. 175–186.
24. Izvolsky, K. I., Demidov, V. V., Nielsen, P. E., and Frank-Kamenetskii, M. D. (2000) Sequence-specific protection of duplex DNA against restriction and methylation enzymes by pseudocomplementary PNAs. *Biochemistry* **39,** 10,908–10,913.
25. Demidov, V. V., Potaman, V. N., Frank-Kamenetskii, M. D., Egholm, M., Buchardt, O., Sönnichsen, S. H., and Nielsen, P.E. (1994) Stability of peptide nucleic acids in human serum and cellular extracts. *Biochem. Pharmacol.* **48,** 1310–1313.
26. Uhlmann, E., Peyman, A., Breipohl, G., and Will, D. W. (1998) PNA: synthetic polyamide nucleic acids with unusual binding properties. *Angew. Chem. Int. Ed.* **37,** 2796–2823.
27. Sanger, F., Nicklen, S., and Coulson, A. R. (1977) DNA sequencing with chain-terminating inhibitors. *Proc. Natl. Acad. Sci. USA* **74,** 5463–5467.

28. Kuhn, H., Demidov, V. V., Frank-Kamenetskii, M. D., and Nielsen, P. E. (1998) Kinetic sequence discrimination of cationic bis-PNAs upon targeting of double-stranded DNA. *Nucleic Acids Res.* **26,** 582–587.
29. Kuhn, H., Demidov, V. V., Nielsen, P.E., and Frank-Kamenetskii, M. D. (1999) An experimental study of mechanism and specificity of peptide nucleic acid (PNA) binding to duplex DNA. *J. Mol. Biol.* **286,** 1337–1345.
30. AutoRead sequencing kit instructions XY-056-00-05, rev. 2 (1996) Pharmacia Biotech.
31. Armitage, B., Koch, T., Frydenlund, H., Ørum, H., Batz, H.-G., and Schuster, G. B. (1997) Peptide nucleic acid-anthraquinone conjugates: strand invasion and photoinduced cleavage of duplex DNA. *Nucleic Acid Res.* **25,** 4674–4678.
32. Norton, J. C., Waggenspack, J. H., Varnum, E, and Corey, D. R. (1995) Targeting peptide nucleic acid-protein conjugates to structural features within duplex DNA. *Bioorg. Med. Chem.* **3,** 437–445.
33. Corey, D. R. (1997) Peptide nucleic acids: expanding the scope of nucleic acid recognition. *Trends Biotechnol.* **15,** 224–229.
34. Koch, T. (1999) PNA oligomer synthesis by Boc chemistry, in *Peptide Nucleic Acids: Protocols & Applications* (Nielsen, P. E., and Egholm, M., eds.), Horizon Scientific Press, Wymondham, UK, pp 21–37.
35. Peffer, N. J., Hanvey, J. C., Bisi, J. E., Thomson, S. A., Hassman, F. C., Noble, S. A., and Babiss, L. E. (1993) Strand-invasion of duplex DNA by peptide nucleic acid oligomers. *Proc. Natl. Acad. Sci. USA* **90,** 10,648–10,652.
36. Demidov, V. V. and Frank-Kamenetskii, M. D. (2001) Sequence-specific targeting of duplex DNA by peptide nucleic acids via triplex strand invasion. *Methods* **23,** 108–122.
37. Demidov, V. V., Yavnilovich, M. V., and Frank-Kamenetskii, M. D. (1997) Kinetic analysis of specificity of duplex DNA targeting by homopyrimidine PNAs. *Biophys. J.* **72,** 2763–2769.
38. Krasil'nikova, M. M. and Veselkov, A. G. (1996) Enhancing the specificity of peptide-nucleic acid binding with DNA. *Mol. Biol.* (translated from *Molekulyarnaya Biologiya* (Russian)) **30,** 226–230.
39. Cherny, D. Y., Belotserkovskii, B. P., Frank-Kamenetskii, M. D., Egholm, M., Buchardt, O., Berg, R. H., and Nielsen, P. E. (1993) DNA unwinding upon strand displacement of binding of PNA to double stranded DNA. *Proc. Natl. Acad. Sci. USA* **90,** 1667–1670.
40. Smolina, I. V., Demidov, V. V., and Frank-Kamenetskii, M. D. (2002) Pausing of DNA polymerase on duplex DNA template due to ligand binding. *J. Mol. Biol.* (submitted).

9

Colorimetric Detection of PNA-DNA Hybridization Using Cyanine Dyes

Miaomiao Wang and Bruce A. Armitage

1. Introduction

The high affinity and sequence selectivity with which peptide nucleic acid (PNA) oligomers bind to complementary DNA and RNA makes them attractive hybridization probes for diagnostics. As is the case for all detection schemes, some type of signaling event is required in order to demonstrate successful hybridization. This chapter focuses on optical detection methods, although electrochemical ***(1)*** and surface plasmon resonance ***(2)*** methods have also been reported. Optical methods are of advantage because of the real-time monitoring capability in standard techniques, such as polymerase chain reaction (PCR), as well as the potential for use in vivo in conjunction with fluorescence microscopy.

Fluorescence is one of the most commonly used methods for detecting hybridization using DNA probes and the same is true for PNA. A number of modifications to the standard PNA structure have provided fluorescence detection schemes. For example, moving the exocyclic amino group of adenine from position 6 to 2 on the purine ring yields 2-aminopurine (2-ap; *see* **Fig. 1** for chemical structures of fluorophores and quenchers used in various formats), which fluoresces at 367 nm (excitation at 307 nm) when incorpo-

From: *Methods in Molecular Biology, vol. 208: Peptide Nucleic Acids: Methods and Protocols*
Edited by: P. E. Nielsen © Humana Press Inc., Totowa, NJ

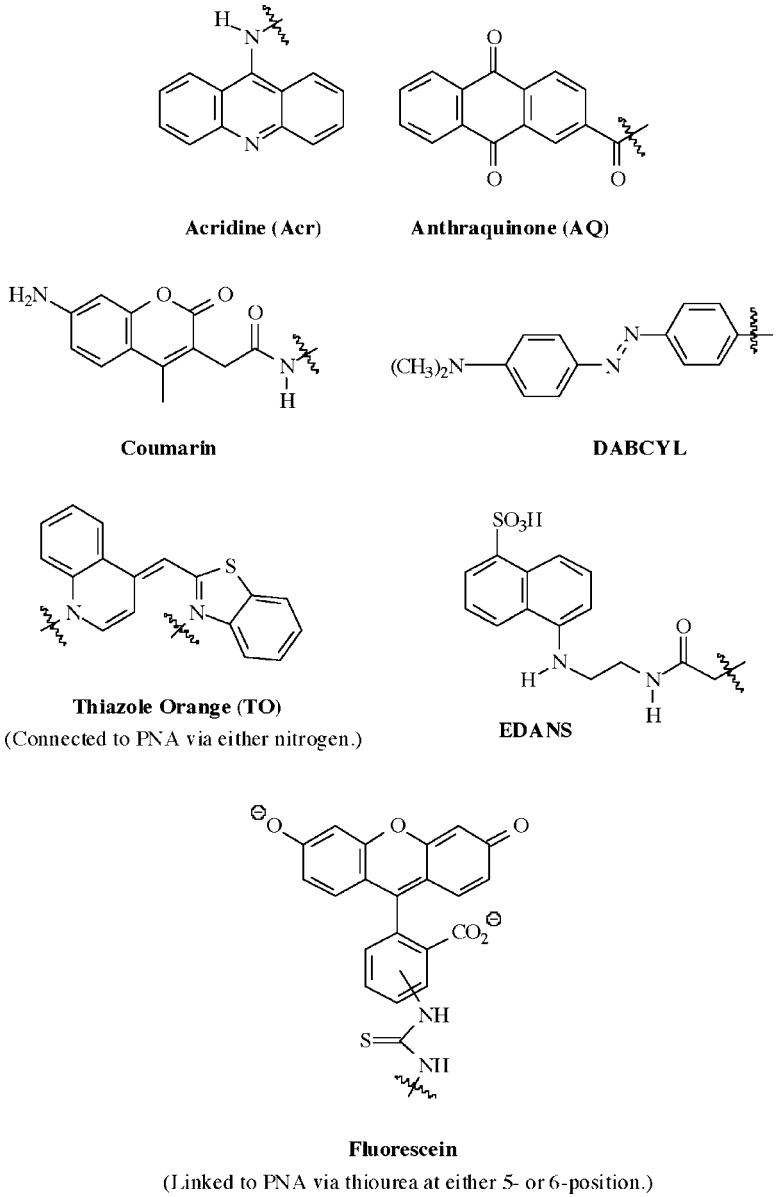

Fig. 1. Chemical structures of fluorophores, quenchers and cyanine dye used in PNA-based DNA detection systems.

rated into PNA. Moreover, when the 2-ap PNA is hybridized to a complementary DNA strand, the fluorescence of the 2-ap is reduced, allowing real-time monitoring of hybridization. This modification

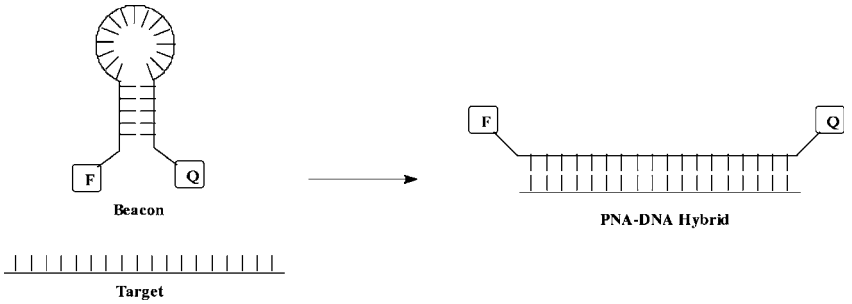

Fig. 2. The molecular beacon concept ([*see* **ref. *5***]). In the hairpin form, the fluorophore (F) and quencher (Q) are close, allowing effective quenching by energy transfer. Upon hybridization, F and Q are separated, relieving quenching.

has been used to measure the kinetics of PNA-DNA hybridization ***(3,4)***. There are three drawbacks to using this technique for detection of hybridization, however. First, substitution of adenine with 2-ap leads to a decrease in thermal stability of 2–3°C. Second, the sensitivity is not particularly high, because the decrease in fluorescence upon hybridization is only 15%. Finally, it is generally easier to detect an increase in fluorescence against a dark background than a decrease against a bright background.

Several methods have been reported that rely on an increase in fluorescence to report hybridization. The first of these is an adaptation of the very successful molecular beacons originally developed for DNA. A molecular beacon is a hairpin DNA with a fluorophore and quencher attached to opposite ends of the hairpin (**Fig. 2**) ***(5)***. This places the fluorophore and quencher at close distance leading to a dark background. When the beacon hybridizes to its target DNA, the hairpin opens, separating the fluorophore and quencher by 30–50 Å and causing a large increase in fluorescence intensity. A similar approach has been taken with PNA, in which a hairpin was designed having an acridine fluorophore and anthraquinone quencher incorporated into the stem such that they would be held in a face-to-face orientation to maximize quenching ***(6)***. The acridine was excited at 417 nm and the spectra from 430–600 nm were recorded. Opening of the PNA hairpin upon hybridization to a

complementary DNA target resulted in a 10-fold increase in fluorescence. However, the hairpin had a significant amount of background fluorescence, which could be due to some fraction of hairpins in which either the acridine or anthraquinone (or both) were not stacked within the stem helix. In addition, this design requires that the two groups be covalently linked to the PNA backbone, rather than to the termini, leading to a significantly more complex synthetic scheme than terminal functionalization.

A chimeric hairpin was also designed in which one side of the stem was a biotinylated DNA while the other side of the stem and the entire loop was composed of PNA ***(7)***. The DNA and PNA components were linked by a disulfide bridge and a coumarin fluorophore and DABCYL quencher were attached to the ends of the PNA and DNA portions of the stem, respectively. The full hairpin was immobilized in streptavidin-coated microtiter plates. Addition of oligonucleotides or PCR amplicons with the target sequence yielded detectable fluorescence enhancements due to hybridization with the beacon and the effect was sequence-specific. The choice of coumarin for the fluorophore was nonideal, given the low quantum yield and tendency of the fluorophore to photobleach; however, DABCYL is a universal quencher ***(8)*** and thus a wide range of fluorophores could be used.

The two examples previously described follow the original molecular beacon design faithfully in terms of utilizing a hairpin secondary structure to minimize fluorescence in the unhybridized state. However, subsequent work illustrated that a specific secondary structure is not essential when using PNA. This is because single-stranded PNAs evidently adopt a collapsed structure in aqueous solution, most likely because of the relatively hydrophobic *N*-[2-aminoethyl]glycine backbone. This structure, although not well-defined, is sufficient to position a fluorophore and quencher in close proximity, leading to quenching in the unhybridized state and relief of quenching upon hybridization. For example, Seitz reported a probe in which the fluorophore was EDANS (a dimethylaminonaphthalene sulfonate derivative) and the quencher was DABCYL ***(9)***. The system was excited at 335nm, and fluorescence from 400–600 nm was observed. Hybridization induced ca. five-fold fluorescence enhancement within

5 min of mixing the probe and target at room temperature. The sensitivity of the assay was limited by the fact that the unhybridized PNA probe had residual fluorescence, which is not surprising because the collapsed conformation of the probe need not place the fluorophore and quencher in direct contact.

PNA-based molecular beacons have been simplified even further through the incorporation of the fluorophore thiazole orange (TO), which is an asymmetric cyanine dye that exhibits a large fluorescence enhancement at 510 nm (excited at 470 nm) when bound to a nucleic acid target ***(10,11)***. By conjugating TO to the N-terminus of the PNA, this so-called "light-up probe" has a much higher sensitivity than the other fluorescence detection systems based on PNA (~50-fold enhancement in fluorescence) ***(12)***. Unfortunately, the background fluorescence can be significant in the light-up probes and is sequence-dependent ***(13)***. (Mixed base sequences have much greater background fluorescence than homopyrimidine PNAs.) The tethered TO fluorophore can evidently bind to the single-stranded PNA ("back-binding") giving the residual fluorescence. Whether the sequence-dependence of the residual fluorescence is due to selectivity in the binding of TO to ssPNA or to sequence-dependent variation in the collapsed secondary structure of the PNA is unresolved. Nevertheless, in addition to the higher sensitivity, the light-up probes benefit from simpler synthetic requirements than the other molecular-beacon designs, which require both a fluorophore and quencher to be incorporated within the same sequence.

Fluorescence polarization can also be used to follow PNA hybridization ***(14)***. When a fluorophore is excited with polarized light, the emission can also be polarized, provided the fluorophore's rotational mobility is restricted on the time scale of fluorescence (usually 1–10 nanoseconds for organic fluorophores). The orientation of the fluorophore dictates the intensity of the emitted light, which is polarized either parallel or perpendicular to the excitation beam polarization. Fluorescence polarization measures the ratio of the two vectors, and thus illustrates the difference in the orientation, which is dependent on the fluorophore's environment. Fluorescein-labeled PNA was used in conjunction with polylysine to amplify the signal. When PNA hybridizes to its DNA target, the motion of

the fluorescein is restricted to some extent, but the difference in polarization relative to unbound PNA is relatively small. However, addition of polylysine results in formation of a PNA-DNA-polylysine complex. With sufficiently high molecular-weight polylysine, the difference in mobility between free and hybridized PNA is amplified, leading to a two-fold increase in fluorescence polarization. With a relatively short PNA 9-mer probe, very good discrimination between a fully matched and single mismatch sequence was achieved. A linear relationship between concentration of target DNA and the fluorescence polarization signal was not evident, so some modification of the system will likely be required to achieve quantitative analysis of DNA.

In contrast to these fluorimetric methods, our group recently reported the use of cyanine dyes as small molecule ligands and colorimetric indicators for PNA-DNA hybrids ***(15)***. The dyes are relatively inexpensive, and since no covalent bond is required to attach the dye to the PNA, unmodified PNA can be used. Given the high cost of custom PNA synthesis and added expense incurred upon modifying the structure, this is a significant advantage. Upon binding to PNA-DNA, the dyes show significant changes in optical properties such as UV-vis absorbance, circular dichroism, and fluorescence. For example, the dye **DiSC2(5)** exhibits a ca. 120 nm shift to shorter wavelength of the main absorption band. This results in an instantaneous color change from blue to purple, providing a simple colorimetric indicator for PNA hybridization. Importantly, **DiSC2(5)** has successfully bound to all sequences tested (ca. 20 different sequences screened). Here we will discuss in greater detail the use of cyanine dyes as indicators for PNA-DNA hybridization. (*See* **Notes 1–3** for factors to consider in designing the PNA probe and selecting the target sequence.)

2. Materials

1. Commercial suppliers of cyanine dyes. A variety of cyanine dyes are available through Aldrich Chemical Company (Milwaukee, WI) and Molecular Probes, Inc (Eugene, OR). **DiSC2(5)** was originally available from both sources, but is now available only from Aldrich. It is quite inexpensive ($25/g) and given the high extinc-

tion coefficient (ε_{651} = 260,000 M^{-1} cm^{-1} in methanol), very little dye is required for most assays (1–10 μ*M* dye concentration in 100–1000 μL total volume).

2. PNA oligomers. Custom-synthesized PNA oligomers are available from PE Biosystems (www.pebio.com). Useful information regarding the design of appropriate PNA sequences is also available at the company's web site.
3. Dye stock solutions. Cyanine dyes exhibit good solubility in methanol and DMSO. Stock solutions containing 1–2 m*M* dye are readily prepared in these solvents. Solutions should be stored in the dark to prevent photobleaching of the dye (*see* **Note 4**). Concentrations can be determined spectrophotometrically using the manufacturer's extinction coefficient (ε_{651} = 260,000 M^{-1} cm^{-1} in methanol for **DiSC2(5)**).

3. Method

3.1. Sample Preparation

Dye binding to PNA-DNA hybrids is virtually instantaneous and yields an immediate visible color change. Thus, the "rate-limiting step" in using **DiSC2(5)** to detect PNA-DNA hybrids will likely be the actual formation of the hybrid. Hybridization can be fast for unstructured, single-stranded targets and in these cases, the PNA and dye can be added according to the following procedure:

1. The DNA target is suspended in aqueous sodium phosphate buffer (10 m*M*, pH 7.0; NaCl and EDTA can also be included without interfering with the dye). The concentration of target can be varied, although we can readily detect 1 μ*M* strand concentration visually. The buffer should also include ca. 10% methanol in order to prevent adsorption of the dye to the walls of the sample container. (A neutral detergent such as Tween-20 can also be used for this purpose. However, anionic detergents such as sodium dodecyl sulfate (SDS) should be avoided because these will compete more favorably than neutral surfactants or cosolvents for binding of the cationic dye.)
2. The desired amount of PNA is pipeted from a stock, aqueous solution and the sample is mixed.
3. The dye is added by pipet or 10 μL syringe from a methanol or dimethyl sulfoxide (DMSO) stock solution and the sample is mixed. A

ratio of one dye per two base pairs of PNA-DNA duplex is usually sufficient to achieve tight binding.

Folding of the DNA into secondary and tertiary structure will impose kinetic barriers to hybridization. In these cases, a preannealing step may be required. This involves mixing of the DNA and PNA following **steps 1** and **2**, then heating to 60–90°C (depending on the stability of the DNA selfstructure) followed by slow cooling to the assay temperature (normally 15°C). The dye can then be added according to **step 3**. (*see* **Note 5**.)

3.2. Detection of Hybridization

Qualitative detection of PNA-DNA hybridization can be made visually, because **DiSC2(5)** undergoes a striking blue-purple color change upon binding. Alternatively, a UV-vis spectrophotometer can be used to record the absorbance spectrum, since the dye exhibits λ_{max} = 648 nm in the buffer and 534 nm when bound to the PNA-DNA (**Fig. 3**). Samples can be prepared in cuvets for standard spectrophotometers or in microtiter plates for use in plate readers. The latter can be particularly useful for parallel screening of many different targets. We have not yet investigated whether quantitative detection of PNA-DNA hybrids is possible with the cyanine dyes.

3.3. Detection of Single-Base Mismatches

The cyanine dyes can give false-positives when the PNA hybridizes to a single-base mismatch target. This is because the high affinity of PNA for DNA allows hybridization even in the event of a mismatch. The high affinity of the dye for PNA-DNA then leads to effective binding. However, we have found that the thermal stability of the dye aggregate is depressed by the mismatch ***(15)***. This effect likely occurs because the mismatch perturbs the regular helical structure of the PNA-DNA hybrid, which negatively impacts the stability of a dye aggregate assembled thereon. Thus, recording "melting curves" at either 648 nm or 534 nm for known matched and mismatched targets will yield different T_m values for the dye aggregates, allowing discrimination between matched and mismatched targets in unknown samples. (It should be noted that the

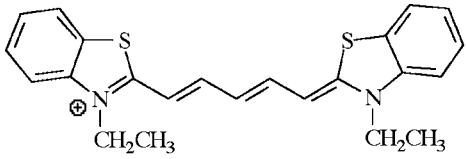

DiSC2(5)

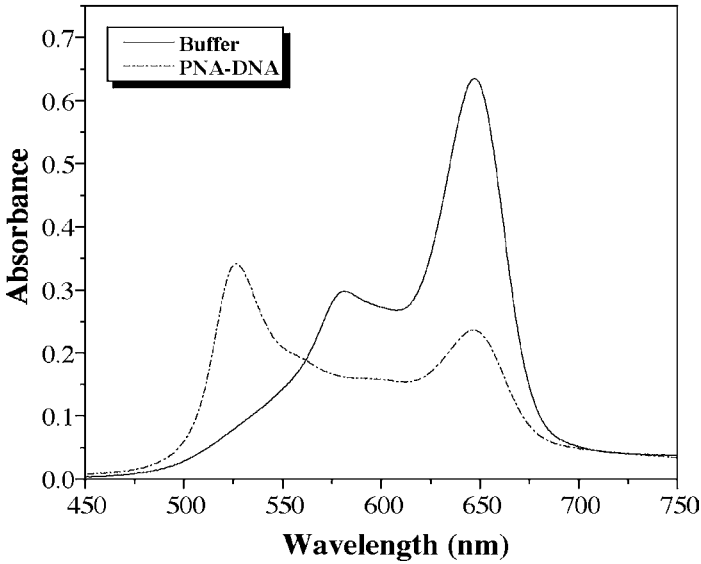

Fig. 3. Chemical structure of colorimetric PNA-DNA indicator **DiSC2(5)** and UV-vis spectra for the dye in buffer (solid line) and in PNA-DNA (dashed line).

melting temperature for the aggregate is usually between 20–30°C, which is well below the melting temperature for the PNA-DNA hybrids.) In these experiments, a sample is prepared as described earlier, heated to 40°C (i.e., above the dye aggregate melting temperature), then cooled to ca. 5–10°C at a rate of 1°C per min. The absorbance at 648 or 534 nm is collected at periodic intervals, such as every 0.5 or 1.0°C. Plotting the absorbance as a function of temperature and then taking the first derivative yields an estimate of the melting temperature of the dye aggregate.

4. Notes

1. Nonspecific binding of the dye. The cyanine dyes studied to date are both cationic and hydrophobic. This leads to their binding to most polyanionic species, including double- and single-stranded DNA. Thus, it would be very difficult to detect a PNA-DNA hybrid in the presence of a large excess of unhybridized DNA. This limitation might be circumvented if a biased PCR procedure is followed in which a relatively short section of only the target strand of a DNA sample is amplified, followed by addition of the PNA and dye for detection.
2. Short PNA-DNA hybrids. We have noted that the affinity of **DiSC2(5)** for PNA-DNA hybrids is noticeably lower when the hybrid is short (<10 base pairs). This is likely due to the fact that the dye assembles on the PNA-DNA helix as an aggregate, and the stability of the dye aggregate will naturally depend on its length. Because most applications will use longer PNA probes, this should not be a practical problem.
3. PNA-RNA targets. We have not yet investigated whether cyanine dyes bind to PNA-RNA duplexes. However, **DiSC2(5)** binds tightly to PNA_2-RNA triplexes, so it would be very surprising if the dye failed to bind to PNA-RNA.
4. Photobleaching. The purple color and 534 nm absorption band fade noticeably when samples are left under room light for ca. 1 h. Cyanine dyes typically are susceptible to photobleaching and this property is enhanced in aqueous vs organic solvents. Photobleaching can be accelerated even further when dye aggregates are formed, as in the case with PNA-DNA hybrids. Thus, measurements should be recorded promptly after addition of the dye to the sample.
5. Thermal degradation of the dye. Cyanine dyes are susceptible to thermal degradation in aqueous solutions. Thus, manipulations that require heating of the sample above 60°C should be done prior to addition of the dye.

References

1. Wang, J., Palecek, E., Nielsen, P. E., Rivas, G., Cai, X., Shiraishi, H., et al. Peptide nucleic acid probes for sequence-specific DNA biosensors. *J. Am. Chem. Soc.* **118,** 7667–7670.

2. Jensen, K. K., Ørum, H., Nielsen, P. E., and Nordén, B. (1997) Kinetics for hybridization of peptide nucleic acids (PNA) with DNA and RNA studied with the BIAcore technique. *Biochemistry* **36,** 5072–5077.
3. Gangamani, B. P., Kumar, V. A., and Ganesh, K. (1997) N. 2-Aminopurine peptide nucleic acids (2-apPNA): intrinsic fluorescent PNA analogues for probing PNA-DNA interaction dynamics. *Chem. Commun.* 1913–1914.
4. Gangamani, B. P., Kumar, V. A., and Ganesh, K. N. (1997) Spermine conjugated peptide nucleic acids (spPNA): UV and fluorescence studies of PNA-DNA hybrids with improved stability. *Biochem. Biophys. Res. Commun.* **240,** 778–782.
5. Tyagi, S. and Kramer, F. R. (1996) Molecular beacons: probes that fluoresce upon hybridization. *Nat. Biotechnol.* **14,** 303–308.
6. Armitage, B., Ly, D., Koch, T., Frydenlund, H., Ørum, H., and Schuster, G. B. (1998) Hairpin-forming peptide nucleic acid oligomers. *Biochemistry* **37,** 9417–9425.
7. Ortiz, E., Estrada, G., and Lizardi, P. M. PNA molecular beacons for rapid detection of PCR amplicons. *Mol. Cell. Probes* 1998, **12,** 219–226.
8. Tyagi, S., Bratu, D., and Kramer, F. R. (1998) Multicolor molecular beacons for allele discrimination. *Nat. Biotechnol.* **16,** 49–53.
9. Seitz, O. (2000) Solid-phase synthesis of doubly labeled peptide nucleic acids as probes for the real-time detection of hybridization. *Angew. Chem. Int. Ed. Engl.* **39,** 3249–3252.
10. Lee, L. G., Chen, C., and Liu, L. A. (1986) Thiazole Orange: a new dye for reticulocyte analysis. *Cytometry* **7,** 508–517.
11. Rye, H. S., Quesada, M. A., Peck, K., Mathies, R. A., and Glazer, A. N. (1991) High-sensitivity two-color detection of double-stranded DNA with a confocal fluorescence gel scanner using ethidium homodimer and thiazole orange *Nucleic Acids Res.* **19,** 327–333.
12. Svanvik, N., Westman, G., Wang, D., and Kubista, M. (2000) Light-up probes: thiazole orange-conjugated peptide nucleic acid for detection of target nucleic acid in homogeneous solution. *Anal. Biochem.* **281,** 26–35.
13. Svanvik, N., Nygren, J., Westman, G., and Kubista, M. (2001) Free-Probe Fluorescence of "Light-Up Probes" *J. Am. Chem. Soc.* **123,** 803–809.

14. Nikiforov, T. T. and Jeong, S. (1999) Detection of hybrid formation between peptide nucleic acids and DNA by fluorescence polarization in the presence of polylysine. *Anal. Biochem.* **275,** 248–253.
15. Smith, J. O., Olson, D. A., and Armitage, B. A. (1999) Molecular recognition of PNA-containing hybrids: spontaneous assembly of helical cyanine dye aggregates on PNA templates. *J. Am. Chem. Soc.* **121,** 2686–2695.

10

PNA-Mediated PCR Clamping

Applications and Methods

Deborah G. Murdock and Douglas C. Wallace

1. Introduction

About 90% of sequence variants in humans are differences in single bases of DNA, called single nucleotide polymorphisms (SNPs). When two individuals are compared, their genomic DNA differs at ~1/1000 nucleotides ***(1)***. Neutral polymorphisms may be responsible for subtle differences between individuals, such as hair and eye color, or may be silent identifiers of variability and relatedness. Other polymorphisms cause genetic diseases such as hemophilia and are referred to as mutations. Polymorphisms within an individual may cause cancer or other diseases, are responsible for the variability of our immune response, and have been implicated in the aging process. Identification of polymorphisms can therefore be useful in diagnosis of genetic disease, detection of tumors, study of immune response and aging, identification of microbial strains, and developing relatedness trees between humans or other organisms.

Several methods exist to detect single nucleotide DNA polymorphisms, the two most common being DNA sequencing and restriction fragment-length polymorphism (RFLP) analysis. Sequencing of cloned genomic DNA or polymerase chain reaction

From: *Methods in Molecular Biology, vol. 208: Peptide Nucleic Acids: Methods and Protocols*
Edited by: P. E. Nielsen

(PCR)-amplified products is the most direct polymorphism detection method, but can be labor intensive and expensive. RFLP analysis of restricted genomic DNA by Southern blotting, or of digested PCR products by agarose gel electrophoresis requires that the polymorphism creates or eliminates a restriction site. Both sequencing and RFLP analysis are ineffective when the polymorphism exists as a small percentage of the total DNA population. Allele-specific PCR-based methods of polymorphism identification are able to detect small levels of point mutations, but the approach is limited by the fact that most primer-template mismatches have no significant effect on the amplification process ***(2)***.

Peptide nucleic acid (PNA)-mediated PCR clamping is a versatile and sensitive method to identify single nucleotide changes in DNA molecules, even when these changes exist as a small percentage of the total DNA. As first described by Ørum et al. ***(3)***, PNA clamping specifically blocks amplification of a given DNA template, while allowing amplification of another template that differs by as little as one nucleotide. While PNAs are DNA mimics in terms of their capability to bind to DNA in a sequence specific manner, PNA molecules have properties unique from DNA that allow PNA clamping. First, PNA/DNA interactions are generally 1°C per base pair more stable than the corresponding DNA/DNA duplex. As a result, a PNA molecule can be designed that is complementary to a DNA template at a PCR primer binding site such that it will competitively block DNA primer binding (or, less efficiently, to a region adjacent to a primer binding site to cause arrest of elongation by the DNA polymerase). Secondly, PNAs cannot function as primers for DNA polymerase, and as such will eliminate amplification when competitively excluding a DNA primer in PCR. Lastly PNA/DNA duplexes are much more destabilized by single base-pair mismatches than are DNA/DNA duplexes. This property allows design of PNA molecules that competitively exclude DNA primers from one template, but not from another template that differs by one base pair. Therefore, in an amplification reaction containing DNA with mixed template varying at one nucleotide, PNA molecules can be

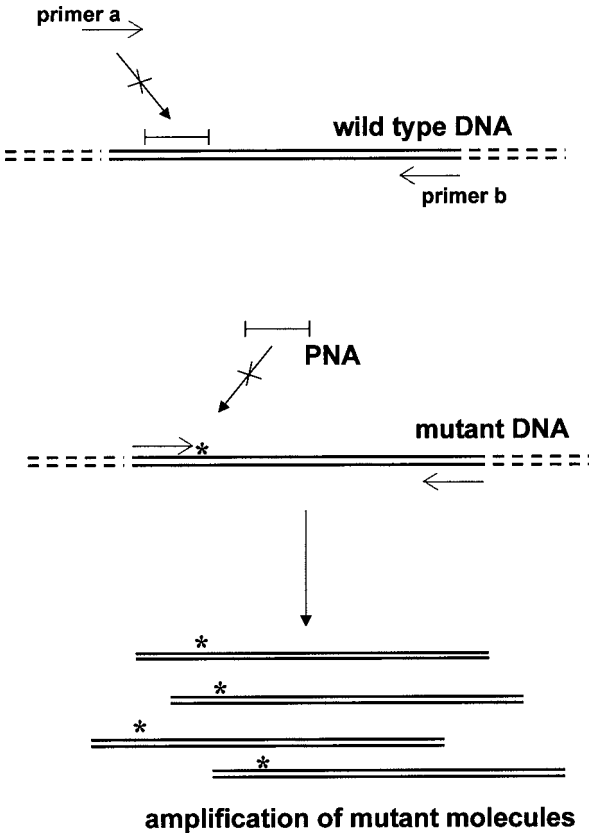

Fig. 1. PNA-mediated PCR clamping methodology. Primers for PCR are shown as arrows. Bars represent PNA. Asterisks represent polymorphisms. Under the appropriate cycling conditions, the PNA will bind to the wild-type, but not the mutant template, blocking annealing of the upstream primer, and allowing amplification of only the mutant molecules.

used to selectively block amplification of one DNA template while allowing amplification of the other (**Fig. 1**). This blockage is very efficient, even when the blocked template is in vast excess, resulting in detection of a template present at a ratio of 1/20,000 in some reaction conditions. In addition, PNA clamping is faster and easier than most techniques that are presently used to identify point mutations, while at the same time providing great sensitivity and specificity.

The versatility of PNA clamping can be illustrated by the various applications of the technique reported in the literature. In addition to allowing basic point mutation detection for identification of genetic disease ***(4–6)***, the tremendous sensitivity of the technique has proven useful in many different applications where the mutation or variation is at a very low level and difficult to identify by standard point mutation detection methods. Low levels of variation seen in cancer ***(7–10)***, mtDNA disease and aging ***(5)***, somatic mutation mosaicism ***(11)***, mRNA editing ***(12)***, and microbial mixed communities ***(13)*** have all been evaluated by PNA clamping methods. These applications, and the modifications of PNA clamping described in each, are reviewed below.

1.1. Diagnostic Detection of Single Nucleotide Changes in Genetic Disease

1.1.1. Familial Thrombophilia

A single base change in the Factor V gene causes inherited resistance to activated protein C, resulting in familial thrombophilia. This mutation, a G to A change at nucleotide 1691, has a high occurrence in the Caucasian population, and constitutes a significant risk factor for thromboembolic events. Behn and Schuermann ***(6)*** reported a PNA clamping based technique to allow diagnosis of the Factor V mutation. Genomic DNA was prepared from individuals homozygous for the Factor V mutation or the normal allele, as well as individuals heterozygous for the mutation. PNA molecules were designed to bind to either the wild type or the mutant sequence surrounding nucleotide 1691. These PNAs partially overlap with the sequence of the PCR primer flanking the mutation, and were shown to block PCR amplification of their complementary template, presumably by primer exclusion. The affects of several experimental factors, such as PNA annealing temperature, primer annealing temperature, $MgCl_2$ concentration, concentration of template DNA, and PNA concentration were also evaluated. The authors conclude that the PNA-medicated PCR clamping technique is an attractive alternative for determination of factor V alleles.

1.1.2. Hereditary Hemochomatosis

Hereditary hemochromatosis (HH), an iron overload disease, is the most prevalent identified inheritable disease, afflicting 1.5 million Americans. 83% of all diagnosed HH patients of Northern European ancestry have a common mutation, the C282Y mutation in the *HFE* gene ***(14)***. HH is frequently undiagnosed, and can be the cause of liver disease, cardiovascular disease, arthritis, and diabetes. Because this disease is treatable by therapeutic phlebotomy, early diagnosis is valuable.

Kyger et al. ***(4)*** report the application of PNA clamping to detect the common C282Y mutation in HH. PNA molecules corresponding to both mutant and wild-type sequences were designed, and the melting temperatures of these PNA molecules in complex with wild-type and mutant primers were measured in a Beckman spectrophotometer with a Peltier temperature controller. The melting temperature of the wild type PNA (75°C) was reduced by 18°C (to 58°C) when the DNA template differed by one nucleotide; and the melting temperature of the mutant PNA (72°C) was reduced by 11°C. In contrast, the melting temperatures of the primers (65°C and 64°C) were reduced to 60°C by one mismatch. These PNA molecules were used in test reactions containing completely wild-type, completely mutant, or heterozygous DNA template. In a variation on previously reported PNA methods, Kyger et al. ***(4)*** used a LightCycler to perform real time fluorescent PCR, eliminating the need for postamplification steps such as agarose gel electrophoresis. Real-time PCR also reduces the time necessary to obtain results to less than 1 h. These PNA molecules were shown to block PCR amplification of their cognate wild-type or mutant template, and Kyger et al. ***(4)*** conclude that PNA clamping performed with real time fluorescence PCR provides a rapid genetic assay to distinguish HH patients from carriers and normal individuals.

1.2. Detection of Oncogenic Point Mutations

There is a growing demand for methods that allow the detection of mutations that cause cancer in order to provide early detection,

prognosis, and risk assessment. Detection of cancer-causing mutations is complicated by the fact that these mutations may constitute a very small fraction of the total in tissues and bodily fluids. Mutations in the *ras* and *p53* proto-oncogenes are found to be a frequent cause of human malignancies. A large percentage of these *ras* and *p53* gene mutations are found within a small number of "hot spot" positions. Because PNA clamping is extremely sensitive, and one PNA can be used to distinguish between several mutations at a given hot spot; PNA clamping has been successfully applied to the detection of cancer-causing point mutations.

Thiede et al. ***(7)*** used PNA clamping to detect point mutations in the *ras* proto-oncogene. Because cancer-causing mutations are known to cluster in a 4–5 base pair span of DNA in codons 12 and 13 of the *ras* gene, a PNA was designed complementary to the wild-type version of that region of the DNA. PNA clamping with this one PNA can theoretically detect any of the twelve mutations that occur in codons 12 and 13 of *ras*. This hypothesis was tested on six of the twelve possible *ras* mutations derived from several tumors that had been previously characterized. While the PNA completely blocked amplification of *ras* from a wild-type sample, amplification occurred from all known *ras* mutant samples. The nature of the mutation was confirmed by sequencing the product. Therefore, PNA clamping was able to detect all six mutations regardless of the site or type of mutation. Additionally, the sensitivity of the technique was tested by creating mixtures of wild type and heterozygous template. The mutation could be detected at a level of one mutation in a background of 200 wild-type alleles (1/200). While direct sequencing confirmed detection of the mutant allele with PNA, sequence analysis of the same DNA amplified without PNA failed to detect the mutation, illustrating the enrichment of the mutation in the PNA-clamping mediated reaction. Thiede et al. ***(7)*** conclude that PNA clamping can detect several hot spot mutations with one reaction, and that this method is very sensitive, detecting 1 mutant allele in a background of 200 wild-type. This same technique was adapted by Takahashi et al. ***(15)*** to measure the mutagenicity of bisphenol A, a chemical used in the production of polycarbonate plastic products.

Human tissue culture cells were treated with different concentrations of bisphenol A, and levels of *ras* codon 12 mutations were measured. It was reported that these mutations can be seen when present at about 0.005% in genomic DNA.

PNA clamping has also been applied to detection of mutations in the *p53* gene. Previously, point mutations in *p53* had been evaluated using the PCR-SSCP (single-strand conformational polymorphism) technique. PCR-SSCP, however, only allows detection of a mutant allele if it is over 2–5% of the total DNA, making detection impossible in certain tissues and body fluids. Behn and Schuermann ***(16)*** used a PNA mediated "mutant enriched" PCR-SSCP technique to evaluate *p53* from brush cytology material. In order to improve the level of detection, Behn and Schuermann enriched the PCR product used for SSCP detection for mutant molecules by using PNA clamping, reducing amplification of the wild-type template. Cancer-causing mutations in the *p53* gene frequently occur at hot spots in codons 248 and 249, allowing the use of one PNA to evaluate several mutations. PNAs were designed complementary to both *p53* hot spots, with primers flanking the mutation and not overlapping the PNA (elongation arrest). The resulting mutant enriched product was subjected to the SSCP technique. Serial dilution experiments showed that 1 mutation in 200 wild-type molecules could be detected (0.5%) with this method. This mutant enriched PCR-SSCP technique was then used to evaluate the *p53* hot spot alleles in brush cytology material from 20 different lung cancer patients. While no mutations could be found in these patients with traditional PCR-SSCP, PNA-mediated "mutant enriched" PCR-SSCP found mutations in four of these samples. These mutations were confirmed by excision of the polymorphic band, reamplification, and sequencing. All mutations found were in the *p53* hot spots, and all were different.

An adaptation of the method described earlier was reported to detect mutations in both *p53* and *ras* from exfoliated tissue material ***(8)***. Again, elongation arrest based PNA-enriched PCR was used to partially block wild-type allele amplification in the first PCR reaction, enriching the product for mutant alleles. Instead of SSCP

analysis, however, mutant alleles were detected by performing a second nested round of amplification on the enriched product with primers engineered to create a restriction site at the wild type locus. The resulting product was digested with the appropriate restriction enzyme, and any mutant product was seen as undigested product by agarose gel electrophoresis. This method was tested on mixtures of DNA from wild type and *p53* or *ras* mutant cell lines. Without PNA, mutant alleles could be detected at a level of 5%, while addition of PNA allowed detection of mutant alleles at a level of 1 in 1000, an improvement of 50-fold. The method was then used to examine brush cytology material taken from 20 patients with lung cancer that had been previously examined for mutations in *p53* and *ras*. While 19 mutations had been identified with repetitive PCR-RFLP based enrichment procedures, 13 could be identified with PNA-enriched RFLP analysis described here. This procedure is not as sensitive as the previous procedure used, but has the advantage of being more rapid and able to identify many different mutations with one set of primers. Finally, this method was used to evaluate *p53* and *ras* mutations in sputum samples taken from 23 lung cancer patients. Eight lesions were detected in this manner, and seven of them were confirmed by analysis of lavage samples taken during bronchoscopy, indicating that this method is sensitive enough to detect mutations in material taken in a noninvasive manner.

In addition to the elongation arrest-based methods described earlier, primer exclusion-based PNA clamping has also been applied to detect mutations in the *p53* gene. This method was successful in detecting point mutations in DNA derived even from formalin-fixed, paraffin-embedded samples. Myal et al. ***(10)*** used a PNA molecule complementary to the hot spot in the *p53* gene with a primer differing from the PNA only in length. In a test reaction containing dilutions of DNA from two breast cancer cell lines, PNA clamping completely blocked wild-type *p53* amplification, and could detect a mutation in the hot spot region when present at 0.05% of wild type. This is a 10-fold improvement in detection from that obtained previously with fresh or frozen tissue.

Rhodes et al. ***(9)*** also report the use of PNA to enhance the sensitivity of allele specific PCR to detect mutations in the *ras* gene. The PNA used in this study was a 19mer complementary to normal K-*ras* sequence at nucleotides 26–45 and overlapping with the binding site of one of the PCR primers by 5 nucleotides. This PNA was incubated with the template DNA for 1 h at 37°C, followed by amplification of the template in the presence of the PNA. The product of the PNA-clamped amplification was then diluted and subjected to allele-specific PCR. The authors report that adding the PNA-clamping step before the allele-specific PCR step increased the detection limit of allele-specific PCR 5–10-fold.

1.3. Detection of Mitochondrial DNA Mutations

Inherited mitochondrial DNA (mtDNA) mutations have been shown to cause a variety of degenerative diseases, and the accumulation of somatic mtDNA mutations have been implicated in aging. Detection of mutations in mtDNA is complicated by the fact that each cell contains hundreds to thousands of mtDNAs, and a mutant cell can contain any proportion of mutant or wild-type molecules, a condition known as heteroplasmy. As a result, it is often important to be able to detect low proportions of mutant mtDNAs in maternal relatives at risk for a disease, or in the tissues of aging individuals. Murdock et al. ***(5)*** have applied the PNA-clamping PCR technique to detect two pathogenic point mutations: the tRNA-Leu np3243 mutation causing mitochondrial myopathy, encephalopathy, lactic acidosis, and strokelike episodes (MELAS); and the tRNA-Lys np8344 mutation causing myoclonic epilepsy and ragged red muscle fibers (MERRF), and the age-related np414 mutation. PNA molecules were designed to overlap with the PCR primer binding site, allowing amplification of only mutant DNA template. The method was shown to be extremely sensitive, being capable of detecting mutations at the level of 0.1% of total molecules, without false positives in the absence of mutant molecules. Moreover, it was shown that the reaction can be multiplexed to identify more than one mutation per reaction. Using this technique, the levels of three

point mutations, the $tRNA^{Leu(UUA)}$ 3243 mutation causing MELAS; the $tRNA^{Lys}$ 8344 mutation causing MERRF; and the np 414 mutation adjacent to the control region promoters, were evaluated in human brain and muscle from individuals of various ages. While none of the mutations were detected in brain samples from individuals ranging in age from 23–93, the 414 mutation could be detected in muscle from individuals 30 yr and older. These data demonstrate that the 3243 and 8344 mutations do not accumulate with age to levels greater than 0.1% in brain and muscle. By contrast, the 414 mutation accumulates with age in normal human muscle, though not in brain. The reason for the striking absence of the 414 mutation in aging brain is unknown.

1.4. Determination of Somatic Mosaicism (GNAS1)

McCune-Albright syndrome is a disease marked by the triad of polyostotic fibrous dysplasia, skin pigmentation, and endocrine disorders. MAS has been shown to be caused by somatic missense mutations in codon 201 of the *GNAS1* gene. Because these mutations are mosaic, they can be difficult to detect in the wild-type DNA background. While MAS is uncommon, fibrous dysplasia (FD) of bone not associated with skin or endocrine abnormalities is a frequent and serious skeletal disorder. Bianco et al. ***(11)*** used PNA clamping PCR to investigate the occurrence of mutations in the *GNAS1* gene in DNA from cultures of fibrous dyplastic lesions dissected from non-MAS FD patients. Mutations in codon 201 (R201C or R201H) were found in all eight FD patients tested, suggesting that both FD and MAS are caused by mutations in the *GNAS1* gene, and that the phenotypic differences are a result of different patterns of somatic mosaicism.

1.5. Microbial Mixed Community Analysis

The analysis of the diversity of complex microbial environments is often performed by determining the sequence of the 16S rRNA genes present in the mixed culture. This can be achieved most simply by direct PCR amplification of the 16S rRNA gene from the

microbial mixture without culturing, followed by cloning and sequencing of the resultant product. In cases where one bacterial strain predominates, or some strains are present in very small ratios, it would be helpful to selectively block amplification of some 16S rRNA gene variants. von Wintzingerode et al. ***(13)*** investigated the use of PNA clamping to enrich for 16S rRNA genes with polymorphisms not frequently found in clone libraries taken from complex microbial cultures. A PNA molecule was designed with an eight base pair overlap with the binding site of one of the 16S rRNA primers.

This PNA was shown to block amplification of completely complementary rDNAs, but not rDNAs containing one or two mismatches. This PNA was then used in a test reaction that contained a 1:100 ratio of polymorphic to normal rDNA. The resulting product was cloned to create an rDNA library, and individual cloned DNAs were screened by dot blot hybridization. Twenty-eight of 34 clones tested were positive in PNA clamping-derived libraries, while only one of 34 clones was positive in the library created without PNA.

PCR clamping was then used to create libraries from an anaerobic dechlorinating consortium of bacterium. This consortium had recently been shown to contain several representatives of recently described phylogenetic groups. Both primer exclusion and elongation arrest-based PCR clamping were performed, although elongation arrest-based PCR clamping was less successful at eliminating amplification. Binding of PNA to the most abundant rDNA sequences allowed the identification of variant rDNA sequences that had not been identified in previous experiments.

1.6. Analysis of mRNA Editing of apoB

Apolipoprotein B (apoB) is the major component of chylomicrons and low density lipoproteins (LDL) in the cell. ApoB exists in two forms, apoB-100, the full-length form, and apoB-48, which is the product of mRNA editing. This mRNA editing, which changes the CAA-Gln codon at 2153 to a UAA stop codon, is species- and tissue-specific. Because the level of the edited message can be very low, a radioactive reverse transcription (RT)-PCR primer extension

method had been previously used to detect it. Zhong et al. ***(12)*** describe a PNA-mediated PCR clamping method to detect low levels of mRNA editing of apoB.

To create a test system for the method, Zhong et al. reverse transcribed mRNA from a HepG2 cell line that has no editing of apoB messages, and from transfected HepG2 cells that have 4% editing of the apoB message. The DNA from the reverse transcription was mixed at various ratios to create template samples with 0, 0.5, 1.0, 2.0, or 4.0% "edited" DNA. Primer-exclusion PCR clamping was then performed in the presence of a PNA molecule that overlaps the primer at 4 nucleotides. The products of PCR clamping were subjected to a primer extension assay to determine the extent to which they contained selectively amplified "edited" DNA. While the "0%" sample contained only a background band, the other samples with PNA added contained 90% "edited" product. The 0.5% "edited" template yielded 89% "edited" product, representing nearly a 180-fold increase. The authors conclude that PNA-mediated PCR clamping can serve as a sensitive nonradioactive new method to detect apoB mRNA editing.

1.7. Cloning IgG Variable Region

The cloning of immunoglobulin variable region genes from hybridomas is used to harvest single-chain Fv (scFv) with predefined specificities that can be used therapeutically. Hybridomas are created by fusing a B-cell line containing the functional scFv gene of interest to a cell line derived from the mouse myeloma MOPC-21. Cloning of the scFv is often complicated by the fact that these hybridomas express an aberrant nonfunctional kappa (*ab*Vκ) light chain transcript from the MOPC-21 derivative. Primers designed to amplify variable regions cannot distinguish between the functional gene from the fused B cell, and the aberrant Vκ transcript from MOPC-21. In addition, the MOPC-21 transcript has been reported to be preferentially amplified by RT-PCR, resulting in a preponderance of *ab*Vκ clones.

Cochet et al. ***(17)*** applied the PNA-mediated PCR-clamping method to block the elongation of the MOPC *ab*Vκ cDNA from hybridomas, while allowing the amplification of the functional scFv cDNA from the fused B cell. A PNA molecule was designed complementary to the CDR3 region of the *ab*Vκ gene, six nucleotides carboxy terminal to the PCR primer binding site. cDNA was created by reverse transcription of mRNA from the hybridoma, and was used as template in PNA-mediated clamping PCR. The products from reactions performed in the presence and absence of PNA were cloned and screened for specific Vκ alleles. While all inserts from the PCR performed without PNA were typed as MOPC *ab*Vκ, over half of the clones derived from the PCR performed in the presence of PNA were shown to contain the functional scFv cDNA.

The authors conclude that PCR clamping provides a useful tool to improve the cloning efficiency of specific immunoglobulin variable regions produced by hybridomas.

1.8. Determination of Allelic Allocation

Cytochrome P4501A1 *(CYP1A1)* plays an important role in the bioactivation of procarcinogenic xenobiotics. Four polymorphisms, designated m1, m2, m3, and m4, have been identified in the human *CYP1A1* gene, and the frequency of these base changes varies among ethnic groups. Two of the four polymorphisms have been proposed to increase enzymatic activity of the protein, and as such have been suggested to be biomarkers for increased susceptibility to certain malignancies, especially lung cancer. M1 and m3 occur in the 3' flanking region of the gene, while m2 and m4 are in adjacent codons of the gene, both causing amino acid changes. Diagnosing not only the polymorphisms, but also their allelic combinations (m1/m2, m1/m4, m2/m4) could have important toxicological consequences.

To determine the allelic allocation of m1, m2, and m4 polymorphisms, three PNA molecules differing only at the polymorphic site were used to block amplification of wild-type, m2, or m4 alleles ***(18)***. The resulting PCR products could then be tested for the sec-

Allelic allocation option 1

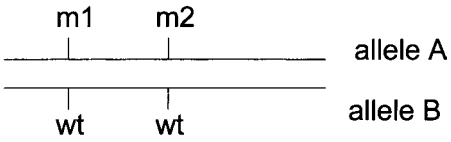

Block with PNA wild type → amplify allele A

Block with PNA m1 → amplify allele B

Block with PNA m2 → amplify allele B

Allelic allocation option 2

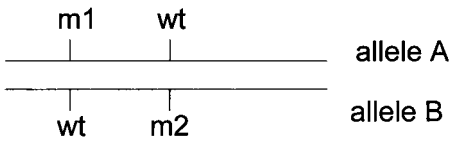

Block with PNA wild type → no amplification

Block with PNA m1 → amplify allele B

Block with PNA m2 → amplify allele A

Fig. 2. Determination of allelic allocation. Option 1, in which polymorphisms m1 and m2 occur on the same allele, can be distinguished from option 2, in which both polymorphism occur on different alleles, by PNA clamping-mediated PCR. In option 1, a product is created whether the added PNA binds to the wild-type or the polymorphic sequences. In option 2, no product is amplified when a wild-type specific PNA is added.

ond polymorphism by restriction digestion. For example, to analyze the linkage of m1 and m2, a segment of *CYP1A1* was amplified from DNA simultaneously heterozygous for both m1 and m2 in the presence of PNA specific for m1, m2, or wild-type alleles. As shown in **Fig. 2**, if m1 and m2 are on different alleles (allelic allocation option 2), then the wild-type PNA would block amplification of both

alleles, and no product would result. On the other hand, if m1 and m2 are on the same allele, then one allele would be amplified in the presence of each PNA. The presence of m1 on the amplified allele can then be verified by restriction-digestion analysis of the PCR product. Mrozikiewicz et al. ***(19)*** use PNA clamping to show that m1 and m2 mutations are always on the same allele in heterozygote individuals, and that m1 and m4 were always on distinct DNA strands in six individuals, and further evaluate the frequency of these *CYP1A1* mutations in the Turkish population.

In this report, we outline the procedures used to identify the np414 mutation in mitochondrial DNA with PNA-clamping mediated PCR. This protocol should be easily adaptable to the identification of most single nucleotide polymorphisms.

2. Materials

2.1. Polymerase Chain Reaction

1. 10X PCR buffer: 100 m*M* Tris-HCl, 15 m*M* $MgCl_2$, 500 m*M* KCl, pH 8.3 (Roche Molecular Biochemicals, Indianapolis, IN).
2. PCR nucleotide mix: 10 m*M* each of the sodium salts of dATP, dCTP, dGTP, and dTTP) (Roche Molecular Biochemicals, Indianapolis, IN).
3. PNA (Applied Biosystems, Foster City, CA) (*see* **Note 1**). T414T (H-TTG GCG GTA TGC ACT-CONH2) Synthesized PNAs arrive in dried form, and should be rehydrated in H_2O, separated into 10 reaction aliquots, lyophilized again in a vacuum dessicator, and stored at –70°C until needed.
4. 40–60 ng total genomic DNA or 1 ng plasmid DNA template.
5. Taq DNA polymerase, 5 units/µL (Roche Molecular Biochemicals).
6. PCR primers (*see* **Note 2**):
   primer 386.for = 5'-ccagatttcaaattttggcgg-3'
   primer 780.rev = 5'-actcactggaacggggatgc-3'
7. H_2O (*see* **Note 3**). DNase-free water (Life Technologies, Rockville, MD) or reagent-grade ultrapure water purified by the MilliQ purification system (Millipore Corporation, Bedford, MA).

2.2. Restriction Analysis of PCR Product

1. Restriction endonuclease *Fok*I 5U/µL (Roche Molecular Biochemicals).

2.3. Agarose Gel Electrophoresis

1. 3:1 agarose (BioWhittaker Molecular Applications, Rockland, MN).
2. TBE buffer: 89 m*M* Tris-HCl base, 89 m*M* Boric acid, 2 m*M* EDTA.
3. 10 mg/mL ethidium bromide solution (Life Technologies, Rockville, MD).
4. DNA molecular-weight marker: pBR322 DNA-*MspI* digest (New England Biolabs, Inc., Beverly, MA).
5. 6X DNA loading buffer: 0.25% bromophenol blue, 0.25% xylene cyanol, 30% glycerol.

3. Methods

3.1. Polymerase Chain Reaction

1. For each template to be investigated, amplification is performed in the presence and absence of PNA. The following reagents are mixed in thin wall 0.2 mL PCR tubes to create 50 µL reactions: 5.0 µL 10X PCR buffer, 1.0 µL 10 m*M* each dNTP mix, 1.0 µL 20 µ*M* primer 386.for, 1.0 µL 20 µ*M* primer 780.rev, 1.0 µL genomic (40–60 ng) or plasmid DNA (1 ng) template, 0.5 µL Taq DNA polymerase (5U/µL), 1.0 µL 100 µ*M* PNA T414T or H_2O, 39.5 µL H_2O.
2. The reactions are then performed under the following cycling conditions: 1 cycle of 94°C for 2 min, 25 cycles of 94°C for 30 s (denaturation), 69°C for 30 s (PNA annealing), 56°C for 30 s (DNA primer annealing), 72°C for 30 s (extension), 1 cycle of 72°C for 5 min.
3. To increase the sensitivity of the PNA-clamped reaction, a second round of PCR can be performed on 1 µL of 1/100 diluted product from the first reaction. PNA is not added to the second amplification reaction, because detection from the second reaction was found to be more sensitive in the absence of PNA. Therefore, wild-type DNA amplification products should be distinguished from mutant products by restriction-enzyme digestion.

3.2. Optional Confirmation of Point Mutation by RFLP Analysis

1. Confirmation that the product generated by PNA-clamping PCR has a mutation can be achieved in several ways (*see* **Note 4**). The mtDNA np414 mutation creates a *Fok*I restriction-enzyme recognition site that can be used for confirmation. The reaction conditions are as follows: 10 µL PCR product, 2 µL enzyme buffer,1 µL *Fok*I, 7 µL H_2O.
2. Reactions are incubated for 1.5 h at 37°C.

3.3. High-Resolution Gel Electrophoresis Analysis of Small DNA Fragments

1. Loading dye is added directly to the reaction, and the entire volume is loading into one well of a 3.5% agarose gel containing 0.5 µg/mL ethidium bromide (*see* **Note 5**).
2. The DNA is run at high voltage (100 volts for 11 cm gel for approx 1 h), and visualized with UV light.

4. Notes

1. PNA design. We have found that a 15-mer PNA works well for PNA clamping. A 15-mer PNA will generally have a melting temperature of about 70°C, with a single mismatch lowering the melting temperature by approx 15°C. The mismatch should be in the center of the PNA where it is the most destabilizing. PNAs should be designed anti-parallel to the DNA template, with not more than 4 purines or 3 guanines in a row and an overall purine content of not more than 60%. Self-complementarity should be avoided, because PNA with palindromes or hair-pins tend to aggregate.
2. The design of the primer that competes with the PNA for template binding is very important. The 3' end of this competitive primer should partially overlap with the PNA, but preferably should not contain the polymorphic nucleotide. This allows confirmation of the polymorphism in the PCR product if the change creates or destroys a restriction site. The melting temperature of the competitive primer should be lower than the PNA/DNA melting temperature, but higher than the mismatched PNA/DNA melting temperature. The length of the competitive primer is the most useful variable in optimizing PNA clamping

reaction conditions. Because the polymorphic restriction site will be very close to the end of the PCR product, the second primer should be sufficiently close to the first such that the resulting restricted bands can be resolved from one another by gel electrophoresis.

3. High-performance PCR applications appear to be very sensitive to the quality of the water used in the reaction. We have successfully used both commercially available DNase-free water, and reagent-grade ultrapure water purified by the MilliQ purification system for PNA-clamping reactions.
4. Optimally, the results of PNA-clamping are read as the presence or absence of a PCR product. In some cases, however, the clamping is not complete, and the results must be verified by alternative techniques that confirm the presence of a polymorphism. If the polymorphism creates or eliminates a restriction-enzyme site, restriction digestion followed by agarose or acrylamide (*see* **Note 5**) gel electrophoresis may be performed. If the polymorphism does not create a restriction site, one may be created in some cases in combination with a mismatch primer ***(8)***. Other alternatives are described in the applications listed in the introduction of this chapter, and include sequencing ***(7,11)***, radioactive ASA ***(9)***, radioactive primer extension assay ***(12)***, SSCP ***(16)***, and real-time fluorescent PCR ***(4)***.
5. The design of the PNA and primers in primer exclusion-based PNA clamping requires that any restriction-enzyme sites created or destroyed by the polymorphism will create very small DNA fragments. These fragments may still be evaluated by agarose gel electrophoresis if the following conditions are used. 3:1 agarose in TBE buffer provides very good resolution of small DNA fragments. The gels should be run with ethidium bromide in the gel (as opposed to poststained) for short times with high voltages to avoid diffusion of small bands.

References

1. Kwok, P. Y., Deng, Q., Zakeri, H., Taylor, S. L., and Nickerson, D. A. (1996) Increasing the information content of STS-based genome maps: identifying polymorphisms in mapped STSs. *Genomics* **31,** 123–126.
2. Kwok, S., Kellogg, D. E., McKinney, N., Spasic, D., Goda, L., Levenson, C., and Sninsky, J. J. (1990) Effects of primer-template

mismatches on the polymerase chain reaction: human immunodeficiency virus type 1 model studies. *Nucleic Acids Res.* **18,** 999–1005.

3. Ørum, H., Nielsen, P. E., Egholm, M., Berg, R. H., Buchardt, O., and Stanley, C. (1993) Single base pair mutation analysis by PNA directed PCR clamping. *Nucleic Acids Res.* **21,** 5332–5336.
4. Kyger, E. M., Krevolin, M. D., and Powell, M. J. (1998) Detection of the hereditary hemochromatosis gene mutation by real-time fluorescence polymerase chain reaction and peptide nucleic acid clamping. *Anal. Biochem.* **260,** 142–148.
5. Murdock, D. G., Christacos, N. C., and Wallace, D. C. (2000) The age-related accumulation of a mitochondrial DNA control region mutation in muscle, but not brain, detected by a sensitive PNA-directed PCR clamping based method. *Nucleic Acids Res*. **28,** 4350–4355.
6. Behn, M. and Schuermann, M. (1998) Simple and reliable factor V genotyping by PNA-mediated PCR clamping. *Thromb. Haemost.* **79,** 773–777.
7. Thiede, C., Bayerdorffer, E., Blasczyk, R., Wittig, B., and Neubauer, A. (1996) Simple and sensitive detection of mutations in the ras proto-oncogenes using PNA-mediated PCR clamping. *Nucleic Acids Res.* **24,** 983–984.
8. Behn, M., Thiede, C., Neubauer, A., Pankow, W., and Schuermann, M. (2000) Facilitated detection of oncogene mutations from exfoliated tissue material by a PNA-mediated 'enriched PCR' protocol. *J. Pathol.* **190,** 69–75.
9. Rhodes, C. H., Honsinger, C., Porter, D. M., and Sorenson, G. D. (1997) Analysis of the allele-specific PCR method for the detection of neoplastic disease. *Diagn. Mol. Pathol.* **6,** 49–57.
10. Myal, Y., Blanchard, A., Watson, P., Corrin, M., Shiu, R., and Iwasiow, B. (2000) Detection of genetic point mutations by peptide nucleic acid-mediated polymerase chain reaction clamping using paraffin-embedded specimens. *Anal. Biochem.* **285,** 169–172.
11. Bianco, P., Riminucci, M., Majolagbe, A., Kuznetsov, S. A., Collins, M. T., Mankani, M. H., et al. (2000) Mutations of the GNAS1 gene, stromal cell dysfunction, and osteomalacic changes in non-McCune-Albright fibrous dysplasia of bone. *J. Bone Min. Res.* **15,** 120–128.
12. Zhong, S., Nguyen, N. Y., and Eggerman, T. L. (1999) Detection of apolipoprotein B mRNA editing by peptide nucleic acid mediated PCR clamping. *Biochem. Biophys. Res. Comm.* **259,** 311–313.

13. vonWintzingerode, F., Landt, O., Ehrlich, A., and Gobel, U. B. (2000) Peptide nucleic acid-mediated PCR clamping as a useful supplement in the determination of microbial diversity. *Appl. Environ. Microbiol.* **66,** 549–557.
14. Feder, J. N., Tsuchihashi, Z., Irrinki, A., Lee, V. K., Mapa, F. A., Morikang, E., et al. (1997) The hemochromatosis founder mutation in HLA-H disrupts beta2-microglobulin interaction and cell surface expression. *J. Biol. Chem.* **272,** 14,025–14,028.
15. Takahashi, S., Chi, X. J., Yamaguchi, Y., Suzuki, H., Sugaya, S., Kita, K., et al. (2001) Mutagenicity of bisphenol A and its suppression by interferon-alpha in human RSa cells. *Mutat. Res.* **490,** 199–207.
16. Behn, M. and Schuermann, M. (1998) Sensitive detection of p53 gene mutations by a 'mutant enriched' PCR-SSCP technique. *Nucleic Acids Res.* **26,** 1356–1358.
17. Cochet, O., Martin, E., Fridman, W. H., and Teillaud, J. L. (1999) Selective PCR amplification of functional immunoglobulin light chain from hybridoma containing the aberrant MOPC 21-derived V kappa by PNA-mediated PCR clamping. *Biotechniques* **26,** 818–820, 822.
18. Mrozikiewicz, P. M., Landt, O., Cascorbi, I., and Roots, I. (1997) Peptide nucleic acid-mediated polymerase chain reaction clamping allows allelic allocation of CYP1A1 mutations. *Anal. Biochem.* **250,** 256–257.
19. Aynacioglu, A. S., Cascorbi, I., Mrozikiewicz, P. M., and Roots, I. (1998) High frequency of CYP1A1 mutations in a Turkish population. *Arch. Toxicol.* **72,** 215–218.

11

PNA Clamping Techniques for the Determination of Oncogene Mutations

Marcus Schuermann and Moira Behn

1. Introduction

Activating point mutations of the *ras* and *p53* type can be used as genetic markers to screen for the presence of neoplastic cells in human tissue ***(1,2)***. The high frequency of activating K-*ras* and *p53* mutations found in most solid tumors and the fact that a large percentage of these are found within a relatively small number of so-called "hot-spot" positions has encouraged the development of PCR techniques which at the same time provide a high degree of sensitivity.

While the determination of oncogene mutations in clonal material is relatively easy, the methodology at hand becomes technically limiting as soon as determination is performed on material taken from body fluids or areas outside the tumor bulk phase. In these cases, the number of cancer cells may be either too small to allow direct detection or, as is often the case cells bearing oncogene mutations are often contained in a majority of normal cells. These can be representing "contamination" from adjacent normal tissue, exfoliated cells from the same organ or immunoreactive cells which have been invading the tissue. Existing techniques have met this issue in

From: *Methods in Molecular Biology, vol. 208: Peptide Nucleic Acids: Methods and Protocols*
Edited by: P. E. Nielsen © Humana Press Inc., Totowa, NJ

the past trying to enrich for mutant alleles either by positive selection through oligonucleotide-driven allele-specific amplification (called polymerase chain reaction [PCR]-ASA ***[3]***) or by providing a negative selection on wild-type alleles. The latter is possible through the choice of naturally occurring or artificially introduced palindroms around the sequence of interest, which allow a selection of mutant alleles by restriction endonuclease digestion (referred to as PCR-RFLP = analysis by generation of artificial restriction fragment length polymorphism) ***(4–7)***. Although these protocols ensure a relatively high sensitivity ***(4,8)*** of determining up to 1 mutant allele in 10,000 normal alleles the reamplification steps required to obtain this sensitivity bear an increasing risk of *Taq* polymerase-borne infidelity.

To meet these obvious limitations an alternative strategies has been developed on the basis of allele exclusion by using synthetic peptide nucleic acid molecules (PNAs) ***(9)***. PNAs are oligonucleotide mimics containing a peptide instead of a ribose-phosphate backbone, which bind strongly and sequence specifically to complementary DNA-strands by Watson-Crick hydrogen bonding. ***(10–12)***. In PCR clamping, a PNA oligomer binds to a target wild-type sequence and, due to its inability to serve as a primer blocks amplification of a DNA-fragment confined by a pair of two outside located DNA oliogonucleotide primers. In the case of a single-base mismatch, the DNA/PNA duplex is significantly destabilized, which allows strand elongation from a bound DNA oligomer to proceed resulting in the detection of PCR fragments, most of which harbor the variant allele. PNA-directed PCR clamping thus can be a useful alternative for selective allele enrichment. Several techniques have been described hence most of which rely on PNA clamping first decribed by Ørum and coworkers ***(9)***. The testing is based on amplification of target nucleic acids by PCR, whereby the addition of PNAs serves in the discriminantion of variant alleles. Based on this technique we describe two modifications that have been successfully applied to improve conventional (single-

strand conformational polymorphism analysis (SSCP) and PCR-RFLP analysis.

1.1. "Mutant-enriched" PCR-SSCP Using PNAs

The technique described is based on the original protocol for SSCP analysis described by Orita et al. ***(13)*** which consists of a PCR step followed by strand separation by electrophoresis on a denaturing acrylamide gel. The advantage of this technique is the rapid detection of variant or mutated alleles over a broad range of the amplified fragment. The resolution of the conventional technique, however, is dependent on the clonal percentage of mutant alleles in the material examined, which usually should lie above 5%. Allele selection by PNA clamping here offers the advantage of extending the sensitivity of detetction by at least one order of magnitude. We tested this hypothesis by designing a PNA spanning the codon 248 and 249 region of the p53 gene (codon 246–250), alternatively the codon 273 hot spot in exon 8 (the PNA being complementary to codon 271–275 of the *p53* gene).

1.2. Combined Allele-Specific Enriched PCR (CASE-PCR)

This method takes advantage of the allele-specific discrimination of PNAs and the PCR-RFLP technique allowing the easy identification of mutant alleles. The method was termed CASE-PCR (combined allele-specific enriched PCR) according to the different character of each PCR step performed and the additive mutant selective effect achieved by this method ***(15)***. The enriched PCR protocol designed by us comprises two PCR steps, a first step involving a mutation-selective PNA oligonucleotide and conventional DNA primers meant to pre-amplify genomic material containing variant alleles of interest (schematically shown in **Fig. 1**). This step requires an additional segment in the PCR profile at higher annealing temperatures in order to allow the preferential association of the PNAs to DNA. The mutant-enriched PCR products then are reamplified using nested primers one of which covers the site of mutation and generates

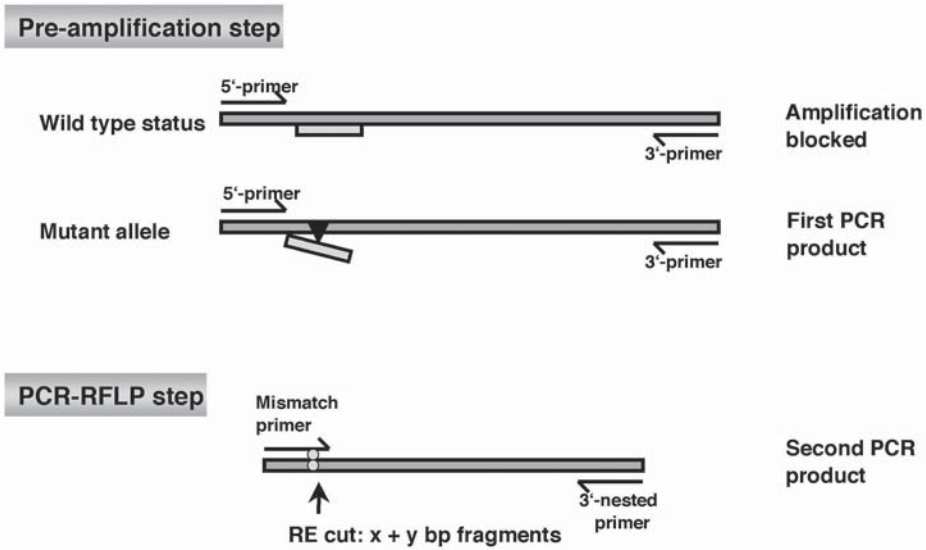

Fig. 1. Schematic representation of the two steps of CASE-PCR. Arrows indicate primer positions. The position of the PNAs is indicated by a bar. A base-pair mismatch due to a missense mutation (black triangle) will block clamping by a complemetary PNA, allowing strand elongation to proceed beyond the PNA-covered sequence. RE, restriction enzyme.

a polymorphism recognized by a restriction endonuclease of choice (diagnostic PCR-RFLP step). Subsequent digestion will then allow the separation of all wild-type fragments by gel electrophoresis.

2. Materials

2.1. Mutant-Enriched PCR-SSCP Using PNAs

2.1.1. DNA-Oligonucleotide Primers

p53, exon7(169nt): p5: 5'-CCTCATCTTGGGCCTGTGTTATCTCCTAGGTTGGCT-3'

p6:5'-CCAGTGTGCAGGGTGGCAAGTGGCTCCTGACCTGGA-3'

p53, exon 8 (196nt): p7: 5'-CTCTTGCTTCTCTTTTCCTATCC-TGAGTAGTGGTAA-3'

p8:5'-CCTCCACCGCTTCTTGTCCTGCTTGCTTACC-TCGCT-3'

2.1.2. PNAs

PNAs were provided by TIB MolBiol (Berlin, Germany).

PNA248-9: GGGCCTCCGGTTCAT- NH_2 (covering p53, codon 246–250)

PNA273: ACAAACACGCACCTC -NH_2 (covering p53 codon 271–275)

2.1.3. PCR Clamping Reaction

1. Reaction buffer: 25 m*M* TAPS, pH 9.3, 50 m*M* KCl, 1.5 m*M* $MgCl_2$, (*see* **Note 1**) and 1 m*M* dithiothreitol (DTT).
2. Nucleotides: 0.2 m*M* of each dATP, dCTP, dGTP, dTTP dissolved in A. bidest.
3. *Taq* DNA-Polymerase (Boehringer Mannheim).
   4. 50–100 ng genomic sample DNA (*see* **Note 2**) dissolved in 50 µL of 10 m*M* Tris-HCl, pH 8.3.

2.2. Combined Allele-Specific Enriched PCR (CASE-PCR)

*2.2.1. DNA-Oligonucleotide Primers for Preamplification Step (*see ***Note 3****)*

Sequences and nomenclature for k-ras amplification according to Mitsudomi et al. ***(16)***.

K-ras, exon 1 (266 bp):

K-*ras* 5': 5' - GTATTAACCTTATGTGTGACATGTTCTAAT - 3'

K-*ras* 3': 5' - ACTCATGAAAATGGTCAGAGAAACC-TTTATCTG - 3'

p53, exon 7 (647 bp) :

p5: 5'-CCTCATCTTGGGCCTGTGTTATCTCCTAGGTTGGCT-3'

p8: 5'-CCTCCACCGCTTCTTGTCCTGCTTGCTTACCT-CGCT-3'

p53, exon 8 (196 bp):

p7: 5'-CTCTTGCTTCTCTTTTCCTATCCTGAGTAGT-GGTAA-3'

p8: 5'-CCTCCACCGCTTCTTGTCCTGCTTGCTTACCTCGCT-3'

2.2.2. DNA-Oligonucleotide Primers for PCR-RFLP Step

Sequences and nomenclature according to Mitsudomi et al. ***(16)***.

K-*ras*, codon 12 (180 bp):

K12MvaI: 5'- CTGCTGAAAATGACTGAATATAAACTTGT GGTAGTTGGACCT - 3'

K12as-1: 5' - CCTTTATCTGTATCAAAGAATGGTCCTGCA-CCAATATGC - 3'

p53, codon 248 (249bp):

248CspI: 5'- ACTACATGTGTAACAGTTCCTGCATGGGCGG CACGGAC - 3'

as24x: 5'- AGAGAAAAGGAAACTGAGTGGGAGCAGTAA GATTC - 3'

p53, codon 249 (246bp):

249Bsu36I: 5'- ACATGTGTAACAGTTCCTGCATGGGCGGC ATGAACCTG - 3'

as24x: 5'- AGAGAAAAGGAAACTGAGTGGGAGCAGTA AGATTC - 3'0

p53, codon 273 (166bp):

273MluI: 5'-TGGTAATCTACTGGGACGGAACAGCTTTG AGACG - 3'

p8: 5'-CCTCCACCGCTTCTTGTCCTGCTTGCTTACCTC GCT-3'

2.2.3. PNAs (see ***Note 4***)

PNAs were provided by TIB MolBiol (Berlin, Germany).

PNAK12-3: TACGCCACCAGCTCC-NH_2 (covering K-ras, codon 10–14)

PNA248-9: GGGCCTCCGGTTCAT- NH_2 (covering p53, codon 246–250)

PNA273: ACAAACACGCACCTC -NH_2 (covering p53 codon 271–275)

2.2.4. Pre-Amplification (PCR Clamping) Step

1. Reaction buffer: 25 m*M* TAPS, pH 9.3, 50 m*M* KCl, 1.5 m*M* $MgCl_2$, 1 m*M* DTT, 3.75% glycerol (7.5% glycerol in case of PNAK12-3).
2. Nucleotides: 0.2 m*M* of each dATP, dCTP, dGTP, dTTP dissolved in A. bidest.
3. *Taq* DNA-Polymerase (Boehringer Mannheim).
4. Genomic sample DNA dissolved in 50 µL of 10 m*M* Tris-HCl, pH 8.3.

2.2.5. PCR-RFLP Step

1. Reaction buffer: 60 m*M* Tris-SO_4, pH 9.1, 18 m*M* $(NH4)_2SO_4$, 1.5 m*M* $MgCl_2$;
2. Nucleotides: 0.2 m*M* of each dATP, dCTP, dGTP, dTTP dissolved in A. bidest.
3. *Taq* DNA-Polymerase (Boehringer Mannheim).

3. Methods

3.1. Mutant-Enriched PCR-SSCP Using PNAs

3.1.1. PCR-Clamping Reaction (Step 1)

The PCR step is performed in a total volume of 25 µL reaction buffer, 0.2 mM of each dNTP, 50–100 ng of DNA, 25 pmol of each primer, 12.5 pmol of PNA, 3.75% glycerol (7.5% glycerol in case of PNAK12-3) and 1 unit of Taq DNA-Polymerase. To prevent unspecific polymerization prior to thermal cycling, the mixture is directly placed into a pre-heated thermocycler and kept at 94°C for 5 min. PCR amplification over 24 cycles with the following parameters: 94°C, 60 s, 73°C 60 s in case of PNA248-9 or alternatively

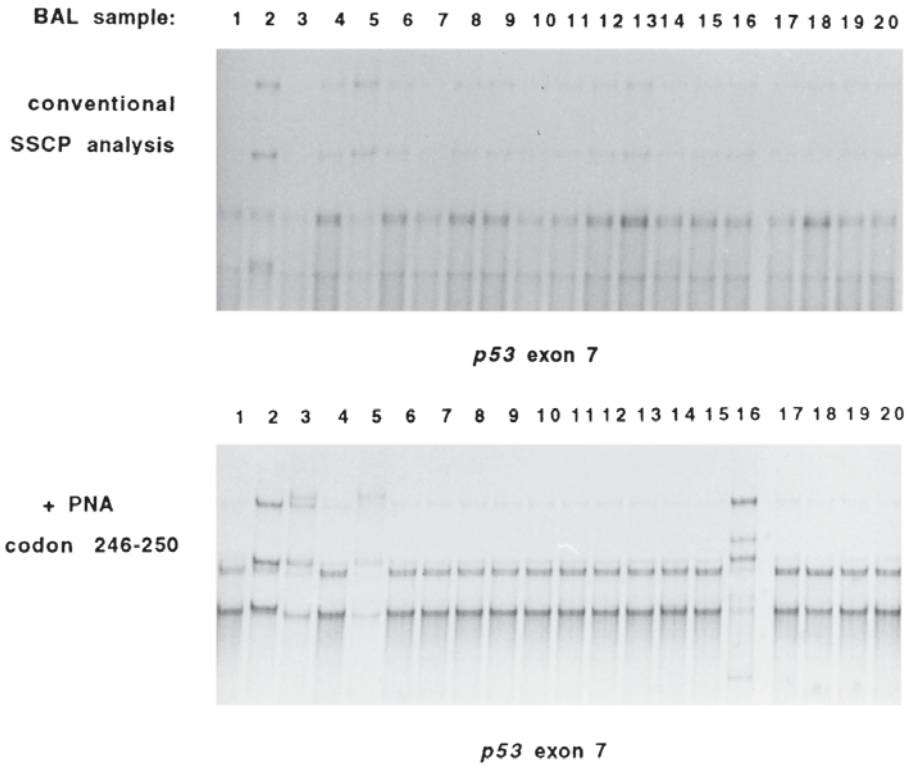

Fig.2. Example of a PCR-SSCP gel using a PNA oligonucleotide largely blocking the amplification of wild-type *p53* alleles. A clear polymorphism becomes visible in lanes 3, 4, and 16, which is not seen in the absence of added PNA. Following mutant-enriched SSCP-PCR, aliquots of the radiactively labeled PCR amplification product was loaded onto a MDE-gel and run overnight (*see* details in **Subheading 3.**).

68°C in case of PNA273; 54°C 60 s; and 72°C 120 s. The additional step at 73°C or 68°C, respectively, is chosen in order to allow the preferential annealing of the PNA to DNA.

3.1.2. Reamplification (Step 2)

One µL of the resulting PCR-amplified DNA from **step 1** is reamplified using identical PCR clamping conditions but this time adding 0.1 µCi 33P-cCTP in a 25 µL reaction volume.

3.1.2.1. SSCP-Analysis

Following the mutant-enriched-PCR 3 µL of α[^{33}P]-dCTP labeled PCR amplification product is added to 12 µL of sequencing stop solution (95% formamide, 10 m*M* NaOH and tracking dyes, heated to 95°C for 3 min and loaded onto a MDE-gel (Hydrolink™; at the size of 40 × 20 cm and 1.5 mm thickness) according to the manufacturer's specification (*see* **Note 5**). The gel is run in 1/2 × TBE (50 mL TBE + 950 mL dH_2O) at 4°C and 4 Watts overnight (about 14 h) and the labeled fragments are visualized by autoradiography. An example of a PCR-SSCP gel is shown in **Fig. 2** demonstrating the gain in sensitivity by PNA-mediated allelosuppression.

3.2. Combined Allele-Specific Enriched PCR (CASE-PCR)

3.2.1. PNA-PCR Parameters (Pre-Amplification)

Each reaction is performed in a volume of 25 µL reaction buffer (*see* **Subheading 2.2.4.**) containing 0.2 m*M* of each dNTP, 50 ng of DNA, 25 pmol of each primer, 75 pmol of PNA, and 1 unit of *Taq* DNA-Polymerase. To prevent unspecific polymerization prior to thermal cycling, hot start is performed by 5 min preheating at 94°C. The PCR reaction itself is performed over 24 cycles with the following conditions: 60 s at 94°C, 60 s at 73°C (PNA248-9) or, alternatively, at 68°C (PNAs K12-3 and 273), 60 s at 54°C and 120 s at 72°C (*see* **Note 6**).

3.2.2. Purification of PCR Products

DNA fragments resulting from the first amplification are purified by centrifugation through quick-spin columns (QIAquick PCR Purification Kit; Qiagen). The samples are then diluted 1:100 to 1:300 and 2 µL are taken for the PCR-RFLP analysis.

3.2.3. PCR-RFLP Analysis

Two µL of diluted pre-amplified products of first step are amplified over 30 cycles in a volume of 50 µL containing the following

buffer components: PCR-RFLP reaction buffer (*see* **Subheading 2.2.5.**), 0.2 m*M* of each dNTP, 25 pmol of each primer, and 2 Units *Taq* DNA polymerase (50 µL of total reaction volume). PCR parameters: 60 s at 94°C, 60 s at 60°C; 120 s at 72°C. The number of cycles can be reduced to 24 if more than 100 ng of input material is taken.

3.2.4. Endonuclease Digestion of PCR-RFLP Products

Five microliter aliquots of the PCR-RFLP reaction are digested with 25 units of the following respective enzymes. These are for K-*ras* codon 12: *Mva*I (Boehringer Mannheim), for *p53* codon 248: *Csp*I (Stratagene), *p53* codon 249: *Bsu36*I (Stratagene), and *p53* codon 273: *Mlu*I (Boehringer Mannheim). The digestion is performed for 3 h in a total volume of 25 µL under conditions recommended by the supplier (PCR reaction components are ignored). 20 µL of the digestion products are electrophoresed through a 3% ethidium bromide stained Nu Sieve® Agarose gel (Biozym, FMC Rockland). The PCR-RFLP step yields products of comparable intensities that are either completely digested in case of wild-type status or are digestion resistant in case of a given K-*ras* or *p53* hot spot mutation.

3.3. Additional Comments

3.3.1. Mutant-Enriched PCR-SSCP

The mutant-enriched PCR-SSCP method allows the rapid, efficient, and sensitive detection of oncogene "hot spot" mutations in material containing only a minority of tumor cells ***(14)***. The limit of detection is in the range of 0.5–1% variant (mutant) alleles, whereas with conventional PCR-SSCP at least 5 %, i.e., the inclusion of PNAs in the reaction step, provides an additional 10-fold increase in sensitivity. A further advantage is that a single PNA can also detect mutations in adjacent neighboring codons simultaneously. Several PNAs strategically designed to cover the majority of *p53* missense lesions could therefore prove a useful way to screen for *p53* mutations in exfoliated material from body fluids. The PCR

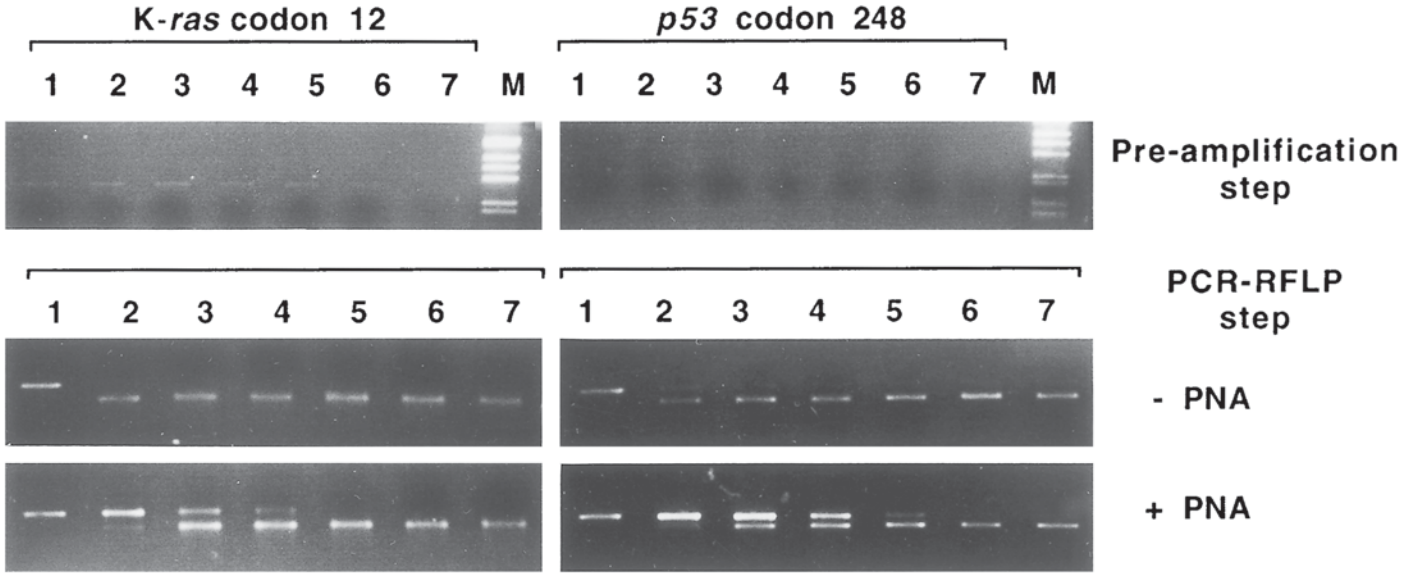

Fig. 3. Analysis of oncogene mutations by CASE-PCR. DNA from a cell line harboring a homozygous K-*ras* codon 12 or *p53* codon 248 mutation was diluted into DNA from a cell line with wild-type K-*ras* (*p53*) status to yield 200 ng genomic DNA per vial. Top: Example of reaction products after 24 cycles of PNA-clamping. Bottom, reaction products after PCR-RFLP (total of 48 cycles) either in the presence or absence of specific PNA. Lane 1, mutant cell line, no dilution; lane 2, diluted 1:10, lane 3, $1:10^2$; lane 4, $1:5 \times 10^2$; lane 5, $1:10^3$, lane 6, 5×10^3; lane 7, negative control. Samples were processed as described in **Subheading 3.** The gel electrophoresis separates residual wild-type alleles from enriched restriction resistant mutant forms (running as retarded bands). M = molecular DNA marker.

clamping is largely independent of salt concentration, and tolerates a relatively large temperature gradient with respect to both the DNA and PNA hybridization temperatures.

3.3.2. Combined Allele-Specific Enriched PCR-SSCP

The use of PNAs in the reaction generally offers the advantage to examine allelic mutations in several hot-spot positions (e.g., K-*ras,* codons 12, 13; *p53*, codons 248, 249) as long as these are covered by one PNA molecule. By serial dilution of K-*ras* mutant DNA into wild-type background we determined a safe limit of detection in the range of one mutant allele in 10^3 wild-type alleles (example shown in **Fig. 3**). We estimate the specific enrichment effect of the PCR clamping step to be about 50-fold ***(15)***. Although other PCR-RFLP based protocols are able to still lower the sensitivity to approx 1 allele in 10^4 this procedure implies three to four successive PCR steps with up to 100 PCR cycles, thereby augmenting the risk of amplifying *Taq*-polymerase borne errors. In our hands the limitation to two successive PCR steps (involving 48–54 PCR cycles) provides a technically reliable way to screen for single codon oncogene mutations but still offers a sufficiently high sensitivity to account for low-abundance alleles. A similar technique has been described based on the combination of PNA-clamping and allele-specific PCR ***(18)***. While this method is even more sensitive, the ASA step requires a larger collection of allele-specific primers to cover all possible mismatches in each individual codon to be examined, which limits the number of hot spot positions that can be analyzed. Moreover, different sequence-specific primer-template combinations occur in each case that need subtle adjustment of PCR conditions.

4. Notes

1. High concentrations of $MgCl_2$ are normally recommended to stabilize PNA/DNA binding; however, we found an optimal specificity at

around 1.5 m*M*. Concentrations above 2.5 m*M* yielded false positive results, presumably by weakening the PNA association.

2. The clamping reaction is relatively dependent on the amount of input genomic DNA. For this reason no less than 50 ng of DNA should be taken; we find an optimum around 100 ng. Otherwise, a preamplification step is required.
3. The design of mismatch primers and primer combinations have been chosen to allow uniform amplification conditions at 60°C . The type of restriction enzyme chosen and the excessive amounts added in the reaction should regularly ensure a complete digest within 3 h.
4. PNA oligomers should be always identical to the noncoding strand of the wild-type allele and chosen so that a 15- nucleotide segment around the "hot spot" mutation site is covered.
5. Instead of ordinary polyacrylamide gels we recommend the use of (mutation detection enhancement)MDE-gels, which provide a high-density resolution optimal for the detection of subtle differences in the electrophoretic mobility of certain allele variants.
6. Conditions of the PCR clamping reaction have been identical to those described by Thiede et al. ***(17)*** With a limitation to 24–30 amplification cycles, the first step usually reveals specific PCR products of varying intensities, most of which are barely visible in ethidium bromide stained gels.

References

1. Huebner, K., Ohta, M., Lubinski, J., Berd, D., and Maguire, H. C., Jr. (1996) Detection of specific genetic alterations in cancer cells. *Sem. Oncol*. **23,** 22–30.
2. Loda, M. (1994) Polymerase chain reaction-based methods for the detection of mutations in oncogenes and tumor suppressor genes. *Hum. Pathol.* **25,** 564–571.
3. Weber, J. L. (1990) Human DNA polymorphisms and methods of analysis. *Curr. Opin. Biotechnol.* **1,** 166–171.
4. Jacobson, D. R. and Mills, N. E. (1994) A highly sensitive assay for mutant ras genes and its application to the study of presentation and relapse genotypes in acute leukemia. *Oncogene* **9,** 553–563.

5. Kahn, S. M., Jiang, W., Culbertson, T. A., Weistein, I. B., Williams, G. M., Tomita, N., and Ronai, Z. (1991) Rapid and sensitive nonradioactive detection of mutant K-ras genes via 'enriched' PCR amplification. *Oncogene* **6,** 1079–1083.
6. Levi, S., Ubano-Ispizua, A., Gill, R., Thomas, D. M., Gilbertson, J., Foster, C., and Marshall, C. J. (1991) Multiple K-ras codon 12 mutations in cholangiocarcinomas demonstrated with a sensitive polymerase chain reaction technique. *Cancer Res*. **51,** 3497–3502.
7. Mills, N. E., Fishman, C. L., Scholes, J., Anderson, S. E., Rom, W. N., and Jacobson, D. R. (1995) Detection of K-ras oncogene mutations in bronchoalveolar lavage fluid for lung cancer diagnosis. *J. Natl. Cancer Inst.* **87,** 1056–1060.
8. Mao, L., Hruban, R. H., Boyle, J. O., Tockman, M., and Sidransky, D. (1994) Detection of oncogene mutations in sputum precedes diagnosis of lung cancer. *Cancer Res.* **54,** 1634–1637.
9. Ørum, H., Nielsen, P. E., Egholm, M., Berg, R. H., Buchardt, O., and Stanley, C. (1993) Single base pair mutation analysis by PNA directed PCR clamping. *Nucleic Acids Res.* **21,** 5332–5336.
10. Buchardt, O., Egholm, M., Berg, R. H., and Nielsen, P. E. (1993) Peptide nucleic acids and their potential applications in biotechnology. *Trends Biotechnol.* **11,** 384–386.
11. Nielsen, P. E. (1995) DNA analogues with nonphosphodiester backbones. *Annu. Rev. Biophys. Biomol. Struct*. **24,** 167–183.
12. Agrawal, S. and Iyer, R. P. (1995) Modified oligonucleotides as therapeutic and diagnostic agents. *Curr. Opin. Biotechnol.* **6,** 12–19.
13. Orita, M., Suzuki, T., and Hayashi, K. (1989) Rapid and sensitive detection of point mutations and DNA polymorphisms using the polymerase chain reaction. *Genomics* **5,** 874–879.
14. Behn, M. and Schuermann, M. (1998) Sensitive detection of p53 gene mutations by a 'mutant enriched' PCR-SSCP technique. *Nucleic Acids Res.* **25,** 1356–1358.
15. Behn, M., Thiede, C., Neubauer, A., Pankow, W., and Schuermann, M. (2000) Facilitated detection of oncogene mutations from exfoliated tissue material by a PNA-mediated 'enriched PCR' protocol. *J. Pathol.* **190,** 69–75.

16. Mitsudomi, T., Steinberg, S. M., Nau, M., Carbone. D., D'Amico, D., Bodner, S., et al. (1992) p53 gene mutations in non-small-cell lung cancer cell lines and their correlation with the presence of ras mutations and clinical features. *Oncogene* **7**, 171–180.
17. Thiede, C., Bayerdorffer, E., Blasczyk, R., Wittig, B., and Neubauer, A. (1996) Simple and sensitive detection of mutations in the ras proto-oncogenes using PNA-mediated PCR clamping. *Nucleic Acids Res.* **24,** 983–984.
18. Rhodes, C. H., Honsinger, C., Porter, D. M., and Sorenson, G. D. (1997) Analysis of the allele-specific PCR method for the detection of neoplastic disease. *Diagn. Mol. Pathol.* **6,** 49–57.

12

PNA Fluorescent *In Situ* Hybridization for Rapid Microbiology and Cytogenetic Analysis

Brett Williams, Henrik Stender, and James M. Coull

1. Introduction

Hybridization-based assays for the detection of nucleic acids including *in situ* hybridization are increasingly being utilized in a wide variety of disciplines such as cytogenetics, microbiology, and histology. Generally *in situ* hybridization assays utilize either cloned genomic probes for the detection of DNA sequences or oligonucleotide probes for the detection of DNA or RNA sequences. Alternately, peptide nucleic acid (PNA) probes are increasingly being utilized in a variety of *in situ* hybridization assays ***(1,2)***. The neutral backbone of the PNA molecule allows for the PNA probes to bind to DNA or RNA under low ionic-strength conditions that will either disfavor reannealing of complimentary genomic sequences or are denaturing for RNA secondary structure but are favorable for PNA/DNA or PNA/RNA hybridization ***(3,4)***. For *in situ* hybridization assays, these unique properties of PNA probes offer significant advantages that allow for the development of fast, simple, and robust assays.

This chapter outlines two protocols that have exploited the unique physico-chemical properties of the PNA molecule in the develop-

From: *Methods in Molecular Biology, vol. 208: Peptide Nucleic Acids: Methods and Protocols*
Edited by: P. E. Nielsen

ment of *in situ* hybridization assays for the targeting of chromosome specific human alpha satellite sequence and for the definitive identification of microorganisms by targeting species-specific rRNA sequences.

1.1. Culture Identification by PNA FISH

Fluorescence *in situ* hybridization using PNA probes (PNA-FISH) is a new molecular method for definitive identification of microorganisms using fluorescein-labeled PNA probes targeting species-specific rRNA sequences ***(5–8)***. Due to the high cellular abundance of rRNA, individual cells can be detected directly by fluorescence microscopy ***(9)*** and thus identified directly in primary cultures, thereby eliminating the requirement for subculture to obtain pure isolates.

rRNA sequence analysis today is a well-established method for phylogenetic analysis of microorganisms ***(10)*** and has further enabled design of specific probes against the rRNA of most microorganisms of clinical, industrial, and environmental interest. As a result, molecular diagnostic methods using rRNA sequences are rapidly replacing the classic phenotypic-identification methods based on biochemical analysis and morphological characteristics.

The noncharged backbone of PNA allows hybridization to be performed under low-salt conditions that are denaturing for rRNA secondary structure but favorable for PNA-RNA hybridization ***(11)***. This enables use of PNA probes targeting rRNA sequences in highly structured regions where many species-specific target sequences are found. Furthermore, the relative hydrophobic character of PNA makes PNA probes able to easily diffuse through the hydrophobic cell wall of fixed bacteria and yeasts. *See* **Fig. 1**.

1.2. Molecular Cytogenetic Analysis Using PNA FISH

FISH has become firmly established in cytogenetics, with the vast majority of FISH probes in use being derived from cloned genomic probes. Recently, the utility in FISH assays of directly labeled PNA probes that have been designed from human satellite or telomeric

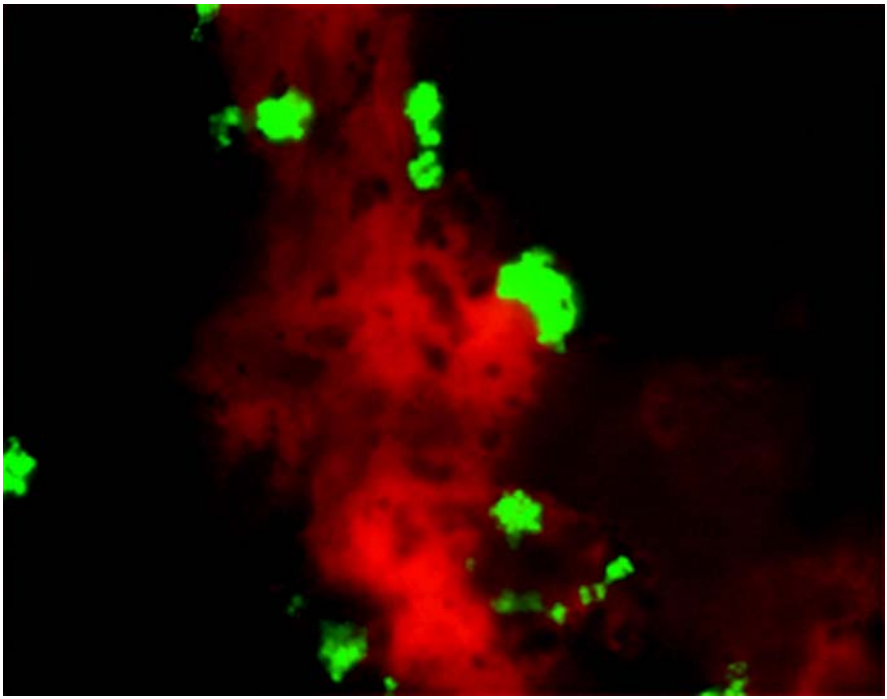

Fig. 1. Identification of *Staphylococcus aureus* from blood culture by PNA-FISH. Identification is based on bright fluorescent cells and thus combines the specificity provided by molecular technologies with the typical cell morphology.

repeat sequence has been demonstrated by a number of investigators ***(13–16)***. As mentioned previously, PNA probes can bind to DNA under low ionic-strength conditions that disfavor reannealing of complimentary genomic strands. This advantage is particularly important for *in situ* hybridization experiments that target repetitive sequences, because both the length and the repetitive nature of the target sequences will effectively favor renaturation over hybridization with labeled probes ***(13)***. These properties of PNA have been exploited in the following protocol; the sensitivity of which when used with a mixture of short synthetic PNA probes is comparable to large cloned probes. *See* **Fig. 2**.

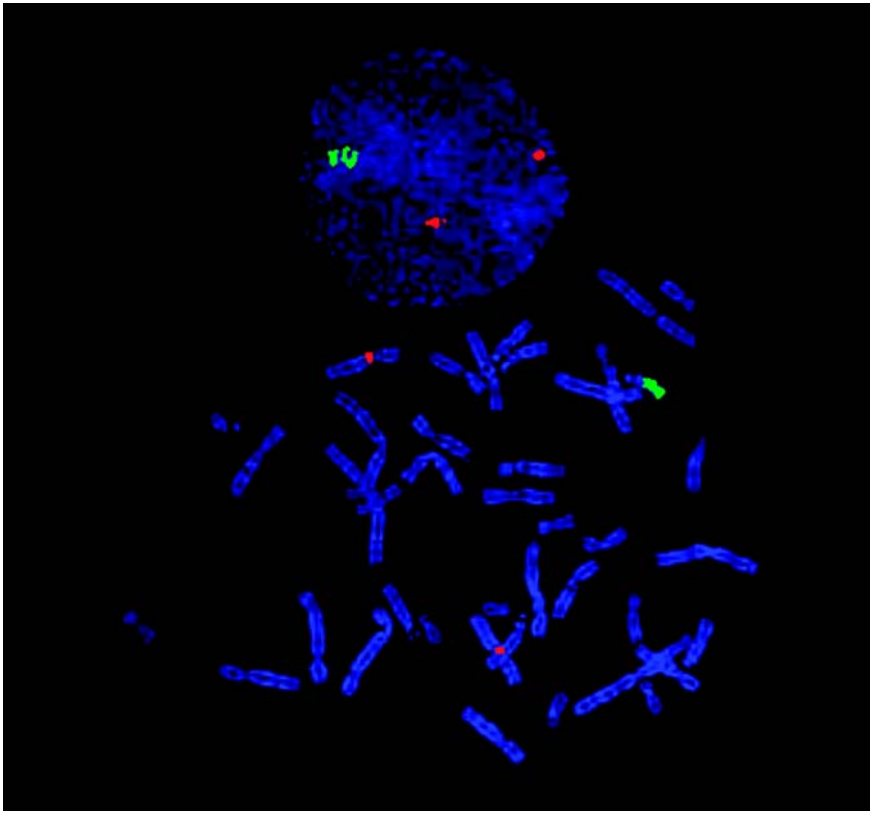

Fig. 2. Detection and enumeration of the X andY chromosomes in human cells with sex chromosome abnormalities. A mixture of Cy3 and fluorescein labeled PNA probes specific for the X centromere and Yq12 region, respectively, were used.

2. Materials

2.1. Culture Identification by PNA FISH

1. Filter-sterilized PBS. It is recommended to add 1% Triton X-100 for culture media containing material, such as charcoal, to prevent nonspecific binding of PNA.
2. Fluorescein-labeled PNA probe targeting rRNA: Typically, PNA probe sequences of approx 15 bases with T_m values in the range of 60–70°C are optimal. Fluorescein-labeled PNA probes targeting

Escherichia coli 16S rRNA, *Pseudomonas aeruginosa* 16S rRNA, *Salmonella enterica* 23S rRNA, *Staphylococcus aureus* 16S rRNA, *Dekkera bruxellensis* 26S rRNA as well as universal probes targeting eubacterium 16S rRNA and eukarya 18S rRNA are available from Boston Probes (Bedford, MA), whereas custom-made PNA probes can be obtained from Applied Biosystems (Foster City, CA). It is recommended to re-suspend and store PNA probes in 50% aqueous N,N-dimethyl formamide (DMF) at –18°C prior to use.

3. Hybridization Buffer: 10% (w/v) dextran sulfate, 10 m*M* NaCl, 30% (v/v) formamide, 0.1% (w/v) sodium pyrophosphate, 0.2% (w/v) polyvinylpyrrolidone, 0.2% (w/v) ficoll, 5 m*M* Na_2EDTA, 0.1% (v/v) Triton X-100, 50 m*M* Tris-HCl, pH 7.5. Store at 2–8°C. (*see* **Note 1**).
4. Wash Solution: 25 m*M* Tris-HCl or CAPSO, pH 10.0, 137 m*M* NaCl, 3 m*M* KCl. Store at 2–8°C, preferably as a 60X stock solution.
5. IMAGEN Mounting Fluid (DAKO, Ely, UK). Store at 2–8°C. Alternatively, VectaShield Mounting Medium (Vector Laboratories, CA) may be used, although it tends to give a more reddish smear background (*see* **Note 2**).
6. Ethanol (Histology Grade).
7. Milli Q or deionized water.
8. Teflon-coated microscope slides with 14-mm diameter wells for FISH (ClearCell, Erie Scientific, Portsmouth, NH) (*see* **Note 3**).
9. Coverslips with a 0.15 mm thickness (No. 1).
10. Incubator or hybridization chamber at 55 ± 1°C.
11. Water bath (55 ± 1°C). The temperature of the water bath should be checked using a thermometer in the water.
12. Coplin jar for slides.
13. Fluorescence microscope equipped with a 60× or 100× oil objective, a 100 W mercury lamp, and a FITC/Texas Red dual band filter. The use of a 50 W lamp reduces the fluorescent signal. The FITC/Texas Red double filter provides excellent discrimination between autofluorescence and specific signal, because autofluorescence will appear reddish whereas cells detected by the fluorescein-labeled PNA probe will be bright green. In particular clusters of cells and yeast cells tend to autofluoresce and therefore make it difficult to distinguish between positive and negative results using a standard FITC-filter (*see* **Note 4**).
14. Immersion oil. The immersion oil used must comply with the microscope objective and be nonfluorescent.

2.2. Molecular Cytogenetic Analysis Using PNA-FISH

2.2.1. Reagents

1. Labeled PNA Probes: Typically, PNA probe sequences of approx 18–20 bases with T_m values in the range of 65–75°C are optimal. Chromosome specific centromere and pan telomere probes are available from Boston Probes, custom-made PNA probes can be obtained from Applied Biosystems. It is recommended to store the PNA probes in 50% aqueous DMF at –18°C prior to use (1) (*see* **Note 5**).
2. Hybridization buffer: 20 m*M* Tris-HCl, pH 7.5, 70% formamide (Gibco-BRL), 1X Denhardt's solution (Sigma), 10 m*M* NaCl, 100 mg/mL tRNA (Sigma), 100 µg/mL salmon sperm DNA (Sigma), pH 7.0–7.5.
3. Metaphase chromosome and Interphase cell suspension.
4. Ethanol (histology grade).
5. Mill-Q H_2O.
6. Carnoy's Fixative (3:1 methanol/acetic Acid): 3 parts methanol (J.T. Baker) to 1 part glacial acetic acid (J.T. Baker).
7. 20X SSC 1% Tween 20: 3 *M* NaCl, 0.3 *M* Sodium Citrate, 1% (v/v) Tween 20, pH 7.0–7.5. 2X SSC 0.1% Tween 20. Prepare 50 mL for each experiment (sufficient for 5 slides) by making a 1 in 10 dilution of the 20X SSC 1% Tween 20.
8. 10X PBS 1% Tween 20: 27 m*M* KCl, 15 m*M* KH_2PO_4, 1.4 *M* NaCl, 8 m*M* Na_2HPO_4, 1% (v/v) Tween 20, pH 7.5. 1X PBS 0.1% Tween 20. Prepare 50 mL for each experiment (sufficient for 5 slides) by making a 1 in 10 dilution of the10X PBS, 1% Tween Wash Solution.
9. Mounting medium: Vector Shield (Vector Laboratories) containing 100 ng/mL of DAPI.

2.2.2. Equipment

1. Suitably equipped epifluorescence microscope with appropriate filters (*see* **Note 6**).
2. Microscope slides: Gold Seal precleaned slides, dipped in 100% ethanol, and polished with a lint free cloth (*see* **Note 7**).
3. Cover slips (22 × 22 mm): 0.15 mm thickness Corning brand No. 1.
4. Pipettes (10 µL and 20 µL).
5. Sterile pipet tips.

6. Graduated cylinders.
7. Water bath (55–60°C).
8. Incubator or heating block (70–80°C).
9. Humidified chamber at room temperature.
10. Forceps.
11. Coplin jars (50 mL).

3. Methods

Before starting the assay procedure, prepare working-strength wash solution and start to preheat (*see* **Note 8**).

3.1. Culture Identification by PNA-FISH

3.1.1. Preparation of Smears

1. Place one drop of phosphate-buffered saline (PBS) in a well on a microscope slide.
2. Transfer a small drop (10–50 µL) of re-suspended culture or a small part of a colony to the PBS and mix gently to emulsify.
3. Allow the smears to air-dry.
4. Fix the smears by passing the slide through the blue cone of a Bunsen burner three to four times, by heating for 20 min at 60°C, or by methanol for 5 min ***(12)***.
5. Immerse the slide in 80% ethanol for 5–10 min. This step primarily serves to disinfect the smear, but may also supplement fixation of the cells.
6. Air-dry until the smears are dry (approx 10 min). The smears may be stored for up to 14 d at 2–8°C prior to hybridization, preferably placed in a sealed foil bag with a desiccant.

3.1.2. Hybridization

1. Dilute the fluorescein-labeled PNA probe in Hybridization Buffer. Typically, a concentration in the range of 100–500 n*M* is optimal, but it is recommended to carefully titrate individual probes using a panel of representative species. The diluted PNA probe in the Hybridization Buffer should be stored at 2–8°C and is stable for up to 1 yr.

2. Add one drop of PNA probe in Hybridization Buffer to the well on the microscope slide with the smear.
3. Add coverslip and try to avoid air bubbles trapped by coverslips, as this will reduce the hybridization efficiency.
4. Incubate for 90 min at 55°C.

3.1.3. Stringent Wash

1. Immerse slide in preheated Wash Solution at 55°C in a Coplin jar placed in a water bath at 55°C (*see* **Note 8**).
2. Carefully remove the coverslip.
3. Incubate for 30 min. at 55°C.

3.1.4. Mounting

1. Add one drop of Mounting Medium to the smear.
2. Add coverslip and try to avoid air bubbles as that may interfere with microscopic examination.

3.1.5. Microscopical Examination

1. Examine slides using a fluorescence microscope. The cell smear appears in general brown/reddish. Positive identification is observed as bright green fluorescent cells and further supported by cell morphology. The intensity may vary between individual cells due differences in the amount of rRNA and/or permeability of the cell wall. The slides are stable when stored in the dark for at least 14 d.

3.2. Molecular Cytogenetic Analysis Using PNA-FISH

3.2.1. Slide Preparation

1. Spot the cell suspension onto a cleaned microscope slide using your current laboratory procedure. Evaluate the metaphase cells using phase-contrast microscopy. Using a 20X phase objective, the metaphase chromosomes should appear gray/black and free of cytoplasm. If there is excessive cytoplasm present it is not advisable to proceed with the hybridization (*see* **Note 9**)
2. After preparing the slides, for optimal chromosome morphology and staining intensity, the slides should be aged for at least 4 h at room

temperature (preferably overnight) before proceeding with the hybridization steps. Alternatively, slides can be stored at –20°C; slides are typically stable for at least 6 mo when stored correctly (*see* **Note 10**).

3.2.2. Hybridization

1. If the slides have been stored in the freezer, allow the slides to warm to room temperature before use.
2. Prepare the PBS wash solution by adding 1X PBS, Tween Wash Solution to a Coplin jar and warm to 57 ± 1°C.
3. Dilute the labeled PNA probe in Hybridization Buffer. Typically, a concentration in the range of 4–100 n*M* is optimal. The diluted PNA probe in Hybridization Buffer should be stored at 2–8°C and is stable for up to 1 yr.
4. Apply a 10 µL aliquot of probe solution to the target area of the slide. Immediately place a 22 × 22 mm glass coverslip over the probe solution and allow the solution to spread evenly under the coverslip. Try to avoid air bubbles because they may interfere with hybridization.
5. Place the slides in an incubator preheated to 70 ± 1°C for 5–8 min (*see* **Note 11**).
6. Prepare a humidified hybridization chamber by placing a damp paper towel in a container at room temperature and cover the chamber with a lid. Remove the slide from the incubator or heating block and place the slide into the humidified hybridization chamber. Reseal the container.
7. Incubate at room temperature for 30 min.

3.2.3. Posthybridization Washes

1. Immerse the slide(s) in 1X PBS, 0.1% Tween Wash Solution at room temperature to remove the coverslip.
2. Transfer the slide(s) to the prewarmed 1X PBS, 0.1% Tween Wash Solution and wash the slide at 57 ± 1°C for 20 min.
3. Rinse the slide(s) in 2X SSC 0.1% Tween wash solution for 1 min.
4. Drain the excess fluid from the slide and apply 20 µL of Mounting Media containing DAPI counterstain to the target area and place a 22 × 22 mm glass coverslip. Try to avoid air bubbles because they may interfere with visualization.
5. Place a tissue over the slide and gently apply pressure with your fingers to squeeze out the excess mounting media.

6. Store the slide in the dark for 15–30 min to allow the DAPI to stain the cells before viewing under the microscope.
7. The slides may be viewed immediately or stored at 4°C or –20°C in the dark. Slides are typically stable for at least 6 mo when stored correctly.

3.2.4. Microscopy Examination

The DAPI counterstain is used as a general DNA stain to aid in the location of metaphase spreads and interphase cells. The fluorescent signals are viewed using an epifluorescence microscope equipped with appropriate excitation and emission filters. In metaphase spreads, the centromere of the chromosome of interest will fluoresce brightly (the color of which will depend on the fluorochrome(s) used). In interphase cells the centromeric signals will be present as bright fluorescent spots. The hybridization efficiency of the PNA probes should be greater than 90% for metaphase and interphase cells.

4. Notes

1. The Hybridization Buffer contains 30% formamide. There is a possible risk of harm to unborn child. It is irritating to eyes, respiratory system, and skin. Wear suitable protective clothing and gloves.
2. Care should be taken when using the Mounting Medium because it may cause skin irritation. Skin should be flushed with water if contact occurs.
3. The use of other slides should be carefully evaluated in respect to the thickness of the teflon-coating, cell-adhesive characteristics, and background spots due to unspecific binding of PNA probes.
4. It is important that the microscope is functioning properly. Make sure that the microscope bulb is correctly adjusted and is not aged above its specified lifetime.
5. PNA probes are compatible with a wide range of reporter molecules including fluorochromes for the direct detection of the PNA probe such as fluoroscein, rhodamine, and the alexa and cyanine series of dyes. For indirect detection of PNA probes, alkaline phosphatase, peroxidases, biotin, DNP, and digoxigenin labels have been utilized.
6. The epifluorecent microscope should be equipped with at least a 10× plan Fluorite objective for locating cells of interest and a 60× and/or

Table 1
Examples of Filters for Common Fluorochromes

Part No.	Ex	Em
Omega XF05/Chroma 31000 (DAPI filter set)	365	400
Omega XF22/ Chroma 41001 (FITC filter set)	485	530
Omega XF34/ Chroma 41007 (Cy3 filter set)	535	590

a 100× oil plan fluorite NA 1.3–1.4 objectives for observing the cells at high magnification. Below are examples of filters from Omega and Chroma suitable for three of the common fluorochromes used *in situ* hybridization experiments (*see* **Table 1**).

7. The use of clean slides cannot be overemphasized. There are a number of protocols for cleaning microscope slides, the simplest of which is to soak the slides in ethanol and wipe clean with a lint free cloth as described earlier. Other approaches include soaking in detergent, followed by rinsing in deionized water and either kept in distilled water until use or dipped in ethanol and rapidly air-dried.
8. It is important that the temperature of the Wash Solution has reached a temperature of 55°C prior to immersion of the slides.
9. The temperature and humidity of the environment in which the slides are made should be optimized to 20–23°C and 50–60%, respectively. If excessive cytoplasm is present, prepare another slide as follows: spot the cell suspension onto a cleaned microscope slide, as the spot takes on a grainy appearance add 1–2 drops of fixative (3:1 methanol:acetic acid). Allow the slides to dry and re-evaluate.
10. If the slides are to be subjected to a hybridization experiment immediately after preparation, then the following steps may be helpful in maintaining chromosome morphology and signal intensity:
    a. Prepare the pretreatment solution by adding 50 mL of 2X SSC wash solution to a Coplin jar and warm to 55 ± 1°C.
    b. Add the slides to the prewarmed 2X SSC wash solution for 5 min.
    c. Dehydrate the slides for 1 min in each of the cold ethanol (70, 85, 100%) series. Air-dry.
    d. Proceed with the hybridization steps.
11. If you are using a programmable heating block then the block should be programmed to gradually increase (90 s) the temperature to 75°C,

hold the temperature for 90 s at 75°C and then ramp down the temperature to room temperature (90 s). If the heating block is humidified, the slides may be left on the heating block for the 30-min hybridization step at room temperature before proceeding with the posthybridization wash steps.

References

1. Buchardt, O., Egholm, M., Berg, R. H., and Nielsen, P. E. (1993) Peptide nucleic acids and their potential applications in biotechnology. *Trends Biotechnol.* **11,** 384–386.
2. Thisted, M., Just, T., Pluzek, K. J., Hyldig-Nielsen, J. J., Nielsen, K. V., Mollerup, T. A., et al. (1999) Application of peptide nucleic acids probes for *in situ* hybridization, in *Peptide Nucleic Acids, Protocols and Applications* (Nielsen, P. E and Egholm, M., eds.), Horizon Scientific Press, Wymondham, Norfolk, UK pp. 99–119.
3. Nielsen, P. E., Egholm, M., Berg, R. H., and Buchardt, O (1991) Sequence selective recognition of DNA by strand displacement with a thymine-substituted polyamide. *Science* **254,** 1497–1500.
4. Egholm, M., Buchardt, O., Christensen, L., Behrens, C., Freier, S. M., Driver, D. A., et al. (1993) PNA hybridizes to complementary oligonucleotides obeying the Watson-Crick hydrogen bonding rules. *Nature* **365,** 556–568.
5. Oliveira, K., Hyldig-Nielsen, J. J., Kurtzman, C., and Stender, H. (2001) Differentiation between Candida albicans and Candida dubliniensis by fluorescence *in situ* hybridization using PNA probes, in Annual Meeting of the American Society of Microbiology, Washington DC, P.C-387.
6. Oliveira, K., Procop, G., Wilson, D., Coull, J., and Stender, H. (2002) Rapid Identification of Staphylococcus aureus directly from Blood Cultures by fluorescence *in situ* hybridization with peptide nucleic acid probes. *J. Clin. Microbiol.* **40,** 247–251.
7. Stender, H., Lund, K., K. Petrsen, K. H., Rasmussen, O. F., Hongmanee, P., Miorner, H., and Godtfredsen, S. E. (1999) Fluorescence *in situ* hybridization assay using peptide nucleic acid probes for differentiation between tuberculous and nontuberculous mycobacterium species in smears of mycobacterium cultures. *J. Clin. Microbiol.* **37,** 2760–2765.
8. Stender, H., Kurtzman, C., Hyldig-Nielsen, J. J., Sørensen, D., Broomer, A., Oliveira, K., et al. (2001) Identification of

Brettanomyces (Dekkera bruxellensis) from wine by fluorescence *in situ* hybridization using peptide nucleic acid probes. *Appl. Environ. Microbiol.* **67,** 938–941.

9. Delong, E. F., Wickham, G. S., and Pace, N. R. (1989) Phylogenetic stains: Ribosomal RNA-based probes for the identification of single cells. *Science* **243,** 1360–1363.
10. Woese, C. R. (1987) Bacterial evolution. *Microbiol. Rev.* **51,** 221–271.
11. Stender, H., Fiandaca, M., Hyldig-Nielsen, J. J., and Coull, J. (2002) PNA for rapid microbiology. *J. Microbiol. Meth.* **48,** 1–17.
12. Pezzlo, M. (1998). Aerobic bacteriology, in *Essential Procedures for Clinical Microbiology* (Isenberg, H. D., ed.), American Society for Microbiology, Washington DC. pp. 51–57.
13. Taneja, K. L., Chavez, E. A., Coull, J., and Lansdorp, P. M. (2001) Multicolor fluorescence *in situ* hybridization with peptide nucleic acid probes for enumeration of specific chromosomes in human cells. *Genes Chrom. Cancer* **30,** 57–63.
14. Chen, C., Wu, B., Wei, T., Egholm, M., and Strauss, W. M. (2000) Unique chromosome identification and sequence-specific structural analysis with short PNA oligomers. *Mamm. Genome* **11,** 384–391.
15. Lansdorp, P. M., Verwoerd, N. P., Van de Rijke, F. M., Dragowska, V., Little, M. T., Dirks, R. W., et al. (1996) Heterogeneity in telomere length of human chromosomes. *Hum. Mol. Genet.* **5,** 685–691.
16. Ruler, N., Dragowska, W., Thronbury, G., Roosnek, E., and Lansdorp, P.M., (1998) Telomere length dynamics in human lymphocyte subpopulations measured by flow cytometry. *Nature Biotechnol.* **16,** 743–747.

13

Detection of Point Mutations Using PNA-Containing Electrophoresis Matrices

Gabor L. Igloi

1. Introduction

1.1. Background

Conventional nucleic acid/nucleic acid hybridization ***(1)*** can be one of the most sensitive procedures for detecting sequence polymorphisms. It forms the basis for many of the diagnostic or screening methods used at present. However, even the most successful of chip-based technologies encounter difficulties in distinguishing between hetero- and homozygous mutational events ***(2)***.

Affinity electrophoresis of macromolecules, depending on the noncovalent interaction of two species, requires the immobilization of one interacting partner in a matrix ***(3)***. The principle of affinity electrophoresis is analogous to other affinity techniques; a molecule in the mobile phase interacts specifically during its passage through the matrix with an immobilized ligand causing a mobility shift (**Fig. 1A**). Peptide nucleic acids (PNA) physically mixed with an electrophoresis medium are effectively immobilized owing to their minimal electronic charge. Electronic neutrality, together with salt-

From: *Methods in Molecular Biology, vol. 208: Peptide Nucleic Acids: Methods and Protocols*
Edited by: P. E. Nielsen © Humana Press Inc., Totowa, NJ

independent base-pair specificity *(4)*, are the properties of PNA that make them ideal candidates as ligands in an affinity electrophoretic partnership. The observed interaction is sensitive to parameters known to affect the stability of base pairs, such as temperature and concentration, enabling a predictable optimization of signal resolution and a single base-mismatch discrimination *(5)*. The matrix selectively retards complementary nucleic acids in a sequence-specific manner that is highly sensitive to mismatches and can readily be automated using commercial fluorescence-based DNA sequencers.

The ability of short PNA oligomers (11-mers) to discriminate between fully complementary and single-base mismatched DNA was established in a model system *(5)* and leads to the application of this property to the diagnostic screening of point mutations *(6,7)*. This requires the generation of PCR amplicons harboring the suspected polymorphic site that will be probed by the entrapped PNA during size fractionation (**Fig. 1B**). Here we will consider two alternative matrices: polyacrylamide slab gels *(6)* and fluid capillary electrophoretic media *(7,8)*; the design of the experimental components are identical. The observed effect is governed by conditions known to influence conventional hybridization. Consequently, base-pairing during electrophoresis is sensitive to temperature and the characteristic T_m of a PNA/DNA hybrid is dependent on the concentration of the interacting strands. Hence, either by raising the temperature or by decreasing the concentration of the trapped PNA one can destabilize the duplex and vica versa.

This concept of hybridization in real time can be applied to clinically relevant hetero- and homozygous mutation detection as exemplified here for the hereditary hemochromatosis C282Y mutation. The polymerase chain reaction (PCR) product from a heterozygous mutation is thereby resolved into two electrophoretically distinct species: a retarded fully complementary strand and a nonretarded mismatched strand *(6,7)*.

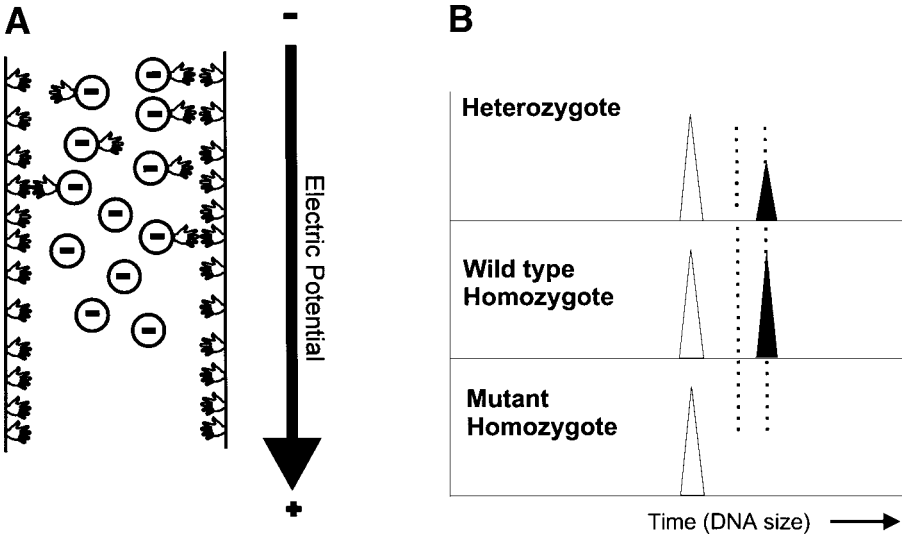

Fig. 1. Principle of affinity electrophoretic mutation detection. **(A)** Schematic view of an affinity interaction driven by an electric potential. The negative ions having an affinity for the immobilized partner are retarded during their passage through the matrix. The positive counter ions have been omitted for clarity. **(B)** Schematic representation of the behavior of DNA fragments bearing a point mutation in a matrix containing PNA that is complementary to the wild-type (black) sequence. The mobility of each species may be referred to an unrelated, noninteracting molecule (internal standard) (unshaded). Mutant alleles (gray) do not base pair efficiently with the entrapped PNA and their signals appear at earlier time points. Note the doublet characteristic for heterozygous loci.

1.2. Design of the Components

1.2.1. PNA

PNAs of 11 residues in length have shown to give adequate specificity in hybridization. They have been synthesized with one or more N-terminal linkers ([2-(N-Boc-2-aminoethoxy)ethoxy]acetic acid) that, according to the manufacturers, prevents rearrangement reactions. The additional terminal NH_2 group, with an estimated pK_a of ~8.5 may confer a slight overall positive charge to the molecule.

This has, in practice, no influence on the fractionation because the migration, if any, of the PNA will be in the opposite direction to that of the DNA. The PNA may be designed to be complementary to either strand and to the wild-type or mutant sequence. This fact permits a certain flexibility in the sequence chosen. The mutation site is optimally discriminated at internal positions of the PNA; position 4 from either end may be the best ***(5)***, but adequate resolution is also achieved at other positions. Of greater importance, as far as the PNA synthesis is concerned, is an avoidance of palindromic sequences and polyG stretches. Of significance for the hybridization, is that G:T mismatches are very stable and therefore, poorly discriminatory ***(5)***. Thus for G→A mutations it would make sense not to target the PNA to the wild-type G because in the mutant this could pair with the complementary T. If several PNAs are to be combined in one system, as in multiplexing (*see* **Subheading 3.4.**), one should aim to maintain similar GC contents to avoid extreme variations in T_m, although these can be compensated by appropriate choice of concentrations (*see* **Note 3**).

1.2.2. Primer

The general design principles of PCR primers apply. Additionally, and in contrast to conventional hybridization, one should be aware that affinity electrophoretic interaction has so far only been observed with amplicons where the PNA binding sequence is close (<25 bases) to either end ***(6)***. Thus, one of the primers should lie adjacent to (but not overlapping) the PNA binding sequence. If this appears impracticable, one may tail the primer with a restriction site such as *Bsg*I (nnnGTGCAG(N_{16}/N_{14})) (the lower case n denote bases added to increase the cleavage efficiency of the enzyme) permitting subsequent removal of much of the primer sequence, thereby bringing the PNA-binding site closer to the amplicon terminus. Because fluorescent detection is envisaged for all analyses discussed here, the distal primer, forming the strand complementary to the PNA probe, must bear a fluorescent label. The optical characteristics of the label are dictated by the detection system. For routine

multicolor screening, one should consider synthesizing the desired primer(s) bearing different fluorescent dyes. More economically, the PCR primer(s) may be 5'-terminally tailed with an unrelated common sequence (e.g., the universal M13 -20 primer). The primary unlabeled amplicon obtained with such primer(s) may be reamplified using variously labeled M13 -20 primers. In the case of fluorescein, the postsynthetic, enzymatic dye incorporation ***(9)*** has also been applied. PCR products are obtained by standard 3-temperature cycle protocols.

In designing PCR primers, one should bear in mind the length of the expected amplicon. As far as the mobility shift is concerned, effects have been observed for products of greater than 400 bp ***(6)***. However, and particularly noticeable in the case of slab gel-based systems, shorter fragments lead to faster analysis times. Routinely, amplicons in the region of 100–150 bp have been preferred.

1.2.3. The Matrix

All analyses are carried out under nondenaturing, but non-single-stranded conformational polymorphism (SSCP), conditions. For slab gels, 0.5X MDE gel (FMC Bioproducts, Rockland ME) has been used. One achieves better separation/resolution with this product than with polyacrylamide, under the same conditions. In the case of capillary electrophoresis, 2% native GeneScan polymer (Applied Biosystems, Foster City) in 1X TBE (*see* **Subheading 3.3.**) has been the medium of choice.

2. Materials

2.1. PCR for Detecting Hereditary Hemochromatosis C282Y

1. PCR primers: 5’ CCTGGGGAAGAGCAGAGATAT and a fluorescein-bearing 5’ Flu-TCAGTCACATACCCCAGATCAC.
2. PCR reaction mix: 2 µL 10X PCR buffer (Amersham-Pharmacia): 2 µL 2.5 m*M* dNTP (Amersham-Pharmacia); 10 pmol of each primer, approx 250 ng human DNA, 2.5 U Taq DNA polymerase (Amersham-Pharmacia), in 20 µL total volume.

3. Methods

3.1. Sample Preparation for Slab-Gel Electrophoresis

1. Run the PCR at 94°C for 5 min and then 30 cycles at 94°C, 55°C, and 72°C for 30 s each (Applied Biosystems GeneAmp PCR System 9600).
2. *Bsg*I digestion (where required): 5 µL PCR product, 5 µL 10X Buffer (New England Biolabs), 5 µL 0.8 m*M* S-adenosyl methionine (supplied with the enzyme), 1 µL (3U) *Bsg*I (New England Biolabs) in 50 µL total volume; 37°C, 1 h.
3. Dilute the PCR reaction 1:20 with water.
4. Add 3 µL 1% dextran blue in deionized formamide to 3 µL diluted PCR product (or an appropriate amount directly from the *Bsg*I digest).
5. Denature the sample at 95°C for 2 min and chill on ice (*see* **Note 1**).
6. Apply 3 µL to gel (*see* **Subheading 3.2.**).

3.2. Slab Gel Preparation Exemplified for Use With the ALF DNA Sequencer

1. Prepare the gel cassette with 0.35 mm spacers as for sequencing, i.e., washed, dried, assembled (*ALF DNA sequencer (Amersham-Pharmacia)* (*see* **Note 2**).
2. Mix the gel components as follows:
   a. 9 mL 2X MDE gel solution (FMC Bioproducts, Rockland, ME).
   b. 3.6 mL 10X Tris-borate buffer (1.0 *M* Tris-HCl, 0.83 *M* boric acid, 10 m*M* EDTA).
   c. A defined amount of PNA, 1–500 n*M* (*see* **Note 3**).
      PNA: (e.g., complementary to the wild-type) N-term O-CGT GCCAGGTG C-term (*see* **Note 4**) in a total of 36 mL.
3. Initiate polymerization by the addition of 130 µL fresh 10% ammonium persulphate and 30 µL TEMED. Pour gel and place sample slotformer in position.
4. After polymerization (approx 30 min), insert the gel cassette into the instrument and connect the thermostat plate to an external water bath (such as MultiTempII, Amersham-Pharmacia) to permit cooling below ambient temperature, if necessary.
5. Run gel at 34W constant power in 0.8X TBE running buffer.

3.3. Capillary Electrophoresis Exemplified for Use with the ABI310 Genetic Analyzer

A higher throughput, greater automation and more economic use of PNA is achieved using capillary electrophoresis *(7)*:

1. Prepare Amplicons as in Subheading 3.1., or alternatively by a two-step labeling procedure (*see* **Subheading 3.4.**).
2. Prepare the electrophoretic medium as follows:
   Stock solution of 2% GeneScan polymer: 1.43 g GeneScan polymer (Applied Biosystems), 0.5 g 10X TBE, 3.07 g H_2O. This solution is stable for several weeks at 4°C. Running buffer: 1X TBE (89 m*M* Tris-HCl, 89 m*M* boric acid, 2 m*M* Na_2EDTA). The PNA is diluted directly into the GeneScan polymer to an optimal final concentration (*see* text). One mL is usually ample for dozens of runs.
3. Run sample under standard conditions.

3.4. Two-step Fluorescent Labeling for Capillary Electrophoresis

1. Run first round PCR: Cycling is performed with 5 min at 94°C followed by 30 cycles of 94°C, 30 s; 62°C, 30 s; 72°C, 30 s
   a. PCR reaction mix: 2 µL 10X PCR buffer (Amersham-Pharmacia), 2 µL 2.5 m*M* dNTP (Amersham-Pharmacia), 20 pmol of each primer, approx 250 ng human DNA, 2.5 U Taq DNA polymerase (Amersham-Pharmacia), in 20 µL total volume.
   b. Primers: Unlabeled PCR primers:
      5' CCTGGGGAAGAGCAGAGATAT
      5'gtaaaacgacggccagtgTCAGTCACATACCCCAGATCAC, where the lowercase letters denote a 5' terminal universal M13–20 sequence that is used for fluorescent labeling during reamplification.
2. Run second round PCR: After completion of the first round PCR reaction, dilute the solution 1/50 and use 1 µL for reamplification using the untailed primer above and either FAM-, JOE, or TAMRA-labeled M13-20 primers under the same conditions as in the first round of amplification.
3. Prepare samples for electrophoresis (without further purification) by mixing 1 µL of reamplified solution with 2 µL ROX-labeled size marker (Promega, Madison) and 15 µL deionized formamide. De-

naturation at 90°C for 2 min is followed by quenching in ice.
4. Inject samples at 1 kV, 10 s (*see* **Note 7**) and perform the run at the chosen temperature at up to 12 kV(*see* **Note 8**).

3.5. Technical Discussion

As in the case of slab gels, preliminary optimization of PNA concentration and temperature is essential. However, with capillary electrophoresis this requirement is considerably less labor-intensive and much faster. Polymer solutions containing varying amounts of PNA are prepared and after analyzing the temperature dependence (*see* **Note 9**) at one concentration — a matter of an hour or so (*see* **Fig. 2**) — one changes the polymer for the next concentration and repeats this process using the same sample (*see* **Note 10**). Once optimal conditions have been determined, these may be retained for routine analysis with this PNA/DNA combination. It is advisable to include an internal unrelated marker with each sample, in particular for the identification of homozygous mutants (*see* **Note 11**). Here one must rely on detecting a signal shift with respect to the wild-type, in contrast to the resolution of a single peak to a doublet for the heterozygote. The internal marker may be a size standard, the labeled complementary strand, or one can relate all migrations to the signal from the free excess-labeled PCR primer.

3.5.1. Two-Dimensional Multiplex Analysis

A further increase in throughput can be achieved with multicolor sequencers by making use of the spectral resolution of the available dyes, for instance with color-coded samples. At present, four colors are generally available permitting three different samples to be analyzed simultaneously, if one color is reserved for the internal standard. Additionally, the concept of two-dimensional multiplex analysis has been introduced ***(8)***. For multiplexing, fluorescent amplicons corresponding to different mutation sites may be designed such that their sizes (the first "dimension"), as resolved by electrophoresis, identify the regions of the target DNA that is to be

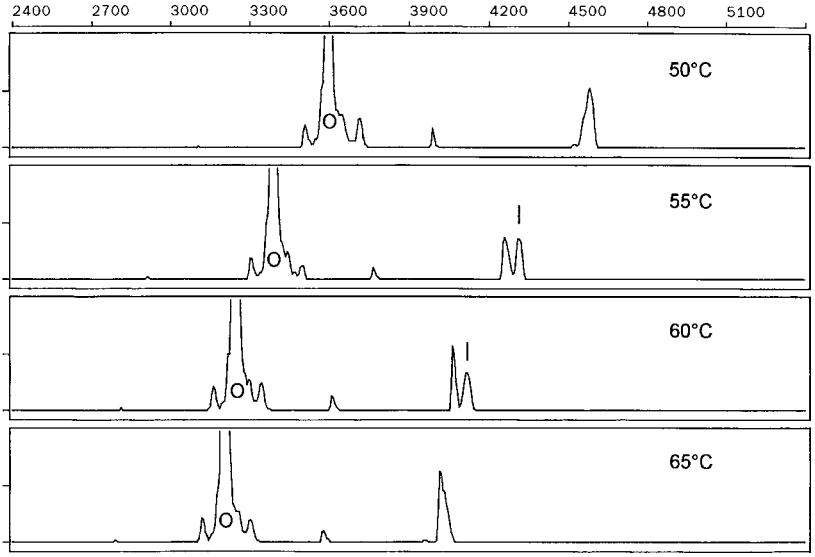

Fig. 2. Temperature dependence of hybridization. The sample was a PCR product (103bp) from a heterozygous C2982Y mutant in human HLA-H DNA. Preinjection electrophoresis was set to 10 s. Electrophoresis was at 6 kV (*see* **Note 8**) for 20 min at the given temperatures in the presence of 2 n*M* PNA. Excess fluorescein labeled primer is marked with O while the PCR product appears around 4600 data points, at 50°C. At 55°C, the resolution between wild-type (retarded, marked with a vertical line) and mutant product is about 20 s. At 50°C the single mismatch between PNA and mutant allele is insufficient for discrimination; it also hybridizes efficiently to the PNA. On increasing the temperature to 55°C, the base pairing of the mismatched strand is weakened and resolution of the alleles is observed. At 60°C, the fully base-paired wild-type strand begins to dissociate from the entrapped PNA, resolution is decreased and lost almost entirely at 65°C.

analyzed. In this way, during electrophoresis and in the presence of a mixture of appropriate PNAs, a virtual or dynamic array of fragments is created each component of which can hybridize specifically *in situ* only to its corresponding PNA (the second "dimension"). Hybridization causes a visible shift in the signal (compared to an internal size marker) at a sector within the electrophoretogram that identifies the locus of the mutation (*see* **Fig. 3**).

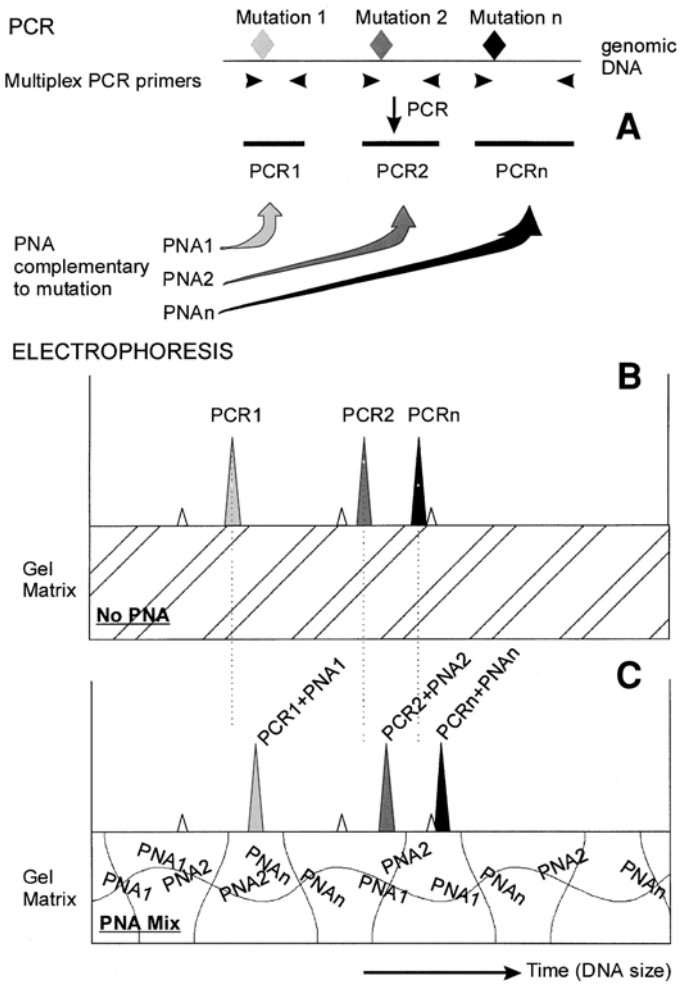

Fig 3. Two-dimensional multiplex analysis. **(A)** Schematic representation of a multiplex PCR giving amplicons of varying, defined, sizes covering n mutational loci. PNA probes are designed to be fully complementary to the mutant allele. **(B)** Schematic view of the electrophoretic fractionation of the amplicons from (A) in the absence of entrapped PNA. **(C)** Addition to the electrophoretic matrix of a mixture of PNAs targeted to the mutant allele leads, upon electrophoresis, to a shift of signals relative to an internal size standard (small unshaded triangles), as shown, if the PCR product hybridizes to the PNA. The position of the fragment in the electrophoretogram can be correlated to the nature of the mutation. Use of color-coded amplicons permits an enhanced throughput.

In this way two unrelated physical properties of the analyte (the molecular size and the base sequence) are used to identify (rather than merely detect) several point mutations simultaneously. Furthermore, the multicolor capability of current DNA sequencers permits several (at present up to 3) color-coded samples covering n polymorphic loci to be run in parallel, giving a $3 \times n$ multiplicity.

The criteria for PNA and primer design outlined earlier are now somewhat restricted, relying on primer sets that are compatible with multiplex PCR. The amplicons for each targeted mutation must have significant size differences (e.g., 20 bp). On the other hand, although any single analytical run will be performed at a given temperature, the PNA concentration dependence of the resolution (or T_m) still permits some choice in PNA design. The application of this approach has been documented for the simultaneous detection of three common point mutations in the human hereditary hemochromatosis gene ***(8)***.

4. Notes

1. Denaturation is obligatory. Double-stranded DNA does not interact with PNA under these conditions.
2. One may choose to apply a thin coating of BindSilane (Amersham-Pharmacia) to the top 1 cm of the inner glass plate, to stabilize the sample slots.
3. In order to determine the optimal PNA concentration that is to be used for routine analysis, preliminary runs at various temperatures and PNA concentrations are required. For PNA 11-mers the concentration range should lie between 1 and 500 n*M*. Hence, a series of gels is constructed containing 1, 25, 100, 250, and 500 n*M* PNA, for instance, and each gel is run with standard samples (*see* **Note 5**) at 4–5 different temperatures, e.g., 35, 40, 45, 50, and 55°C. (*see* **Note 6**). Each gel may be reused several times (preferably using fresh sample slots), although physical changes to the gel at high temperatures (>65°C) prevent repeated use at such extremes. (One should also bear the physical limitations of the thermostatting plate at high temperatures in mind.) Furthermore, low temperatures (<25°C) can lead to smearing of the signal. At the optimal PNA concentration, one observes a temperature dependent resolution of the hybridizing species from the noninteracting signal. For routine analy-

sis, the temperature giving the greatest resolution at the given PNA concentration is used. Evaluation may be carried out with the Fragment Manager software (Amersham-Pharmacia).

4. O represents a [2-(N-Boc-2-aminoethoxy)ethoxy]acetic acid linker that is said to stabilize the PNA with respect to rearrangements. PNA obtained from the manufacturer (Applied Biosystems) in an unpurified form and is purified by gel filtration over Sephadex NAP5 columns (Amersham-Pharmacia). 0.2 mL fractions are collected and the UV-absorbing material combined and stored at –20°C. Repeated freeze-thaw cycles appear not to affect the PNA.
5. Standard samples should comprise amplicons from wild-type and from genotyped point mutations, preferably heterozygous, as one then observes a resolution of a single signal to a doublet upon affinity interaction.
6. Note that there may be quite a narrow temperature/concentration range. If no resolution is observed, a narrower temperature range, e.g., 2°C steps should be attempted. It is advisable once a temperature has been located to perform a further analysis in the absence of PNA to ensure that any effects are not due to SSCP, which would complicate the interpretation. At temperatures of approx 50°C, this is unlikely to be the case.
7. The injection parameters should be adjusted according to the signal strength observed. This depends on the yield of PCR product and, to a certain extent, on the nature of the fluorescent dye.
8. Signals from 150 bp samples appear within 15 min, at these settings. The running voltage is a compromise between analysis speed and visual resolution. At higher voltage, resolution may not be observed in real-time, although postrun analysis performed with the GeneScan software (ver. 3.0) (Applied Biosystems) can still distinguish resolved peaks.
9. Cooling of the ABI310 below ambient temperature is not possible without structural alterations to the instrument.
10. Samples remain in a denatured form for at least 48 h at room temperature. They may be re-denatured for further application, although there is some loss of signal intensity.
11. It should be noted that in contrast to gel-based systems where lanes within one gel are usually directly comparable, it is not advisable, despite the good reproducibility, to rely on comparisons of fragment migration between separate capillary-electrophoretic runs.

References

1. Southern, E. M. (1975) Detection of specific sequences among DNA fragments separated by gel electrophoresis. *J. Mol. Biol.* **98,** 503–517.
2. Hacia, J. G. (1999) Resequencing and mutational analysis using oligonucleotide microarrays. *Nature Genet.* **21,** 42–47.
3. Igloi, G. L. (1993) Affinity electrophoresis of nucleic acids: general principles and their application to nucleic acids, in *Molecular Interactions in Bioseparations* (Ngo, T. T., ed.), Plenum, New York, pp. 511–531.
4. Eriksson, M. and Nielsen, P. E. (1996) PNA-nucleic acid complexes. Structure, stability, and dynamics. *Q. Rev. Biophys.* **29,** 369–394.
5. Igloi, G. L. (1998) Variability in the stability of DNA-Peptide Nucleic Acid (PNA) single-base mismatched duplexes. Real-time hybridization during affinity electrophoresis in PNA-containing gels. *Proc. Natl. Acad. Sci.USA* **95,** 8562–8567.
6. Igloi, G. L. (1999) Automated detection of point mutations by electrophoresis in peptide-nucleic acid containing gels. *BioTechniques* **27,** 798–808.
7. Igloi, G. L. (2000) Automated detection of point mutations by electrophoresis in peptide-nucleic acid containing gels, in *Polymorphism Detection and Analysis* (Burczak, J. D. and Mardis, E. R., eds.), Eaton, Westborough, MA, pp. 445–455.
8. Igloi, G. L. (2001) Simultaneous identification of mutations by dual-parameter multiplex hybridization in peptide nucleic acid-containing virtual arrays. *Genomics* **74,** 402–407.
9. Igloi, G. L. (1996) Enzymatic fluorescence and biotin labeling of primers for PCR sequencing. *Methods Mol. Biol.* **65,** 23–28.

14

Lipid-Mediated Introduction of Peptide Nucleic Acids Into Cells

Dwaine A. Braasch and David R. Corey

1. Introduction

The development of general chemical approaches for controlling gene expression would facilitate investigations into the details of cellular function ***(1)***. Antisense oligonucleotides have been widely used to block the expression of genes or alter splicing ***(2)***, but their use has suffered from questions regarding their potency and specificity. In addition, successful antisense experiments often require a large effort to identify oligomers with adequate activity ***(3)***. Peptide nucleic acids (PNAs) bind with exceptionally high affinity to complementary sequences and possess an uncharged backbone that is unlikely to prompt interactions with the many cellular proteins that bind anionic macromolecules ***(4)***. It is reasonable to hypothesize, therefore, that PNAs may possess advantages as antisense agents. In addition, PNAs have an unmatched ability to invade duplex DNA, suggesting that they may bind to chromosomal targets and act as antigene agents ***(4)***.

Such speculation, however, is meaningless in the absence of efficient methods for delivering PNAs into cells. In this contribution we describe the delivery of PNAs into cells as PNA-DNA heterodu-

From: *Methods in Molecular Biology, vol. 208: Peptide Nucleic Acids: Methods and Protocols*
Edited by: P. E. Nielsen © Humana Press Inc., Totowa, NJ

plexes complexed with cationic lipid *(5–7)*. This method is rapid, reproducible, and relies on lipid-mediated transfection techniques that are well-established and familiar to many laboratories. Importantly, no synthetic modification of the PNA is required.

1.1. Challenges to Intracellular Usage of PNAs

Research to evaluate the effects of PNAs inside cells faces a series of complex challenges. PNAs do not spontaneously enter cultured mammalian cells with good efficiency, so the first challenge is their delivery. We describe one solution to this problem, the use of PNA-DNA-lipid complexes. Other solutions include electroporation *(8)*, membrane permeablization with streptolysin O *(9)*, and attachment of PNAs to peptides that assist membrane translocation *(10,11)*. The second challenge is that PNAs must be able to locate their target sequences when introduced at concentrations that are not toxic to cells. In our experience we have been able to use PNAs to block the expression of luciferase mRNA and to inhibit human telomerase, demonstrating that PNAs can effectively recognize their intracellular targets. The final challenge is that binding of PNAs to nontarget nucleic acids or proteins, which is likely to be unavoidable, should be limited and not produce unintended phenotypes that might confuse the interpretation of experiments. Comparison of the effects of fully complementary and mismatch PNAs is a powerful strategy for addressing this final challenge.

1.2. DNA-PNA-Lipid Complexes

In designing a method for PNA delivery we sought to develop a strategy that would be simple and rely on existing technology. We did not wish to covalently modify the PNA because such modifications, while straightforward, add a level of complexity that we would prefer to avoid. We had become familiar with the use of cationic lipids to deliver 2'-O-methyl RNA oligonucleotides, and found that this approach was highly efficient. PNAs cannot be delivered in complex with cationic lipid alone because they lack a negatively charged backbone, but we reasoned that a PNA annealed to a DNA

oligomer with a negatively charged backbone could be delivered as a PNA-DNA-lipid complex.

It was not obvious that this strategy would work, because to succeed the PNA must bind DNA strongly enough to be transported as a complex but not so strongly that it cannot be released once inside the cell (*see* **Notes 1** and **2**). The approach taken was to design DNA oligomers that were fully complementary to the PNA of interest. No phosphorothioate substitution is needed to stabilize the DNA, as the efficiency of delivery may be dependent on the degradation of the delivery DNA upon introduction into cells. It is preferable to test two or three potential transport DNAs to ensure that one has an adequate affinity for the PNA and can deliver the PNA into cells effectively. Typically we design the transport DNA molecules to be 15 nucleotides in length with a 4-base overhang in either direction relative to the PNA. Melting temperature (T_m) values are then obtained for the PNA-DNA complexes. PNA-DNA duplexes with T_m values between 50° and 75°C have permitted delivery of active PNAs ***(7)***. PNA-DNA complexes with promising T_m values are then complexed with lipid and added to cells.

2. Materials

1. PNA monomers and synthesis reagents were obtained from Applied Biosystems (Foster City, CA).
2. PNAs can be synthesized using either manual or automated protocols. Automated synthesis can be achieved on an Expedite 8909 (Applied Biosystems) using Fmoc PNA monomers ***(12)***. Manual synthesis ***(13,14)*** can be accomplished using monomers protected by either tBoc or Fmoc protecting groups. Once a PNA is synthesized, fluorescent groups, biotin, or other labels can be added to the free N-terminus prior to deprotection. PNAs are purified and analyzed as described. A detailed description of our methods for PNA synthesis and purification can be found at (http://hhmi.swmed.edu/Labs/dc/DCHome.html).
3. Rhodamine-labeled PNAs were synthesized as described ***(15)***.
4. PNA storage solution: Milli-Q purified water. If PNAs are purified using buffers that contain TFA, residual TFA will lead to a pH ~ 5.5

upon dissolution in water. This low pH is convenient because it increases PNA solubility.

5. PNA-DNA annealing buffer: 2.5X phosphate buffered saline (PBS) final concentration from a 10X stock. 10.4 m*M* KH_2PO_4, 1551.7 m*M* NaCl, 29.6 m*M* Na_2HPO_4 without calcium and magnesium, pH 7.4 (Invitrogen, Carlsbad, CA).
6. PNA-DNA melting temperature buffer: 0.1 *M* Na_2HPO_4, pH 7.4.
7. DNA oligonucleotides, LipofectAMINE™, and OptiMEM® were obtained from Invitrogen (*see* **Note 3**). Oligonucleotides from other suppliers are also suitable.
8. DU145 and COS-7 cells were obtained from American Type Cell Culture (ATCC), Rockville, MD.
9. Tissue culture medium: High glucose DMEM (Mediatech cellgro™, Fisher Scientific, Norcross, GA) supplemented with 10% fetal bovine serum (FBS) premium select (Atlanta Biologicals, Norcross, GA), 20 m*M* HEPES buffer, pH 7.4, antibiotics (5,000 U/mL Penicillin, 10 mg/mL Streptomycin, Sigma, St. Louis, MO) and 1X anti-PPLO reagent (Invitrogen). Culture cells at 37°C in a 5% CO_2 incubator.
10. Cell culture plates used include 48- and 96-well flat-bottom tissue-culture treated polystyrene (Costar®, Corning Costar, Corning, NY) and 96-well opaque flat-bottom plates for luminescence assays (Costar®).

3. Methods

3.1. Solubilization of PNAs

PNAs are readily soluble in aqueous solutions at pH 6.0 or lower, and somewhat less soluble at higher pH levels. Solubility can be enhanced by the addition of charged amino acid residues at the termini of PNAs. After drying, hydrate the pellet with 200 µL of sterile Milli-Q filtered water and allow the tube to sit at room temperature for 5–10 min undisturbed. Heating solutions containing PNAs can also enhance solubility. We recommend always heating PNAs to 55°C immediately prior to use to ensure that aggregation is minimized. If this is not done, the effective concentration of PNA is likely to be less than that determined when the

PNA was first dissolved. We have found that this aggregation is one of the greatest obstacles to successful use of PNAs by new users.

3.2. Annealing of PNAs to DNA Oligonucleotides

PNAs can be delivered into cultured cells by annealing PNAs to complementary DNA oligonucleotides and then adding cationic lipid (LipofectAMINE™, Invitrogen) to transport the DNA-PNA complex. This method is rapid and takes advantage of the existing expertise and protocols for use of cationic lipid. An important consideration for use of this method is the amount of overlap between PNA and DNA. We find that only those complexes with a T_m between 50°C and 70°C yield effects inside cells *(7)*.

1. Check the concentration of PNA and DNA independently. As noted earlier, heat the PNA to 55°C prior to quantitation to ensure that it is fully solubilized.
2. Calculate the volume of PNA and DNA that are required to prepare 50 µL of a 100 µ*M* stock solution of PNA:DNA heteroduplex.
3. In a thin-walled PCR tube, add 12.5 µL of 10X (PBS). This will result in a 2.5X PBS concentration in the final solution. Buffering is necessary to neutralize the acidic nature of PNA solutions.
4. Calculate the residual volume available by subtracting the required volumes of PNA, DNA, and 10X PBS from the 50 µL total volume. Add that volume of sterile water to the tube containing the PBS.
5. Add the volumes of DNA to the tube and mix gently.
6. Add the volume of PNA to the tube and mix lightly. It is not uncommon for a precipitate to form at this point; it will dissipate during the annealing process.
7. Place tube(s) in a thermal cycler and anneal according to the following temperature profile. Reductions in temperatures should occur in 1 min with hold times indicated. 95°C, 5 min, 85°C, 1 min, 75°C, 1 min, 65°C, 5 min, 55°C, 1 min, 45°C, 1 min, 35°C, 5 min, 25°C, 1 min, 15°C, 1 min; hold at 15°C. After annealing is complete, the PNA:DNA complexes should be maintained at 4°C until use and characterized by T_m evaluation. We have found that annealed samples that have been stored at –20°C or –80°C require reannealing prior to T_m analysis and/or transfection. Samples stored at 4°C for over 3 mo have been successfully analyzed without adversely affect-

ing results. We have never observed a PNA to become unusable after storage, even those several years old.

8. In addition to using a PNA that is fully complementary to the target site, always use one or more mismatch-containing PNAs as controls (*see* **Note 4**).

3.3. Determination of T_m

Our method for delivery of PNAs into cells requires that hybridization be strong enough to allow the PNA to bind to DNA outside the cell while permitting the DNA to be released inside the cell. To achieve reliable results, therefore, it is necessary to determine T_m values for this process. If a T_m is below 55°C or above 75°C it is unlikely that the PNA will function as desired. It will either not bind to the DNA strongly enough to be transported, or it will bind too tightly and will not be released upon entry into the cell.

An essential feature to determining if a T_m is reliable is the fact that the denaturation and annealing profiles be reversible. We have developed the following technique for determining accurate T_m values.

1. Using a quartz cuvet (Spectrosil® Far UV Quartz type 26.100 stoppered cell (Uvonic Instruments, Plainview, NY) with a 10-mm path and a 15-mm Z-dimension), add 145 µL of 0.1*M* Na_2HPO_4, pH 7.4.
2. Add 5 µL of freshly annealed 100 µ*M* PNA:DNA, mix by pipetting up and down. (Note: for consistency, it is better to premix the 145 µL of 0.1 *M* Na_2HPO_4 buffer and the 5 µL of freshly annealed 100 µ*M* PNA:DNA in a 500 µL microcentrifuge tube and then transfer the mixed solution into the cuvet).
3. Overlay sample with 145 µL of mineral oil and place in temperature-controlled spectrometer (Hewlett Packard Diode Array Spectrometer with a Peltier temperature regulator and TEMPCO Software, Hewlett Packard Company, Wilmington, DE).
4. Setup software on spectrophotometer to collect data from 9°C to 96°C and from 96°C to 9°C in 3°C increments with an equilibration time of 0.1 min at each temperature. To maximize the difference between annealed and denatured states, the absorbance of the sample should be collected at 274 nm with a 500 nm reference reading. (Note: Other temperature ranges or increments may be used; however, temperature increments between 1°C and 3°C are preferred

because they produce smoother transitions and more reliable determination of T_m).

5. After the cuvet chamber or block has reached the starting temperature, allow sample to equilibrate for 5 min before starting temperature ramping.
6. Save the data file (*.dta) and import it into a spreadsheet program (Microsoft Excel) as a comma delimited file.
7. Convert the temperatures in the data file into degrees Kelvin (required for the nonlinear curve fit analysis to follow).
8. Removal of mineral oil from the cuvet can be difficult, but we have found that chloroform and ethanol work well in combination with a Scienceware™ Vacuwash™ cell washer apparatus (Bel-Art Products, Pequannock, NJ).

3.4. T_m Analysis

The transition data collected in **Subheading 3.3.** was analyzed by means of a nonlinear curve-fitting technique that employed equations derived from van't Hoff thermodynamic parameters of double-stranded DNA helices ***(16)***. Equations were derived such that independent determination of ΔH_m (transition enthalpy) and the T_m for both the denaturation and annealing profiles were entered as nonlinear fit procedures into SigmaPlot (SPSS). Likewise, formulae were entered into SigmaPlot to determine baselines based on the fit data for the transitions in both directions. Baselines for native and denatured conditions were plotted for both transitions in conjunction with the nonlinear fit. Under ideal conditions, the two plots should overlay one another, as should the baselines, reflecting the reversibility of denaturation and annealing.

3.5. Transfection of PNA:DNA Complexes into Anchorage-Dependent Cells

Transfection protocols will need to be optimized for each cell line. We have found that it is convenient to use fluorophore-labeled PNAs to established optimal transfection conditions because their introduction into cells can be readily observed by microscopy or fluorescence-activated cell sorting (FACS) analyses. Factors that

should be considered during the optimization process include, cell line, cell-plating density, lipid type, and lipid to PNA:DNA ratio. When optimizing the conditions for a given cell line, as little lipid as possible should be used without compromising transfection efficiency. We recommend that lipid be minimized because it is associated with cell toxicity and can prevent reattachment of cultured cells.

To determine guidelines for the use of PNAs as antisense agents we transfect reporter vectors. An example procedure is given below for transfecting COS-7 cells with PNAs, along with luciferase and ß-galactosidase reporter systems in a 48-well format.

1. Beginning with a 75-cm^2 tissue culture flask of cells grown to confluence, trypsinize the cells according to standard procedures. After the cells have been suspended in fresh tissue-culture medium, draw up the entire volume of cell suspension into a 10 mL pipet. Dispense back into flask with the tip of the pipet pressed lightly against the bottom of the flask to disrupt aggregates of cells, yielding a single-cell suspension that results in counts that are more accurate.
2. Perform a cell count in triplicate using a cell counter (Beckman Coulter, Fullerton, CA) or by hemacytometer and average the results.
3. From the original trypsinized cell suspension, prepare a suspension of cells such that 250 µL will contain 11,000–13,000 cells. Plate cells at 11,000–13,000 cells per well in a 48-well tissue-culture plate (Falcon) 4–6 h prior to transfection. For accuracy, dispense 250 µL of cell suspension into each well using a Repeater™ (Eppendorf™) pipetter and a 12.5 mL Combitip™. After dispensing cells, replace cover on plate and disperse cells evenly within the wells by sliding the plate back and forth gently bumping the plate against the front lip of the Laminar flow hood work surface.
4. Warm the previously prepared 100 µ*M* PNA:DNA annealed hybrid stock mixture to room temperature (the stock may have been stored at 4°C).
5. Determine the specific concentration range of PNA to be tested. Calculate the final volumes required for all inhibitor concentrations based on the number of experimental wells for each concentration. Include extra if needed for dilutions in addition to plating volume. We have found that 5×10^{-8}µL of LipofectAMINE™ per n*M* inhibitor per cell per well serves as a good conversion for a 48-well format and for scaling to other multi-well formats.

6. For example, for a 48-well format, if the highest concentration of inhibitor to be tested is 200 n*M*, and six wells will receive this concentration plus extra volume is required for diluting to 100 n*M* and 25 n*M* in a serial manner, then a total of 3.2 mL of 200 n*M* inhibitor solution is required (16-well equivalents assuming 200 µL per well). If we use the conversion factor from **step 5**, then 5×10^{-8}µL of LipofectAMINE × 200 n*M* × 12,000 cells/well × 16 wells = 1.9 µL LipofectAMINE would be required. If 3.2 mL of a 200 n*M* solution of inhibitor is required then the calculated amount of the 100 µ*M*-annealed PNA-DNA heteroduplex needed would be 6.4 µL. The steps involved in the preparation of PNA:DNA heteroduplexes for transfection appear in **Fig. 1**.
7. The next step involves forming a stock concentration of PNA-DNA-LipofectAMINE complex. This is achieved by diluting the 1.9 µL LipofectAMINE with 148 µL of OptiMEM® in a 12 × 75 mm tube. In another tube, dilute the 6.4 µL of 100 µ*M* annealed PNA-DNA heteroduplex with 144 µL OptiMEM. Allow these two solutions to equilibrate for 5 min.
8. Combine the two solutions from **step 7**. Tap tubes gently 15× to disperse contents and form micelles.
9. Incubate for 15 min in the dark at room temperature for PNA-DNA-LipofectAMINE micelle formation. While waiting, aspirate off the culture medium and wash cells with 250 µL OptiMEM® per well. Set up tubes for dilutions by placing OptiMEM diluent in each tube.
10. Dilute concentrated PNA-DNA-LipofectAMINE complexes (*see* **step 9**) by adding 2.9 mL OptiMEM, for a final volume of 3.2 mL (*see* **step 6**).
11. Perform serial dilution of the 200 n*M* PNA-DNA-LipofectAMINE mixture by pipetting up and down 4-times prior to transferring to the next tube.
12. Aspirate off the 250 µL of OptiMEM wash and replace with inhibitor solution. Dispense 200 µL per well working backward through the dilution scheme for a given PNA:DNA. Extended periods without culture medium or wash solution can dehydrate the cells and deleteriously affect assay results.
13. Allow cells to incubate with the inhibitor mixture at 37°C overnight. If no reporter system transfection is required, then aspirate off the inhibitor transfection mixture and replace with prewarmed complete tissue-culture medium until the resulting assay is performed (*see* **step 19**). If a reporter system transfection is required *see* **steps 14–19**.

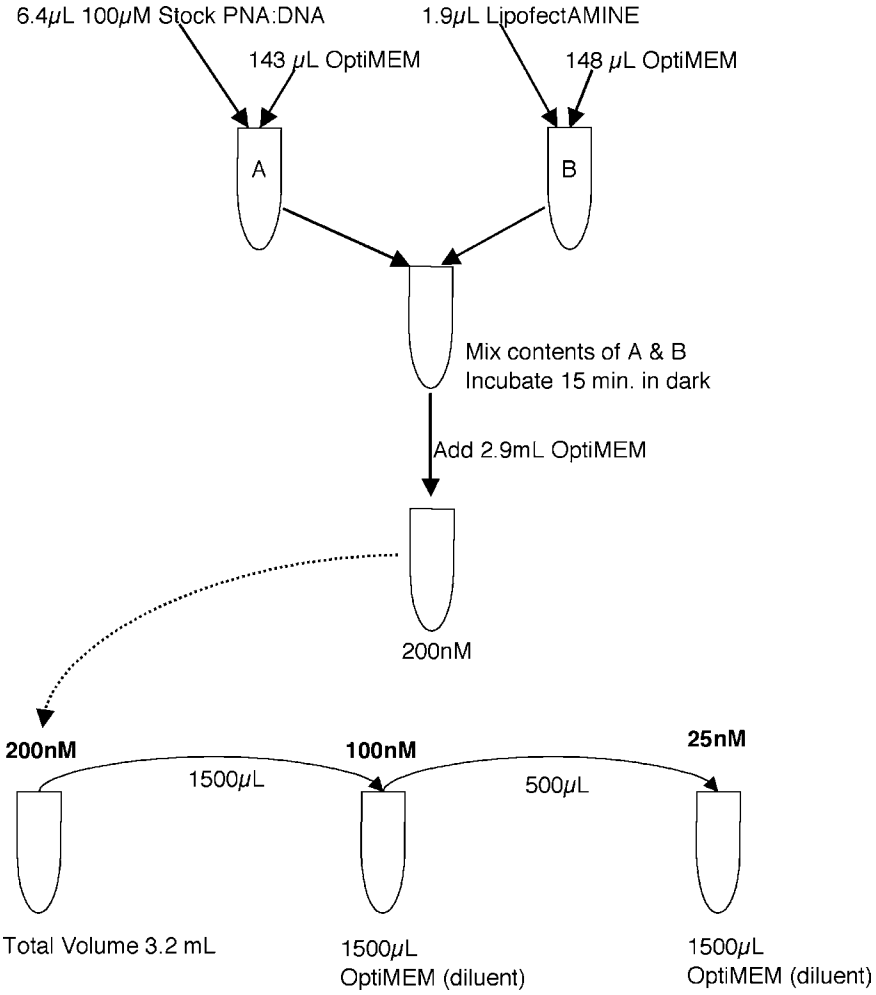

Fig. 1. Transfection scheme.

Reporter Vector Transfection

14. The vector solution required is based on 40 µL per well and 48 wells per plate plus a little extra (i.e., 52 wells). In one tube combine 19.8 µL OptiMEM/well and 0.2 µL LipofectAMINE. In another tube combine 19.5 µL OptiMEM/well with 0.5 µL of vector mix assuming a total of 100 ng of vector(s)/well. Allow the tubes to equilibrate for 5 min.

15. Combine the two solutions from above. Tap tubes gently 15× to disperse contents and form PNA-DNA-lipid complexes.
16. Dilute mixed complex with 10 µL OptiMEM per well and dispense 50 µL per well and transfect for 6 h in a 37°C, 5% CO_2 incubator.
17. Aspirate off transfection solution and replace with 250 µL of tissue-culture medium, or medium containing a specific activator if applicable.
19. Incubate at 37°C for 36–40 h prior to conducting assay(s) for the effects of the PNA.

4. Notes

1. This protocol for the introduction of PNAs as PNA-DNA-lipid complexes has proven to be reliable. The method worked as planned the first time it was tested for the delivery of anti-telomerase PNAs. Since then, it has been equally successful in the hands of several laboratory coworkers for inhibition of telomerase or antisense inhibition of luciferase expression.
2. This approach has several limitations, however: the first limitation is that the method requires annealing and then complex formation with lipid. Relative to approaches that allow PNA to be directly added to cells, such as use of PNA-peptide conjugates, these steps add complexity and make transfection a relatively labor-intensive process. This is particularly important if one wishes to do lengthy studies on the effects of gene inhibition over more than a few days. That said, we have not found PNA-peptide conjugates to be a particularly effective strategy for achieving reliable delivery of PNAs, thus complicating the analyses for intracellular effects. This negates the added convenience of PNA conjugates, at least in our hands.
3. A second limitation is that the lipid is toxic at high concentrations, reducing the amount of PNA that can be delivered. Toxic effects and nonsequence-specific gene inhibition begin to appear in COS-7 cells when more than 500 n*M* PNA is delivered. This limitation for PNA concentration is likely to vary from cell line to cell line, and one can vary the lipid used to achieve better effects. Similarly, some cell lines will be resistant to transfection with cationic lipid and will not be amenable to our technique at all. Finally, it is absolutely necessary to determine the melting temperature of the DNA-PNA hybrid, and this also adds an additional step.

4. PNAs bind to complementary sequences with exceptionally high affinity. Owing to the strong hybridization properties of PNAs, users of PNAs are often asked whether PNAs will also bind to unintended targets, preventing their use as specific agents in cells. Having transfected over 25 different PNAs into cells using this method, we have never observed toxic effects or unexpected cellular phenotypes; nor have nonsequence-specific effects been observed or deemed to be a problem. This result is in contrast to our other experiences with phosphorothioate-substituted oligonucleotides, in which unpredictable toxic effects were frequently observed.

Acknowledgments

This work was support by grants from the National Institutes of Health (GM60624) and by the Robert A. Welch Foundation (I-1244).

References

1. Stockwell, B. R. (2000) Frontiers in chemical genetics. *Trends Biotech.* **18,** 449–455.
2. Koller, E., Gaarde, W. A., and Monia, B. P. (2000) Elucidating cell signalling mechanisms using antisense technology. *Trends Pharm. Sci.* **21,** 142–148.
3. Stein, C. A. (1999) Keeping the biotechnology of antisense in context. *Nature Biotechnol.* **17,** 209.
4. Nielsen, P. E., Egholm, M., Berg, R. H., and Buchardt, O. (1991) Sequence-selective recognition of double stranded DNA by a thymine-substituted polyamide. *Science* **254,** 1497–1500.
5. Herbert, B.-S., Pitts, A. E., Baker, S. I., Hamilton, S. E., Wright, W. E., Shay, J. W., and Corey, D. R. (1999) Inhibition of telomerase in immortal human cells leads to progressive telomere shortening and cell death. *Proc. Nat. Acad. Sci.USA* **96,** 14,726–14,281.
6. Hamilton, S. E., Simmons, C. G., Kathriya, I., and Corey, D. R. (1999) Cellular delivery of peptide nucleic acids and inhibition of human telomerase. *Chem. Biol.* **6,** 343–351.
7. Doyle D. F., Braasch, D. A, Simmons, C. G., Janowski, B. A., and Corey, D. R. (2001) Intracellular delivery and inhibition of gene expression by peptide nucleic acids. *Biochemistry* **40,** 53–64.

8. Shammas, M. A., Simmons, C. G., Corey, D. R., and Shmookler-Reis, R. J. (1999) Inhibition of telomerase reverses immortality of transformed. *Oncogene* **18,** 6191–6200.
9. Faruqi, A. F., Egholm, M., and Glazer P. M. (1997) Peptide nucleic acid targeted mutagenesis of a chromosomal gene in mouse cells. *Proc. Natl. Acad. Sci.USA* **95,** 1398–1403.
10. Simmons, C. G., Pitts, A. E., Mayfield, L. D., Shay, J. W., and Corey, D. R. (1997) Synthesis and membrane permeability of PNA-peptide conjugates. *Bioorg. Med. Chem. Lett.* **7**, 3001-3007.
11. Pooga, M., Soomets, U., Hallbrink, M., Valkna, A., Saar, K., Kahl, U., et al. (1998) Cell penetrating PNA constructs regulate galanin receptor levels and modify pain transmission in vivo. *Nature Biotech.* **16,** 857–861.
12. Mayfield, L. D. and Corey, D. R. (1999) Automated synthesis of peptide nucleic acids (PNAs) and peptide nucleic acid-peptide conjugates *Anal. Biochem.* **268,** 401–404.
13. Norton, J. C., Waggenspack, J. J., Varnum, E., and Corey, D. R. (1995) Targeting peptide nucleic acid protein conjugates to structural features within duplex DNA. *Bioorg. Med. Chem.* **3,** 437–445.
14. Goodwin, T. E., Holland, R. D., Lay, J. O., and Raney, K. D. (1998) A simple procedure for solid-phase synthesis of peptide nucleic acids with N-terminal cysteine. *Bioorg. Med. Chem. Lett.* **8,** 2231–2234.
15. Mayfield, L. D. and Corey, D. R. (1999) Enhancing solid phase synthesis by a noncovalent protection strategy: efficient coupling of rhodamine to peptide nucleic acids. *Bioorganic Med. Chem. Lett.* **9,** 1419–1422.
16. Atkins, P. W. (1990) *Physical Chemistry*, 4th ed. W. H. Freeman and Company, New York, p. 219.

15

Synthesis of Cell-Penetrating Peptide-PNA Constructs

Margus Pooga, Ursel Soomets, Tamas Bartfai, and Ülo Langel

1. Introduction

Small synthetic molecules that can specifically inhibit translation or transcription hold great promise as potential antisense and antigene drugs. The polyamide/peptide nucleic acid (PNA) ***(1)***, along with locked ***(2)*** and morpholino ***(3)*** nucleic acids, is one of the most promising synthetic DNA mimics for these "antisense applications." Extremely high stability in biological fluids ***(4)*** as well as *in vivo* conditions in general, low toxicity, strong and specific pairing with complementary single stranded RNA/DNA are the main advantages of PNA. The heteroduplexes of PNA with RNA or with DNA have remarkably higher stability as compared to naturally occurring homo- or heteroduplexes of RNA and DNA ***(5)***. High thermal stability of PNA-containing duplexes is mainly based on the lack of intra-molecular electrostatic repulsion, but also on hydrophobic interactions and less favorable hydration ***(6)***.

The advantages of PNA are also implying some drawbacks in the case of antisense applications. Peptide nucleic acid oligomers are very stable in vivo because they are not recognized by nucleases

From: *Methods in Molecular Biology, vol. 208: Peptide Nucleic Acids: Methods and Protocols*
Edited by: P. E. Nielsen © Humana Press Inc., Totowa, NJ

and do not interact with many other proteins. As a consequence PNA can not activate RNase H, a step which is considered to be important for classical ***(7)*** antisense efficacy, because this leads to degradation of the mRNA in the heteroduplex with antisense oligonucleotide.

Lower avidity to interact with proteins may lay behind another main problem of PNA application in vivo, the poor cellular uptake. "Naked" PNA is less efficient ly taken up by cells in culture, as compared to DNA oligomers and most of the DNA-mimics with charged backbone ***(8)***. Supplementing of cell-culture medium by moderate or small amounts of PNA (concentration in range 0.1–5 μ*M*) results in uptake of tiny amounts of unmodified PNA with negligible effects, while microinjection of respective PNA has yielded profound antisense/antigene effects ***(9)***. Unfortunately, owing to the lack of charge on PNA backbone, PNA oligomers cannot be included into liposomes of cationic lipids that are routinely used to facilitate the uptake of DNA oligomers and its analogs ***(10)***.

Somewhat surprisingly, it was discovered that PNA oligomers are more easily taken up by different types of cells in culture at high concentration (above 20 μ*M*) ***(11,12)***. As observed earlier, the internalized PNA is initially localized in the cell interior in granular (vesicular) structures, probably in endosomes. Later, about 6–8 h after the PNA was added to the extracellular medium, and especially after 24 h, PNA is distributed diffusely all over the cytosol and has also reached the nuclei ***(11)***. Unmodified PNA, especially when present in high concentration (10 μ*M* and higher) is exceptionally well taken up by the neuronal cells both in cell culture and in vivo conditions as compared to other cell types ***(13)***.

Improved cellular uptake of PNA by many cell types has been achieved by covalent coupling it to a DNA oligomer ***(14)*** and internalization of these chimeras can be even increased by preparing liposomes ***(15)*** of cationic lipids and PNA-DNA. The receptor mediated endocytosis can be exploited to deliver PNA oligomers into the cell interior, e.g., D-analog of insulin-like growth factor (IGF) enabled transport of 12-mer PNA into mouse 3T3 cells that express

IGF receptor ***(16)***. However, most efficient uptake of PNA is achieved by taking advantage of Cell-Penetrating Peptides (CPP) ***(17).***

A relatively new strategy for cellular delivery of hydrophilic macromolecules is based on the ability of CPPs to translocate from the medium surrounding the cells into the cell interior without receptor-mediated endocytosis in a non ATP energy dependent manner ***(18)***. Molecules, which are either coupled to CPP by a covalent bond or form a strong complex with CPP, are carried into the cells by these peptides. Most often used CPPs are penetratin ***(19)***, Tat derived peptide ***(20)***, membrane-targeting sequence (MTS) ***(21)*** and transportan ***(22),*** as well as their numerous analogs.

PNA is purely synthetic linear oligomeric molecule and can be assembled on the resin for solid-phase peptide synthesis as one continuous chain with CPP. This approach has given relatively low synthesis yields in our hands and we do not routinely use it to prepare PNA-CPP constructs of long PNA chain. Moreover, in the case of strong covalent coupling the intracellular localization of delivered PNA is predetermined by the preferential whereabouts of the transporter peptide, which in turn can decrease the efficacy of PNA to find and interact with its target on mRNA or gene. Instead, we have synthesized separately the PNA oligomer and a transporter peptide and connected these preferentially by a disulfide bond ***(23)***. Disulfide bond is stable in the tissue-culture medium, but after internalization, it is rapidly cleaved in the strongly reducing cellular environment enabling specific and differential intracellular targeting of both, PNA and transport peptide, respectively.

2. Materials

2.1. Solid-Phase Synthesis of Peptide and PNA

2.1.1. Reagents

1. *t*-butyloxycarbonyl (*t*-Boc) protected amino acids **(24)**, *t*-butyloxycarbonyl (*t*-Boc) protected PNA monomers, stored at –20°C.
2. *p*-methylbenzylhydrylamine (MBHA) resins.

a. for peptide synthesis substitution, 1.02 mmol/g.
b. for PNA synthesis, resin was downloaded to 0.16 mmol/g (*see* **Note 1**).

3. Hydroxybenzotriazole (HOBt).
4. 2-(1H-benzotriazole-1-yl)-1,1,3,3-tetramethyluronium tetrafluoroborate (TBTU).
5. Kaiser Test reagents:
   Solution A: mix solutions a and b.
   a. 200 m*M* KCN in pyridine: dilute 2 mL of KCN solution (65 mg in 100 mL of water) in 100 mL of pyridine. KCN is highly toxic, unused aqueous KCN solution should be stored at 4°C in the dark;
   b. Dissolve 40 g of phenol in 10 mL of absolute ethanol. Phenol can cause severe burns. Phenol should be kept in the dark.

   Solution B: Ninhydrin solution: Prepare 5% (w/v) ninhydrin solution in ethanol (500 mg of ninhydrin in 10 ml of ethanol).
6. Solvents and scavengers: methylene chloride (DCM), trifluoroacetic acid (TFA), *N*,*N*-diisopropylethylamine (DIEA), 100% ethanol, *N*,*N*-dimethylformamide (DMF), dimethylsulphoxide (DMSO), acetonitrile, trifluoromethanesulfonic acid (TFMSA), dimethylsulfide (DMS), *p*-cresol, dimercaptoethane.

2.1.2. Equipment

1. Applied Biosystem peptide synthesizer, model 431A.
2. Applied Biosystem peptide/PNA synthesiser, model 433A.
3. High-performance liquid chromatography (HPLC) system.
4. C18 preparative HPLC column, C18 semipreparative HPLC column.
5. Lyophilizer.

2.2. Treatment of Cells with CPP-PNA Conjugates and Detection of Biotinyl-PNA

Solutions:

1. 10X PBS, pH 7.2: 0.2 *M* potassium phosphate, 1.5 *M* NaCl.
2. Fixative: 4% (w/v) paraformaldehyde, 0.2% (v/v) glutaric dialdehyde in phosphate-buffered saline (PBS).
3. Blocking solution: 5% (w/v) fat-free milk powder in PBS.
4. Bis-Benzimide solution: 1 mg/mL in water (*see* **Note 2**).

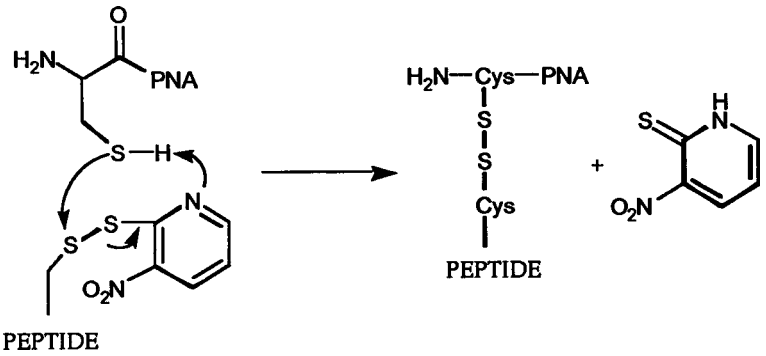

Fig. 1. Synthesis of cell penetrating PNA constructs by application of Cys(Npys).

3. Methods

3.1. Synthesis of Cell Penetrating Peptide-PNA Constructs

Transport peptides were synthesized in a stepwise manner on solid support on an Applied Biosystem Model 431A peptide synthesizer. *tert*-Butyloxycarbonyl amino acids were coupled as 1-hydroxybenzotriazole (HOBt) esters to a *p* methylbenzylhydryl-amine, MBHA, resin to obtain C-terminally amidated peptides ***(24)***. PNA oligomers with a general sequence biotin-Cys-PNA were synthesiszed on downloaded MBHA resin mainly manually.

It was assumed that free N-terminal α-amino group could be necessary for transportan internalisation, therefore PNA oligomer was coupled to ε-amino group of Lys^{14} residue in the middle of transportan. First, Fmoc-protected Lys was introduced into the transportan sequence and 3-nitro-2-pyridinesulphenyl (Npys) derivative of cysteine was coupled manually to ε-amino group of this Lys residue. Sequence of penetratin was modified by adding an extra Npys-cysteine at N-terminus. The unsymmetrical disulfides were obtained by reacting an extra Cys containing PNA oligomer with (Npys)-Cys-CPP (**Fig. 1**). The peptides with S-Npys protected Cys have been shown to react rapidly with thiols to form disulphides at high yields ***(25)***.

3.1.1. Synthesis of Cys(Npys) Derivatives of Transport Peptides

1. Add DCM to 1 eq of unprotected peptide-resin, mix for 5 min, and drain.
2. Add 20% (v/v) piperidine/DMF to peptide-resin, mix for 1 min, and drain.
3. Repeat **step 2**, mix for 10 min, and drain.
4. Wash 5 times with DMF and twice with DCM.
5. Perform Kaiser test.
6. Dissolve 3 eq of Boc-Cys(Npys) in DCM, add 3 eq of HOBt, and 3 eq of TBTU.
7. Add this solution to peptide resin, add 6 eq DIEA. The optimal volume of solution is approx 20 mL per gram resin. Add DMF, if necessary.
8. Mix for 20 min.
9. Wash with DCM, ethanol, DMF, base (5% DIEA in DCM), DMF, 3× with DCM. The optimal volume of each washing is about 20 mL per gram of resin and all washes are carried out for 1 min.
10. Perform Kaiser test.
11. After coupling the peptide-resin can be stored at 4°C. If the first coupling is not complete (blue color in Kaiser test), then re-coupling is recommended (perform **steps 6–11**).

3.1.2. Cleavage of Peptides from Resin and Purification

1. Final deprotection of the peptide resin to remove *t*-Boc groups. Add approx 20 mL of 50% (v/v) TFA/DCM solution per gram of resin, mix for 1 min, drain.
2. Repeat **step 1**, but mix for 20 min, drain.
3. Wash with DCM, ethanol, DMF, base, DMF, base, DMF, 3× with DCM.
4. Perform Kaiser test.
5. Remove the formyl and benzyl type protective groups from peptide side chains by using the low TFMSA method. Treat the resin with the of TFMSA/TFA/*p*-cresol/DMS/dimercaptoethane (10/50/30/8/2 v/v). Mix all the components on ice and lastly add carefully TMFSA. Take 1 mL of mixture per 50 mg of peptide-resin and mix on ice for 2 h.
6. Wash the deprotected resin with DCM, ethanol, DMF, base, DMF, base, and three times with DCM.

7. Cleave the peptides from the MBHA resin using hydrogen fluoride according to the manufacturer's specifications (*see* **Note 3**).
8. After cleavage, dissolve crude peptide in aqueous solution of 10% acetic acid and freeze-dry.
9. Purify crude peptide by reverse phase HPLC technique (C18 preparative HPLC column).
10. Freeze-dry the fractions.
11. Find the product of correct molecular mass by mass spectrometry.
12. Store freeze-dried peptides in the dark at 4°C (*see* **Note 4**).

3.1.3. Synthesis and Purification of Cell-Penetrating Peptide-PNA Constructs

1. Dissolve for conjugation 1 eq of peptide and 1.5 eq of Cys-PNA in deoxygenized mixture of dimethyl sulfoxide (DMSO)/DMF/0.1 m*M* KH_2PO_4, pH 4.45 (v/v; 3/1/1) (*see* **Note 5**).
2. Stir solution overnight in the dark in the nitrogen atmosphere (*see* **Note 4**).
3. Purify the crude CPP-PNA construct by reversed phase HPLC (C18 semi-preparative HPLC column). Elute constructs using a 50 min gradient (solvent A: 0.1% TFA in water; solvent B: 0.1% TFA in acetonitrile) of 20% to 100% solvent B. Record the absorbance at both 260 and 220 nm (*see* **Note 6**).
4. Freeze-dry the construct.
5. Verify the product by matrix-assisted laser desorption/ionization–time-of-flight (MALDI-TOF) mass spectrometry.
6. Store the construct at –20°C.

3.2. Treatment of Cells with CPP-PNA Conjugates

We cultivate human Bowes melanoma cells for our antisense experiment in 2 mL of MEM medium on Petri dishes, 35 mm diameter. All values suggested in the protocol are optimal for these dishes and volumes. Scale the amounts up or down depending on the dishes or wells that you are using.

1. Seed the cells 12–24 h before the treatment with CPP-PNA conjugates to have a 40–50% of the confluence at the start of experiment. Use standard techniques and cultivate the cells in medium that is recommended for respective cell-lines.

Prepare:

a. As minimum two dishes (wells)/compound/concentration.
b. Two negative controls: medium only and medium + PBS.
c. PNA only (at maximal concentration of used construct).
d. CPP only (at maximal concentration of used construct).

2. Dissolve the CPP-PNA in Milli Q quality water at 0.1 or 0.2 mM concentration and determine the actual concentration:
   a. Add the calculated amount of water to the lyophilized construct, vortex and let dissolve for 5 min.
   b. Make a 1:50 dilution of the stock solution for determination of the actual concentration.
   c. Incubate the diluted solution 10 min at 75°C to melt the putative PNA duplexes and measure its optical density (OD) at 260 nm, preferably at 75°C (or 60°C).
   d. Calculate the concentration of CPP-PNA stock, using the respective extinction coefficients (e_{260}): A = 13.7 mL/mmol·cm; C = 16.6 mL/mmol·cm; G = 11.7 mL/mmol·cm; T = 8.6 mL/mmol·cm.
3. Prepare 10X solutions of the CPP-PNA construct for applying.
   a. Make 180 mL of water solution to contain the calculated amount of CPP-PNA construct for 2 mL of medium.
   b. Incubate the solution for 10 min at 75°C and transfer onto ice.
4. Prepare the cells for treatment.
   a. Aspirate the medium.
   b. Apply 1 mL of serum-free medium.
5. Apply constructs.
   a. Add to each 10X CPP-PNA stock solution 20 mL 10X PBS and 800 mL of prewarmed serum-free medium.
   b. Vortex the mixture and apply drop-wise to cells all over the dish.
   c. Incubate the cells with constructs in CO_2 incubator for 4 h or overnight (recommended).
   d. Aspirate the serum-free medium, add 2 mL of serum containing medium and grow them for 24–48 h.
6. Assay for the effects.

3.3. Detection/Visualization of PNA Oligomers and CPPs in the Cells

The intracellular localization of delivered PNA oligomers is usually determined either by indirect immunofluorescence using PNA

modified with biotin or applying to cells PNA directly labeled with fluorochrome.

The cells for experiment (e.g., Bowes, COS, RINm5F, HeLa) are cultivated on sterile round glass coverslips either separately in the wells of the 24-well plate or directly in Petri dishes used for bioassays.

1. Seed the cells on sterile round glass coverslips (No.1, d 12 mm) placed in the 24-well plate. Let the cells to attach to glass surface at least for 12–24 h and use for internalization assay the cells of about 40–60% confluence.
2. Aspirate the medium and add 2–5 μ*M* solution of biotin-PNA-CPP or biotin-CPP in serum-free culture medium (recommended) or in serum-containing medium (*see* **Note 7**)
3. Transfer the cells to CO_2 thermostat at 37°C and incubate from 15 min to 4 h. (*see* **Note 8**).
4. Wash the coverslips gently with PBS (two times 2 min).
5. Fix the cells for 30 min with the mixture of 4% paraformaldehyde and 0.2% glutaric dialdehyde in PBS.
6. Wash the coverslips briefly with PBS (two times 1 min).
7. Permeabilize the cells with cold methanol at –20°C for 10 min.
8. Wash the cells briefly with PBS (two times 1 min).
9. Block the sites for nonspecific binding with 5% (w/v) fat-free milk powder in PBS for 20 min.
10. Rinse the cells with PBS.
11. Visualize the localization of biotinyl-PNA by staining with avidin-TRITC (Sigma; diluted 1:200 in 2% fat-free milk in PBS) for 30 min (*see* **Note 9**).
12. Counter-stain the nuclei for 5 min with 0.3 μg/mL bis-benzimidine in PBS.
13. Wash the preparate with PBS (three times 3 min).
14. Mount the coverslips (e.g., with Slow Fade, "Molecular Probes" or similar) on object glass and seal the edges with transparent nail polish. (*see* **Note 10**).
15. Observe the samples using fluorescence microscope.

4. Notes

1. High loading of resin in PNA synthesis causes aggregation of growing oligomers.

2. Store bis-benzimidine solution at –20°C, fixative and the blocking solution at +4°C, for prolonged storage supplement blocking solution with 0.01% NaN_3.
3. As scavenger use only *p*-cresol. Cys(Npys) residue is sensitive to *p*-thiocresol.
4. Npys-group is light sensitive and therefore stirring is carried through in the dark.
5. Organic solvents such as DMSO are used to increase solubility of PNA.
6. The final yield of the construct was 35–65%. Yield depends on the length and sequence of PNA.
7. The optimal concentration of biotinylated compound is in range 2–5 μ*M*, although we have used successfully 1–10 μ*M* concentrations.
8. Optimal staining intensities are usually achieved by using incubation times of 30 min for biotin-CPP and 1–2 h for biotin-PNA-CPP.
9. We prefer conjugates of avidin with TRITC or FITC for detection of biotinylated peptides or PNA in cells, because these had yield in our hands higher intensity of fluorescence signal as compared to respective conjugates of streptavidin.
10. All the washings and stainings are performed at room temperature, if not stated otherwise.

References

1. Nielsen, P. E., Egholm, M., Berg, R. H., and Buchardt, O. (1991) Sequence-selective recognition of DNA by strand displacement with a thymine-substituted polyamide. *Science* **254,** 1497–1500.
2. Wahlestedt, C., Salmi, P., Good, L., Kela, J., Johnsson, T., Hökfelt, T., et al. (2000) Potent and nontoxic antisense oligonucleotides containing locked nucleic acids. *Proc. Natl. Acad. Sci. USA* **97,** 5633–5638.
3. Summerton, J. (1999) Morpholino antisense oligomers: the case for an RNase H-independent structural type. *Biochim. Biophys. Acta* **1489,** 141–158.
4. Demidov, V. V., Potaman, V. N., Frank-Kamenetskii, M. D., Egholm, M., Buchard, O., Sonnichsen, S. H., and Nielsen, P. E. (1994) Stability of peptide nucleic acids in human serum and cellular extracts. *Biochem. Pharmacol*. **48,** 1310–1313.

5. Egholm, M., Christensen, L., Dueholm, K. L., Buchardt, O., Coull, J., and Nielsen, P. E. (1995) Efficient pH-independent sequence-specific DNA binding by pseudoisocytosine-containing bis-PNA. *Nucleic Acids Res.* **23,** 217–222.
6. Ratilainen, T., Holmen, A., Tuite, E., Haaima, G., Christensen, L., Nielsen, P. E., and Norden, B. (1998) Hybridization of peptide nucleic acid. *Biochemistry* **37,** 12,331–12,342.
7. Knudsen, H. and Nielsen, P. E. (1996) Antisense properties of duplex- and triplex-forming PNAs. *Nucleic Acids Res.* **24,** 494–500.
8. Bonham, M. A., Brown, S., Boyd, A. L., Brown, P. H., Bruckenstein, D. A., Hanvey, J. C., et al. (1995) An assessment of the antisense properties of RNase H-competent and steric-blocking oligomers. *Nucleic Acids Res.* **23,** 1197–1203.
9. Hanvey, J. C., Peffer, N. J., Bisi, J. E., Thomson, S. A., Cadilla, R., Josey, J. A., et al. (1992) Antisense and antigene properties of peptide nucleic acids. *Science* **258,** 1481–1485.
10. Lebedeva, I., Benimetskaya, L., Stein, C. A., and Vilenchik, M. (2000) Cellular delivery of antisense oligonucleotides. *Eur. J. Pharm. Biopharm.* **50,** 101–119.
11. Chinnery, P. F., Taylor, R. W., Diekert, K., Lill, R., Turnbull, D. M., and Lightowlers, R. N. (1999) Peptide nucleic acid delivery to human mitochondria. *Gene Ther.* **6,** 1919–1928.
12. Sei, S., Yang, Q. E., O'Neill, D., Yoshimura, K., Nagashima, K., and Mitsuya, H. (2000) Identification of a key target sequence to block human immunodeficiency virus type 1 replication within the gag-pol transframe domain. *J. Virol.* **74,** 4621–4633.
13. Tyler, B. M., McCormick, D. J., Hoshall, C. V., Douglas, C. L., Jansen, K., Lacy, B. W., et al. (1998) Specific gene blockade shows that peptide nucleic acids readily enter neuronal cells in vivo. *FEBS Lett.* **421,** 280–284.
14. Uhlmann, E. (1998) Peptide nucleic acids (PNA) and PNA-DNA chimeras: from high binding affinity towards biological function. *Biol. Chem.* **379,** 1045–1052.
15. Nastruzzi, C., Cortesi, R., Esposito, E., Gambari, R., Borgatti, M., Bianchi, N., et al. (2000) Liposomes as carriers for DNA-PNA hybrids. *J. Contr. Release* **68,** 237–249.
16. Basu, S. and Wickström, E. (1997) Synthesis and characterization of a peptide nucleic acid conjugated to a D-peptide analog of insulin-

like growth factor 1 for increased cellular uptake. *Bioconjug. Chem.* **8,** 481–488.

17. Lindgren, M., Hällbrink, M., Prochiantz, A., and Langel, Ü. (2000) Cell-penetrating peptides. *Trends Pharmacol. Sci.* **21,** 99–103.
18. Derossi, D., Chassaing, G., and Prochiantz, A. (1998) Trojan peptides: the penetratin system for intracellular delivery. *Trends Cell Biol.* **8,** 84–87.
19. Prochiantz, A. (1996) Getting hydrophilic compounds into cells: lessons from homeopeptides. *Curr. Opin. Neurobiol.* **6,** 629–634.
20. Vivés, E., Brodin, P., and Lebleu, B. (1997) A truncated HIV-1 Tat protein basic domain rapidly translocates through the plasma membrane and accumulates in the cell nucleus. *J. Biol. Chem.* **272,** 16,010–16,017.
21. Rojas, M., Yao, S., Donahue, J. P., and Lin, Y. Z. (1997) An alternative to phosphotyrosine-containing motifs for binding to an SH2 domain. *Biochem. Biophys. Res. Commun.* **234,** 675–680.
22. Pooga, M., Hällbrink, M., Zorko, M., and Langel, Ü. (1998) Cell penetration by transportan. *FASEB J.* **12,** 67–77.
23. Pooga, M., Soomets, U., Hällbrink, M., Valkna, A., Saar, K., Rezaei, K., et al. (1998) Cell penetrating PNA constructs regulate galanin receptor levels and modify pain transmission in vivo. *Nat. Biotechnol.* **16,** 857–861.
24. Soomets, U., Lindgren, M., Gallet, X., Hällbrink, M., Elmquist, A., Balaspiri, L., et al. (2000) Deletion analogues of transportan. *Biochim. Biophys. Acta* **1467,** 165–176.
25. Bernatowicz, M. S., Matsueda, R., and Matsueda, G. R. (1986) Preparation of Boc-[S-(3-nitro-2-pyridinesulfenyl)]-cysteine and its use for unsymmetrical disulfide bond formation. *Int. J. Pept. Protein Res.* **28,** 107–112.

16

Antisense Inhibition of Bacterial Gene Expression and Cell Growth

Liam Good

1. Introduction

Antisense agents are very attractive for research and therapeutics development because they offer possibilities to inhibit any gene using simple design rules. In practice, however, antisense design is very difficult and clinical progress has been only sporadic. Fortunately, new nucleic acid analogs and mimics such as peptide nucleic acid (PNA) have been developed and these greatly improve the prospects for therapeutic development ***(1)***. In this chapter we describe antisense PNAs that inhibit bacterial genes. This area of antisense technology attracts relatively little attention ***(2–6)***, however, bacteria are accessible to antisense inhibition and PNA chemistry in particular gives some important advantages ***(7)***. There are strong motivations to pursue this work, including the need for new types of antimicrobials for medicine and also research needs for flexible tools for genetic analyses of diverse bacteria. So far, our attempts to develop antisense PNAs for bacteria have been very encouraging ***(2–4)***.

Although bacterial applications for antisense technology attracts less attention than eukaryotic applications, bacteria may be particularly amenable to antisense control. Bacterial genomes are much

From: *Methods in Molecular Biology, vol. 208: Peptide Nucleic Acids: Methods and Protocols*
Edited by: P. E. Nielsen © Humana Press Inc., Totowa, NJ

smaller than those of higher eukaryotes and this naturally improves the prospects for target binding and gene-specific effects. Furthermore, bacterial genes are structurally less complex and we understand more about their gene regulation. Finally, bacteria do not possess internal organelles that limit cellular distribution or target access. Therefore, bacteria are attractive systems for antisense development, in terms of both feasibility and potential applications.

There is a major challenge, however, when considering antisense agents for bacteria. Most microbes possess stringent cell barriers to protect themselves from harmful molecules in their environment ***(8)***. Antisense agents large enough for genome-wide sequence selectivity are inherently larger than most drugs and too large for efficient diffusion into microbes. Our first efforts using 15-mer standard antisense PNAs showed only poor potency in wild-type *Escherichia coli* ***(2,3)***. However, antisense PNAs function very well in cell lysates. Also, certain permeable mutant strains with a defective lipopolysaccharide (LPS) layer are more susceptible to PNA and the cell barrier of wild-type bacteria can be chemically permeabilized to increase susceptibility to PNA ***(9)***. Therefore, antisense PNA effects in *E. coli* appear to be significantly limited by poor passage across the outer membrane.

Although standard PNAs show poor cell uptake, they show promising sequence specificity and a true antisense mechanism of action. Therefore, PNAs that can gain cell entry are likely to provide potent antisense agents. Fortunately, there are many possibilities to modify PNA to overcome cell barriers ***(10)***. To improve potency, we first reasoned that shorter PNAs should be able to pass the outer barrier more efficiently. Comparison of different sized PNAs showed that shorter PNAs are indeed more potent, presumably because of improved uptake ***(4)***. To further improve uptake we searched for a cell-permeabilizing agent that could be directly attached to PNA. A recent literature report described a simple version of such a peptide (KFFKFFKFFK), and when attached to PNA the resulting peptide-PNA conjugate is much more potent than the standard version ***(4)***.

As an example of the improved potency provided by the modified PNAs, a short peptide-PNA targeted to the essential fatty acid

biosynthesis *acpP* gene can prevent growth in a gene-specific manner and is bactericidal within a few hours of treatment at (8 μg/mL) ***(4)***. Furthermore, the anti-*acpP* effect can be used to clear a bacterial infection of cultured human cells without apparent toxicity to the human cells. Therefore, antisense PNAs show desirable properties for antimicrobial development, and the gene specific effects provide new tools for gene-function studies.

This chapter describes relatively simple guidelines for designing antisense PNAs and peptide-PNAs. Although uncertainties remain regarding optimum design strategies and there are many more options to explore with modified versions of PNA, the molecules described here display robust antisense effects. Also included here is a description of straightforward and inexpensive assays to assess antisense effects on reporter and essential genes. Finally, the Notes Subheading offers additional hints and a description of controls that can help ensure true antisense effects.

2. Materials

2.1. PNAs and Peptide-PNAs

Synthesis of standard modified peptide.PNAs is described in Chapters 2, 3, and 4.

2.2. E. coli Culture and PNA Teatment

1. *E. coli* K12 from the Coli Genetic Stock Center (Yale University).
2. Mueller Hinton broth (MHB) (e.g., Sigma M-9677).
3. 96-well microtiter plates (e.g., Costar 7424).
4. Spectrophotomer with temperature control and shaking capacity (e.g., Molecular Dynamics Spectromax).

2.3. Reporter Gene Expression and Measurements

1. IPTG stock: 100 m*M* isopropyl β-D-thiogalactopyranoside.
2. Cell-permeabilization buffer (2X): 50 m*M* Tris-PO_4, 4 m*M* dithiothreitol (DTT), 4 m*M* trans-1,2-diaminocyclohexane-N;N; *N*';*N*'-tetraacetic acid, 20% glycerol, 2% Triton X-100, 100 μg/mL polymyxin B sulfate.

3. Z buffer: 0.06 *M* Na_2HPO_4, 0.04 *M* NaH_2PO_4, 0.01 *M* KCl, 0.001 *M* $MgSO_4$, 0.05 *M* 2-mercaptoethanol, pH 7.0.
4. Stop solution: 0.5 *M* sodium carbamate.

2.4. Effects on Bacterial Cell Viability

1. Luria Bertani plates: 1.5% agar, 0.5% yeast extract, 1% tryptone, 0.5% NaCl (w/v).
2. Glass beads (2 mm diameter).

3. Methods

3.1. Target-Site Selection and PNA Sequence Design

Empirical screening remains the most important method to identify susceptible mRNA target sites and active antisense agents. Uncertainty about mRNA higher-order structure and antisense-agent binding properties prevents a fully rational approach. However, some sensible guidelines have emerged that can increase the success rate when designing antisense agents for eukaryotic applications ***(11)***. For bacterial applications, there is less experience to draw from, however, in some respects the situation is eased by our better understanding of prokaryotic translation control and the lower cell complexity in bacterial. Overall, the difficult question of target-site selection and antisense sequence design appears to be easier for bacteria than for eukaryotes.

In bacterial systems, there is strong evidence that the mRNA start codon region is susceptible to antisense inhibition. First, bases within this region are recognized by ribosomal components during recruitment and assembly of an active translation apparatus ***(12,13)***. Second, in the natural examples of antisense inhibition in bacteria, the start codon region is the usual target ***(14)***. Third, there are several examples of attenuated mRNAs where the start codon region is sequestered within a double-stranded region ***(15)***. Finally, we have experienced consistent success when designing antisense PNAs that target the start codon region. Therefore, the start codon region in most bacterial mRNAs is likely to be susceptible to antisense inhi-

bition. At this time, the size of the susceptibility window is uncertain, so we suggest mRNA target sites within the start codon and Shine-Dalgarno sequences.

For bacterial applications antisense PNAs from 9–12-mer in length are recommended. This length range is short relative to our first design efforts and much shorter that those typically used by antisense researchers. However, one must consider that most PNA sequences display high affinity binding properties and bacterial genomes are relatively small. Indeed, a 12-mer target sequence can be unique within the transcription products of the *E. coli* genome. Also, shorter PNAs are more likely to efficiently enter cells. Most importantly, "side-by-side" comparisons have shown that this range improves antisense potencies over longer versions and we have successfully designed many short PNAs ***(4)***.

While considering the mRNA target site, one also must consider sequence composition. There are several potential pitfalls to avoid. First, it seems best to avoid self-complementarity. Second, a low GC content could result in a low binding affinity, particularly with short PNAs ***(16)***. Third, a high G content can be problematic for synthesis and solubility. Finally, the target site should be examined for uniqueness within the bacterial genome. This can be carried out using the Blast algorithm ***(17)*** (http://www.ncbi.nlm.nih.gov/BLAST/: with word size set to 10 and the –e value set to 10,000), or by visiting http://genolist.pasteur.Fr. Note that target sites spanning the AUG start codon or containing a consensus Shine-Dalgarno sequence are less likely to be unique and should be carefully checked.

Standard 9–12-mer antisense PNAs can provide reasonable antisense effects against *E. coli*. In addition, further improvements are possible by attaching PNA to cell-permeabilizing peptides ***(4)***. The synthesis of such peptide-PNAs is described in Chapter 4. Typically, the short, cell-permeabilizing peptide KFFKFFKFFK is conjugated directly to PNA oligomers as illustrated in **Fig. 1**. Although there are many alternative peptides, this sequence has proven reliable both for synthesis and antisense efficacy. Indeed, antisense assays using KFFKFFKFFK-PNA conjugates show that the attached peptide can improve potency up to two orders of magni-

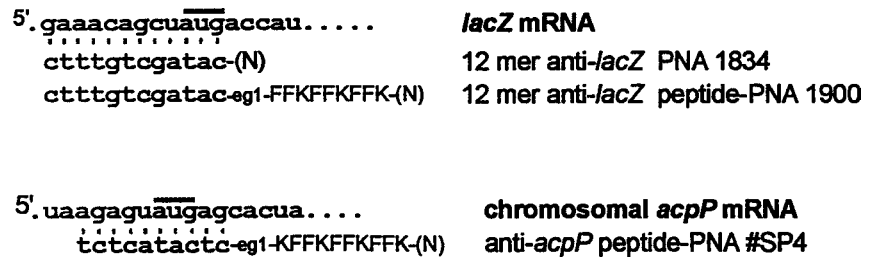

Fig. 1. Structure of antisense PNAs and peptide-PNAs. Wild- type chromosomal *E. coli* β-galactosidase (*lac*Z) and *acpP* mRNA start codon target sequences and examples of antisense PNAs and peptide-PNA conjugates. The *lac*Z gene is targeted as a reporter gene and *acpP* is an essential gene central to fatty acid biosynthesis. N indicates the PNA amino terminus, corresponding to the 5' end of a conventional oligonucleotide.

tude. Antisense PNA design for bacterial applications can proceed in four steps, as follows:

1. Target-site selection within the start codon region.
2. Select antisense PNA length (10–12-mer) and composition.
3. Ensure target-site uniqueness.
4. Optional attachment of a cell-permeabilizing peptide.

3.2. E. coli *Cell Culture and PNA Susceptibility Testing in Liquid Culture*

E. coli cells are cultured and treated with PNA inhibitors in accordance with standarized methods for antimicrobial testing ***(18)*** (*see* **Note 1**). This can be conveniently carried-out using 100 µL cultures in a 96-well plate, with growth monitored during incubation by recording culture turbidity at regular time intervals. The compiled data provide a growth curve for up to 96 cultures, as shown in **Fig. 2**. The results from all wells can be plotted to visualize the effect of inhibitors on cell growth (*see* **Fig. 2**).

1. Prepare a fresh overnight culture of *E. coli*, when grown in MHB at 37°C the cell density will be approx 10^9colony-forming units (cfu) mL (*see* **Note 2**).
2. Dilute cells 1:10000 into experimental 100 µL MHB cultures within microtiter plates wells to provide an inoculum of 10^5 cfu/mL. Add

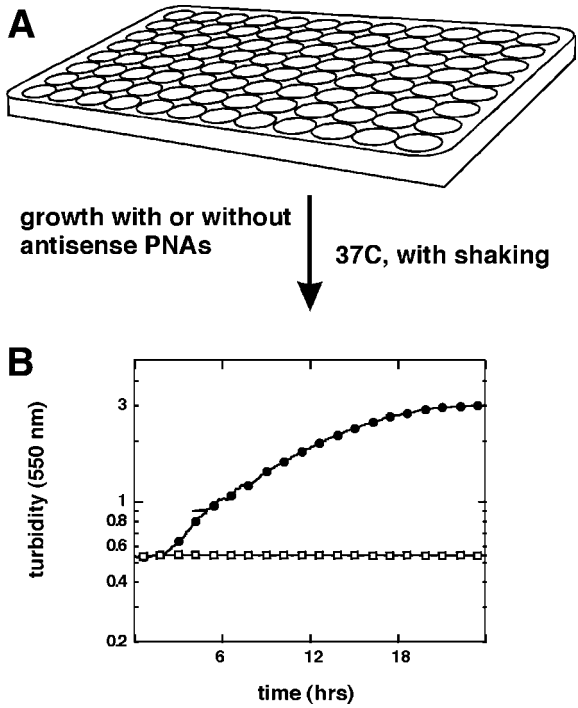

Fig. 2. *E. coli* culture conditions, PNA treatment and growth monitoring. (**A**) Pre-grown *E. coli* K12 are used to inoculate 100 mL of MHB at 10^5 cfu/ml in the wells of a 96-well microtiter plate. PNA is added in the nanomolar or low micromolar range. Plates are incubated at 37°C with shaking for 5 s each 5 min, followed by a turbidity measurement at 550 nm. (**B**) Cell growth is indicated as increased turbidity using OD_{550} measurements, and the turbidity measurements are indicated in the graph, adjusted to a 1 cm path length.

PNA, which is handled according to directions given in **Note 3**.

3. Incubate cultures overnight at 37°C for 18 h in an automated spectrophotomer where the plates are shaken for 5 s each 5 min and this is followed by an absorbance (**A**) reading at 550 nm.

3.3. Reporter Gene Expression and Measurements

There are a variety of reporter gene systems that can be efficiently used in bacteria. To test PNA antisense effects we have used β-galactosidase gene (*lacZ*), β-lactamase, luciferase, and the green fluorescence protein (GFP). The *lacZ* reporter system is advanta-

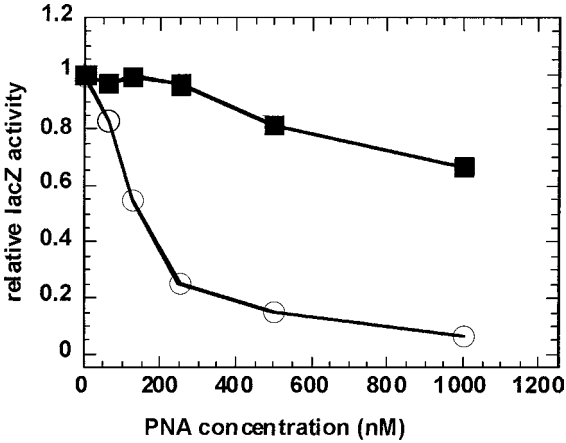

Fig. 3. *lacZ* inhibition with peptide-PNAs in *E. coli.* The values represent relative enzyme activities in *E. coli* K12 cultures grown in MHB. Antisense effects with 12 mer PNA 1834 (open circles) and the peptide-PNA conjugate 1900 (closed circles). Note the dose response and improved potency provided by the peptide.

geous because it is chromosomally encoded in most strains, inducible, and expression can be accurately and inexpensively quantified ***(19)***. For antisense inhibition, the *lacZ* gene in *E. coli* is induced with 50 μ*M* isopropyl β-D-thiogalactopyranoside (IPTG) and assayed with the substrate *o*-nitrophenyl-β-galactoside (ONPG) and A_{420} measurements, as follows:

1. Aliquot samples 10 μL of the final *E. coli* culture into microtiter plate wells. To create a standard curve, place dilutions containing blank and 1–10 μL aliquotes of a control culture into parallel wells.
2. Add 50 μL of Cell-Permeabilization Buffer, incubate 30 min at room temperature.
3. Add 100 μL Z buffer containing ONPG.
4. Incubate until a pale yellow color appears, add 50 mL Stop Solution, record A_{420}, and calculate relative *lacZ* expression by comparison to values obtained for the standard curve.

An example of antisense inhibition of *lacZ* is shown in **Fig. 3**. The figure includes results for a standard antisense PNA, a control

mismatched PNA, and a more active peptide-PNA. Note that a dose response is observed and the IC_{50} is in the mid-nanomolar range for the peptide-PNA.

3.4. Antisense PNA Effects on Cell Viability

The antisense PNAs described in this chapter are very promising compounds for antimicrobial development in at least two ways. Antisense PNAs targeted against essential genes are potential new antimicrobials and they also can indicate which genes in a pathogen are susceptible targets for more conventional antimicrobial development. Furthermore, the bacteriostatic vs bactericidal effects of gene inhibition can be studied by determining the number of cfu in cultures treated with PNA ***(18)***. To do this, small samples can be taken at multiple time points during PNA treatment, and the number of viable cells in the sample is indicated by determining the number of cfu, as follows:

1. From experimental cultures prepared as described in **Subheading 3.2.**, collect 5 µL of the bacterial culture and dilute over 4 orders of magnitude in MHB.
2. Spread onto prewarmed LB plates using glass beads or a glass hockey stick.
3. Incubate overnight at 37°C and calculate the number of cfu in the liquid culture.

As an example, **Fig. 4** illustrates the bactericidal effects of a peptide-PNA targeted to the essential *acpP* gene. Note that complete killing was observed within a few hours of incubation. Finally, Note 4 describes some important controls that can be included in antisense experiments.

4. Notes

1. Bacterial species. We are most familiar with antisense PNAs directed against *E. coli* K12 and the permeable mutant AS19, which is more sensitive to PNAs. Experiments in progress indicate that antisense PNAs can be applied to a variety of bacterial species, however, it is too early to predict the phylogenetic range of susceptible species.

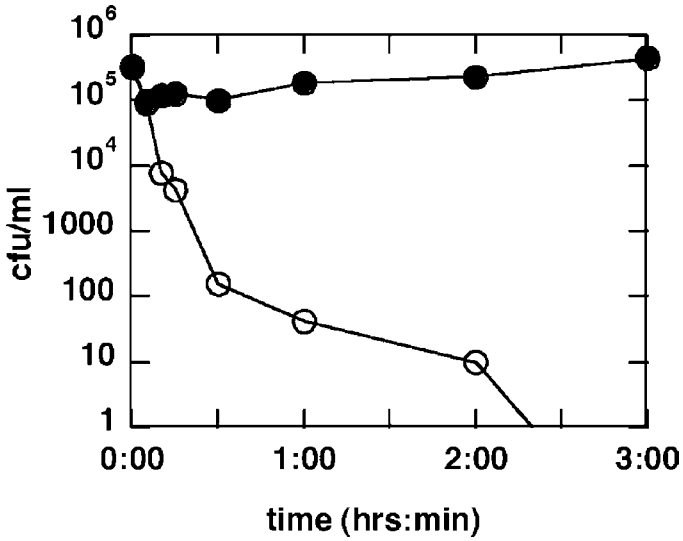

Fig. 4. Bactericidal antisense effects of an anti-*acpP* peptide PNA. Cultures of *E. coli* K12 (open circles) and K12/*acpP-1* (closed circles) were established in MHB at 10^5 cfu/mL and treated with PNA at 2 μ*M*. The number of cfu was determined by plating.

2. Growth media. For most applications, MHB is recommended for cell growth and PNA treatment. Previously, when using standard antisense PNAs, it was necessary to use dilute media to obtain robust antisense effects. The modified peptide-PNAs described here are effective in MHB, which is standard for antimicrobial susceptibility testing.
3. Storage and handling of antisense peptide-PNAs. PNAs should be stored in water at –70°C in small aliquots to minimize freeze-thaw damage, and special care should be taken with peptide-PNAs, because the peptide component can be susceptible to protease degradation. Siliconized or similarly coated tubes and microtiter plates are recommended to reduce problems with PNA adherence.
4. Controls for antisense specificity. Antisense agents potentially can effect cells in a variety of ways and also bind to more than just the intended RNA. For many antisense applications this is an important concern, and controls are needed to evaluate specificity. In addition to measuring expression of the targeted gene, the usual control is to include within the experiment antisense agents that are not fully

complementary to the target site. These can be constructs with mismatched or scrambled sequences where the overall base composition remains the same. Also, when possible, binding site-altered versions of the targeted gene can be included to ensure specificity.

References

1. Toulme, J. J. (2001) New candidates for true antisense. *Nat. Biotechnol.* **19,** 17–18.
2. Good, L. and Nielsen, P. E. (1998) Antisense inhibition of gene expression in bacteria by PNA targeted to mRNA, *Nat. Biotechnol.* **16,** 355.
3. Good, L. and Nielsen, P. E. (1998) Inhibition of translation and bacterial growth by peptide nucleic acid targeted to ribosomal RNA, *Proc. Natl. Acad. Sci. USA* **95,** 2073–2076.
4. Good, L., Awasthi, S. K., Dryselius, R., Larsson, O., and Nielsen, P. E. (2001) Bactericidal antisense effects of peptide-PNA conjugates. *Nat. Biotechnol.* **19,** 360–364.
5. Harth, G., Zamecnik, P. C., Tang, J. Y., Tabatadze, D., and Horwitz, M. A. (2000) Treatment of Mycobacterium tuberculosis with antisense oligonucleotides to glutamine synthetase mRNA inhibits glutamine synthetase activity, formation of the poly-L-glutamate/glutamine cell wall structure, and bacterial replication. *Proc. Natl. Acad. Sci. USA* **97,** 418–423.
6. White, D. G., Maneewannakul, K., von Hofe, E., Zillman, M., Eisenberg, W., Field, A. K., and Levy, S. B. (1997) Inhibition of the multiple antibiotic resistance (mar) operon in *Escherichia coli* by antisense DNA analogs, *Antimicrob. Agents Chemother. 41*, 2699–2704.
7. Nielsen, P. E. (2001) Peptide nucleic acids as antibacterial agents via the antisense principle, *Exp. Opin Invest. Drugs* **10,** 331–341.
8. Nikaido, H. (1994) Prevention of drug access to bacterial targets: permeability barriers and active efflux, *Science* **264,** 382–388.
9. Good, L., Sandberg, R., Larsson, O., Nielsen, P. E., and Wahlestedt, C. (2000) Antisense PNA effects in escherichia coli are limited by the outer-membrane LPS layer. *Microbiology* **146,** 2665–2670.
10. Haaima, G., Lohse, A., Buchardt, O., and Nielsen, P. E. (1996) Peptide nucleic acids (PNA) containing thymine monomers derived from chiral amino acids: hybridization and solubility properties of d-lysine PNA. *Angewandte Chem.* **35,** 1939–1941.

11. Myers, K. J. and Dean, N. M. (2000) Sensible use of antisense: how to use oligonucleotides as research tools. *Trends Pharmacol. Sci.* **21,** 19–23.
12. Shine, J. and Dalgarno, L. (1974) The 3'-terminal sequence of *Escherichia coli* 16S ribosomal RNA: complementarity to nonsense triplets and ribosome binding sites. *Proc. Natl. Acad. Sci. US A.* **71,** 1342–1346.
13. Osada, Y., Saito, R., and Tomita, M. (1999) Analysis of base-pairing potentials between 16S rRNA and 5' UTR for translation initiation in various prokaryotes. *Bioinformatics* **15,** 578–581.
14. Wagner, E. G. and Simons, R. W. (1994)Antisense RNA control in bacteria, phages, and plasmids. *Annu. Rev. Microbiol.* **48,** 713–742.
15. Lovett, P. S. (1996) Translation attenuation regulation of chloramphenicol resistance in bacteria: a review. *Gene* **179,** 157–162.
16. Giesen, U., Kleider, W., Berding, C., Geiger, A., Orum, H., and Nielsen, P. E. (1998) A formula for thermal stability (Tm) prediction of PNA/DNA duplexes. *Nucleic Acids Res.* **26,** 5004–5006.
17. Altschul, S. F., Gish, W., Miller, W., Myers, E. W., and Lipman, D. J. (1990) Basic local alignment search tool. *J. Mol. Biol.* **215,** 403 –410.
18. Amsterdam, D. (1996) Susceptibility testing of antimicrobials in liquid media, in *Antibiotics in Laboratory Medicine*, (Lorian, V., ed.), Williams & Wilkins, Baltimore, pp. 52–111.
19. Miller, J. H. (1972) *Experiments in Molecular Genetics*. Cold Spring Harbor Laboratory Press, Cold Spring Harbor, NY.

17

In Vitro Transcription from Peptide Nucleic Acid/DNA Strand Displacement Loops

Niels Erik Møllegaard and Peter E. Nielsen

1. Introduction

Escherichia coli RNA polymerase holoenzyme consists of a core enzyme with subunit composition, $\beta\beta'\alpha_2$, capable of elongation of transcription and an additional subunit, sigma (σ) that binds to the core enzyme and allows specific promoter recognition and transcription initiation. Primarily two DNA consensus sequences centered around –10 and –35 are included in the process of promoter recognition and opening. The open complex includes a region where base pairing is disrupted over a region of ~12 bp. When the open complex is formed, the sigma subunit is released and a processive elongation complex is formed ***(1–3)***.

However, transcription initiation can take place from single stranded mismatch bubbles of approx 12 bp in length with no similarity to the two consensus sequences in DNA. It has been shown that *E. coli* RNA polymerase can utilize synthetic RNA/DNA bubble complexes containing an RNA/DNA duplex and a single-stranded DNA loop for transcription elongation ***(4)***. Furthermore, it has even been shown that *E. coli* RNA polymerase can initiate transcription from synthetic bubbles even in the absence of an RNA primer ***(5)***. These results show that RNA polymerase has strong

From: *Methods in Molecular Biology, vol. 208: Peptide Nucleic Acids: Methods and Protocols*
Edited by: P. E. Nielsen © Humana Press Inc., Totowa, NJ

affinity for single stranded regions, which is sufficient to direct transcription in the 5' to 3' direction.

An exclusive way of introducing single-stranded templates for RNA polymerase in naturally occurring DNA sequences is by the employment of peptide nucleic acids (PNA). Homopyrimidine PNAs are able to bind to complementary double-stranded DNA by triplex invasion, where the PNA forms a $(PNA)_2$/DNA triplex with one strand while the other strand is displaced, forming a single-stranded loop ***(6–9)***.

It has been shown that transcription can be directed in the 5' to 3' direction from single-stranded loops formed by PNA strand displacement, which allows a unique construction of DNA targets for RNA polymerase. Transcription from such "PNA promoters" is dependent on the length of the single-stranded region, and can be designed to be just as efficient as *E. coli* promoters ***(10)***. PNA-induced transcription suggests some exciting uses of PNA as general sequence-specific gene activators, which may have implications in genetic therapy.

In this chapter the *E. coli* RNA polymerase is used to demonstrate transcription from PNA promoters. However, PNA-induced transcription initiation can also be performed by using phage polymerases and Hela cell extract. Furthermore transcription initiation by PNA has been demonstrated in human cell lines ***(11)***.

2. Materials

1. Plasmid and DNA fragment with a target for PNA (*see* **Note 1**).
2. PNA incubation buffer: The PNA-DNA complex is assembled in a low salt buffer, as for instance in 10 m*M* Tris-HCl, pH 8.0.
3. PNA specific for DNA target in the template (*see* **Note 2**).
4. *E. coli* RNA polymerase transcription buffer: 40 m*M* Tris-HCl, pH 7.9–8.0, 120 m*M* KCl, 5 m*M* $MgCl_2$, 0.1 m*M* dithiothreitol (DTT), 1 m*M* (each) ATP, CTP, and GTP, and 0.1 m*M* UTP and 5 µCi ^{32}P UTP.
5. Transcription buffer used in reverse transcriptase primer extension is the same as in **step 4**. except that no ^{32}P UTP is used and 1 m*M* UTP is added instead of 0.1 m*M*.

6. *E. coli* RNA polymerase.
7. AMV reverse transcriptase.
8. 5X AMV reverse transcriptase buffer: 250 m*M* Tris-HCl, pH 8.3, 250 m*M* KCl, 50 m*M* $MgCL_2$, 2.5 m*M* spermidine, and 50 m*M* DTT.
9. DeoxyNTP mix: 1 m*M* dATP, dGTP, dTTP, and dCTP.
10. Primer for primer extension.
11. Ethanol 96%.
12. Ethanol 70%.
13. 1X TBE: 90 m*M* Tris-borate, 1 m*M* EDTA, pH 8.3.
14. Polyacrylamide gel: 8–10%, 0.3% *bis*-acrylamide, 7 *M* urea, 1X TBE buffer.
15. Gel-loading buffer: 80% formamide in 1X TBE buffer, 0.05% bromophenol blue, and 0.05% xylene cyanole.

3. Methods

3.1. "Run-Off" Transcription

1. DNA restriction fragments containing PNA targets is isolated by standard techniques (*see* **Note 3**).
2. PNA-DNA complexes are formed by incubating PNA with DNA fragments in 10 m*M* Tris-HCl, pH 8.0, in a total volume of 25 µL for 1 h at 37°C. (*See* **Note 4**).
3. The reaction mixture is adjusted in a total volume of 50 µL to contain the concentration of the transcription buffer with 5 µCi ^{32}P UTP.
4. 100 n*M* RNA polymerase is added and incubation is performed at 37°C for 10–30 min (*see* **Note 5**).
5. The RNA is recovered by precipitation with 100 µL ethanol.
6. RNA is dissolved in 10 µL gel loading buffer.
7. A sample of the RNA is run on 8–10% denaturing polyacrylamide gels.
8. Visualize radioactive bands by phosphoimager or autoradiography.

3.2. Reverse Transcriptase Primer Extension

1. PNA-DNA complexes are formed by incubating the PNA with the supercoiled circular closed DNA vector in 10 m*M* Tris-HCl, pH 8.0, in a total volume of 25 µL for 1 h at 37°C.

2. The reaction mixture is adjusted to contain the concentration of the transcription buffer with 1 m*M* of all four nucleotides.
3. 100 n*M* RNA polymerase is added and incubation is continued at 37°C for 10–30 min.
4. The RNA is recovered by precipitation with 100 µL ethanol.
5. The samples are dissolved in 200 µL H_2O and extracted with 200 µL phenol. The phenol is removed and extraction with 200 µL chloroform is performed.
6. The samples are precipitated with 400 µL ethanol.
7. The RNA pellet is dissolved in 30 µL H_2O.
8. A ^{32}p-labeled primer (labeled by standard techniques) is added. Primer-template hybridization is done by slow cooling from 90°C to 45°C.
9. Reverse transcriptase buffer is added together with a final concentration of 100 m*M* dATP, dGTP, dTTP, and dCTP.
10. 20 units AMV reverse transcriptase is added and incubation is done at 37°C for 1 hr in a total volume of 50 µL (*see* **Note 6**).
11. The DNA is recovered by 100 µL ethanol.
12. The DNA is dissolved in 10 µL gel loading buffer.
13. A sample of the DNA is run on 8–10% denaturing polyacrylamide gels together with sequence reactions (*see* **Note 7**).
14. Visualize radioactive bands by phosphoimager or autoradiography.

3.3. Example

A construct (pA_9GT_9CKS) where a double PNA target (two targets on opposite strands) is cloned into the Sal I site of plasmid bluescriptKS+ was used in the example shown here. The target for PNA is a homopurine/homopyrimidine target with the sequence TTTTCTTTTT/AAAAGAAAAA and the PNA used is a bis PNA, H-$(lys)_3$-TTJTTJTTTT$(eg1)_3$TTTTCTTCTT-lys-NH_2, where J and eg1 designate the synthetic nucleobase pseudoisocytosine and an ethylene glycol type linker, respectively ***(12)***. Binding of PNA results in a complex with two single-stranded regions separated by six bp, which are single-stranded at the condition used for transcription (*see* **Fig. 1**).

The 477 bp PvuII fragment from pA_9GT_9CKS is purified and used for the in vitro transcription assay. No active *E coli* promoters

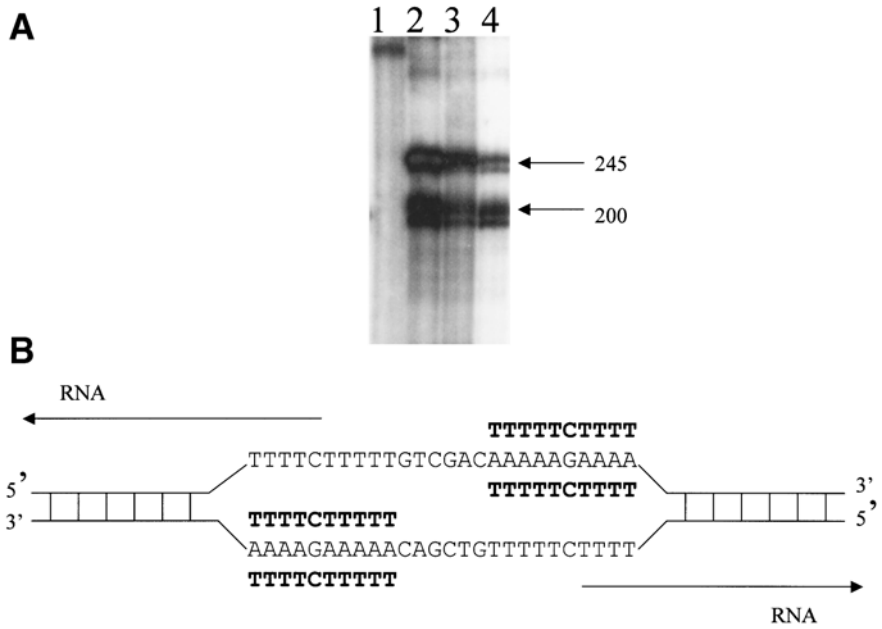

Fig. 1. In vitro transcription initiation from PNA/DNA strand displacement loops. A double PNA target is used, where PNA binds to opposite strands, which allows transcription in two directions. **(A)** Transcription in the absence of PNA is shown in lane 1. Lane 2 and 3 contains samples from transcription in the presence of 100 nM PNA and 10 and 100 n*M* RNA polymerase, respectively. Transcription in the presence of 100 n*M* PNA and 20 n*M* core RNA polymerase is shown in lane 4. Arrows indicate the two RNA products. **(B)** The model shows the two single-stranded regions and the two RNA products appearing from transcription in the 5' to 3' direction. The PNA forming the two triple helixes is shown in bold letters.

at in vitro conditions are present within the fragment. The product appearing when the reaction is performed in the absence of PNA has been ascribed to RNA polymerase binding and initiation from the ends of the fragment (lane 1 in **Fig. 1**). PNA induced transcription gives rise to two transcription products of 200 and 245 bases corresponding to initiation at both single-stranded regions and going in opposite direction towards the ends of the fragment. This is shown for two concentrations of RNA polymerase in lane 2 and 3 of **Fig. 1**.

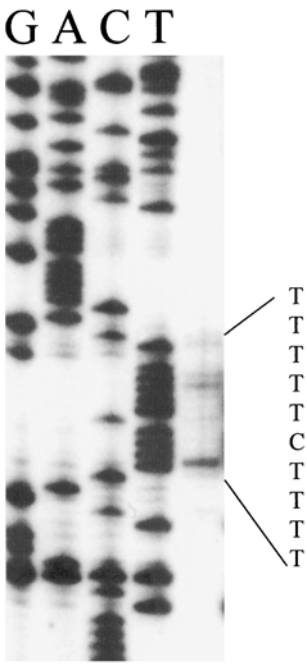

Fig. 2. Reverse primer extension in the presence of 100 n*M* PNA and 100 n*M* RNA polymerase. The sequence of the displaced region is displayed.

In addition it is shown that transcription from the displacement loop can proceed in the absence of the sigma factor (lane 4), which indicates that the RNA polymerase-DNA complex in the PNA promoter resemble more an elongation complex than an initiation complex. Subsequently this suggests that the role of *E. coli* promoters is to provide a platform for RNA polymerase binding and the creation of a transcription loop.

To determine the initiation site of transcription induced by PNA a reverse transcriptase primer extension experiment is performed (*see* **Fig. 2**). Transcription is conducted on a supercoiled template including a PNA target of the same sequence as in the DNA fragment used in the transcription assay of **Fig. 1**. Primer extension in only one direction is shown using a labeled primer that binds to the 5' region of the RNA product of 200 bp. In addition a sequence ladder using the same primer is run along side the primer extension

sample. The result shows that initiation of transcription is taking place at the single-stranded region within the sequence TTTTCTTTTT. It is noted that transcription is initiated from several positions within the loop.

4. Notes

1. The length of the single stranded region may have effect on the efficiency of transcription. It has been shown that two PNA targets positioned in *cis* (~26 bases are single-stranded) exhibit a stronger transcription than a single PNA target (~10 bases are single-stranded) ***(10)***.
2. PNA binding is most efficient when bis-PNA with J bases (pseudoisocytosine) are used. Bis PNAs form triple-stranded complexes of higher thermal stability than monomeric PNA. The J base placed in the strand parallel to the DNA complement (Hoogsteen strand) allows a pH-independent DNA binding.
3. RNA polymerases have affinity for DNA ends and especially when the ends in a DNA fragment are protruding. It is therefore recommended to use blunt-ended templates.
4. To obtain full PNA-DNA complex formation, we recommend performing a PNA titration to find the optimal concentration of PNA.
5. A RNA polymerase titration is recommended.
6. Other reverse transcriptase than AMV can be used.
7. Sequence reactions are performed with the primer used for primer extension.

References

1. Burgess, R. R., Travers, A. A., Dunn, J. J., and Bautz, E. K. (1969) Factor stimulating transcription by RNA polymerase. *Nature* **4,** 43–46.
2. McClure, W. R. (1985) Mechanism and control of transcription initiation in prokaryotes. *Annu. Rev. Biochem.* **54,** 171–204.
3. Von Hippel, P. H., Bear, D. G., Morgan, W. D., and McSwiggen, J. A. (1984) Protein-nucleic acid interactions in transcription: a molecular analysis. *Annu. Rev. Biochem.* **53,** 389–446.
4. Daube, S. S. and von Hippel, P. H. (1992) Functional transcription elongation complexes from synthetic RNA-DNA bubble duplexes. *Science* **258,** 1320–1324.

5. Aiyar, S. E., Helmann, J. D., and deHaseth, P. L. (1994) A mismatch bubble in double-stranded DNA suffices to direct precise transcription initiation by *Escherichia coli* RNA polymerase. *J. Biol. Chem.* **6,** 13,179–13,184.
6. Cherny, D. Y., Belotserkovskii, B. P., Frank-Kamenetskii, M. D., et al. (1993) DNA unwinding upon strand-displacement binding of a thymine-substituted polyamide to double-stranded DNA. *Proc. Natl. Acad. Sci. USA* **90,** 1667–1670.
7. Hanvey, J. C., Peffer, N. J., Bisi, J. E., et al. (1992) Antisense and antigene properties of peptide nucleic acids. *Science* **258,** 1481–1485.
8. Nielsen, P. E., Egholm, M., Berg, R. H., and Buchardt, O. (1991) Sequence-selective recognition of DNA by strand displacement with a thymine-substituted polyamide. *Science* **254,** 1497–1500.
9. Egholm, M., Buchardt, O., Nielsen, P. E., and Berg, R. H. (1992) Peptide nucleic acids (PNA). Oligonucleotide analogues with an achiral peptide backbone *J. Amer. Chem. Soc.* **114,** 9677–9678.
10. Møllegaard, N. E., Buchardt, O., Egholm, M. and Nielsen, P. E. (1994) Peptide nucleic acid. DNA strand displacement loops as artificial transcription promoters. *Proc. Natl. Acad. Sci. USA* **91,** 3892–2895.
11. Wang, G., Xu, X., Pace, B., et al. (1999) Peptide nucleic acid (PNA) binding-mediated induction of human gamma-globin gene expression. *Nucleic Acids Res*. **27,** 2806–2813.
12. Egholm, M., Christensen, L., Dueholm, K. L., Buchardt, O., Coull, J., and Nielsen, P. E. (1995) Efficient pH-independent sequence-specific DNA binding by pseudoisocytosine-containing bis-PNA. *Nucleic Acids Res.* **23,** 217–222.

18

In Vitro and In Vivo Studies on the Pharmacokinetics and Metabolism of PNA Constructs in Rodents

Edward Kristensen

1. Introduction

This chapter describes fast and simple methods for early evaluation of the pharmacokinetic parameters of peptide nucleic acid (PNA) oligomers in vitro and in vivo. The in vitro methods are based on incubation of the PNAs with plasma and selected tissue homogenates from rodents. These high-throughput screening assays provide valuable information on biological stability and metabolic pathways in the early structure optimization and lead candidate selection processes. Further, a method is presented for extraction and analysis of PNA oligomers from biological samples (plasma/serum, bile, urine, and tissue) obtained from animal studies. Design of a pilot pharmacokinetic study in rodents is described for preliminary evaluation of key pharmacokinetic parameters such as systemic clearance, volume of distribution, and elimination half-life. Application of both in vitro and in vivo methodologies are demonstrated using a 12-mer PNA.

From: *Methods in Molecular Biology, vol. 208: Peptide Nucleic Acids: Methods and Protocols*
Edited by: P. E. Nielsen © Humana Press Inc., Totowa, NJ

2. Materials

1. The high-performance liquid chromatography (HPLC) system (Waters) consisted of an Alliance 2690 (pump, autosampler, and degasser), a PDA UV absorbance detector Model 996 (195 – 600 nm), and Millennium[32] Chromatography software version 3.2. HPLC separation was performed on a Waters Symmetry 300™ C18, 2.1 × 150 mm (3.5 µm particles with 300 Å pore size) analytical column (Waters) equipped with a Zorbax Eclipse XDB-C18 (5 µm particles with 80 Å pore size) guard column (Agilent) (*see* **Note 1**), using linear gradient elution of solvent A (0.1% TFA in water) and solvent B (0.1% TFA in acetonitrile) from 2% to 75% solvent B over 8 min. The column was operated at 50°C. Samples were kept in the autosampler at 5°C. Solvent flow was 0.4 mL/min. Polypropylene (PP) test tubes and containers (Sarsted) were generally used for all solutions containing the test PNA (*see* **Note 2**). Samples were centrifuged in a Hettich Rotina 46R centrifuge and evaporated to dryness in a SpeedVac AES 2010 from Savant.
2. NMRI mice (female, 25 g body weight) were obtained from M&B (Denmark) for in vivo studies. Plasma and tissue from sacrificed animals were used for in vitro stability/metabolism studies.
3. The mixed purine-pyrimidine sequence, standard PNA (H-TTCAAA CATAGT-LysNH_2) was synthesized and purified as TFA salt using tBoc chemistry (*see* Chapter 2). The compound was used both as test and reference compound. Other chemicals were purchased from Fluka, Sigma, Merck, or ICN Biochemicals and used as received.
4. Trifluoroacetic acid (TFA).
5. Acetonitrile (ACN).
6. Tris(hydroxymethyl)aminomethane (Tris).
7. Sucrose.

3. Methods

3.1. In Vitro Metabolism in Plasma and Tissue Homogenates

3.1.1. HPLC Test Solution (see **Fig. 1**)

1. Prepare a stock solution of PNA (1 mg/mL) in water. The stock solution is stable for at least 3 mo after preparation when stored at 4°C in the dark.

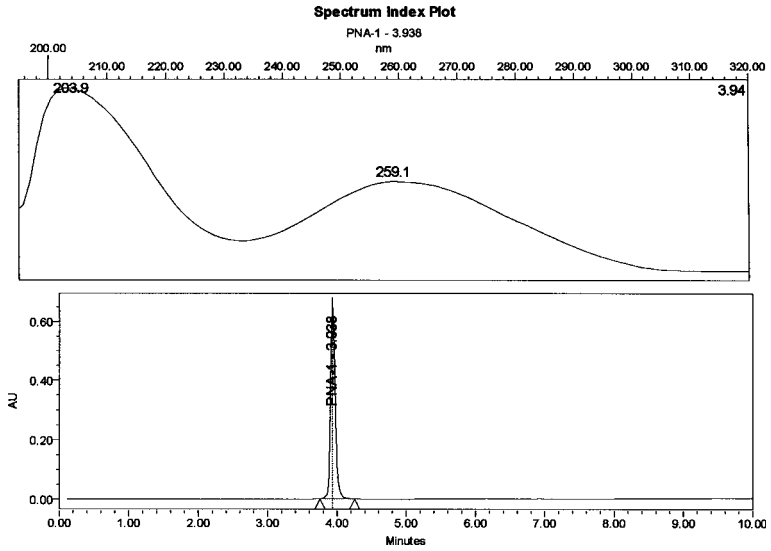

Fig. 1. HPLC chromatogram (UV detection, 260 nm) of PNA-1.

2. Dilute 0.025 mL of the stock solution (1 mg/mL) with 0.1% TFA in water ad 0.250 mL. Dilutions are only used on the day of preparation.
3. Inject 0.01 mL (~1000 ng) of the diluted solution on the HPLC for test of column, gradient and the HPLC-system.

3.1.2. Preparation of Tissue Homogenates for In Vitro Studies

1. Sacrifice the animal and rapidly excise relevant tissues (liver, kidneys, lungs). Immediately place the tissue in 0.25 *M* sucrose at 0°C for rapid cooling and removal of external blood.
2. After cooling (3–5 min), dry the tissue by blotting with paper. Weigh and transfer each tissue to clean PP test tubes.
3. To each tissue add 0.25 *M* sucrose in water to a final concentration of 150 mg tissue/mL, using a density of 1 mg/mL for the tissue.
4. Cut the tissue into pieces and homogenize it for 1–5 min (depending on tissue) in, e.g., Ultra-Turrax™ T25 homogenizer (IKA).
5. Centrifuge the homogenate in a refrigerated centrifuge (4°C) for 30 min at 3000 rpm (corresponding to approx 1000*g*) to isolate subcellular fractions.

6. Carefully decant the supernatant (~ the post mitochondrial supernatant) and transfer it to polypropylene containers. Store the supernatant at –80°C pending use (*see* **Note 3**).

3.1.3. In Vitro Metabolism Studies

1. Mix 0.025 mL 0.1 *M* Tris-HCl buffer, pH 7.4, 0.135 mL of water and 0.025 mL of the tissue homogenate (or plasma).
2. Pre-incubate the mixture at 37°C for 2 min, then add 0.015 mL of the PNA stock solution (1 mg/mL).
3. After incubation for (e.g.) 15 min stop the enzymatic reactions by adding 0.300 mL of 16.6% ACN in 0.1% TFA in water. Immediately transfer the mixture to an ice-water bath (0°C).
4. Freeze the mixture at –18°C for 30 min; subsequently thaw the mixture at 4°C and centrifuge it at 3000 rpm for 10 min (approx 1000*g*) at 4°C.
5. Transfer 0.200 mL of the supernatant directly to HPLC autosampler vials. Inject 0.010 mL aliquots into the HPLC system.
6. Prepare additional blind samples where the PNA test compound is replaced with water. The blind samples are incubated and analyzed as described for the test samples.
7. Prepare and analyze a reference solution by mixing 0.015 mL of the PNA test compound with 0.025 mL 0.1 *M* Tris-HCl buffer, pH 7.4, 0.160 mL water, and 0.300 mL 16.6% ACN in 0.1% TFA in water.
4. Collect a urine sample in a polypropylene tube by applying a slight pressure on the bladder of the anaesthetized animal. Store urine samples at –18°C pending analysis.
5. Decapitate the anaesthetised animal and collect the blood in 2 mL EDTA-treated glass tubes. Place and keep the tube in an ice-bath until centrifugation. Separate plasma by centrifugation at 3000 rpm (approx 1500*g*) at 4°C for 10 min and transfer the plasma to polypropylene test tubes. Store the samples at –18°C pending analysis.
6. Prepare additional blind samples where the PNA test compund is replaced with water. The blind samples are incubated and analyzed as described for the test samples.
7. Prepare and analyze a reference solution by mixing 0.015 mL of he PNA test compund with 0.025 mL 0.1 *M* Tris-HCl buffer, pH 7.4, 0.160 mL water, and 0.300 mL 16.6% ACN in 0.1% TFA in water.
8. Recovery in the incubated samples is calculated from the HPLC areas using the reference solution prepared in **step 7** as standard, corresponding to 100% recovery (no metabolism).

9. Metabolites are identified in the HPLC chromatograms based on comparisons of test samples and blind samples.

3.2. In Vivo Pharmacokinetics in Rodents

The pharmacokinetic profile of PNA-1 was investigated in a pilot study with i.v. administration to NMRI mice. NMRI mice were dosed intravenously with the PNA and single animals were sampled (plasma and urine) at fixed time points until 6 h after dosing. Plasma and urine concentrations of PNA-1 were determined using a preliminary analytical method based on solid-phase extraction and reversed phase (RP)-HPLC analysis. Quantification was based on electronically integrated peak areas using a series of spiked plasma (urine) samples (calibrators) covering the expected concentration range in the samples. Based on peak areas, the recovery of PNA-1 was estimated to be >95%. The limit of quantification (LOQ) was approx 100 ng/mL when assaying aliquots of 0.20 mL plasma. Concentration data were analyzed by noncompartmental methods using the Pharsight software WinNonlin version 3.0. Key parameters were calculated as follows: Clearance (CL) as the i.v. dose divided by area under the plasma concentration curve (AUC); volume of distribution (V) as CL divided by the elimination rate constant (k), and the elimination half-life ($t_{\frac{1}{2}}$) as log2 divided by k. Further information on calculation and interpretation of the various pharmacokinetic parameters can be found in text books on pharmacokinetics (e.g., **ref. *1***).

3.2.1. In Vivo Study

1. Prepare the dose formulation (2.50 mg/mL) by dissolving 5 mg PNA in 2 mL of 5% glucose in water.
2. Dose each of eight female NMRI mice (25 g body weight) with 0.10 mL of the dose formulation by slow injection (10–15 s) into a tail vein.
3. Anaesthetize (CO_2) one animal at each the following times after dosing: 2, 5, 15, 30, 60, 120, 240, and 360 min.
4. Collect a urine sample in a polypropylene tube by applying a slight pressure on the bladder of the anaesthetized animal. Store urine samples at 18°C pending analysis.
5. Decapitate the anaesthetized animal and collect blood in 2 mL EDTA-treated glass tubes. Place and keep the tune in an ice-bath

until centrifugation. Separate plasma by centrifugation at 3000 rpm (approx 1500*g*) at 4°C for 10 min and transfer the plasma to polypropylene test tubes. Store the samples at –18°C pending analysis.

3.2.2. Extraction and Analysis of Plasma and Urine Samples

1. Add 0.8 mL 0.1% TFA to aliquots of 0.2 mL plasma.
2. Activate the Oasis™ SPE columns with 0.25 mL of 0.1% TFA in ACN followed by 0.25 mL of 0.1% TFA in water.
3. Apply each sample to a conditioned SPE extraction column.
4. Wash the SPE column twice with 0.25 mL of 0.1% TFA in water. At each step pass the solution through the column by centrifugation at 3000 rpm (approx 1500*g*) for 5 min.
5. Elute PA251 from the column into clean PP tubes by application of 2×0.5 mL of 0.1 %TFA/40% ACN in water. Centrifuge as described for the washing steps.
6. Evaporate the two compiled eluates to dryness in a SpedVac centrifuge (*see* **Note 4**) without heating (approx duration: 1–2 h).
7. Re-dissolve the sample in 0.1 mL of 0.1% TFA in water. Centrifuge (3000 rpm, 5 min) and transfer the supernatant to autosampler vials. Inject 0.080 mL into the HPLC column.
8. Prepare a series of spiked plasma and urine blind samples (calibrators) covering the expected concentration range in the samples (0.1–100 µg/mL). Extract and analyze the calibrators as described in **steps 1–8** for the samples.
9. Calculate concentration in the study samples from a calibrator-based standard curve using peak areas as the response factor.
10. Analyze concentration data by noncompartmental methods and estimate pharmacokinetic parameters (e.g., AUC, $t_{1/2}$, CL; V_z).

3.3. Results and Discussion

3.3.1. In Vitro Studies

Representative HPLC chromatograms are shown in **Fig. 2**. Recovery of PNA-1 after in vitro incubations with plasma and tissue homogenates is listed in **Table 1**. PNA-1 was very stable in all matrices tested. No peaks originating from metabolites were detected in any of the HPLC chromatgrams of the incubated

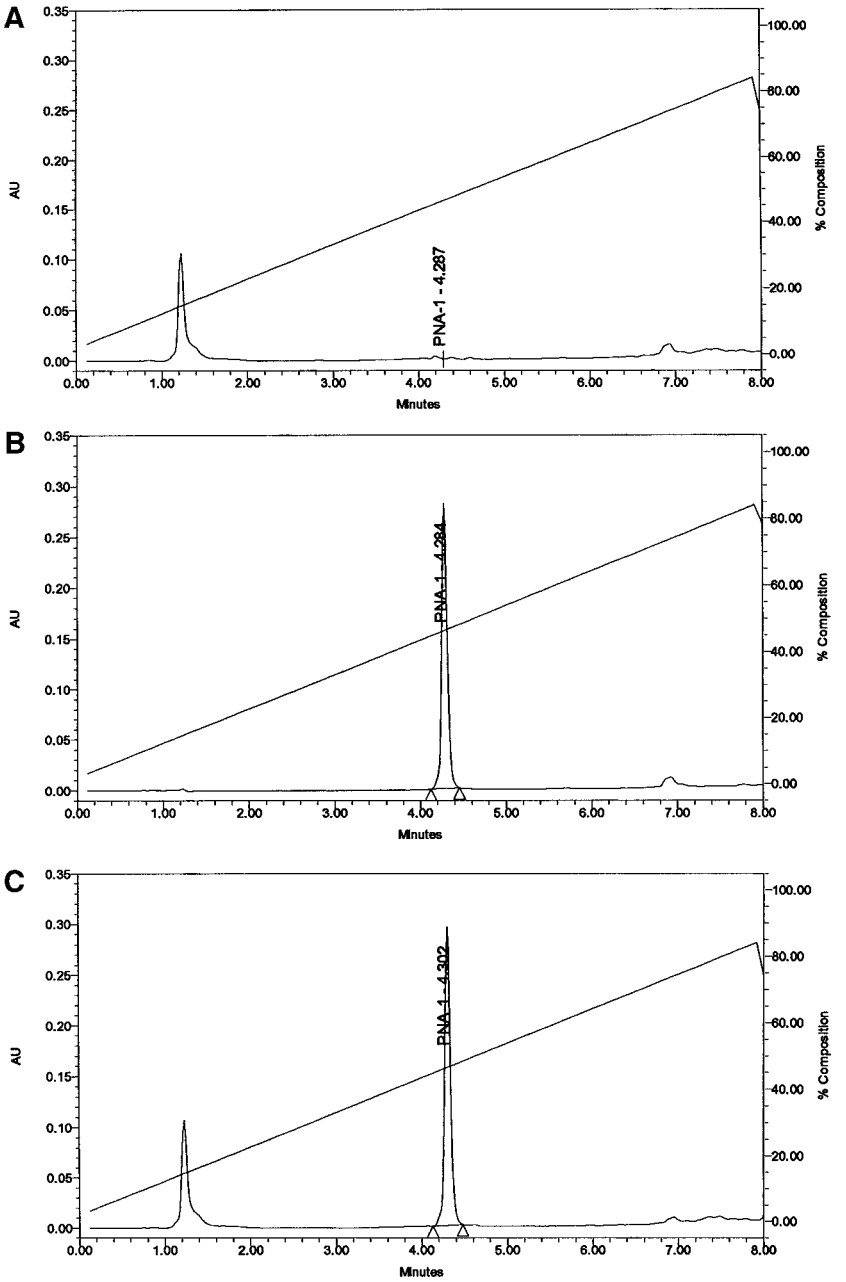

Fig. 2. HPLC chromatograms of samples from in vitro incubation of PNA-1 with liver homogenate: **(A)** liver blank; **(B)** reference sample, liver blank spiked with 0.015 mg PNA-1; and **(C)** test sample incubated for 15 min.

Table 1
Recovery and Turnover of PA251 After Incubation for 15 min with Tissue Homogenates and Plasma

Tissue	Recovery (%)
Liver	98
Kidney	99
Lung	100
Plasma	99

samples. These findings are consistent with previous reports on the biological stability of PNA oligomers *(2)*.

Using the BSA Protein Assay (*see* **Note 3**) the following protein concentrations were measured in tissue homogenates and plasma: liver: 20 mg/mL; kidney: 11 mg/mL; lung: 13 mg/mL, and plasma: 58 mg/mL. However, because the in vitro stability of PNA-1 was very high with recoveries >98%, it was not possible to calculate reliable turnover rates.

3.3.2. In Vivo Studies

PNA-1 was measurable in all plasma samples taken after administration to the mice (*see* **Fig. 3**). Representative chromatograms are shown in **Fig. 4**. AUC was calculated to be 28.7 h × µg/mL. The elimination half-life ($t_{1/2}$) was approx 0.9 h. Clearance (CL) was estimated to be 6 mL/min/kg and the volume of distribution (V_z) to be 0.5 L/kg. Highest urine concentration was measured in the sample taken 0.5 h after dosing. Metabolites of PNA-1 were not detected in any of the plasma and urine samples, concordant with an excellent biological stability of the PNA oligomer.

Because only one animal was sampled at each time point, very crude estimates of the key pharmacokinetic parameters were obtained. For more accurate parameter estimates, additional studies should be performed using more animals per time point in a sampling scheme optimized based on the outcome of the pilot study.

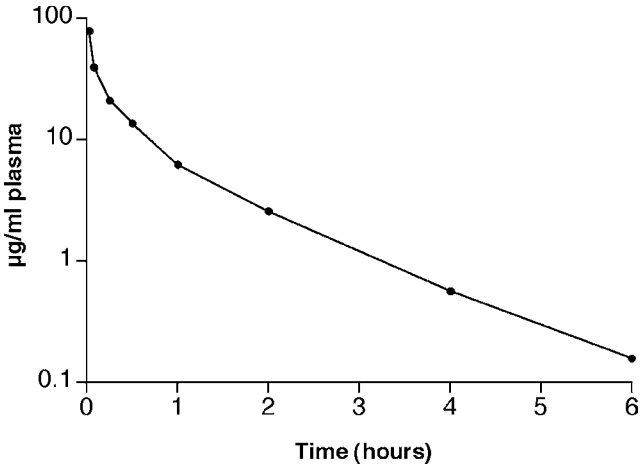

Fig. 3. Plasma concentration of PNA-1 following single i.v. administration of 10 mg/kg to female NMRI mice.

4. Notes

1. The advantages of small-bore chromatography (1–2 mm ID) are ascribed to the increased mass sensitivity achieved. Mass sensitivity and concentration sensitivity are the two ways of deeming the detection limits of a chromatographic system. The smaller the column ID, the smaller the mass that can be detected. Good column alternatives are: 1) Protein C4 (214TP5115), 2.1 × 150 mm (5 µm particles with 300 Å pore size) from Vydac; 2) Protein/peptid C18 (218TP5215), 2.1 × 150 mm (5 µm particles with 300 Å pore size) from Vydac; 3) Symmetry300™ C4, 2.1 × 100 mm (3.5 µm with 300 Å pore size) from Waters; and 4) Symmetry300™ C18, 2.1 × 100 mm (3.5 m particles with 300 Å pore size) from Waters.
2. PNAs tend to bind strongly to glass and some types of plastic (e.g., polystyrene). It is recommended to test the degree of binding to the test tubes prior to use. We have good experience with polypropylene tubes where the binding is <0.1%.
3. When comparing tissue fractions for their ability to catalyze drug biotransformation, a measure of the tissue protein is required. Protein is readily determined by, e.g., the colorimetric method of BCA Protein Assay reagent. Rate of metabolism can be calculated in *mg PNA/min/mg protein* from the formula:

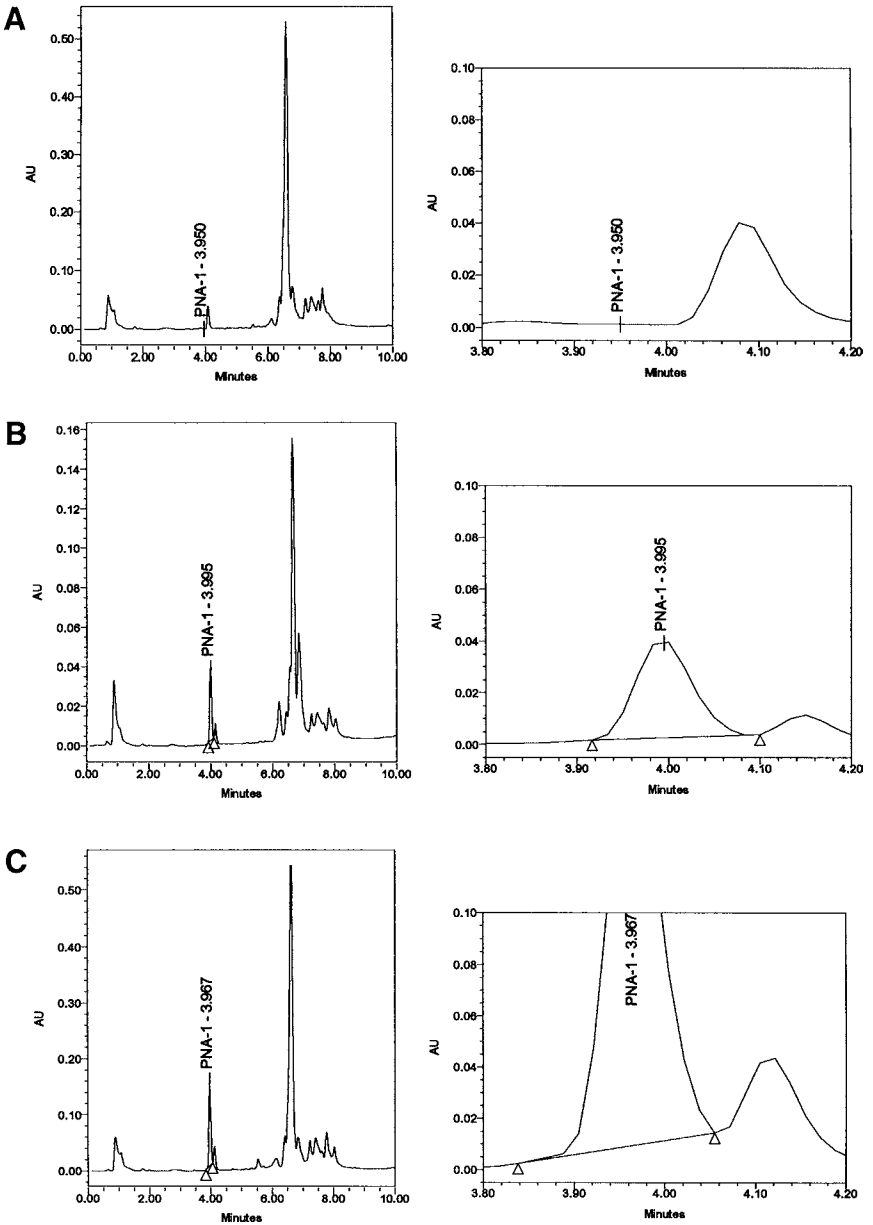

Fig. 4. HPLC chromatograms of plasma from in vivo studies on PNA-1 in mice: **(A)** plasma blank; **(B)** reference sample, plasma spiked with 0.15 mg PNA-1; and **(C)** test sample obtained 15 min after drug administration

$$[Area_{ref} - Area_{spl}] \times C / Area_{ref} \times T \times (P/0.025)$$

where:

$Area_{ref}$ is HPLC area of the PNA peak in the reference solution,
$Area_{spl}$ is HPLC area of the PNA in the test solution,
C is initial concentration in the test solution (mg/mL),
T is incubation time (15 min),
P is protein concentration in the homogenate (mg/mL).

4. SpeedVac evaporation generally works well for biological samples. However, for some nonbiological samples strong binding to the test tubes (i.e., low recovery) has been observed following SpeedVac evaporation. For such samples, higher recoveries are achieved if evaporation is done by freeze-drying or by N_2-streaming at room temperature.

References

1. Welling, P. G. and Tse, F. L. S. (1988) *Drugs and the Pharmaceutical Sciences, vol. 23: Pharmacokinetics*. Marcel Dekker Inc., New York. (eds.).
2. Demidov, V., Potaman, V. N., Frank-Kamenetskii, M. D., Buchardt, O., Egholm, M., and Nielsen, P. E. (1994) Stability of peptide nucleic acids in human serum and cellular extracts. *Biochem. Pharmacol.* **48,** 1309–1313.